



HAL
open science

New biopolymers with possible use in dentistry and orthopaedics

Teodora Zecheru

► **To cite this version:**

Teodora Zecheru. New biopolymers with possible use in dentistry and orthopaedics. Chemical Sciences. Université d'Angers, 2008. English. NNT : . tel-00448235

HAL Id: tel-00448235

<https://theses.hal.science/tel-00448235>

Submitted on 18 Jan 2010

HAL is a multi-disciplinary open access archive for the deposit and dissemination of scientific research documents, whether they are published or not. The documents may come from teaching and research institutions in France or abroad, or from public or private research centers.

L'archive ouverte pluridisciplinaire **HAL**, est destinée au dépôt et à la diffusion de documents scientifiques de niveau recherche, publiés ou non, émanant des établissements d'enseignement et de recherche français ou étrangers, des laboratoires publics ou privés.

**UNIVERSITATEA POLITEHNICA DIN BUCUREȘTI
FACULTATEA DE CHIMIE APLICATĂ ȘI ȘTIINȚA
MATERIALELOR**

TEZA DE DOCTORAT

**NOI BIOPOLIMERI CU POSIBILE UTILIZĂRI ÎN
DOMENIUL STOMATOLOGIC ȘI ORTOPEDIC**

**NEW BIOPOLYMERS WITH POSSIBLE USE IN
DENTISTRY AND ORTHOPAEDICS**

CONDUCĂTORI DE DOCTORAT

Prof.dr.ing. Corneliu CINCU

Pr. Daniel CHAPPARD

DOCTORAND

Ing. Teodora ZECHERU

2008

NEW BIOPOLYMERS WITH POSSIBLE USE IN THE FIELD OF DENTISTRY AND IN THE FIELD OF ORTHOPAEDICS

A thesis submitted in the fulfilment of the requirements
for the degree of Doctor of Philosophy
by **Teodora ZECHEU** (chem. eng.)

University POLITEHNICA of Bucharest, ROMANIA
Faculty of Applied Chemistry and Materials Science
Department of Science and Engineering of Polymers

and

University of Angers, FRANCE
Faculty of Medicine
Laboratory of Histology-Embryology – INSERM U922

October 2008

TABLE OF CONTENTS

Acknowledgements	iii
Abstract of the thesis	v
1. LITERATURE OVERVIEW	1
1.1. General introduction.....	2
1.2. History of controlled delivery.....	3
1.3. State-of-the-art in drug release mechanisms for polymeric drug delivery.....	5
1.4. Micro and nanocontainers for drug delivery.....	7
1.5. Amphiphiles, lipids, and self-assembly.....	8
1.6. Polymers and block-copolymers.....	10
1.7. Aggregation of amphiphilic block-copolymers in aqueous media.....	14
1.8. Polymeric containers.....	18
1.9. Tissue Engineering	19
1.10. Angiogenesis concept.....	20
1.11. General concept of drug delivery	28
1.12. General concept of surface immobilization.....	41
1.13. Poly (2-hydroxyethyl methacrylate).....	42
1.14. Economic figures.. ..	45
1.15. Future Opportunities and Challenges.....	46
2. PURPOSE OF THE THESIS	48
3. P(MMA-CO-TIPA) MICROBEADS FOR TUMOUR DETECTION	53
3.1. Introduction.....	54
3.2. Synthesis procedures.....	55
3.2.1. Synthesis of the iodine-containing monomer, TIPA.....	55
3.2.2. Synthesis of TIPA-containing microbeads.....	55
3.2.3. Synthesis of copolymers for biological tests.....	56
3.3. Characterisation studies.....	57
3.3.1. FT-IR spectrophotometry.....	57
3.3.2. SEM and EDX analyses of the p(MMA-co-TIPA) micobeads.....	59
3.3.3. Determination of reactivity ratios of the monomers.....	65
3.3.4. <i>In vitro</i> mineralisation potential of p(MMA-co-TIPA).....	72
3.3.5. <i>In vitro</i> cytotoxicity evaluation of p(MMA-co-TIPA) copolymers.....	75
3.4. Conclusions and perspectives.....	77
4. HEMA-BASED MICROBEADS FOR DRUG DELIVERY SYSTEMS	78
4.1. Introduction.....	79
4.2. Experimental.....	80
4.2.1. Synthesis of 2-Methacrylic Acid 3-Guanidinopropyl Ester.....	80
4.2.2. Synthesis of the polymers.....	81
4.3. Results and discussion.....	85
4.3.1. SEM analysis.....	86
4.3.2. FT-IR analysis.....	91
4.3.3. Swelling behaviour.....	91
4.3.4. FOM analysis.....	91
4.3.5. <i>In vitro</i> tests.....	93
4.3.6. <i>In vivo</i> tests. Organs distribution analysis.....	94
4.4. Conclusions.....	97
5. POLYMERIC BIOCOMPATIBLE STRUCTURES FOR CONTROLLED DRUG RELEASE OBTAINED BY PRECIPITANT POLYMERISATION	98
5.1. Introduction.....	99
5.2. Experimental.....	99
5.3. Results and discussion.....	100
5.3.1. Elemental analysis.....	100
5.3.2. Swelling tests.....	102
5.3.3. Scanning electron microscopy.....	103
5.3.4. Biocompatibility tests.....	105
5.4. Conclusions.....	110

6. COMPARATIVE STUDIES ON DIFFERENT HEMA-BASED POLYMERIC COMPOSITIONS AND THALIDOMIDE-LOADING	111
6.1. Introduction.....	112
6.1.1. Systems and methods.....	112
6.1.2. Staining.....	112
6.1.3. Calcification studies.....	113
6.1.4. Thalidomide.....	114
6.2. Synthesis procedures.....	118
6.2.1. Synthesis of the copolymers.....	118
6.2.1.1. Synthesis of microbeads.....	119
6.2.1.2. Synthesis of pellets.....	120
6.2.2. Drug loading for bone metastases.....	121
6.3. Characterisation studies.....	122
6.3.1. Fluorescence study.....	122
6.3.2. FT-IR and RAMAN Spectroscopy.....	124
6.3.3. Swelling tests.....	130
6.3.4. Mineralization tests.....	132
6.3.5. SEM and EDX.....	134
6.3.6. Spectrophotometrical dosage of calcium and phosphorus.....	144
6.3.7. Size distribution report by volume.....	145
6.3.8. Cytotoxicity evaluation.....	149
6.3.8.1. <i>In vitro</i> evaluation with L929 line cell.....	149
6.3.8.2. <i>In vitro</i> evaluation with EA.hy 926 cells.....	151
6.4. Use of p(HEMA-co-MOEAA) microbeads loaded with thalidomide, in a rat methastases model.....	155
6.5. Conclusions.....	159
7. P(HEMA-CO-DDMA-CO-AA) AND P(HEMA-CO-DDMA-CO-DEAEMA) MICRO- BEADS AND NAFICILLIN LOADING	161
7.1. Introduction.....	162
7.2. Synthesis of the polymers.....	165
7.3. Characterisation studies.....	166
7.3.1. Swelling tests.....	166
7.3.2. Scanning Electron Microscopy.....	169
7.3.3. FT-IR analysis.....	171
7.3.4. Kinetic study of HEMA-AA and AA-dDMA binary systems.....	174
7.3.4.1. Binary system HEMA-AA.....	178
7.3.4.2. Binary system AA-dDMA.....	181
7.3.5. Kinetic study of HEMA-dDMA-AA ternary system.....	186
7.3.6. <i>In vitro</i> studies for polymers biocompatibility testing.....	189
7.4. Conclusions of the synthesis.....	191
7.5. Nafcillin loading to the synthesized copolymers.....	194
7.5.1. Esterification procedure.....	194
7.5.2. Hydrolysis and drug release procedures.....	194
7.5.3. Results.....	195
7.5.3.1. SEM analysis.....	198
7.5.3.2. Nafcillin loading efficiency.....	199
7.5.3.3. <i>In vitro</i> study of nafcillin release.....	200
7.6. Conclusions and perspectives.....	204
8. GENERAL CONCLUSIONS OF THE THESIS	205
References.....	210
List of figures.....	218
List of tables.....	223
 <i>Curriculum Vitae</i>	 224
List of paperworks.....	226

ACKNOWLEDGEMENTS

Completing a thesis is a challenge, but thanking all those who contributed to it is an even greater one. Due to the nature of my studies, many people were involved in one or the other way in it. I want to thank all of them for their invaluable support and guidance during the process of completing this thesis, including those not mentioned here by name.

It was a pleasure for me to work with all the wonderful people from University POLITEHNICA of Bucharest.

First and foremost, I would like to thank Professor Corneliu CINCU for being a great supervisor. His ideas and tremendous support had a major influence on this thesis. He spent a lot of time helping me as well as all the other people in the laboratory. I would like to thank him for his advices and for giving me the chance to take part in several interesting conferences. I learned a lot during this time and I am convinced that this knowledge will help me in the future.

I would like to thank Professor Daniel CHAPPARD for reviewing my thesis. I was glad to have such a supportive co-supervisor. I enjoyed his interest in my research as well as the fruitful discussions. Thank you for the opportunity to become involved in research in the field of bone pathology!

Thanks are also due to the members of my committee, Professor Horia IOVU, Senior Lecturer Marie-Françoise MOREAU, Professor Gheorghe HUBCA, Professor Michel-Felix BASLE, for their valuable input.

Thank you to Professor Ecaterina IONESCU, from University of Medicine and Pharmacy "Carol Davila", Romania, and to Professor Amar ZERROUKHI, from University of Saint-Etienne, France, for the very favorable report evaluations on my thesis.

I also want to thank Professor Lambrache PAPAAGI for introducing me to the Department of Polymers and inspiring me to pursue it as a course of study.

Thank you to Professor Bogdan MĂRCULESCU, Lecturer Edina RUSEN, Lecturer Izabela-Cristina STANCU, Lecturer Cătălin ZAHARIA, for your amazing work in designing and conducting different studies. Discussing the meaning and implications of these studies with you has been truly wonderful. I could not have done it without you. Thank you!

My thanks to my friends and colleagues for the great time I had in our group. I enjoyed the atmosphere, your friendship, and your support. On this occasion, I would like to extend my

appreciation to: Lecturer Sorina-Alexandra GÂREA, Lecturer Paul STĂNESCU, PhD Student Adriana LUNGU and PhD Student Celina PETREA.

I would also want to thank to Eng. Florica RIZEA for her invaluable support during all those four years of research.

Special thanks to Professor Tudor CHERECHEȘ, Professor Doru-Adrian GOGA, Principal Researcher IInd grade Aurora SĂLĂGEANU, Senior lecturer Traian ROTARIU, and to University Assistant Florin MICULESCU for the great collaboration over the years. It was a pleasure to work with all these people and to benefit from their knowledge.

I would like to thank Georgios STAIKOS, from University of Patras, Greece, for the great collaboration on elemental analyses, and also to all the people in Laboratory of Histology-Embryology from University of Angers, France, for the interesting and fruitful discussions. Furthermore, special thanks to Eng. Robert FILMON and PhD Student Hervé NYANGOGA for their help on different biology issues during my stay in Angers.

Last but not least, I wish to thank to my family who has always supported me: to my parents and my sister for instilling the respect and love for academic education, and most of all, to my husband for being patient with me during the past years - especially during the writing of this thesis.

The present thesis has been supported by the Romanian Ministry of Education and Research (MEC) under contract number CEEEX 11/2005 and CNCSIS PN-II-RU-TD-I 21/2007. This financial support is gratefully acknowledged.

ABSTRACTUL TEZEI DE DOCTORAT

Prezenta teză de doctorat a avut drept temă de cercetare studiul unor noi polimeri biocompatibili sintetici cu utilizări în domeniul eliberării controlate de medicamente. În partea de literatură sunt subliniate principiile eliberării controlate și sunt descrise posibilele aplicații ale acestor tipuri de polimeri.

Au fost sintetizați copolimeri pe bază de HEMA prin polimerizare în suspensie, polimerizare precipitantă și polimerizare în masă. Acești copolimeri au fost funcționalizați prin introducerea de monomeri cum ar fi: metacrililoxietil fosfat, guanidino-propil metacrilat, dietilaminoetil metacrilat, clorură de dialildimetil amoniu, metacrililoxietil acetoacetat, clorură de metacrililoxietil trimetilamoniu, glicidil metacrilat, tetrahidrofurfuril metacrilat. Compușii obținuți au fost caracterizați din punct de vedere fizico-chimic și biologic. Au fost studiate rapoartele de reactivitate ale monomerilor în sistemele binare: MMA-TIPA, HEMA-AA, AA-dDMA, și în sistemul ternar HEMA-dDMA-AA.

O altă direcție de cercetare a fost constituită de studiul comportamentului în mediu biologic al acestor copolimeri alături de coloranți fluorescenți, și al unui copolimer pe bază de MMA conținând un monomer iodat, pentru detecție biologică.

În vederea obținerii de sisteme active de eliberare, s-au conceput două sisteme: primul, utilizând un conjugat fizic talidomidă-polimer, iar cel de-al doilea, nafcilină legată chimic de polimer. Legătura polimer-medicament a fost analizată prin FT-IR și UV, și a fost confirmată prin MEB și EDX. Au fost efectuate studii *in vitro* pentru a verifica interacțiunile dintre polimerii încărcăți cu medicament și celule, folosind ca metode de analiză microscopia de fluorescență, în cazul talidomidei, și analize UV-VIS, în cazul nafcilinei.

Rezultatele obținute reprezintă o reală opțiune în vederea utilizării în viitor al acestor copolimeri în domeniul anti-angiogenezei tumorale.

ABSTRACT OF THE DOCTORAL THESIS

The present thesis focuses on the use of biocompatible polymers in controlled drug delivery applications. The principles of controlled drug delivery are outlined and applications of polymers are described.

Series of HEMA-based copolymers were synthesized by suspension-dispersion polymerization, precipitant polymerization and bulk polymerization. Functionalisation was given by introducing monomers such as: methacryloyloxyethyl phosphate, guanidino-propyl methacrylate, diethylaminoethyl methacrylate, diallyldimethyl ammonium chloride, methacryloyloxyethyl acetoacetate, methacryloyloxyethyl trimethylammonium chloride, glycidyl methacrylate, tetrahydrofurfuryl methacrylate. Polymers were physico-chemically and biologically characterized. Reactivity ratios of monomers in different systems were studied: MMA-TIPA, HEMA-AA, AA-dDMA, HEMA-dDMA-AA.

Another approach was the use of HEMA-based copolymers with fluorescent dyes and a iodine MMA-containing copolymer, for biological detection purposes.

To obtain active targeting drug-delivery systems, two methods were used: physical conjugation in case of thalidomide and chemical linkage for nafcillin. Drug insertion was determined by FT-IR and UV spectra, confirmed by SEM and EDX. *In vitro* studies were performed in order to investigate the interactions of these drug-functionalized polymers with cells, in which uptake was followed via fluorescence microscopy, in case of thalidomide, and via UV-VIS studies, in case of nafcillin. No significant cytotoxicity was determined for the artificial polymers in these studies.

Drug release results obtained were interesting, giving a real option for future use in the field of tumour antiangiogenesis.

RESUME DE LA THESE DE DOCTORAT

La thèse présente l'étude des polymères biocompatibles dans le domaine de la libération contrôlée de médicaments. Les principes de la libération contrôlée sont soulignés et les applications des polymères sont décrites.

Séries de copolymères de HEMA ont été synthétisées par polymérisation en suspension-dispersion, polymérisation précipitante et en masse. La fonctionnalisation a été donnée par l'introduction de monomères comme: méthacryloyloxyéthyl phosphate, guanidino-propyl méthacrylate, diéthylaminoéthyl méthacrylate, diallyldiméthyl ammonium chlorure, méthacryloyloxyéthyl acétoacétate, méthacryloyloxyéthyl triméthylammonium chlorure, glycidyl méthacrylate, tétrahydrofurfuryl méthacrylate. Les polymères ont été caractérisés physico-chimiquement et biologiquement. Les rapports de réactivité des monomères dans les systèmes: MMA-TIPA, HEMA-AA, AA-dDMA, HEMA-dDMA-AA ont été étudiés.

Une autre direction a été l'étude du comportement de ces copolymères avec des colorants fluorescents, et d'un copolymère contenant du MMA et un monomère iodé, pour la détection biologique.

Pour l'obtention de systèmes actifs de libération, on a utilisé deux méthodes: liaison physique en cas du thalidomide et liaison chimique pour le nafcilline. La liaison polymère-médicament a été analysée par FT-IR et UV, et a été confirmée par MEB et EDX. On a effectué des études *in vitro* pour vérifier les interactions entre les polymères chargés avec médicaments et les cellules, en utilisant comme méthode d'analyse la microscopie de fluorescence, dans le cas du thalidomide, et l'UV-VIS, pour le nafcilline.

Les résultats obtenus donnent une vraie option pour une future utilisation dans le domaine de l'anti-angiogenèse des tumeurs.

Chapter 1

Literature overview

T. Zecheru, C. Spulber, C.C. Zecheru, T. Chereches, *Advanced technologies and concepts used in diagnosis and treatment*, Fall session 2007 of Romanian Scientists Association (AOSR), 15-16 October, Constanta, Romania.

1.1. General introduction

In the past decade, the interest in biomaterials based on polymers and amphiphilic self-assembling systems has increased enormously. The main reason for this is the need of new materials with enhanced performance to replace classic systems facing the demand of industry for increasingly sophisticated systems. A particular interest has been focused on the preparation of carriers, with special emphasis on the control of their size and morphology at the micro and nanometer scale.

In recent years, there has been a rapid growth in the area of drug discovery, facilitated by novel technologies such as combinatorial chemistry and high-throughput screening. These novel approaches have led to drugs which are generally more potent and have poorer solubility than drugs developed from traditional approaches of medicinal chemistry (Lipinsky, 1998). The development of these complex drugs has resulted in a more urgent focus on developing novel techniques, to deliver these drugs more effectively and efficiently.

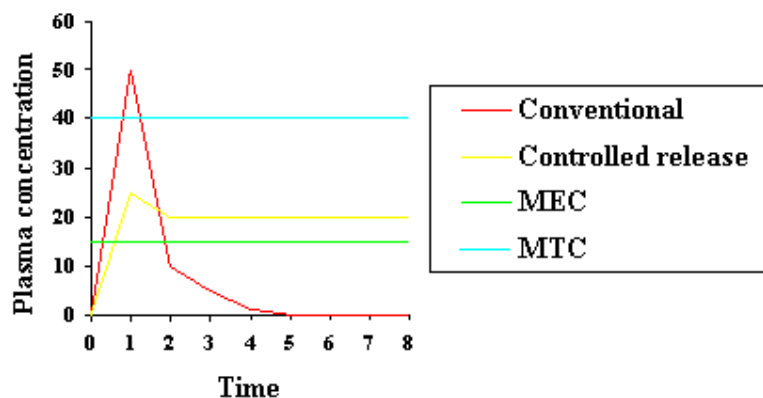


Fig. 1-1. Conventional and ideal drug release profiles (Dziubla, 2003). MEC = maximum desired concentration; MTC = minimum efficient concentration.

As it can be seen in Fig. 1-1, the conventional oral and intravenous routes of drug administration do not provide ideal pharmacokinetic profiles especially for drugs, which display high toxicity and/or narrow therapeutic windows. For such drugs the ideal pharmacokinetic profile will be one wherein the drug concentration reaches therapeutic levels without exceeding the maximum tolerable dose and maintains these concentrations for extended periods of time until the desired therapeutic effect is reached. The same amount of drug is delivered but in therapeutic concentrations for a longer time. With less drug wasted, costs can be reduced.

1.2. History of controlled delivery

The state of the art in drug delivery could be compared to the early years of car production, when "lots of car companies with lots of models" rushed to capitalize on technology and capture a share of the market.

Microencapsulation

Microencapsulation has been the subject of massive research efforts since its inception around 1950. Today, it is the mechanism used by approximately 65% of all sustained release systems. Hundreds of drugs have been microencapsulated and used as sustained release systems.

Some common examples are Arthritis Bayer, Dexatrim Capsules, Dimetapp Elixer, and No Doz (Fig. 1-2). Microencapsulation can be either physical or chemical.



Fig. 1-2. Powdered drugs encapsulated

(http://chsfpc5.chem.ncsu.edu/~franzen/CH795I/lectures/drug_delivery/sld001.htm).

Physical methods include encapsulation by pan coating, gravity-flow, centrifuge, and the Wurster Process. The Wurster Process, invented in 1949 by Professor Dale E. Wurster, is the first technique to microencapsulate any type of particle. This method consists of a high-velocity air stream shot through a cylindrical fluid bed of active ingredients. Coating is applied to the resultant mist of vapour and the particles flow out the top of the cylinder and descend back to the layer of fluid. The air dries the coating, so that each particle is ready to be recoated once it reaches the bottom of the chamber. Number of cycles, temperature, pressure, and humidity are varied to gain desired coating composition and thickness.

Chemical microencapsulation is most frequently achieved by coacervation (1953) (Fig. 1-3). In this technique, the coating precipitates onto a droplet of the drug, much like the way in which a crystal is formed in a supersaturated solution.

Coacervation consists in three stages under constant agitation:

1. A solution must be formed with three immiscible phases, the core material (active ingredient), coating material, and solvent.
2. The liquid coating will deposit around the core material. This is accomplished by mixing the coating phase with the solvent phase (in which the active ingredients reside).
3. The coating is rigidized thermally or by desolvation.

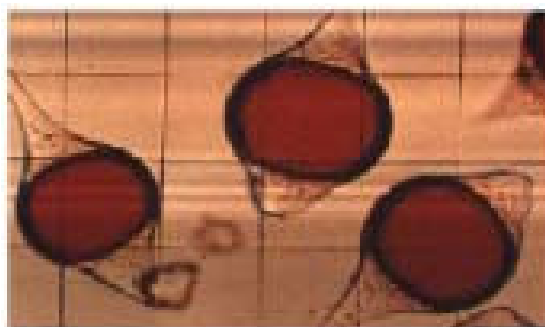


Fig. 1-3. Example of droplets formed by coacervation

(http://chsfpc5.chem.ncsu.edu/~franzen/CH795I/lectures/drug_delivery/sld001.htm).

Implants for drug delivery

Implantable drug delivery systems are being developed since the 1970s' to take the place of traditional drug delivery systems, such as pills and hypodermic injection. However, compared to other forms of drug delivery systems, implants are still in the infancy stage of development. Implantable systems that are currently available include Norplant and various pumps, such as insulin pumps. The systems are designed to deliver drugs directly into the bloodstream at a controlled rate of transmission.

Implantable pumps

Implantable pumps for drug delivery have been developed for treatment of several ailments, such as diabetes and cancer. These pumps reduce the need for repeated insulin or chemotherapy injections and can provide blood samples for analysis without using venipuncture. One advantage of a pump is the elimination of infection that results from repeated injections at the same site. However, there are some disadvantages to implantable pumps systems. Disadvantages include the size of the pump, restricted access to the pump, potential of drug leakage from the reservoir, and possible infection due to implant surgery. The implantable pumps currently being used in humans today are peristaltic pumps. New pump designs include fluorocarbon propellant pumps, and osmotic pumps.

Transdermal drug delivery (1980)

Transdermal drug delivery systems are involved in the continuous administration of drug molecules from the surface of the skin, through its layers, and into the circulatory system. The first transdermal patches were commercially available in the early 1980s. The first was Transderm Scop, marketed by CIBA, which released the anti-motion sickness drug scopolamine. It was followed by nitroglycerin patches that aided in the prevention of angina. Today, the drugs available include scopolamine, nitroglycerine, clonidine (for the treatment of hypertension), nicotine, estradiol (postmenopausal syndrome), and testosterone (hormone replacement therapy).

Methods of transdermal drug delivery

There are two basic dosing systems: one that controls the rate of drug delivery to the skin and one that uses the skin to control the absorption rate. There are two elementary patch designs that correspond to the dosing systems: reservoir system and monolithic system, respectively.

a) The monolithic design

The monolithic design has only three layers: the adhesive layer, a polymer matrix containing the drug molecules, and a waterproof backing. These systems deliver the drug to the skin to saturation, which causes the rate of delivery to the circulatory system to be controlled by the skin. As the amount of drug in the patch decreases below the skin's saturation limit, the rate of delivery from patch to skin will slowly decrease.

b) The reservoir design

The reservoir design is made up of four layers: the adhesive layer that directly contacts the skin, the control membrane, which controls the diffusion of drug molecules, the reservoir of drug molecules, and a water-resistant backing. As this design delivers uniform amounts of the drug over a specified period, the rate of delivery has to be less than the saturation limit of different types of skin.

1.3. State-of-the-art in drug release mechanisms for polymeric drug delivery

The first design concepts for controlled release were passive delivery systems. In passive delivery, unassisted diffusion of solvent and solute is the only means of modulating the rate of drug delivery. Typically, there is a depot of drug contained within a polymer matrix which releases over time. A convenient way to evaluate the release profile from these passive systems is by the following power law

$$\frac{M_t}{M_\infty} = kt^n \quad (1)$$

where M_t is the amount of drug released at a specific time, M_∞ is the total amount of drug released at infinite time, and k and n are both weighting constants that best fit experimental data. While this equation is inherently curve fitting, there is a theoretical basis for its existence.

A solution to Fick's second law on a slab with diffusion across both edges results in the following short time approximation,

$$\frac{M_t}{M_\infty} = \frac{4}{\delta} \left(\frac{Dt}{\pi} \right)^{\frac{1}{2}} \quad (2)$$

where D_t is the diffusion parameter and δ is the wall thickness, which is analogous to equation (1) with $n = 1/2$. When n is equal to 1, this is known as Case II transport. Continuous release occurs with a time-independent delivery scheme, most commonly called zero-order release kinetics.

However, this is just a subset of the actual goal of controlled release. The primary aim of controlled drug delivery is the complete optimization of the therapeutic delivery; that is the ability to deliver to the desired location, a precise dose for a finite period of time. With this ideal system, one could achieve high bioavailability with minimal side effects and drug exposure. To achieve this idealization, systems must be responsive to fluctuations in the patient's needs.

The advantage to implantable drug delivery devices is that they can be designed to meet these aims by providing a means of continually monitored and administered drug delivery.

One of the ways such a profile can be achieved in an ideal case scenario would be by encapsulating the drug in a polymer matrix. The technology of polymeric drug delivery has been studied in detail over the past 30 years and numerous excellent reviews are available (Gombotz and Pettie, 1995; Sinha and Khosla, 1998; Langer, 1998).

And it is not only a matter of convenience and reduced anxiety. In some cases, sustained release is also a more effective way to deliver the drugs - at a slow, steady pace instead of dumping them into the patient's system with periodic doses of pills or injections.

The three key advantages that polymeric drug delivery products can offer are:

- Localized delivery of drug: The product can be implanted directly at the site where drug action is needed and hence systemic exposure of the drug can be reduced. This becomes especially important for toxic drugs which are related to various systemic side effects (such as the chemotherapeutic drugs).
- Sustained delivery of drugs: The drug encapsulated is released over extended periods and hence eliminates the need for multiple injections. This feature can improve patient compliance especially for drugs for chronic indications, requiring frequent injections (such as for deficiency of certain proteins).
- Stabilization of the drug: The polymer can protect the drug from the physiological environment and hence improves its stability *in vivo*. This particular feature makes this technology attractive for the delivery of labile drugs such as proteins.

Interest in this field has increased considerably, especially after the commercial success of products such as Lupron Depot, Zoladex, Norplant and Gliadel, all of which using the principles of sustained and localized drug release.

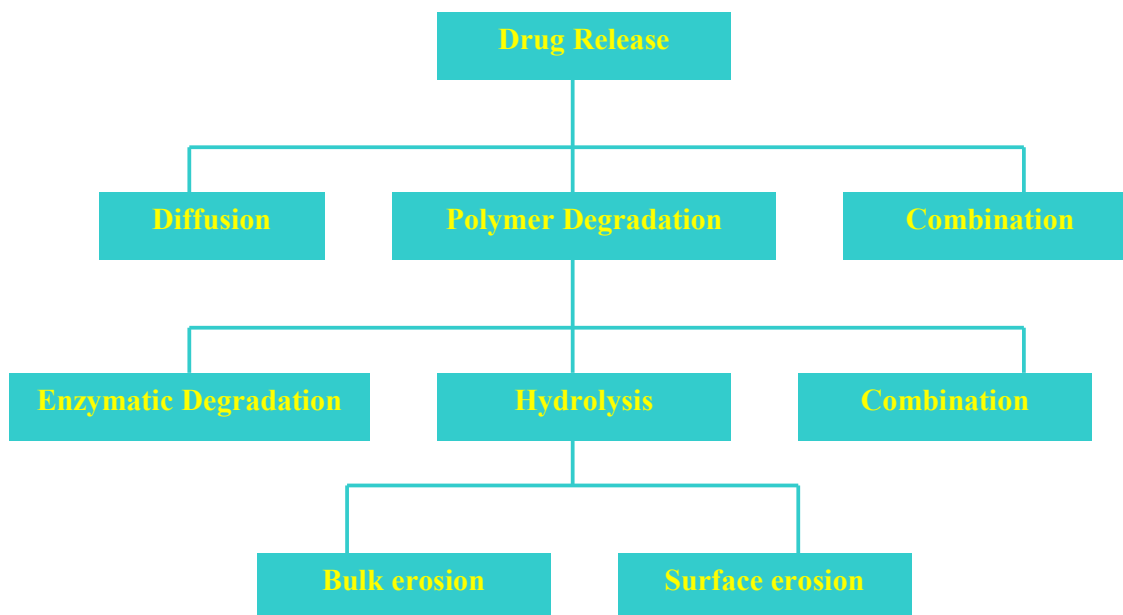


Fig. 1-4. Possible drug release mechanisms for polymeric drug delivery (Dziubla, 2003).

As shown in Fig. 1-4, the drug will be released over time either by diffusion out of the polymer matrix or by degradation of the polymer backbone.

This continuous release of the drug could potentially lead to a pharmacokinetic profile close to the ideal case scenario depicted in Fig. 1-1.

The continuous release of drugs from the polymer matrix could occur either by diffusion of the drug from the polymer matrix, or by the erosion of the polymer (due to degradation) or by a combination of the two mechanisms. Several reviews have been presented on the mechanisms and on the mathematical aspects of drugs release from polymer matrices (Batycky et al., 1997; Brazel and Peppas, 2000; Comets et al., 2000). For a given drug, the release kinetics from the polymer matrix are governed predominantly by three factors, viz. the polymer type, polymer morphology and the excipients present in the system.

1.4. Micro and nanocontainers for drug delivery

As a result of the intensive research in this area several approaches have emerged and two main classes of micro and nanocarriers can be distinguished: spheres and capsules (Fig. 1-5). Microspheres, also termed microparticles or matrix systems, consist of a polymer matrix, in whose pores other molecules can be encapsulated. They can also serve as molds for engineering more sophisticated materials. Microcapsules consist of a polymer shell or membrane surrounding a cavity, and can be thought as reservoir systems. These systems are *per se* encapsulating systems, but have been also used as templates.

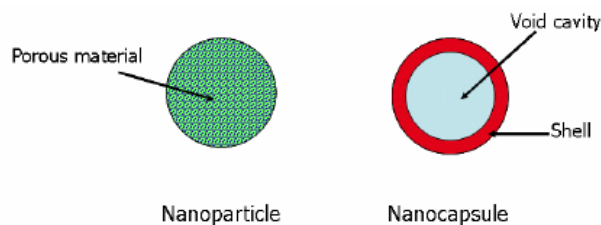


Fig. 1-5. Difference between a porous microparticle and a microcapsule.

Many of these microstructures have been used in different fields. For instance, microcapsules can be used as microreactors, where they provide a compartmentalized volume in which reactions can take place, thus protecting unstable or labile molecules (enzymes, catalysts, etc.) from hostile environments. Microparticles find use in chemistry for chromatography. In the pharmaceutical industry, both systems are used as controlled-release and targeting devices. In cosmetics, these systems are used as protective shells for the encapsulation of labile substances such as antioxidants. Another area of application is agriculture, where micro and nanocarriers can be used to deliver nutrients to poor soils, and also as delivery systems for fungicides, pesticides, and bactericides.

Moreover, in fields such as biochemistry these capsules can serve as matrices to insert membrane proteins and therefore as model systems to study protein association with membranes, or more ambitiously to design artificial ionic pumps and light harvesting systems.

Microstructured materials have evolved from early and simple systems into more sophisticated complex functional structures and hybrid materials. Using self-assembly, these synthetic systems mimic living organisms. A further challenge is to obtain artificial cells based on this type of self-assembled structures, mimicking the structure and behavior of biological cells. First attempts to obtain artificial cells focused mainly in the incorporation of channel proteins and pores into the artificial membranes.

Some of the major *drug delivery vehicles* being researched for delivering drugs are:

- Organic and synthetic polymers and other chemical constructs that can release drugs at a sustained rate, or release them only in certain environments;
- Liposomes;
- Medicated skin patches;
- Implanted devices that can release drugs with an external remote control;
- Powder forms of traditional drugs which can be inhaled and absorbed through the lungs.

1.5. Amphiphiles, lipids, and self-assembly

Early versions of controlled drug delivery are already in common use, such as time-release cold tablets and Nicoderm patches for those trying to quit smoking. But such modes of drug delivery are used mostly with small molecules. Cutting-edge technologies tackle the real challenge:

how to package and deliver complex molecules so that delivery will be accurate, modulated, and effective. Many diseases formerly thought to be untreatable, such as hepatitis C, multiple sclerosis, hormonal disorders, and many cancers, can benefit from protein therapy. But until recently, this required intravenous infusion or frequent injections. With the latest developments in pulmonary delivery and injection of long-lasting doses of proteins or drugs, new horizons are appearing for the treatment of such diseases.

Proteins present a thorny delivery problem, not only because of their large sizes but because they are notoriously sensitive to changes in their surroundings. Their optimal activity often depends on just the right pH, temperature, and conformational structure.

Amphiphilic molecules (Fig. 1-6), which are molecules with a polar and a non-polar moiety, arrange themselves at interfaces or tend to build aggregates in solution. Amphiphiles are surface-active molecules; at the interface they form monolayers, therefore lowering the energy of the system, by lowering its surface tension. Examples of common amphiphiles are lipids and detergents.

Lipids constitute a special case of amphiphiles typically consisting of two fatty acid chains linked by ester or acyl bonds to a common backbone, with the most commonly found lipids in nature being glycerol-based lipids.

In aqueous solution, low molecular-weight amphiphilic molecules can, depending on concentration, structure, temperature, and other parameters, build different aggregates such as micelles, vesicles, and lyotropic liquid crystalline phases ("lyotropic" refers to the fact that such phases are formed by amphiphiles as a function of concentration as well as temperature, in the case in which the phases form in function of the temperature only they are called thermotropic phases). The driving force for such aggregation in aqueous media usually is referred to as the hydrophobic effect.

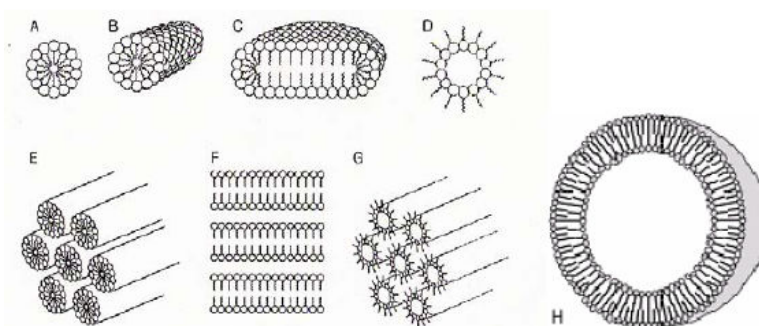


Fig. 1-6. Some different aggregation morphologies found in low molecular amphiphiles: A, spherical micelles; B, rod-like micelles; C, disk-shaped micelles; D, inverted micelles; E, normal cylindrical hexagonal packing; F, lamella; G, inverted cylindrical hexagonal packing; H, double bilayer formation in a spherical vesicle.

The term "hydrophobic effect" was first used by Kauzmann and broadly reviewed by Tanford. According to the IUPAC definition, it is "the tendency of hydrocarbons (or lipophilic hydrocarbon-like groups in solutes) to form intermolecular aggregates in aqueous medium, and analogous intramolecular interactions. The name arises from the attribution of the phenomenon to the apparent repulsion between water and hydrocarbons. However, the phenomenon ought to be attributed to the effect of the hydrocarbon-like groups on the water-water interaction". At a crude approximation, the hydrophobic interaction reduces to the preferential interaction of nonpolar groups among themselves in a water environment, although the process is much more complex than that. Hydration of non-polar species results in higher ordering of the neighboring water molecules which in turn results in highly unfavorable entropic conditions of the water surrounding the solute. The system, therefore, tends to avoid the unfavorable hydrophobic hydration contribution by forming aggregates, thus reducing the contact of the solute with neighboring water molecules.

Nevertheless, the complex thermodynamic factors affecting the hydrophobic effect are still not completely understood and debate among specialists continues. Interesting reviews with the evolution of the concept of the hydrophobic effect throughout time and its thermodynamic implications were recently published (Kost and Langer, 2001; Nahar et al., 2006; Siepmann and Goepferich, 2001).

The hydrophobic effect dictates the self-assembly of lipids into a variety of morphologies. Like lipids, amphiphilic polymers also self-assemble in different structures.

1.6. Polymers and block-copolymers

Polymers consist of structural or repeating units of low molecular weight covalently connected to each other to give high molecular weight compounds. The small molecules that combine with each other to form these macromolecules are called monomers. Based on their architecture, polymers can be classified into linear polymers, branched polymers, and dendrimers. Likewise, branched polymers can be classified according to their structure into comb-like, ramified, or star-like polymers (Fig. 1-7).

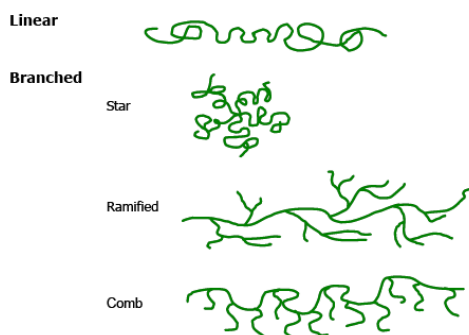


Fig. 1-7. Different types of homopolymer architecture.

Dendrimers (Fig. 1-8) constitute actually a special class of branched polymers, in which the ramifications occur in each monomer, giving thus branched branches.

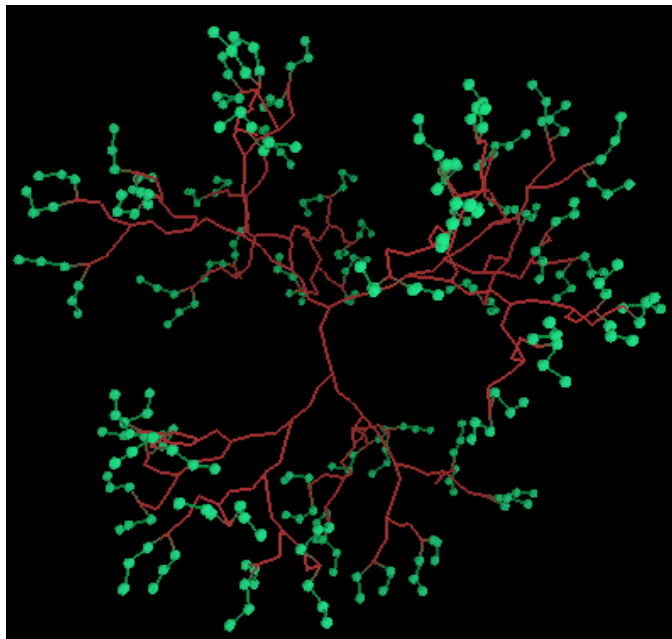


Fig. 1-8. Highly branched dendrimers (biomed.brown.edu/.../Pages/emerging.htm).

A polymer that consists of two different repeating units is referred to as a copolymer, whereas polymers containing only one type of repeating unit are named homopolymers. The sequence in which two different repeating units appear gives rise to a further classification within copolymers. A polymer in which the repeating units alternate is called an alternating copolymer, if the repeating units do not have any specific sequencing the copolymer is known as a random or statistical copolymer. If relative long segments of a monomer are present in a block fashion, it is termed a block-copolymer.

Block-copolymers consist of at least two, covalently bound, segments or blocks of different homopolymers. For instance, a triblock-copolymer can have a general form $A_x-B_y-C_z$, with A, B, C, being different monomer types constituting the different blocks. The subscripts x, y, and z, stand for the degree of polymerisation, i.e. the average number of each monomer units present in each respective block. Branched structures can also be found among copolymers, graft copolymers being one of the most interesting ones.

Graft copolymers can be considered as a special case of block-copolymers, a comb-like structure in which several blocks of homopolymer B are grafted as branches onto a main chain of homopolymer A, known as the backbone (Fig. 1-9).

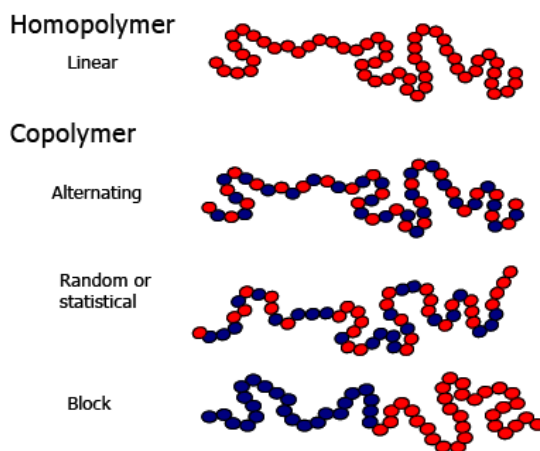


Fig. 1-9. Linear copolymers, statistical or random, alternate and block-copolymers.

In block-copolymers (Fig. 1-10), by covalently linking two intrinsically different homopolymers, macroscopic phase separation is prevented and limited to the nanometer range. This gives rise to the wide variety of morphologies found for this type of polymers in bulk, including cylindrical, and body-centered cubic micellar structures, depending on the relative volume fractions of the blocks.

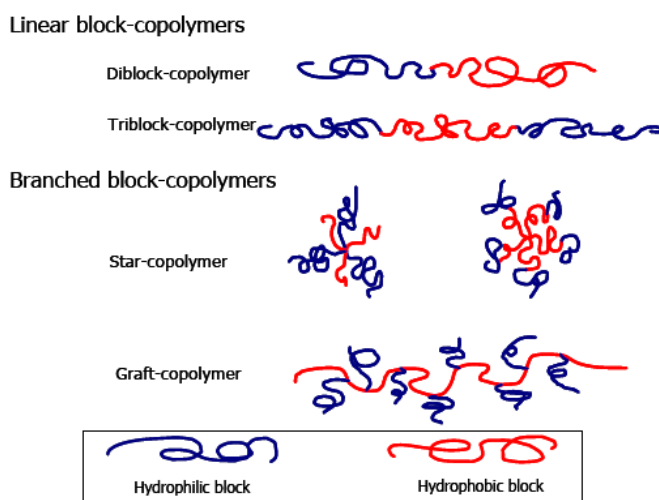


Fig. 1-10. Different architectures of block-copolymers: linear diblock, triblock, star, and graft copolymer.

For amphiphilic block-copolymers the tendency to separate phases manifests itself not only as micro-phase separation in bulk but also as self-assembly in solution. All the parameters that influence the assembly behavior of low molecular amphiphiles also play a role in the self-aggregation process of amphiphilic block-copolymers and analogous superstructures are observed in solution (Fig. 1-11).

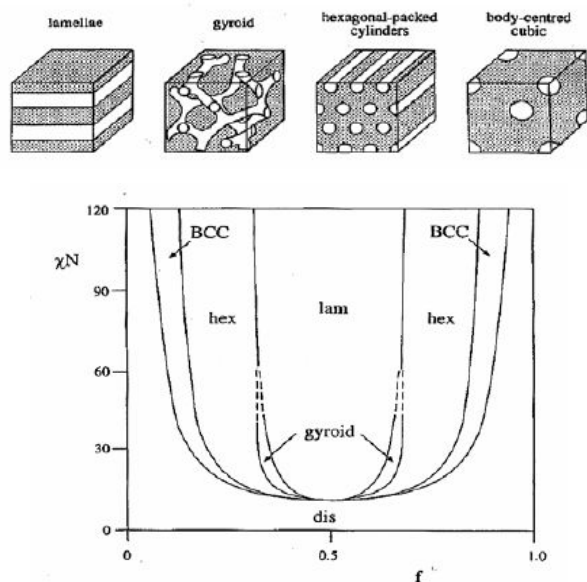


Fig. 1-11. Phase diagram and the corresponding self-assembled structures for block-copolymers in bulk.

Polymers can deliver drugs through dissolution, diffusion, or osmosis.

In **dissolution**, the drug is released over time as the polymer dissolves in the gastrointestinal tract. Mixing and layering polymers with varying dissolution rates controls the rate of release.

In **diffusion**, the release of the drug is controlled by its rate of diffusion out of the polymer.

In **osmosis**, the drug is contained in a polymer consisting of two compartments: one compartment contains the drug and the other contains a biologically inactive agent that can push out the drug under certain conditions – a push layer. When an individual takes the drug in pill form, water penetrates the pill through the membrane of the polymer. This step activates the push layer, which then drives the active ingredient into the gastrointestinal tract through one or more tiny holes on the other side of the pill.

Upon swallowing, the biologically inactive parts of the pill remain intact during its voyage through the gastrointestinal tract and are eliminated in the faeces as an insoluble shell.

Implant-Body Chemical Communication through Diffusion. For biological systems, chemical communication is the exchange of solutes between cells, tissues, organs, and implanted devices. These solutes can either be nutrients/waste for cellular metabolism or chemical signals that elicit a specific biological response, such as drugs and hormones. In biological systems, there is some point at which the process is diffusive. Hence, an understanding of the native diffusion barriers that are found in localized tissue is required to understand what variables are important in the control of the transport rate.

To describe the diffusion of a solute to the circulatory system, it is beneficial to divide the process into two parts, diffusion in the bulk tissue and diffusion through the vessel wall. Tissue diffusion is usually modeled as the diffusion of a porous media. The density of the extra-cellular matrix (ECM) proteins, cellular bodies and their orientation regulates the diffusivity. These bodies can act in two main ways. First, they can take up the diffusing solute, either degrading it or imparting their own diffusive limitations which will result in decreased release. Or, these cells act to block diffusion and increase the path tortuosity. As a result, the diffusivity of the tissue decreases as the tissue proteins and cell bodies become more tightly packed.

Once a solute reaches the blood vessel, the transport into the blood stream is dictated by the permeability of the vessel wall. Primarily the total surface area of the vessels within the tissue and the permeability of the vessel wall regulate this transport. The total surface area is a function of the diameter and the density of the vessels within the tissue. Vessel permeability is dynamic and determined by the balance of signaling proteins in the vicinity. For instance, an increase in vascular endothelial growth factor (VEGF) has proved to increase permeability while an increase in Angiostatin-1 (ANG-1) decreases vessel permeability.

Based upon this description of solute transport from implant to circulatory system, a loose connective tissue with high vascularity and vessel permeability would provide the fastest route for systemic delivery. It may be possible to remodel the tissue surrounding the implant by applying tissue engineering techniques. This work may have implications which can extend to key difficulties being faced in tissue engineering.

1.7. Aggregation of amphiphilic block-copolymers in aqueous media

Amphiphilic block-copolymers, which are hydrophobic and hydrophilic blocks covalently linked together, can be considered macromolecular analogues of low molecular weight surfactants, and are usually referred as superamphiphiles. Mainly, the relative length of the blocks determines the assembly behavior in selective solvents. It has been found that the formation of different morphologies is a function of total and relative block lengths, temperature, block (chemical) composition, type of solvent, and concentration among other variables.

One special feature of block-copolymer chemistry is that it enables to change the chemical composition, length, and structure of the constituting blocks in order to tune the association characteristics and thus the obtained morphologies. Moreover, by playing with the architecture of the blocks different mesophases can be achieved as depicted in Fig. 1-12. At low solvent concentrations spherical micelles, rod-like micelles, and vesicles can form, whereas at higher concentration lyotropic liquid crystalline phases are encountered.

Although it is broadly accepted that an aqueous medium is a prerequisite for the self-aggregation of low molecular weight amphiphiles into superstructures, this is not necessarily the case for block-copolymer amphiphiles. Many examples have been presented in which aggregation takes place in other solvents than water. Nevertheless, the aggregates formed in aqueous solutions

still pose the main interest since they closely resemble biological systems. Systems based on organic solvent will also be further discussed here.

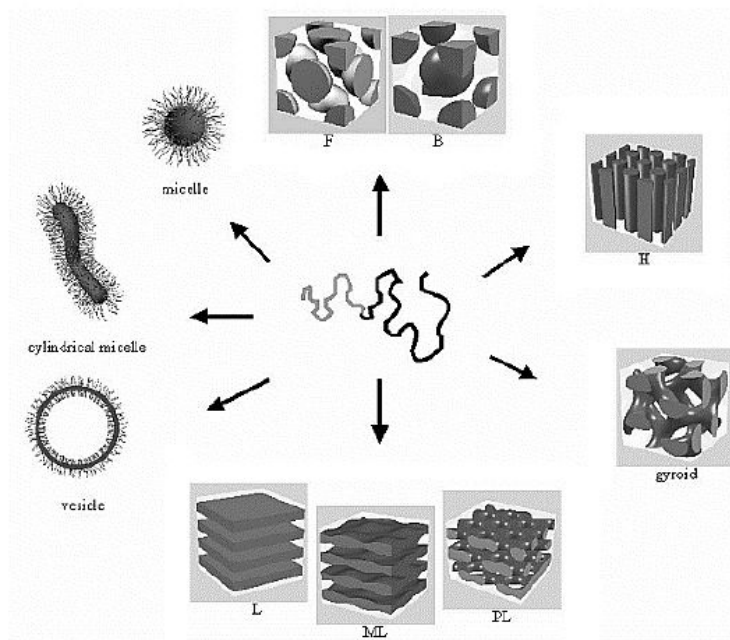


Fig. 1-12. Morphologies of block-copolymer aggregates found in aqueous media.

In the context of micro and nanocarriers, the most interesting superstructures obtained from block copolymers in solution are micelles and vesicles. The individual block-copolymers constituting these aggregates are termed unimers. By thermodynamic considerations, the unimers are in equilibrium with the aggregates in solution, and the aggregates form above what is known as critical aggregation concentration (CAC). Although dictated by thermodynamics, self-assembled structures can and are often kinetically stabilized, that is, shapes, which are not equilibrium ones can be found since they are kinetically trapped.

Micelles

Simple micelles are aggregates with a core-shell structure, occurring in a given concentration range. In aqueous solutions, micellisation results from the selective solubilisation of the shell-forming block, whereas the core is formed by the hydrophobic non-soluble block. Micelles form above what is known as the critical micelle concentration (CMC) and are dynamic systems.

Physical aspects of surfactants and micelles. Surfactants are often used to stabilize microemulsion, emulsion, and suspension systems into which drugs are dissolved. Surfactants decrease the surface tension of multicomponent systems. Thus, the measurement of surface tension is a means to determine the properties of micelles and to understand their effect on solubility, fluid flow, and membrane transport (Fig. 1-13).

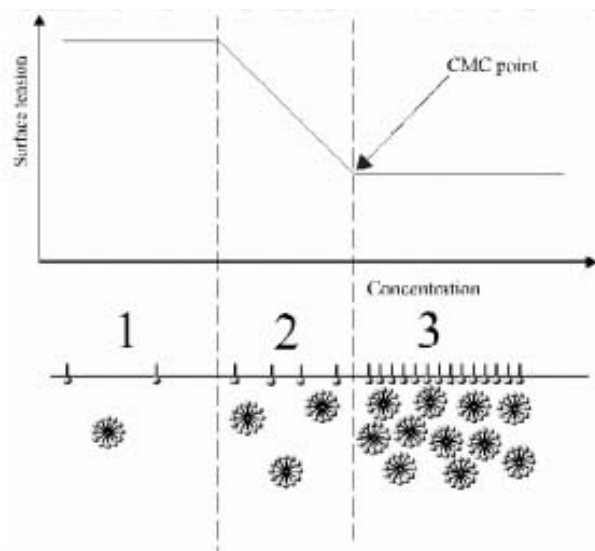


Fig. 1-13. Use of surface tension measurement to determine the CMC
http://chsfpc5.chem.ncsu.edu/~franzen/CH795I/lectures/drug_delivery/sld001.htm.

The slower dynamics of the constituent blocks makes block-copolymer micelles more stable systems compared to lipidic micelles. Intermicellar chain exchange is mainly a function of the type of blocks, i.e. their relative polarity, the overall chain length, and relative block lengths, and can be tailored to be very slow in contrast to lipid micelles, by using blocks with low glass transition temperature (T_g). Also in contrast to aggregates formed from low molecular weight surfactants, self-assembled structures based on block-copolymers show higher structural stability, and have a much lower CAC.

Depending on the asymmetry of the constituting diblocks, the micellar structures can be classified as crew-cut micelles and star micelles. In crew-cut micelles the relative long blocks form the core where the short ones constitute the corona, whereas star micelles have their cores filled with the short hydrophobic chains, and coronas formed by the long hydrophilic ones (Fig. 1-14 c). In the case of triblocks having a hydrophobic middle block, normal micelles form, whereas for triblocks with hydrophobic side chains, flower-like micelles are observed (Fig. 1-14 b). The latter consist of a core of B blocks surrounded by loops of A blocks.

Diblock-copolymers with long hydrophilic chains tend to form micellar aggregates due to the highly positive curvature of the interface. As the length of the insoluble block increases, the curvature decreases and a transition to rod-like micelles is observed. If the length of the insoluble block increases further then lamellar phases are favored. Depending on the concentration stacked lamella or vesicular structures can be formed.

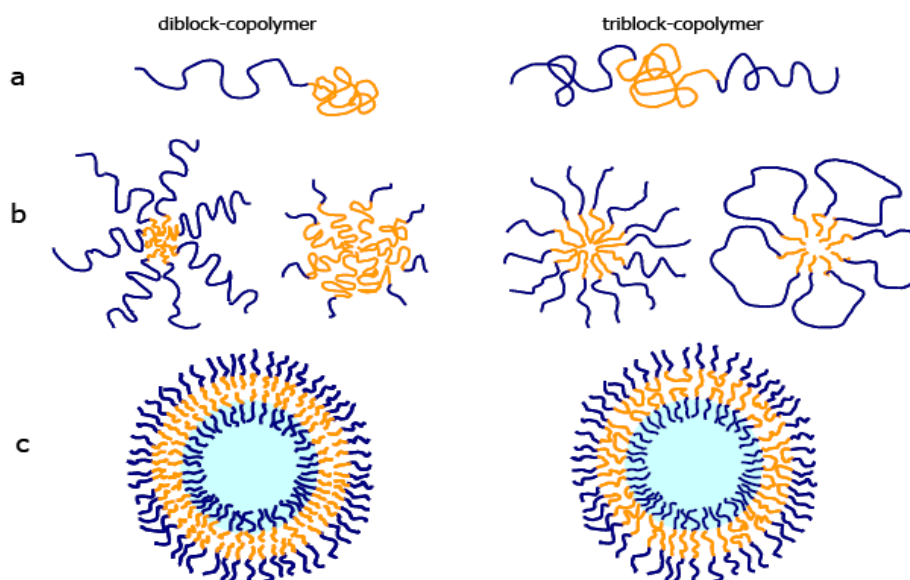


Fig. 1-14. a) unimers in solution, di- and triblock respectively b) star and crew cut micelles for a diblock-copolymer, and normal (ABA) and flower-like (BAB) micelles for a symmetric triblock-copolymer, c) vesicle formation for a diblock and triblock-copolymer respectively.

Vesicles

Vesicular structures are particularly interesting since they are straightforward encapsulation devices, can be used as transport systems, protection devices for labile substances, and nanoreactors, to perform localized chemical reactions at the nanometer level. Vesicles, in the case of lipids, consist of a closed spherical bilayer. Diblock-copolymer vesicles also form closed hollowspherical aggregates with bilayer walls, whereas triblock-copolymers self-assemble into vesicles with a more complex association, such as bilayer and stretched or spanning polymers in the membrane (Fig. 1-14 c). The formation of vesicles from block-copolymers was broadly reviewed.

Polymer vesicles are known for their higher stability and toughness when compared to liposomes. For liposomes leakage of encapsulated substances is related to the fluidity of the lipid bilayer. In this respect, polymer vesicles are more versatile since their fluidity properties can be tailored by tuning the glass transition temperature of the constituting blocks.

At this point it must be noted that when the constituents are synthetic or natural lipids, the resulting structures are preferentially termed liposomes. The term vesicle, which is more general, includes not only lipidic vesicles but also synthetic surfactants and amphiphilic polymers. As the field broadens new terminology emerges. For instance, vesicular structures obtained from peptidic polymers were termed peptosomes, whereas the term polymersomes has been used in relationship to vesicles consisting of polymers.

1.8. Polymeric containers

Since amphiphilic polymers can form vesicles with a small pool of water inside, they can be regarded as micro and nanocontainers. The separation from the outer medium is achieved with the polymer membrane. Two important parameters of the membranes are their permeability and their stability. The advantage of synthetic block-copolymers as the building blocks of these containers is their higher stability over lipids, due to the increased length, conformational freedom, and slower dynamics of the underlying polymers. The thickness of the membrane can be tuned by the nature and length of the hydrophobic chains of the constituting polymers. Additional stability can be obtained by cross-linking the aggregates, thus, freezing their structures achieving solid-state properties. However, this further reduces the permeability of such capsules.

The micro and nanocontainers comprised solely of block-copolymers show a rather low permeability. For practical purposes, an ideal system would be one that is stable enough to resist handling and diverse technological steps, while at the same time being permeable enough to allow encapsulation and release at will, that is, a switchable or tunable system. This can be achieved, for instance, as already demonstrated, by the incorporation of pore proteins in the artificial polymer membrane, such as encountered in cell membranes. Some approaches to regulate the permeability can be triggered by temperature or pH changes. These tunable systems would for example change their conformation depending on one of these parameters.

One can further functionalize these containers by introducing a plethora of functional groups or molecules in different regions of the vesicular structure. For instance, hydrophobic molecules can be buried within the hydrophobic layer of the membrane. Amphiphilic molecules can be anchored by a long apolar chain inserted into the hydrophobic layer, and therefore present the polar heads on the surface of the vesicle (Fig. 1-15).

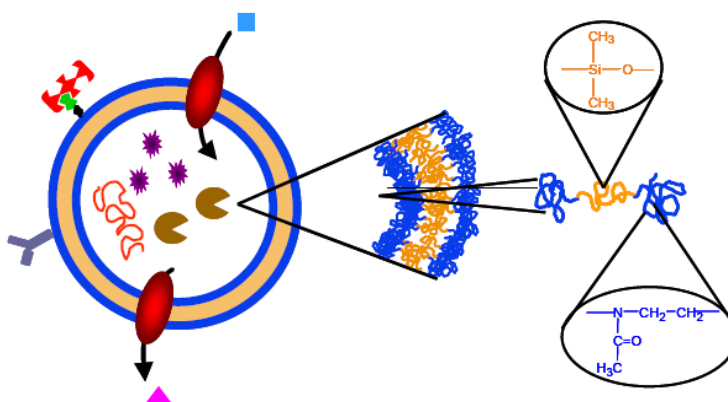


Fig. 1-15. Constitution of some containers and the multiple modifications possible.

Furthermore, hydrophilic molecules can be encapsulated in the inner water pool of the vesicle or can be bound to their inner or outer surface. The most stable way to attach a molecule

to the surface of vesicles is by covalent bonding. This often requires harsh conditions or organic solvents when high yields are desired, which can disturb or destroy the aggregates. To overcome this, one can functionalize the assembling molecules or unimers prior to aggregation. This approach might be useful only for the attachment of low molecular weight molecules, since steric hindrance might disturb the aggregation process when higher molecular weight molecules are anchored to the assembling polymer.

1.9. Tissue Engineering

Biotechnology is contributing to advances in drug delivery through drug, gene and protein discovery, and the resulting knowledge of human biological systems. This enables researchers to create synthetic systems that mimic the already existing biological processes in the body. Also, as researchers learn more about certain diseases, they can discover drug delivery targets that are more specific to the particular disease.

The current development of delivery systems as well as methods of administration is the result of chemical, technical, and biological advances and the subsequent understanding of the body.

Encapsulation of labile molecules is an important technology field found in many areas of chemistry, pharmaceuticals, and biotechnology. Different strategies have been developed and the use for this purpose of microspheres, microcapsules, and liposomes is well established. Nevertheless, it is still a challenge for scientists to design and to fabricate micro- and nanocontainers for various substances with the desired storage, release, and stability properties required for each specific application, therefore this research field is in constant activity. One of the most investigated topics within encapsulation technology is the use of micro- and nanocapsules and particles for drug delivery.

The goal of tissue engineering is to repair an existing tissue/organ or completely regenerate a tissue/organ that has failed to function. In order to achieve this, there are two main strategies currently being pursued.

One method is the *in vitro* regeneration of a tissue/organ from primary cells obtained by the patient, and the subsequent reimplantation of the newly generated tissue.

The other technique is to implant a device that would temporarily provide or assist the functions of the organ/tissue being replaced, while simultaneously allowing the *in situ* formation of a new organ/tissue. Both of these strategies require a biomaterial scaffold, which organizes the growth of cells into the proper configuration to form the desired tissue, and are limited by the depth of cellular penetration into the porous networks. It is believed that this limitation is directly related to the depth of penetration of the vascular which penetrates the scaffolding. Without capillaries being fully extended throughout the scaffold, deeper cells will not be able to achieve the required nutrient/waste exchange rates. In order to specifically select vessel growth, an understanding of the capillary growth physiological pathways is needed.

1.10. Angiogenesis concept

Generalities

Angiogenesis is a physiological process involving the growth of new blood vessels from pre-existing vessels. Though there has been some debate over this, *vasculogenesis* is the term used for spontaneous blood-vessel formation, and *intussusception* is the term for new blood vessel formation by splitting off existing ones.

Angiogenesis is a normal process in growth and development, as well as in wound healing. However, this is also a fundamental step in the transition of tumors from a dormant state to a malignant state.

Cancer cells are cells that have lost control of their ability to divide in a controlled fashion. A tumor consists of a population of rapidly dividing and growing cancer cells. Mutations rapidly accrue within the population. These mutations (variations) allow the cancer cells (or sub-populations of cancer cells within a tumor) to develop drug resistance and escape therapy (Fig. 1-16). Tumors cannot grow beyond a certain size, generally 1-2 mm³, due to a lack of oxygen and other essential nutrients.

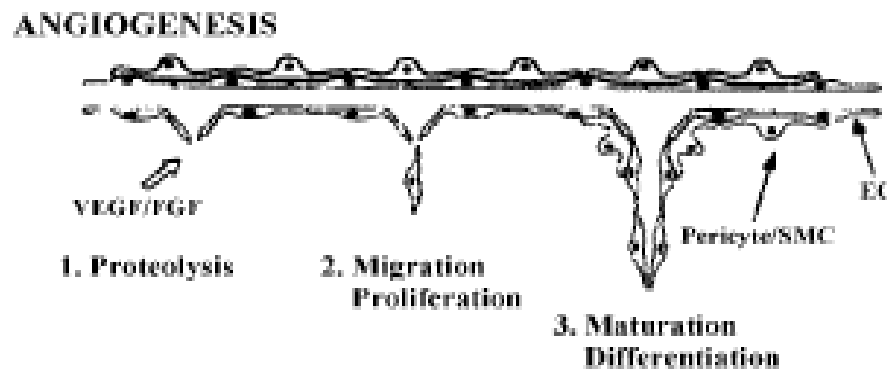


Fig. 1-16. Growth of a capillary during angiogenesis (Dziubla, 2003).

Tumors induce blood vessel growth (angiogenesis) by secreting various growth factors (e.g. Vascular Endothelial Growth Factor or VEGF). Growth factors, such as bFGF and VEGF can induce capillary growth into the tumor, which some researchers suspect supply required nutrients - allowing for tumor expansion. Other clinicians believe that angiogenesis really serves as a waste pathway, taking away the biological end products put out by rapidly dividing cancer cells. In either case, angiogenesis is a necessary and required step for transition from a small harmless cluster of cells, often said to be about the size of the metal ball at the end of a ball-point pen, to a large tumor. Angiogenesis is also required for the spread of a tumor, or metastasis. Single cancer cells can break away from an established solid tumor, enter the blood vessel, and be carried to a distant site, where they can implant and begin the growth of a secondary tumor. Evidence now suggests that the blood vessel in a given solid tumor may in fact be mosaic vessels, comprised of endothelial

cells and tumor cells. This mosaicity allows for substantial shedding of tumor cells into the vasculature. The subsequent growth of such metastases will also require a supply of nutrients and oxygen or a waste disposal pathway.

Endothelial cells have long been considered genetically more stable than cancer cells. This genomic stability confers an advantage to targeting endothelial cells using antiangiogenic therapy, compared to chemotherapy directed at cancer cells, which rapidly mutate and acquire 'drug resistance' to treatment. For this reason, endothelial cells are thought to be an ideal target for therapies directed against them. Klagsbrun et. al. have shown that endothelial cells growing within tumors do carry genetic abnormalities. Thus, tumor vessels have the theoretical potential for developing acquired resistance to drugs. This is a new area of angiogenesis research being actively pursued.

Angiogenesis research is a cutting edge field in cancer research, and recent evidence also suggests that traditional therapies, such as radiation therapy, may actually work in part by targeting the genomically stable endothelial cell compartment, rather than the genomically unstable tumor cell compartment. New blood vessel formation is a relatively fragile process, subject to disruptive interference at several levels. In short, the therapy is the selection agent which is being used to kill a cell compartment. Tumor cells evolve resistance rapidly due to rapid generation time (days) and genomic instability (variation), whereas endothelial cells are a good target because of a long generation time (months) and genomic stability (low variation).

This is an example of selection in action at the cellular level, using a selection pressure to target and differentiate between varying populations of cells. The end result is the extinction of one species or population of cells (endothelial cells), followed by the collapse of the ecosystem (the tumor) due either to nutrient deprivation or self-pollution from the destruction of necessary waste pathways (Fig. 1-17).

Many of the factors involved in vasculogenesis play a crucial role in angiogenesis. There are a host of signals/factors that seem to initiate the angiogenic response, however not all of these signal cascades are understood. It is believed that VEGF and ANG1/ANG2 play a part in most cases of vascular remodeling, and is depicted in figure 18. A start signal is released into the ECM when an area in the body needs to remodel its vasculature. This need can arise in situations such as wound healing, hypoxic tissue, or a tumor induced event. This start signal is either VEGF or ANG2 directly, or signals that induce the release of VEGF/ANG2. When ANG2 hits the TIE2 receptor, it inhibits ANG1 ability to maintain vessel integrity. Hence, the vessel becomes locally unstable. The basement membrane surrounding the blood vessel is digested, the pericytes recede, and if no other signal is present the local endothelial cells will undergo apoptosis. This is believed to be the way the body will digest unneeded vasculature. However, if VEGF is present during this time, the endothelial cells will start migrating chemotaxically toward increasing VEGF.

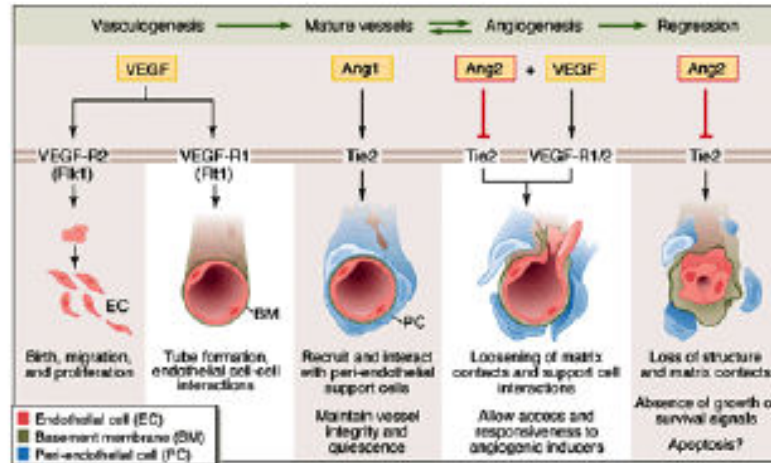


Fig. 1-17. Endothelial cell response to VEGF and ANG1/ANG2 during vasculogenesis and angiogenesis (Dziubla, 2003).

These leading cells do not usually proliferate; rather the endothelial cells that follow will divide and align along the space created by the leading cells to form a lumen. The cells form tube-like structures, which resemble budding blood vessels. These sprouts, the budding vessels, continue to grow until they reach another sprout, and the link to form a functioning capillary. This linking behavior is termed anastomosis. Over time as the ANG2 signal is diminished, the greater concentration of ANG1 allows for the reactivation of the TIE2 receptor, which allows the endothelial cells to call for the support of the pericytes to stabilize these newly formed vessels. It is believed that it is this continual balance of signals, which controls the maintenance, and remodeling of adult vasculature.

Angiogenesis Design

Angiogenesis is an orchestration of complex pro and anti angiogenic regulators, growth kinetics, and adhesion proteins. Events at molecular, cellular, and tissue level all play a part into the final structure of the newly formed vasculature. For this reason, it is difficult to obtain a full understanding of this process through experiment alone. Mathematical modeling of angiogenesis can provide some useful insights into the viability of vessel growth theories and what factors are most likely dominant. The angiogenesis models that have been proposed can be grouped into two main classes of models, continuous models and cellular automata.

In continuous models, contributing factors are expressed explicitly in a series of non-linear PDEs in order to describe the movement and growth of endothelial cells. One of the first descriptions of this type for angiogenesis was by Edelman, where filament and sprout tip densities were described as continuum variables. Terms were also included to allow for branching, anastomosis, and death. Baldwin and McElwain adopted this approach to look at tumor induced angiogenesis. This time, sprout tips chemotactically moved toward a tumor angiogenesis factor

(TAF). In this model, TAF consumption by the migrating endothelial cells was ignored. The most recent model is that of Anderson et al.

$$\frac{\partial n}{\partial t} = D\nabla^2 n - \nabla \cdot (\chi(c)n\nabla c) - \nabla \cdot (\rho n\nabla f) \quad (3)$$

$$\frac{\partial f}{\partial t} = \beta f(1-f)n - \gamma f \quad (4)$$

$$\frac{\partial c}{\partial t} = -\eta mc \quad (5)$$

$$\chi(c) = \frac{\chi_0}{1+ac} \quad (6)$$

In this series of equations, n is the endothelial cell density, D the endothelial cell diffusivity, χ the chemotactic function, c the TAF concentration, ρ the hepatotoxic constant, and f the adhesion protein density. β , γ , and η are positive, scaled parameters.

Equation (3) describes the change in endothelial cell density by typical Fickian diffusion, chemotactic directed and hepatotoxic directed motion. Hepatotoxicity is the tendency of endothelial cells to move in the direction of increasing adhesion protein concentrations. Equation (4) accounts for the endothelial cells tendency to remodel the ECM by simultaneously digesting and secreting adhesion proteins. Also, equation (5) is used to describe growth factor consumption by endothelial cells. As most cells, endothelial cells are limited in their sensitivity to growth factor concentrations.

Any additional amount of growth factor beyond a certain value will have no increasing affect on the chemotaxis of the migrating cells. Equation (6) mathematically describes this limiting behavior. This model is currently the most extensive in its attempt to include many different aspects of angiogenesis.

This extensive nature leads to the inclusion of many curve fitting parameters that bring into question the validity of the model. There are some problems inherent in using continuous models to describe angiogenesis. Since endothelial cells are discrete entities, the use of continuum variables to describe endothelial cells is highly suspect. The definition of the derivative does not apply. Moreover, due to the non-linear nature of these models, explicit solutions are difficult to obtain and finite element method or other numerical solution techniques must be employed. Finally, continuous models are only able to provide statistical trends in cell migration and growth factor concentrations. These models are not able to explicitly demonstrate the growth of vascular networks.

Cellular automata, while not an explicit model, can reproduce many complex phenomena shown by the use of simple rules. Cellular automata, originally created by Von Neumann, are a grid of many cells that can possess discrete values dictated by simple rules. With each step, the state of

every cell is calculated, and the time course of development can be plotted. One of the first and probably most popular cellular automata was developed by John Conway, and is most commonly called "Conway's Game of Life". In this automation, a cell is either alive or dead. If there are two or three live cells near a neighboring cell, then that cell stays alive, otherwise that cell becomes dead. If three live cells surround a dead cell, then the dead cell becomes live. When these rules are repeated over many iterations, complex patterns emerge that resemble patterns of growth and migration seen in nature. By altering the rules that control the automation, it may be possible to elucidate the underlying factors that are involved in many biological processes.

Cellular automata can be divided into three main categories; Eulerian, lattice gases, and solidification models. In Eulerian models, every cell can possess many discrete states, and the state of each cell is dependant upon its previous state and the state of the neighboring cells. This is the type that was evident in the game of life model. In lattice gases, solid particles move around and interact with other particles. In this class, turbulent behavior of gases in complex geometries have been described where more through Navier-Stokes evaluations would have been time-limiting. Finally, solidification models are used to describe events such as crystallization. Moving particles can be irreversibly bound to a lattice point, or cells undergo irreversible changes.

Markus et al. used this final class of models to describe vessel morphogenesis as a sequential series of irreversible steps.

Cellular automata have been applied to simulate the formation of vessel structures in angiogenesis. The rules governing these simulations have been based on both geometric and biological mechanisms. For example, due to the similarities between fractal structures and vessel networks, some groups have based their vessel growth on events such as crystallizations. Other groups have confined the growth of vessel to the migration of the vessel tip (since the forming blood vessel is dependant upon this leading cell). These models use the discretized PDEs to describe probability fields for the neighboring cells of sprout tips. The models work off an Eulerian based cellular automata. At every time point, the change of each cell's sprout tip density is calculated. This change is used to create an array of probabilities that dictate which simulation cell space the sprout tip will move to next (or if it will stay stationary). Then a random number is generated, and the sprout tip moves accordingly. While this method is highly dependant upon the scaled values assumed by the PDE equations, and the time steps selected, these models are capable of recreating the vessel growth, branching and brush tip disorganization of vessels that is commonly seen in tumor-induced angiogenesis.

Effects of Extracellular Matrix Ligands in Angiogenesis

While not discussed in most descriptions of angiogenesis, proteins adhesion play a crucial role in the formation of new blood vessels. The reason for this omission is due to the extensive availability of proteins adhesion in normal extracellular matrix. The basement membrane that surrounds blood vessels is comprised primarily of collagen IV and laminin. There have been many studies that evaluate the *in vitro* and *in vivo* ability of the endothelial cells to form tubules in and

on different membrane proteins. The results of these studies were highly dependant upon variables such as cell type, whether it was a 2D or 3D matrix study, or if the studies were handled *in vivo*. For example, Dvorak demonstrated that collagen I implanted subcutaneous did not induce vascularization, while Hoying et al. showed that the vascular fragments seeded onto collagen I matrices provided vascular growth in 1 week. In spite of these irregularities, one general trend observed is tubule formation occurred most rapidly when in the presence of collagen IV and laminin. It is believed that observed complex behavior is a result of cross-talk that exists between adhesion integrins and growth factor receptors expressed on the endothelial cell surface. Integrins are cell receptor proteins comprised of two subunits, alpha and beta.

There are currently 8 known adhesion integrins that are expressed on most endothelial cells, $\alpha 1\beta 1$, $\alpha 2\beta 1$, $\alpha 3\beta 1$, $\alpha 5\beta 1$, $\alpha 6\beta 1$, $\alpha v\beta 3$, and $\alpha v\beta 5$. It was found that in *in vitro* settings, $\alpha 2\beta 1$ interaction was crucial in the tubule formation in collagen matrices, where as the $\alpha v\beta 3$, and $\alpha 5\beta 1$ integrins were necessary in fibrin matrices. Moreover, in studies where $\alpha v\beta 3$ was ligated, migration on fibronectin (a process mediated by $\alpha 5\beta 1$) was inhibited. The converse effect was also true. Further evidence of cross-talk exists in the work of Friedlander, who demonstrated that when $\alpha v\beta 3$ was blocked, fibroblast growth factor induced angiogenesis was inhibited, but not VEGF angiogenesis. Where as when $\alpha v\beta 5$ was blocked, the reverse was true.

Tissue-Implant Interactions

Classic Foreign Body Response. Implants are foreign bodies that will invoke the natural defense mechanism against such intrusions; the inflammatory response. This process is outlined in Fig. 1-18. Typically the inflammatory response is split into two categories, acute and chronic inflammation. During the acute phase, an influx of fluid, plasma proteins, and neutrophils enter the wound/implant site. These neutrophils accumulate at the site of implantation and start to phagocytize any small debris/bacteria that are present. Phagocytosis is activated when the neutrophils comes into contact with activating factors called opsonins. If an implant surface absorbs opsonins, such as the antibody immunoglobulin G (IgG), the neutrophil will try to engulf the implant. But since there is a large size disparity between the implant and neutrophils, phagocytosis cannot occur. This leads to an event known as frustrated phagocytosis, where the neutrophils dump the contents of lysosomes into the ECM.

This process is highly unfavorable since it is very irritating to the surrounding tissue and leads to chronic inflammation. After the neutrophils have entered the area and cleared away any debris, granulation tissue (highly vascularized tissue) begins to form, and the natural wound healing response continues. At this point the response can split into either a chronic inflammatory response or a foreign body reaction of the acute type. If there is a constant chemical or physical irritation (as in free movement of the implant), the chronic inflammatory response will occur.

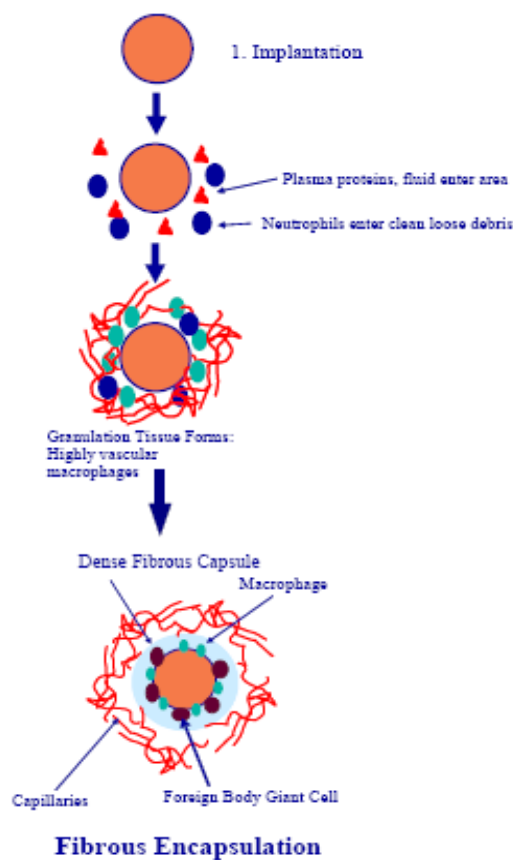


Fig. 1-18. Classic foreign body response typically ends with the surrounding of an implant with a dense fibrous layer called the fibrous capsule (Dziubla, 2003).

If there are no negative chemical or physical signals then classic foreign body response occurs. Typically, the foreign body response results in 3 characteristic layers. A primary layer of macrophages and/or foreign body giant cell formations surrounds the implant. These cells secrete the second layer composed of dense fibrous tissue 30-100 μm in thickness. A third layer of granulation tissue surrounds this fibrous wall. This response is indefinitely stable except for a decrease in cellularity of the primary layer. The dense nature of the fibrous layer greatly impedes the diffusion of most chemical species, as a result prevents any implanted drug delivery device from functioning effectively.

Tissue Response to Porous Materials. The tissue response changes greatly when the implanted material has a porous morphology. Brauker et al. published a paper demonstrating the ability of porous materials to remodel the tissue response. They subcutaneously implanted several hydrophobic materials (PTFE, cellulose acetate, cellulose esters, and acrylic copolymers) with pore sizes ranging from 0.2 to 15 μm . It was found that materials with pores greater than 5 μ were surrounded by highly vascular loose connective tissue. When the pore sizes further increased, evidence of vascular penetration was evident (Fig. 1-19).

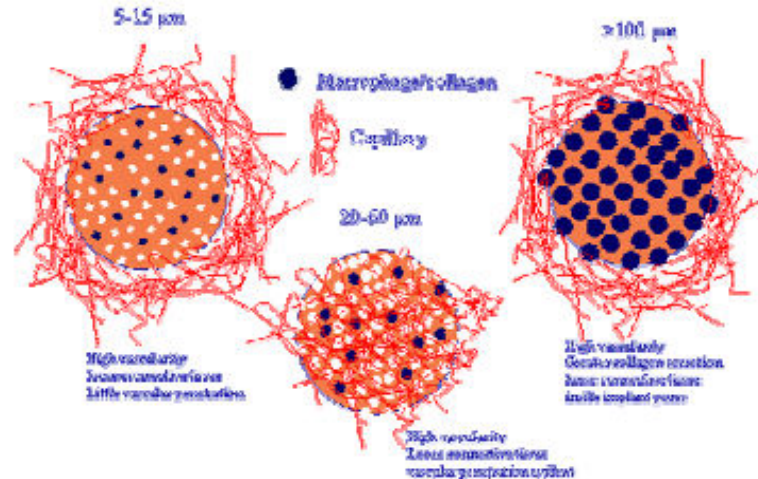


Fig. 1-19. Vascularised tissue response to implants with varying pore sizes (Dziubla, 2003).

The astonishing part of the study was that this vasculature persisted for the entire duration of the study, 1 year. Shwarkawy et al. studied acetylated PVA with pore sizes 5, 60, and 200 μm . Their 5-micron pore size corroborated the results obtained by Brauker et al. However, they noted a very high degree of vascularization of implants with the 60 μm pore size, and when this pore size increased beyond 100 μm , the vascularity of the materials actually decreased.

Shwarkawy also demonstrated that changes in pore size not only effected vascular density but also the response to systemic uptake of drug through a vascularized implant. It was demonstrated that the 60 μm pore material delivered the drug in almost half the time it took for a subcutaneous injection to be taken up systemically. This is due to the increased vascular density as well as increased vascular permeability at these pore sizes.

There are two main theories that have been proposed to describe the dependence of vascular penetration on implant pore size. Padera and Colton have suggested that it is the macrophages degree of attachment onto the material surface that dictates the signals that they send out. When the macrophages are able to spread onto the surface of the material, they release signals that call for the deposition of the tight collagen layer. When these macrophages penetrate into a porous sample, and cannot spread fully on the surface, this signal is not released or released to a reduced extent. However, due to the macrophages being further from a nutrient source, they release signals that initiate angiogenesis. When the macrophages penetrate into the very large pores, they are able to once again release the collagen deposition signals, and the pores become filled with the avascular collagen layer that typically surrounds a nonporous implant.

Rosengren has suggested that it may be implant mobility that controls the degree of implant vascularity. They suggest that smooth implants are capable of high relative motion. This motion shears the adjacent cells inducing necrosis. The degree of necrosis is the cause of the severity of the inflammatory response, hence the thickness of the fibrous capsule. They further suggest that porous materials possess little to no fibrous capsule, because the tissue that

penetrates works to stabilize the relative motion. While it is still not known whether or not these hypotheses are correct or to what degree they are important, it is evident that simple morphological changes have a great effect upon the vascularization of implants.

Chemical vs. Physical Effects. Many of the porous implant studies compared the results of materials with varying surface chemistries. These studies looked at materials of varied hydrophilicity, such as hydrophobic PTFE, and acetylated PVA, to the more hydrophilic cellulose esters and acetates and poly(vinyl alcohol)s. It was found that the ingrowth of vascularized and loose connective tissue was dictated primarily by the pore size rather than chemical properties of the material. However, it would be wrong to assume that no control could be obtained through modifications of the implant surface chemistry. Endothelial cells interact with the ECM through adhesion moieties called integrins. It is believed that cells attach onto synthetic materials through intermediary proteins, such as fibrin, which absorb onto polymer surfaces.

Hence, by changing the protein absorption properties of surfaces, it is possible to alter the adhesion of endothelial cells. Moreover, it is also possible to bind specific adhesion ligands onto surfaces for a more direct control of the cellular attachment. Endothelial cells are able to adhere to the common attachment sequences that are found on fibrin, such as RGD and YISGR. It was found, however, that another adhesion peptide sequence, the RDEV ligand, preferentially bound endothelial cells over fibroblasts, smooth muscle cells, or activated platelets. Through this ligand, it may be possible to explicitly control the formation of capillaries into the implant. Tube formation of the endothelial cells is an essential characteristic for the formation of capillaries, and is controlled by both chemical and physical properties of the material. There has been a significant lack of *in vitro* research showing the effects of synthetic biomaterials on endothelial cell's ability for tube formation. One study coated fibronectin in 10 and 30 μ m stripes. They noted that tube formation occurred on the 10 μ m stripes but not the 30. This study demonstrates the general trend of tube formation that the more adherent the cells are to a surface, the more they spread and are less likely to express tube formation. Also, cells with greater spreading (attachment) exhibited increased proliferation, yet a decrease in cellular mobility. Moreover, tube formation was most prominent in surfaces that exhibited moderate adhesive characteristics. There is also evidence that material stiffness also plays a part on tube formation. Ingber et al. showed that softer, more malleable materials exhibited an increase in cell tube formation.

1.11. General concept of drug delivery

There are several ways to solve the delivery problem, but it requires collaboration among chemists, physiologists, and biomedical engineers. Materials scientists look for new materials and ways to manipulate existing ones in order to fulfil unmet needs.

In the context of drug delivery, the need for materials can generally be broken into two categories: the creation of new materials and better understanding of how to manipulate existing materials.

In both cases and in whatever route of administration, "you go to the unmet needs". The unmet needs lead to where materials can do something. Current needs include reducing the toxicity of drugs, increasing their absorption, and improving their release profile.

In one fertile area of research, scientists are tailoring polymers to address those needs. They are using long-standing polymers like poly(ethylene glycol) (PEG) and newer types like dendrimers. And they are forming polymeric micelles and using polymer-drug conjugates as prodrugs, polymeric carriers for anticancer agents or particles for gene delivery or scaffolds for cell delivery and tissue engineering.

One area that researchers have particularly been focusing on is the delivery of anticancer agents. Polymers have already been shown to form effective delivery systems for localized treatment of cancer.

Polymer carriers have several advantages over other delivery methods such as liposomes and antibodies. Because liposomes (spherical vesicles made of phospholipids) are particles, they get taken up by macrophages. High levels can be found in the liver and spleen, even when the liposomes are given "stealth" characteristics by coating them with PEG. In addition, stealth liposomes have other side effects, such as extravasations, in which the liposome moves from the blood vessel into tissue where it is not wanted. Antibodies, meanwhile, have the disadvantage that most receptors on tumour cells are also present on normal cells, making it hard to find ones that are unique to cancer.

In contrast, polymers allow us to work with a single molecule rather than a large particle. We can choose a material which doesn't go to the liver and the spleen and to which we can bind an anticancer agent using a linkage designed to be more specifically clipped at the tumour tissue. It's in effect a macromolecular prodrug.

Another advantage of polymers is that the linkage can be designed to control where and when the drug is released.

Like many others, we considered the fact that new blood vessels in tumours are "leaky" to passively target tumours. Because tumour blood vessels are more permeable than blood vessels in other tissue, drugs enter tumour tissue fairly easily. This effect, known as the **enhanced permeability and retention effect** (EPR), was first discovered by Hiroshi Maeda of the University of Kumamoto in Japan in 1986.

Recognition capabilities (Fig. 1-20) can be built into drug delivery using molecular imprinting. Monomers polymerise around a template molecule. The template is then removed, leaving a site that will interact selectively with the template. Such a site can be used to trigger drug delivery in response to the presence of a particular compound - for example, insulin in the presence of glucose.

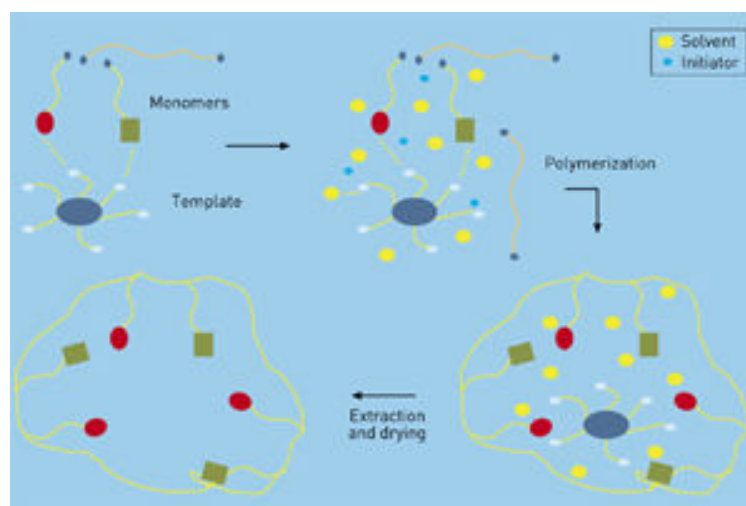


Fig. 1-20. Mechanism of drug recognition (Duncan, 1998).

However, polymer carrier systems also have their disadvantages. Compared to liposomes, which are basically empty vesicles that can be "stuffed full of drug," polymers have a low drug-carrying capacity. The payload that each polymer molecule can carry depends on the number of reactive groups where the drug can be attached.

Basically, the concept behind drug delivery is to provide more constant concentrations in the organism, and to bring the compound with pharmaceutical activity directly to the site of need in order to enhance the effectiveness of action. One way to bring the active substance to the site of action is to modify their bio-distribution by entrapping them in particulate drug carriers such as microspheres, micro and nanocapsules, or liposomes. The need for encapsulation lies in the instability of many drugs, and in some cases it can improve the bioavailability of the therapeutic compounds.

Other reasons for using drug carriers or delivery systems are the poor solubility of some drugs, which may be enhanced by choosing the right carrier. For this, usually micellar systems are used since hydrophobic solutes will solubilize in their cores.

By encapsulating drugs in designed carriers, labile drugs are protected from the hostile conditions that they might encounter for instance at the low pH of the stomach. Furthermore, in many cases adsorption can be enhanced and side effects of therapeutic compounds can be minimized.

Short circulation times in the blood stream due to rapid clearance through uptake by the reticuloendothelial system (RES) might be increased by choosing carriers that are able to avoid the uptake by the RES.

Within the concept of drug delivery two mechanisms must be taken into account to design such carrier systems, sustained or controlled drug delivery and site directed drug delivery. Controlled drug delivery takes place when a polymer, whether natural or synthetic, is combined with a drug or therapeutic agent in such a way that the active agent is released from the material

in a pre-designed fashion. Different profiles for the release of the active substance might be used, for instance, this can be constant over a defined time or cyclic over a time. Additionally, the release can be externally triggered by environmental events.

Site directed or targeted drug delivery occurs when the drug, with the aid of a carrier is delivered to a specific site or organ. Different strategies can be considered, whether the delivery to specific tissues from the circulation is needed or intracellular delivery is required.

Drug delivery based on liposomes

In the past, the interest in liposomes as carriers of molecules was based on their potential to enclose and protect different materials of biological interest and to deliver them, functionally intact and in significant quantities to the interior of many cell types. Nevertheless, in many instances, the use of liposomes proved to be inadequate. The use of liposomes as drug carriers has some limitations, mainly their instability on storage, leading to leaking of the encapsulated material and the easiness of some complement activation leading to recognition by the RES. Two mechanisms are basically used to deliver the substances when using liposomes, a general mechanism of membrane fusion and the more specific receptor mediated endocytosis (Receptor-mediated endocytosis is a process by which cells internalize molecules or viruses. As its name implies, it depends on the interaction of that molecule with a specific binding protein in the cell membrane called a receptor).

By combining liposomes with hydrophilic polymers, more stable systems could be obtained, usually known as Stealth liposomes (Stealth liposomes consist of lipids conjugated with poly(ethylene glycol) (PEG) forming a protecting brush on the surface of the liposomes, and thus repelling the adhesion of proteins to the liposome's surface). In these systems a covalently attached PEG chain minimizes the recognition by the RES and therefore helps prolonging the circulation times. It is not intended to review the vast literature on liposome drug delivery and targeting systems, only some exemplifying references are given. Walde et al. reported an almost exhaustive review on encapsulation with liposomes.

The use of liposomes as carriers for hydrophilic drugs and lipidic micelles for hydrophobic drugs has been one exhaustively explored research area in the field of drug delivery, controlled drug delivery and targeted drug delivery.

Polymer-based drug delivery systems

Since liposomes present some technical limitations, the need to find new and more stable systems increased and new preparation methods for containers were developed. Several systems have been tested within the last decade, mainly consisting of micro and nanospheres. Porous micro and nanoparticles usually show limited encapsulation capacities; in this respect micro or nanocapsules offer a better approach. Block-copolymer micelles and their use as drug vehicles have been also extensively reviewed (Kataoka et al., 2001; Rösler et al., 2001; Kwon and Forrest, 2006). Similar to liposomes, polymeric vesicles could provide a protective environment for labile

molecules to deliver them intact to desired targets. Parameters such as size, surface charge, membrane fluidity and stability, presence of coupling groups on the surface, can be used to design the carrier to be adapted to a wide range of experimental conditions. The use of polymeric carriers for drug delivery brings several advantages, on the one hand the encapsulated substance is protected from degradation, on the other hand processes such as opsonization (one of the first steps in the process by which the body recognizes a foreign body (exogenous protein, molecule, or particle). The immune system produces the proper antibodies or complement proteins (opsonins) which bind to the particle to tag it. Via recognition of the opsonins by the phagocytes, the opsonization process promotes phagocytosis, thus, triggering the immune response) might be avoided or diminished, additionally, targeted delivery might be introduced by using ligands or antibodies.

A range of materials have been employed to control the release of drugs and other active agents. The earliest of these polymers were originally intended for other, nonbiological uses, and were selected because of their desirable physical properties, for example:

- Poly(urethanes) for elasticity;
- Poly(siloxanes) or silicones for insulating ability;
- Poly(methyl methacrylate) for physical strength and transparency;
- Poly(vinyl alcohol) for hydrophilicity and strength;
- Poly(ethylene) for toughness and lack of swelling;
- Poly(vinyl pyrrolidone) for suspension capabilities.

To be successfully used in controlled drug delivery formulations, a material must be chemically inert and free of leachable impurities. It must also have an appropriate physical structure, with minimal undesired aging, and be readily processable. Some of the materials that are currently being used or studied for controlled drug delivery include

- Poly(2-hydroxy ethyl methacrylate);
- Poly(N-vinyl pyrrolidone);
- Poly(methyl methacrylate);
- Poly(vinyl alcohol);
- Poly(acrylic acid);
- Polyacrylamide;
- Poly(ethylene-co-vinyl acetate);
- Poly(ethylene glycol);
- Poly(methacrylic acid).

However, in recent years additional polymers designed primarily for medical applications have entered the arena of controlled release. Many of these materials are designed to degrade within the body, among them:

- Polylactides (PLA);
- Polyglycolides (PGA);
- Poly(lactide-co-glycolides) (PLGA);

- Polyanhydrides;
- Polyorthoesters;
- Polyketals.

They are biodegradable and flexible for applications. Due to these concerns, several new polymers are presently being explored for applications in drug delivery. Some of the new polymers which are in clinical or preclinical development stage are:

- Polyorthoesters (Heller et al., 2000);
- Polyphosphazenes (Allcock, 1994);
- Polyanhydrides (Shieh et al., 1994);
- Polyphosphoesters (Richards et al., 1991).

Originally, polylactides and polyglycolides were used as absorbable suture material, and it was a natural step to work with these polymers in controlled drug delivery systems. The greatest advantage of these degradable polymers is that they are broken down into biologically acceptable molecules that are metabolized and removed from the body via normal metabolic pathways. However, biodegradable materials do produce degradation by-products that must be tolerated with little or no adverse reactions within the biological environment.

Biodegradable polymers can be natural polymers, modified natural polymers, or synthetic polymers.

Natural polymers are called such because they are always biodegradable. Collagen, cellulose, and polysaccharides are examples of natural polymers. For example, collagen has been used for the delivery of protein-based drugs.

Modified natural polymers are natural polymers that are altered in order to suit a particular application. The reason they are modified is that these polymers often take longer to degrade within the body. This problem can be avoided by adding polar functionalities to the polymers. The polar groups are more labile and enhance the degradability of the polymers.

Synthetic polymers have recently been examined for use in drug delivery systems, including polyesters and polyanhydrides.

The very first polymeric controlled-release delivery vaccination systems were developed merely to use a polymer matrix to achieve a desired release profile. Subsequent efforts reduced the size of the spheres from millimetres to microns and used biodegradable polymers like poly(lactic-co-glycolic acid) (PLGA). Progesterone, nitroglycerin, and insulin are a few of the drugs that are currently delivered to the body using polymer-based drug delivery systems. Pharmaceutical coatings, anti-infective applications, and cancer chemotherapeutic drugs are also examples of polymeric drug delivery systems.

Controlled release systems

Controlled release is aimed at obtaining enhanced effectiveness of the therapeutic treatment by minimizing both under- and over-dosing, and it is also known as sustained delivery. A frequently desired feature is to achieve a constant level of drug concentration in the blood

circulation or at the site of action of the substance, with a minimum of intakes per day and a maximum coverage. Usually drug delivery systems that dissolve, degrade, or are readily eliminated are preferred.

Classically three types of processes are involved in the delivery of substances from a carrier system: diffusion, degradation, and swelling followed by diffusion or a combination thereof.

The advantages of sustained delivery systems are mainly the achievement of an optimum concentration, usually for prolonged times, the enhancement of the activity of labile drugs, due to their protection against hostile environments, and the diminishing of side effects due to the reduction of high initial blood concentrations (toxic concentration).

Controlled-release systems can be classified according to the mechanism that controls the release, the most common being diffusion. Diffusion controlled-release takes place when a compound diffuses through the polymer comprising the delivery system.

The type of polymer system dictates whether macroscopic diffusion occurs, which usually takes place in polymer matrices containing pores. On the other hand, diffusion can also occur molecularly among the polymer chains. These types of delivery systems are the simplest ones in the sense that the polymer matrix does not undergo any changes in the body, when this happens the system being known as stimuli-responsive.

More sophisticated features can be introduced in the drug delivery systems in order to obtain systems that might deliver the active substance by responding to changes in the environment.

These systems are then collectively known as environmentally- or stimuli-responsive systems, and can be designed in such a way that they are incapable of releasing the encapsulated material until it is placed in an appropriate biological environment. For instance, swelling-controlled release systems are initially dry and, when in contact with body fluids, will swell. Consequently, in the case of micro and nanospheres, the swelling increases the pore size of the matrix and promotes the diffusion of the active agents into the bulk medium (Fig. 1-21).

Other features of a polymer can be used to externally trigger the swelling, such as changes in pH, temperature, or ionic strength. These systems are usually termed intelligent or environmentally sensitive systems. One additional requirement of these triggered systems is that the structural changes are reversible and repeatable upon additional changes in the external environment.

One subset of this type of release systems makes use of the external trigger in order to deliver their contents in a one-shot fashion, in contrast to swelling which is governed by diffusion. These systems can be actually thought to belong also to site specific delivery systems, since they take advantage of the conditions of the milieu to release drugs where an environmental condition is other than at different sites.

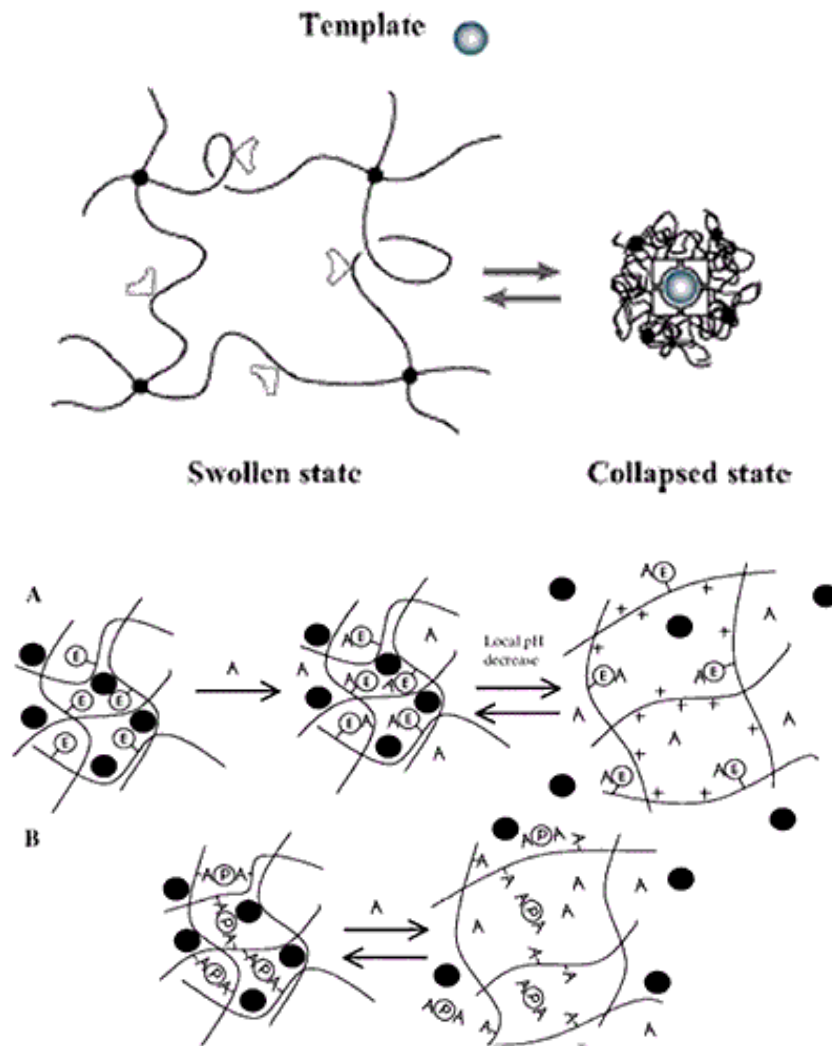


Fig. 1-21. (A) Induced Swelling - the result is ionization, swelling, and release of drug, peptide, or protein; (B) Loss of Effective Cross-links - effective cross-links are reversibly lost and release occurs.

Biodegradable polymers are of great interest since these materials are processed within the body under biological conditions giving degraded sub-units that are easily eliminated by the normal pathways of excretion. In most cases, hydrolysis is the degrading reaction which produces smaller and biologically acceptable by-products. Mainly two types of degradation exist: uniform hydrolysis throughout the matrix and surface degradation, or erosion. The last process results in a release rate that is proportional to the surface area of the particle.

The most commonly used biodegradable polyesters are poly(lactic acid) (PLA) and poly(glycolic acid) (PGA), and especially their copolymers poly(lactic-co-glycolic acid) (PLG), their degradation is controlled by both drug diffusion and polymer erosion. Contrary to this, polyorthoesters show mainly surface-eroding process.

Site specific or Selective targeting

Administration routes. The choice of a delivery route is driven by patient acceptability, the properties of the drug (such as its solubility), access to a disease location, or effectiveness in dealing with the specific disease (Fig. 1-22).



Fig. 1-22. Different administration routes (Mort, 2000).

The most important drug delivery route is the peroral route. An increasing number of drugs are protein- and peptide-based. They offer the greatest potential for more effective therapeutics, but they do not easily cross mucosal surfaces and biological membranes; they are easily denatured or degraded, prone to rapid clearance in the liver and other body tissues and require precise dosing. At present, protein drugs are usually administered by injection, but this route is less pleasant and also poses problems of oscillating blood drug concentrations. So, despite the barriers to successful drug delivery that exist in the gastrointestinal tract (i.e., acid-induced hydrolysis in the stomach, enzymatic degradation throughout the gastrointestinal tract by several proteolytic enzymes, bacterial fermentation in the colon), the peroral route is still the most intensively investigated as it offers advantages of convenience and cheapness of administration, and potential manufacturing cost savings.

Pulmonary delivery is also important and is effected in a variety of ways - via aerosols, metered dose inhaler systems (MDIs), powders (dry powder inhalers, DPIs) and solutions (nebulizers), all of which may contain nanostructures such as liposomes, micelles, nanoparticles and dendrimers. Aerosol products for pulmonary delivery comprise more than 30% of the global drug delivery market. Research into lung delivery is driven by the potential for successful protein and peptide drug delivery, and by the promise of an effective delivery mechanism for gene therapy (for example, in the treatment of cystic fibrosis), as well as the need to replace chlorofluorocarbon propellants in MDIs. Pulmonary drug delivery offers both local targeting for the treatment of respiratory diseases and increasingly appears to be a viable option for the delivery of drugs

systemically. However, the pulmonary delivery of proteins suffers by proteases in the lung, which reduce the overall bioavailability, and by the barrier between capillary blood and alveolar air (air-blood barrier).

Transdermal drug delivery avoids problems such as gastrointestinal irritation, metabolism, variations in delivery rates and interference due to the presence of food. It is also suitable for unconscious patients. The technique is generally non-invasive and aesthetically acceptable, and can be used to provide local delivery over several days. Limitations include slow penetration rates, lack of dosage flexibility and / or precision, and a restriction to relatively low dosage drugs.

Parenteral routes (intravenous, intramuscular, subcutaneous) are very important. The only nanosystems presently in the market (liposomes) are administered intravenously. Nanoscale drug carriers have a great potential for improving the delivery of drugs through nasal and sublingual routes, both of which avoid first-pass metabolism; and for difficult-access ocular, brain and intra-articular cavities. For example, it has been possible to deliver peptides and vaccines systemically, using the nasal route, thanks to the association of the active drug macromolecules with nanoparticles. In addition, there is the possibility of improving the ocular bioavailability of drugs if administered in a colloidal drug carrier.

Trans-tissue and local delivery systems require to be tightly fixed to resected tissues during surgery. The aim is to produce an elevated pharmacological effect, while minimizing systemic, administration-associated toxicity. Trans-tissue systems include: drug-loaded gelatinous gels, which are formed *in situ* and adhere to resected tissues, releasing drugs, proteins or gene-encoding adenoviruses; antibody-fixed gelatinous gels (cytokine barrier) that form a barrier, which, on a target tissue could prevent the permeation of cytokines into that tissue; cell-based delivery, which involves a gene-transduced oral mucosal epithelial cell (OMEC)-implanted sheet; device-directed delivery - a rechargeable drug infusion device that can be attached to the resected site.

Gene delivery is a challenging task in the treatment of genetic disorders. In the case of gene delivery, the plasmid DNA has to be introduced into the target cells, which should get transcribed and the genetic information should ultimately be translated into the corresponding protein. To achieve this goal, a number of hurdles are to be overcome by the gene delivery system. Transfection is affected by: (a) targeting the delivery system to the target cell, (b) transport through the cell membrane, (c) uptake and degradation in the endolysosomes and (d) intracellular trafficking of plasmid DNA to the nucleus.

Drug delivery carriers. Colloidal drug carrier systems such as micellar solutions, vesicle and liquid crystal dispersions, as well as nanoparticle dispersions consisting of small particles of 10–400 nm diameter show great promise as drug delivery systems. When developing these formulations, the goal is to obtain systems with optimized drug loading and release properties, long shelf-life and low toxicity. The incorporated drug participates in the microstructure of the system, and may even influence it due to molecular interactions, especially if the drug possesses amphiphilic and/or mesogenic properties (Fig. 1-23).

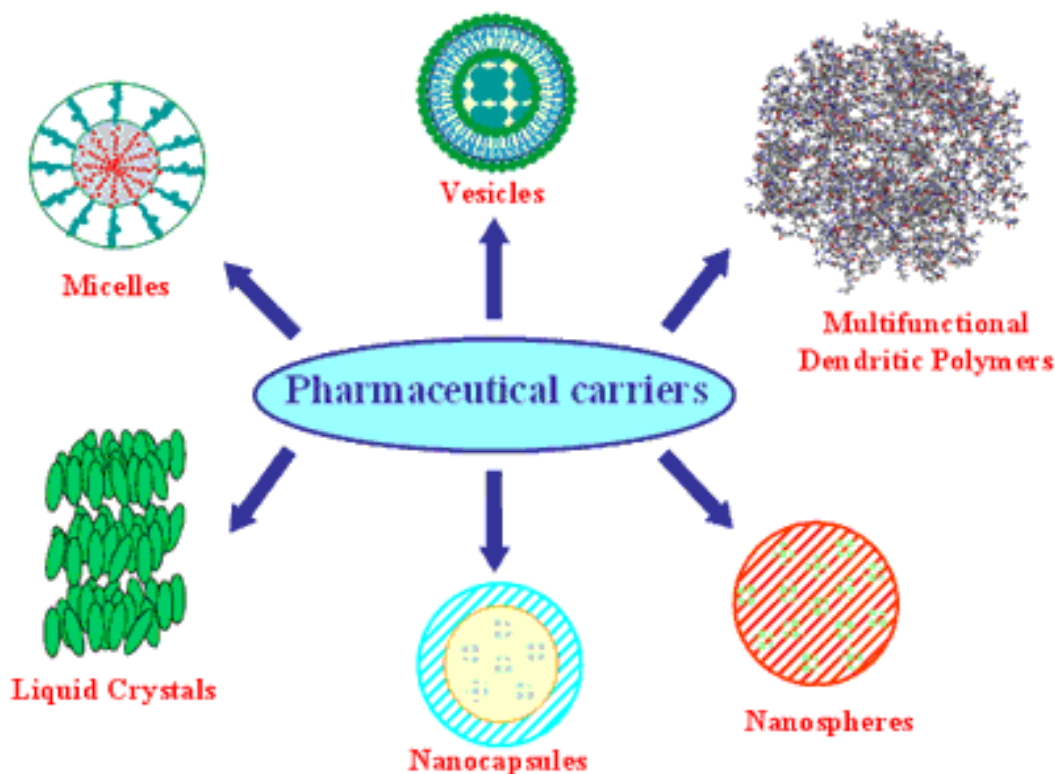


Fig. 1-23. Pharmaceutical carriers (Kaparissides et al., 2006).

Micelles formed by self-assembly of amphiphilic block copolymers (5-50 nm) in aqueous solutions are of great interest for drug delivery applications. The drugs can be physically entrapped in the core of block copolymer micelles and transported at concentrations that can exceed their intrinsic water- solubility. Moreover, the hydrophilic blocks can form hydrogen bonds with the aqueous surroundings and form a tight shell around the micellar core. As a result, the contents of the hydrophobic core are effectively protected against hydrolysis and enzymatic degradation. In addition, the corona may prevent recognition by the reticuloendothelial system and therefore preliminary elimination of the micelles from the bloodstream.

A final feature that makes amphiphilic block copolymers attractive for drug delivery applications is the fact that their chemical composition, total molecular weight and block length ratios can be easily changed, which allows control of the size and morphology of the micelles. Functionalization of block copolymers with crosslinkable groups can increase the stability of the corresponding micelles and improve their temporal control. Substitution of block copolymer micelles with specific ligands is a very promising strategy to a broader range of sites of activity with a much higher selectivity (Fig. 1-24).

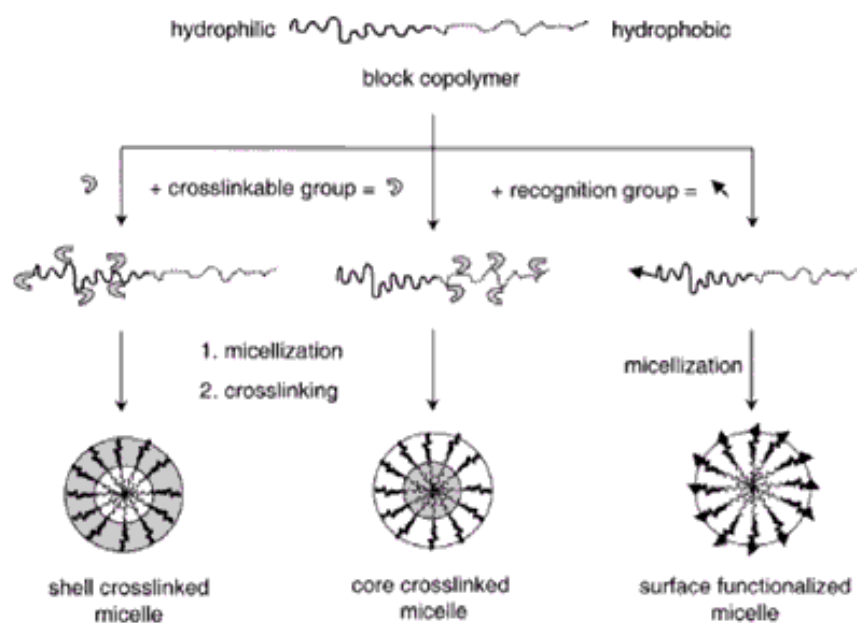


Fig. 1-24. Mechanisms followed by block-copolymers (Kaparissides et al., 2006).

Drugs that are encapsulated in a nanocage-functionalized with channel proteins are effectively protected from premature degradation by proteolytic enzymes (Fig. 1-25). The drug molecule, however, is able to diffuse through the channel, driven by the concentration difference between the interior and the exterior of the nanocage.

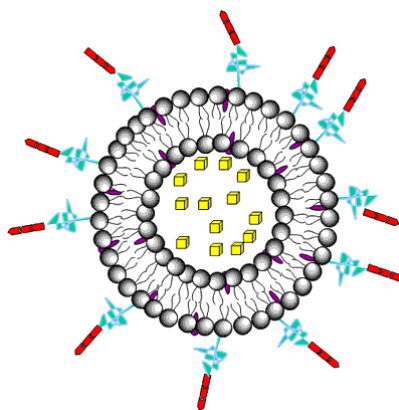


Fig. 1-25. Drug encapsulation in liposomes (Kaparissides et al., 2006).

Site directed targeting to cells or organs is desired to reduce the concomitant negative effects due to the action of the drug in sites other than necessary in the organism. As already mentioned, by encapsulating the drug in a carrier, the distribution process depends on the carriers' characteristics. Moreover, the carrier can be modulated to provide selective targeting to the cell or organ of interest, thus minimizing unwanted systemic side effects. For this purpose, two mechanisms may be used; passive targeting and active targeting.

Passive targeting takes place due to the action of the reticuloendothelial system (RES) in the common response of the organism to destroy foreign materials. Passive targeting is mainly dictated by the physical properties of the carrier and its interaction with plasma proteins. This form of targeting can be used to target diseases that affect the RES, for instance this is used to activate the immune system to destroy tumor cells. Passive targeting usually occurs by phagocytosis of the particle or carrier by the mononuclear phagocytic system, belonging to the RES.

In particular when the disease occurs in cells other than the RES, this kind of uptake must be avoided. In such cases active targeting needs to be used. Active targeted drug delivery occurs when the drug or carrier are directed to specific sites, in particular receptors located on the cell's membrane or tissue of interest, with the aid of a homing device (antibody, ligand, epitope). For instance, to provide recognition to specific target cells, antibodies were covalently attached to the surface of liposomes.

Active targeting usually involves the attachment of a ligand to the surface of the carrier in order to achieve specific ligand-receptor interaction. Once the targeted interaction takes place, the cell's mechanisms, mainly receptor-mediated endocytosis⁶, provides the proper conditions for internalization of the carrier.

Phagocytosis is a potential route for uptake of colloidal drug delivery systems. This benefits the passive targeting of drugs to treat diseases that reside within the cells of the mononuclear phagocytic system (MPS). However, other conditions require the carrier system to avoid the MPS for selective delivery of drugs before achieving any therapeutic response. Attempts made to avoid the MPS include: modification of surface characteristics - enthalpic stabilization; labeling with monoclonal antibodies - immunotargeting using magnetic microspheres - physical manipulation.

Phagocytosis can be avoided by creating a high potential energy barrier between the colloidal particle and the interacting cell surface. This high potential energy barrier can be formed by creating a sterically stabilized surface by introducing a hydrated polymer at the surface of the colloidal particle (enthalpic stabilization). On close approach, polymer chains inter-penetrate with the release of some bounded water molecules, resulting in a positive enthalpy change, which is energetically unfavourable.

Surfactants. Surfactants serve a variety of functions in controlled drug delivery systems. A surfactant is an organic chemical, which contains both hydrophilic and hydrophobic ends. The hydrophobic effect causes an organization of the surfactant into a micelle. A micelle consists of a hydrophilic shell and a hydrophobic core. Micelles are capable of performing a number of different functions and serve as the most useful form of surfactant in drug delivery systems.

Surfactants are used to supplement other delivery methods; however, surfactants can also act as primary carriers of drugs to the body. Because of the micelle's properties, it is able to solubilize drugs into its hydrophobic centre and protect them from the hydrophilic surroundings. In doing so, the micelle can then transport the drug to the area of the body where it will be released.

Surfactants can either be anionic, cationic, ampholytic (both anionic and cationic), or non-ionic. The type of drug dissolved and the conditions of the target site will dictate the type of surfactant used to carry the medicine.

The concentration of the micelle largely influences its properties. There is a finite range in which the micelle will provide maximum utility. This critical micelle concentration (CMC) will determine the effectiveness of the delivery. The composition of the surfactant, the target site in the body, and the type of drug to be delivered must be considered in determining the CMC.

The conditions of the target site are critical to the effectiveness of a surfactant delivery system. Parameters such as temperature, environment, and pH will influence the solubility of a drug inside the micelle.

Surfactants are commonly used to supplement pre-existing delivery systems. A relatively small concentration of surfactant incorporated into a drug can drastically increase the delivery's effectiveness. Surfactants perform the following functions:

1. Increase absorption of drug into cell membrane
2. Increased solubility of drug into carrier
3. Increase stability of drug into delivery system

Therefore, surfactants can complement other drug delivery strategies.

By acting as a wetting agent, surfactants facilitate the absorption of a drug into the cell wall. They increase the contact area between the drug and the cells by encouraging interfacial contact between the drug and the target. Surfactants raise the permeability of membranes, which allows for easier absorption.

However, interactions of surfactants with membranes can cause disruption of biological membranes.

Depending on the type of carrier and the amount of drug that must be dissolved, surfactants can greatly enhance the ability of a solvent to dissolve a drug. Introducing a surfactant into a solution lowers the surface tension and increases the solubility of the organic material into the solvent. Micelles can dissolve many substances in the body. For instance, anionic micelles display significant interaction with certain proteins. A high concentration of surfactants over a long period of time may disturb some bodily processes.

1.12. General concept of surface immobilization

Immobilization onto a surface is a prerequisite in order to use micro and nanocontainers in biosensing devices. Micro and nanoreactors, which are containers functioning as confined reaction vessels with micro and nanoscopic dimensions seem ideal candidates for bio-sensing devices. Immobilized containers could be used as biosensor chips for the detection, identification, and manipulation of biological entities. The containers can be loaded with molecules that could, after reacting with the analyte, give a detectable signal (absorbance, fluorescence, etc). Reactions taking place within a confined nanometer space, protected from the surrounding environment,

seem ideal candidates for sensor devices. Moreover, immobilized vesicles containing channel and receptor proteins can be used as model systems to study the interactions of these receptors. Usually in a bio-sensing device immobilization takes place onto the surface of a transducer, therefore the need to immobilize the containers.

Different approaches can be used to achieve immobilization of molecules onto surfaces: physisorption or adsorption and chemisorption (Fig. 1-26 a, b, and c). Physisorption through van der Waals or hydrophobic interactions is usually not an advantageous approach since the adsorption obtained is weak and reversible and thus the achieved surface modification is not permanent. One example of this type of immobilization is the Langmuir-Blodgett deposition technique, which in its most basic form uses only hydrophobic or hydrophilic interactions. Physisorption can also be obtained by electrostatic forces and the resulting layers show rather good stability. One well-established approach based on electrostatic interactions is known as the layer-by-layer (LbL) deposition of opposite charged molecules onto surfaces.

Covalently attached molecules, the chemisorption, on the other hand, render a much more stable system, and usually the modification is irreversible. One example of such an immobilization strategy is found in self-assembled monolayers (SAMs) on gold, via thiol-gold bond formation. However, the harsh conditions usually needed to promote chemical bonding onto a surface reduce the spectrum of application of chemisorption.

Moreover, in order to promote specific binding between (macro)molecules, one can make use of the readily available and highly specific interactions found in biochemistry (Fig. 1-26 d).

Bio-affinity interactions are widely spread in biologic systems, and include antibody-antigen recognition, ligand-receptor interaction, nucleic acid hybridization or any other biological pair interacting with high affinity.

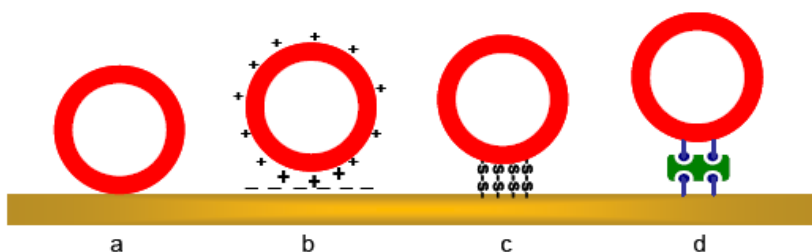


Fig. 1-26. Different strategies for immobilization onto surfaces; a, physisorption; b, electrostatic interaction; c, covalent bonding (S-Au); d, receptor-ligand interaction (e.g. avidin-biotin).

1.13. Poly (2-hydroxyethyl methacrylate)

One of the first polymers studied for biomedical applications was poly (2-hydroxyethyl methacrylate) (PHEMA), as hydrogel. It is a non-ionic hydrogel, and as such exhibits no pH swelling dependence. It was used as one of the first soft contact lenses. Unlike other hydrogels,

the monomer is infinitely soluble in water while the polymer exhibits a limited solubility. This phase behavior allows for the formation of a macroporous sponge structure when reacted in dilute monomer solutions. In the late 1960s, these porous forms of PHEMA were studied for the potential applications of soft tissue replacement, such as breast augmentation and nasal cartilage replacement. However, complications with long-term calcification hindered further development. Then in the 1980s, work was done with pancreatic islet sequestering using PHEMA sponges. While the hydrogels sponge performed well as an immunoisolation device, long-term viability of the islets was not achieved.

PHEMA hydrogel sponge formation is controlled by the thermodynamic phase behavior between the polymer-rich phase, and the aqueous-rich phase during polymerisation. Chirila noted that the formation of the porous structure is dependant upon a kinetic competition between gel point and phase separation. If gelation occurs first, the resulting material is a hydrogel with little to no macropores, but will still contain the typical hydrogel mesh size on the angstrom level. If phase separation occurs first, the resulting material contains water filled spaces that can vary in size from sub micron up to 20 microns in size. The presence of the two different pore sizes present in macroporous PHEMA sponges is schematically shown in Fig. 1-27. Since the sponge formation is dependant upon both polymerisation kinetics and solution thermodynamics, there are many variables that can be altered in order to control the pore morphology of the resulting hydrogel sponge.

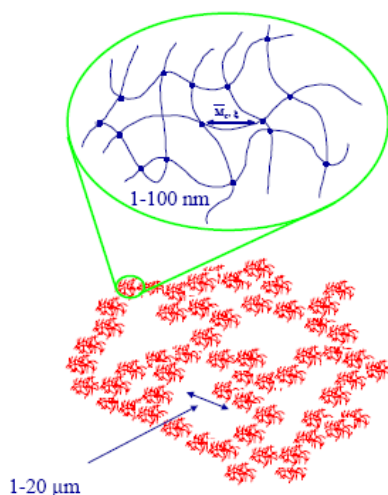


Fig. 1-27. Schematic representation of macroporous PHEMA hydrogel sponges. Interstitial spaces between polymer droplets create a macroporous structure 1-20 μm in size, whereas the polymer network creates a 1-100nm mesh size in the polymer phase (Dziubla, 2003).

The amount of water added to the reaction mixture produces the most dramatic effect upon the size of the pores in a PHEMA sponge. When the water content is below 45-50%, the PHEMA polymer chains remain soluble and do not form a 2 phase system. When the reaction

solution's water content is increased, phase separation occurs with excess water acting as the pore forming agent.

Hence, as we further increase the water content, the number of water molecules excluded from the polymer phase increases creating larger voids between the polymer droplets. It is well established that networks containing 85% water or greater possess pore sizes that are large enough for cellular invasion.

Unfortunately, these high water solutions result in materials with characteristically weak mechanical properties and large pore size distributions.

Since different cross-linking agents possess different solubilities in water, it was hypothesized that by altering the cross-linking agent used it should be possible to alter the networks pore morphology. Chirila et al. performed a rather extensive evaluation of cross-linkers to determine their relative impact upon the networks ability to form large macropores. They determined that using typical concentrations of cross-linker content (0.1-2 % mol.) had very little effect of the ultimate morphology and mechanical strength of the networks formed.

While many studies on cross-linker selection have been performed, little work has been done on the effect of more/less hydrophilic comonomers on the formation of the macropores. The comonomers that have been attempted were more hydrophobic monomers such as methyl methacrylate. This is most likely due to the commonly used hydrophilic comonomers, such as acrylic acid and 2,2-diethylamino methacrylate that result in transparent gels.

The presence of non-reacting, inert, components can also affect the pore size of the resulting polymer sponge. One of the first methods pursued was that of porogens. A porogen is a space filling particulate that prevents polymerisation in specific locations through physical hindrances. Sucrose, glucose, and ice crystals have all been used as void fillers to create macroporous PHEMA hydrogels. The porogen must be selected based on its ability to remain suspended in the reaction mixture, and provide some mechanism of being leached from the next work after the sponge is formed.

Another technique is to control the solubility of PHEMA by addition of a tertiary component. For example, PHEMA solubility decreases with an increase in ion content. As a result, Mikos et al. used salt solutions of varying ionic strength to dilute the reaction mixtures. It was noted that increasing the ion content of the aqueous solution to 0.7 molar, interconnected macropores were obtained at 60 vol% water. Surfactants may also be used to control the network pore structure. However, not much work has been done in this area, since surfactants typically work to reduce the surface repulsions between the two phases and form smaller droplets. These smaller droplets when gelled are expected to possess a smaller pore size. However this is still a promising area of exploration, since it may be possible to form alternate phase structures such as bicontinuous phases, which would be ideal for cellular invasion.

Isotactic PHEMA was found to possess negative temperature dependence in water. While atactic PHEMA is not expected to have as strong of a negative temperature dependence, the mechanisms of this behavior can still exist over short ranges and may effect the phase behavior.

As such, increased temperatures may also function to control the pore morphology by allowing the polymer to phase separate sooner in the reaction.

Temperature not only plays a critical role with the thermodynamics, but also with the kinetics of the polymerisation. Once phase separation occurs, the polymer phase will start to settle out of solution since it is denser than the aqueous phase. Chirila noted this phenomenon by stating that in some reactions, a water layer was evident over the polymer sponge layer. Temperature can reduce this settle out by speeding up the reaction kinetics, and forcing gelation to occur sooner.

Since two phases are present, mechanical agitation can be used to control the distribution of the phases. Dalton synthesized porous tubes of PHEMA hydrogels by reacting the monomer solution in a radially rotating glass tube.

It was found that this rotation resulted in a dense outer layer of polymer (due to centripetal force) and a more porous inner surface. Minor evidence of pore organization under this radial agitation was noticed when HEMA was copolymerised with PEG.

1.14. Economic figures

The global market for advanced drug delivery systems was more than €37.9 billion in 2000 and grew up to €80 billion by 2005 (Kaparissides et al., 2006).

Table 1-1

Global markets for advanced drug delivery systems

Market	Value (billion €)
controlled release	20.0
needle-less injection	0.8
injectable/implantable polymer systems	5.4
transdermal	9.6
transnasal	12.0
pulmonary	17.0
transmucosal	4.9
rectal	0.9
liposomal drug delivery	2.5
cell/gene therapy	4.0
miscellaneous	1.9

Developments within this market are continuing at a rapid pace, especially in the area of alternatives to injected macromolecules, as drug formulations seek to cash in on the €6.2B worldwide market for genetically engineered protein and peptide drugs and other biological therapeutics.

1.15. Future Opportunities and Challenges

The most exciting opportunities in controlled drug delivery lie in the arena of responsive delivery systems, with which it will be possible to deliver drugs through implantable devices in response to a measured blood level or to deliver a drug precisely to a targeted site. Much of the development of novel materials in controlled drug delivery is focusing on the preparation and use of these responsive polymers with specifically designed macroscopic and microscopic structural and chemical features. Such systems include:

- **Copolymers with desirable hydrophilic/hydrophobic interactions.**
- **Block, statistic or graft copolymers.**
- Complexation networks responding via hydrogen or ionic bonding.
- Dendrimers or star polymers as nanoparticles for immobilization of enzymes, drugs, peptides, or other biological agents.
- New biodegradable polymers.
- New blends of hydrocolloids and carbohydrate-based polymers.

These new biomaterials—tailor-made copolymers with desirable functional groups—are being created by researchers who envision their use not only for innovative drug delivery systems but also as potential linings for artificial organs, as substrates for cell growth or chemical reactors, as agents in drug targeting and immunology testing, as biomedical adhesives and bioseparation membranes, and as substances able to mimic biological systems. Successfully developing these novel formulations will obviously require assimilation of a great deal of emerging information about the chemical nature and physical structure of these new materials.

Also, nanoparticles and nanoformulations have already been applied as drug delivery systems with great success; and nanoparticulate drug delivery systems have still greater potential for many applications, including anti-tumour therapy, gene therapy, and AIDS therapy, radiotherapy, in the delivery of proteins, antibiotics, virostatics, vaccines and as vesicles to pass the blood - brain barrier.

Nanoparticles provide massive advantages regarding drug targeting, delivery and release and, with their additional potential to combine diagnosis and therapy, emerge as one of the major tools in nanomedicine. The main goals are to improve their stability in the biological environment, to mediate the bio-distribution of active compounds, improve drug loading, targeting, transport, release, and interaction with biological barriers. The cytotoxicity of nanoparticles or their degradation products remains a major problem, and improvements in biocompatibility obviously are a main concern of future research.

There are many technological challenges to be met, in developing the following techniques:

1. Nano-drug delivery systems that deliver large but highly localized quantities of drugs to specific areas to be released in controlled ways;
2. Controllable release profiles, especially for sensitive drugs;
3. Materials for nanoparticles that are biocompatible and biodegradable;
4. Architectures / structures, such as biomimetic polymers, nanotubes;
5. Technologies for self-assembly;
6. Functions (active drug targeting, on-command delivery, intelligent drug release devices/ bioresponsive triggered systems, self-regulated delivery systems, systems interacting with the body, smart delivery);
7. Virus-like systems for intracellular delivery;
8. Nanoparticles to improve devices such as implantable devices/nanochips for nanoparticle release, or multi reservoir drug delivery-chips;
9. Nanoparticles for tissue engineering; e.g. for the delivery of cytokines to control cellular growth and differentiation, and stimulate regeneration; or for coating implants with nanoparticles in biodegradable polymer layers for sustained release;
10. Advanced polymeric carriers for the delivery of therapeutic peptide/proteins (biopharmaceutics),
And also in the development of:
11. Combined therapy and medical imaging, for example, nanoparticles for diagnosis and manipulation during surgery (e.g. thermotherapy with magnetic particles);
12. Universal formulation schemes that can be used as intravenous, intramuscular or peroral drugs;
13. Cell and gene targeting systems;
14. User-friendly lab-on-a-chip devices for point-of-care and disease prevention and control at home;
15. Devices for detecting changes in magnetic or physical properties after specific binding of ligands on paramagnetic nanoparticles that can correlate with the amount of ligand;
16. Better disease markers in terms of sensitivity and specificity.

Chapter 2

Purpose of the thesis



The purpose of the laboratory work developed during the doctoral stage was to find a strategy for attacking cancerous tumours in order to stop angiogenesis. Endothelial cells are involved in many aspects of vascular biology, including: vasoconstriction and vasodilatation, and hence the control of blood pressure; blood clotting (thrombosis & fibrinolysis); atherosclerosis; formation of new blood vessels (angiogenesis); inflammation and swelling (oedema). Endothelial cells also control the passage of materials and the transit of white blood cells into and out of the bloodstream.

The advantages of controlled delivery systems represent a continuous challenge at the edge among chemistry, physics, biology, and medicine, aiming at: the maintenance of optimum therapeutic drug concentration in the blood or in a cell; predictable and reproducible release rates for extended periods of time; enhancement of activity duration for short half-life drugs; the elimination of side effects, frequent dosing, waste of drug, optimized therapy; better patient compliance.

Controlled release products provide prolonged delivery of a drug while maintaining its blood concentration within therapeutic limits. It is a relatively new field, and, as a result, research in the field has been extremely fertile and has produced many discoveries. Traditionally, the most popular form of drug delivery has been injection and ingestion in tabular form. The justification for a controlled release dosage form over a conventional tablet is either to circumvent problems in drug absorption or metabolism, or to optimize therapy itself. The variety of routes available for drug delivery corresponds to the list of biological membranes in the human body: nasal, gastrointestinal tract, the eye, skin, and even the vaginal mucosa. It should be added to this list implants and targeted delivery.

The polymer must be biocompatible and degradable into non-toxic components that do not create an inflammatory response.

Nano or micropolymeric beads are usually not soluble in the living bodies' plasma. They can swell and liberate drugs diffusively or by enzymatic splitting. By releasing small amounts of drugs over sustained periods of days, weeks and even years, polymeric controlled-release systems greatly improve the effect of the drugs. As the polymer degrades, the drug is released by desorption and diffusion. Desorption is assumed to originate with drug that is initially contained on the sphere surface and in mesopores connected to the outside surface of the microsphere.

In contrast, drug diffusion is delayed by a period of time that is determined by how long it takes for the micropores to coalesce and for the drug to pass out of the inner portions of the macropores, forming the polymeric matrix as water makes contact with the drug, causing it to degrade.

A major problem with standard drug dosing is that 2-3 times a day delivery of drugs results in a quick burst of medication at the time of dosing, followed by a rapid loss of the drug from the body. Most of the side effects of a drug occur during the burst phase of its release into

the bloodstream. Secondly, the time the drug is in the bloodstream at therapeutic levels is very short; most is used and cleared during the short burst.

Polymer technology has given some solutions to these problems. Drugs embedded in polymer beads or in polymer wafers have several advantages. First, most systems allow slow release of the drug, thus creating a continuous dosing of the body with small levels of drug. This should prevent any side effects associated with high burst levels of normal injected or pill based drugs. Secondly, since these polymers can be made to release over hours to months, the therapeutic span of the drug is markedly increased. Often, by mixing different ratios of the same polymer components, polymers of different degradation rates can be made, allowing remarkable flexibility depending on the medication being used. A long rate of drug release is beneficial for people who might have trouble staying on regular dosage, such as the elderly, but is also an ease of use improvement that everyone can appreciate. Most polymers are made to degrade or be cleared by the body over time, so they will not remain in the body after the therapeutic time.

A second major advantage of polymer based drug delivery is that the polymers often can stabilize or solubilize proteins, peptides, and other large molecules (drugs, vitamins) that would otherwise be unusable as medications. Finally, many drug/polymer mixes can be placed directly in the disease area, allowing specific targeting of the medication where it is needed without losing drug to the "first pass" effect.

Obviously the more localized a drug can be delivered, the lower the overall dose needs to be to maintain a therapeutic concentration. This makes medication more effective with lower side effects. It has already been described in the literature part how certain polymer products can achieve localized delivery.

The present thesis proposes the development of new high performance macromolecular structures, the original contribution consisting in:

- the synthesis of iodine-based copolymers for tumour detection by X-rays;
- the synthesis and modification of pHEMA copolymers and terpolymers to render structures able to couple via specific interactions to other molecules and with applications in the field of:
 1. enhanced permeability and retention (EPR) in osseous tumours:
 - a) inclusion of biocompatible dyes for tracking the microparticles during *in vivo* tests;
 - b) incorporation of drugs in controlled release systems;
 2. calcification studies.

The main purpose of the present thesis was to obtain new polymeric microbeads for further use as polymer-drug conjugates to detect and treat metastatic cancers. The ideal drug delivery system should be inert, biocompatible, mechanically strong, comfortable for the patient, capable of achieving high drug loading, safe from accidental release, simple to administer and remove, and easy to fabricate and sterilize.

The goal of the original controlled-release systems obtained was to achieve a delivery profile that would yield a high blood level of the drug over a long period of time. Other microparticles obtained were conceived for tumoral targeting.

If we can give the conjugates by injection, then we have an opportunity to target the micrometastases that can be present throughout the whole organism.

The purpose of the functionalization of copolymers is two-fold: to use them as active targeting delivery systems in the context of active cell targeting and for surface immobilization. Both approaches share a common feature that is the specific interaction of microcontainers towards receptors, whether these are present on the surface of a cell or a sensor.

The following strategy was used in order to introduce specific functionalities: different monomers containing different functionalities were used in order to obtain either amphiphilic or less hydrophilic copolymers. By doing this, the polymers carrying the desired functionalities as end groups self-assemble exposing these moieties on their surface. The functionalities on the microcarrier will function as anchors providing covalent bonding. In these self-assembly systems, the average aggregation number define the average number of functional groups per aggregate, which can be further tailored by modifying the ratios of the comonomers, with respect to the shape and dimensions of the particles. Moreover, specific biocompatible fluorescent dyes were introduced, labeling the structures for visualization purposes.

The characterisation of these functionalized polymers in the view of their use as drug delivery carriers, *in vitro* behaviour and their interaction with specific receptors were studied in two different systems:

1. Microparticles binding and uptake were studied *in vitro* with different cell lines. Encapsulation of fluorescent dyes in the polymer cavities provided a means of visualization of the structures by fluorescent techniques, such as fluorescent microscopy and flow cytometry.

2. Surface immobilized drugs for bone metastasis and dentistry infections treatment was obtained by surface immobilization via anchoring groups. Other hydrophobic monomers were investigated to replace MMA in the copolymers. Their synthesis and characterisation were studied with established techniques, optimized.

Providing control over the drug delivery can be the most important factor at times when traditional oral or injectable drug formulations cannot be used. These include situations requiring the slow release of water-soluble drugs, the fast release of low-solubility drugs, drug delivery to specific sites, drug delivery using nanoparticulate systems, delivery of two or more agents with the same formulation, and systems based on carriers that can dissolve or degrade and be readily eliminated.

Morphology of the polymer matrix plays an important role in governing the release characteristics of the encapsulated drug. HEMA-based polymer matrices were formulated as low degree cross-linked structures, in order to enable drug binding by physical or chemical means and its release by diffusion.

The shape of the polymer is also important to the drug release kinetics. For example, it has been shown that zero order drug release can be achieved using a hemispherical polymer form. Polymer microspheres are the most popular form due to manufacturing advantages as well as ease of administration (injectability by suspending in a vehicle). Polymer microspheres can be

manufactured by using various techniques such as emulsion polymerisation, suspension polymerisation, precipitant polymerisation, etc. Denizli et al. (2003), Horák et al. (2000), and Maeda (1991, and 2000) have very interesting works published in this field.

The type of technique used affects factors such as porosity, size distribution and surface morphology of the microspheres and may subsequently affect the performance of the drug delivery product.

In the experimental part of this work, polymeric microparticles were obtained by dispersive polymerisation and precipitant polymerisation from functionalised biocompatible polymers, which further were marked with a fluorescent biocompatible dye, in order to track their trajectory through the living body to the organ aimed. After positive results, a drug that is supposed to stop tumour angiogenesis and even to destroy the tumours was bond.

2-hydroxyethyl methacrylate (HEMA) and methyl methacrylate (MMA)-based polymers are both biocompatible and biodegradable (very well tolerated by the human organism). Conjugation with some specific drugs is expected to increase the accumulation of these microbeads into tumours and would decrease the drug toxicity for other organs. Iodine-based copolymers were obtained in order to be used as tracking agents of tumours, taking into consideration the EPR effect.

The following aspects were considered:

- copolymerisation of HEMA, which is highly hydrophilic, with hydrophobic comonomers, in order to decrease it's swelling degree in living bodies to a certain extent;
- addition of functionalised comonomers, either positively or negatively charged;
- choice of fluorescent dye;
- loading of a drug that can inhibit the tumour development or even to induce necrosis.

Another approach was to study the *in vitro* mineralization potential of the polymers obtained. In the literature, an important number of studies on the influence of the positive, neutral or negative polymers onto the calcification inhibition are presented. There were performed studies on copolymers from all these categories and the results are presented further.

Chapter 3

p(MMA-co-TIPA) microbeads for tumour detection

Data presented in:

Teodora Zecheru, Cătălin Zaharia, Edina Rusen, Florin Miculescu, Bogdan Mărculescu, Corneliu Cincu, *Synthesis, characterisation and bioavailability of a new copolymer system*, International Conference on Chemistry and Chemical Engineering RICCE 15, 19-22 September 2007, Sinaia, Romania.

3.1. Introduction

When a polymer is introduced in the organism, it should be easy to track and be analysed by X-ray spectroscopy, in order to monitor exactly its position in the body. A negative aspect of polymeric biomaterials in the purpose of detection is represented by their X-ray transparency. X-rays are difficult to pass through organic polymers, due to the lack in high atomic mass elements.

One of the simplest methods of inducing radio-opacity in polymers is to introduce an additive, such as: barium, zirconium, lead, platinum, gold (chemical elements with high atomic mass), or BaSO₄, ZrO₂ (their salts). Unfortunately, these methods lead to some negative effects, due to the incompatibility between inorganic materials and organic matrices: mechanical defects at the contact between radio-opaque material and polymer; exudation of the radio-opaque material from the composite.

This is the reason for replacing inorganic materials with radio-opaque polymers, containing covalent bonds with high-molecular elements. In this purpose, new polymeric biomaterials are designed to combine X-ray visibility, biocompatibility and superior physico-chemical and mechanical properties.

The Enhanced Permeability and Retention (EPR) effect has been observed not only in solid tumours, but also in the case of granuloma and different tissue inflammation. In this case, macromolecules are slowly released through the lymphatic system.

The tumour or inflammatory specific polymer retention can be used for diagnose. Binding nano or microbeads with radio-opaque elements, scintigraphic elements (gallium) or magnetic resonance analysis allow finding better diagnose methods.

One of the most encountered polymers in the field of dentistry, in dental prosthesis, and in orthopaedics, as bone cement, is poly(methylmethacrylate) (pMMA). Copolymers of MMA are widely used in biomedical applications due to their established biocompatibility. Synthetic resins most commonly used in prosthetic dentistry are based on pMMA.

In this chapter of the thesis, the synthesis and characterisation of a range of copolymers of MMA with a iodine-based comonomer is reported, in which the relationship between the copolymer composition and the utility as microbeads for tumoral detection is examined.

The objectives of the present study were: the synthesis of the 2,4,6-triiodophenyl acrylate (TIPA) monomer; the synthesis of p(MMA-co-TIPA) copolymer; physico-chemical, and biological characterisation of the copolymer obtained; determination of the reactivity ratios of the comonomers; evaluation of the copolymer utilisation in tumoral detection.

3.2. Synthesis procedures

3.2.1. Synthesis of the iodine-containing monomer, 2,4,6-triiodophenyl acrylate (TIPA)

The method used for the synthesis of the monomer followed the M. Okamura et al. (2002) procedure (Fig. 3-1), and was modified as follows.

All reagents used were obtained from commercial sources (Sigma, Alfa Aesar, Merck, Chimopar) and used without further purification.

1.9 mL (0.022 moles) of acryloyl chloride were dissolved in 70 mL dichloromethane and the mixture was added dropwise under stirring to a mixture of 10 g (0.019 moles) 2,4,6-triiodophenol and 2.64 mL (0.019 moles) triethylamine dissolved in 100 mL dichloromethane. The solution was stirred below room temperature and kept for 4 hours. The resultant organic compound, TIPA, was collected from the organic and water phases, extraction being carried out from the latter phase. TIPA obtained was washed with 10% in weight NaHCO_3 , 10% in weight NaCl three times each and then dried over anhydrous Na_2SO_4 . The product was separated from dichloromethane by rotoevaporation at 30°C and 10 mmHg. Yield of the light yellow product obtained was $\sim 82\%$.

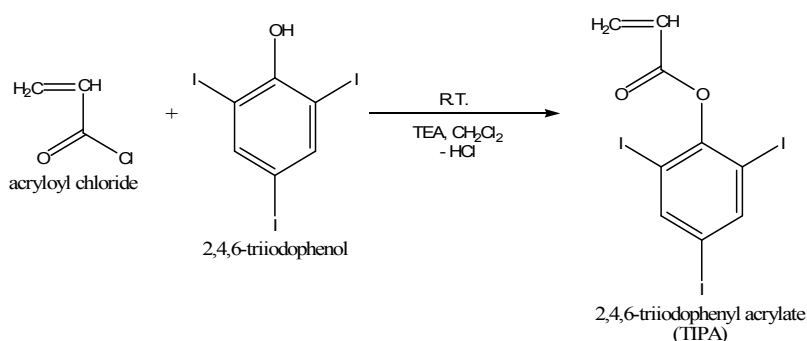


Fig. 3-1. Chemical synthesis of TIPA monomer

3.2.2. Synthesis of TIPA-containing microbeads

Free-radical polymerisation was used for the microparticles obtaining, following the procedure:

Methyl methacrylate (MMA), and 2,4,6-triiodophenol acrylate (TIPA), obtained accordingly the procedure above, were employed as comonomers, benzoyl peroxide (BPO) as initiator, polyvinyl alcohol (PVA) as suspension agent (88-98 hydrolysis grade), all the reagents being purchased from Sigma-Aldrich. Ethanol was employed as non-solvent (Chimopar).

The initiator BPO was purified by recrystallisation from ethanol, and MMA was distilled under reduced pressure.

The synthesis had into the view the obtaining of μm -size particles, using suspension-precipitation polymerisation procedure at a conversion over 90%.

A solution of suspension agent (w/v) in demineralised water (5/100) was introduced into a three-neck reactor. Separately, a solution containing the comonomers (Table 3-1), and BPO initiator (5×10^{-3} mol/L in the solution) was prepared. Monomer: water ratio used was 1:5 (v/v). The comonomer solution was added dropwise to the first one, under mechanical stirring, increasing the temperature to 75°C and the stirring rate to 800 rpm. Polymerisations were performed in a water-bath and under nitrogen atmosphere. An optimal result of the reaction and a high conversion were noticed after 6 hours.

Table 3-1

Comonomer ratios used in the feed compositions for p(MMA-co-TIPA) synthesis

Sample	Comonomer molar ratios in the feed	
	MMA	TIPA
1	95	5
2	93	7
3	90	10

3.2.3. Synthesis of copolymers for biological tests

In order to evaluate their *in vitro* biocompatibility and mineralisation potential, there were obtained bulk copolymers with the same ratios (Fig. 3-2, Table 3-1). Bulk copolymerisations were performed in polyethylene tubes (PE), 5 mm diameter, at 80°C , under nitrogen atmosphere, for 24h. BPO was used as initiator also (5×10^{-3} mol/L).

Cylinders of p(MMA-co-TIPA) obtained were purified by extraction in soxhlet with ethanol for 24h.

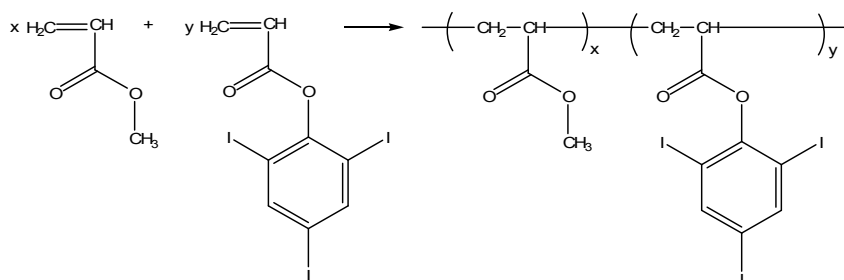


Fig. 3-2. Chemical structure of p(MMA-co-TIPA) copolymer

3.3. Characterisation studies

3.3.1. FT-IR spectrophotometry

A FT-IR spectrophotometer JASCO 6200 with ATR (Attenuated Total Reflectance) modulus SPECAC Golden Gate was used for the tests. Spectra were scanned over the range of 4000-550 cm^{-1} . TIPA monomer and p(MMA-co-TIPA) copolymers were characterised through FT-IR ATR analysis in order to confirm their structures and to identify the main peaks.

In Fig. 3-3 there is given the TIPA spectrum. C-I stretching vibrations appear in the interval of 550-650 cm^{-1} , as a range of weak and medium peaks, while =C-H and =CH₂ from alkene function are observed at 3049 cm^{-1} and C=C sp² from phenyl-ring at 1529 cm^{-1} (stretching vibrations), C-H bending and ring puckering at 793; and a strong band of C=O (str. vib.) from ester functional class at 1743 cm^{-1} . 1135 and 1205 cm^{-1} represent the 2-band stretching vibration O-C bond from ester functional class. At 859 cm^{-1} appears the C-O-C bond from ether functional class. In Fig. 3-4 the FT-IR superposed spectra of p(MMA-co-TIPA) copolymers at different molar ratios are presented. In comparison with the TIPA spectrum, the peak at 3049 cm^{-1} disappears, and the ones at 2945 cm^{-1} , representing CH₃, CH₂ and CH stretching vibrations and 1420 and 1360 cm^{-1} from CH₂ and CH₃ deformation of alkanes, increases. The peak at 1538 cm^{-1} increases with the ratio of TIPA following a gain in phenyl functions (C-C sp²); so does the peak at 1725 cm^{-1} , of C=O from ester function, displaced due to steric effects while polymerisation of two esters, one being a methacrylate-ester and the other - an acrylate-ester.

The spectra show that iodine bonds C-I are present also, due to the peaks in the interval 650-550 cm^{-1} (701, 668, and 566 cm^{-1}); in the same time, the peak in the monomer for ether functional group at 859 cm^{-1} is displaced to 862 cm^{-1} (C-O-C bending vibrations).

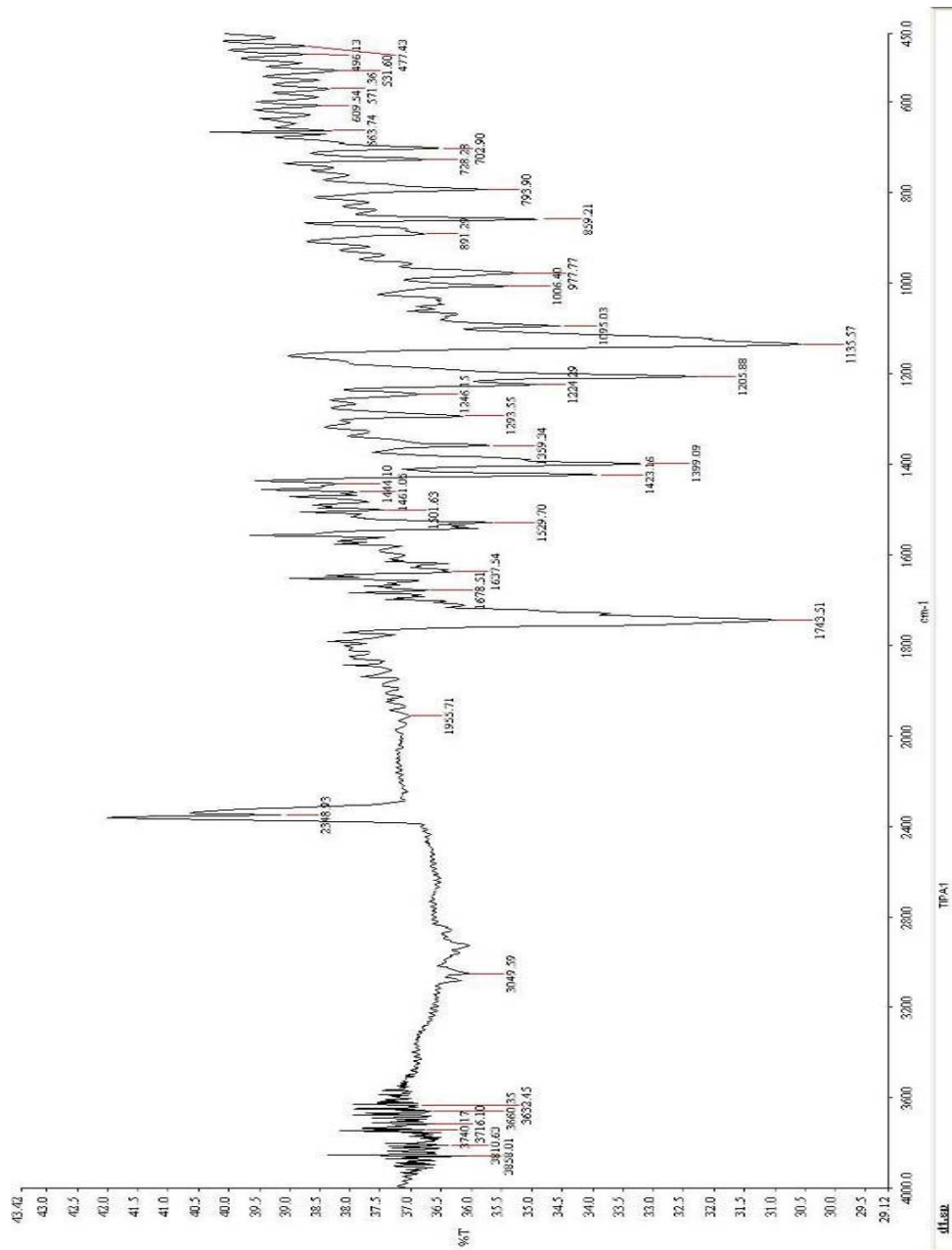


Fig. 3-3. FT-IR spectrum of TIPA monomer

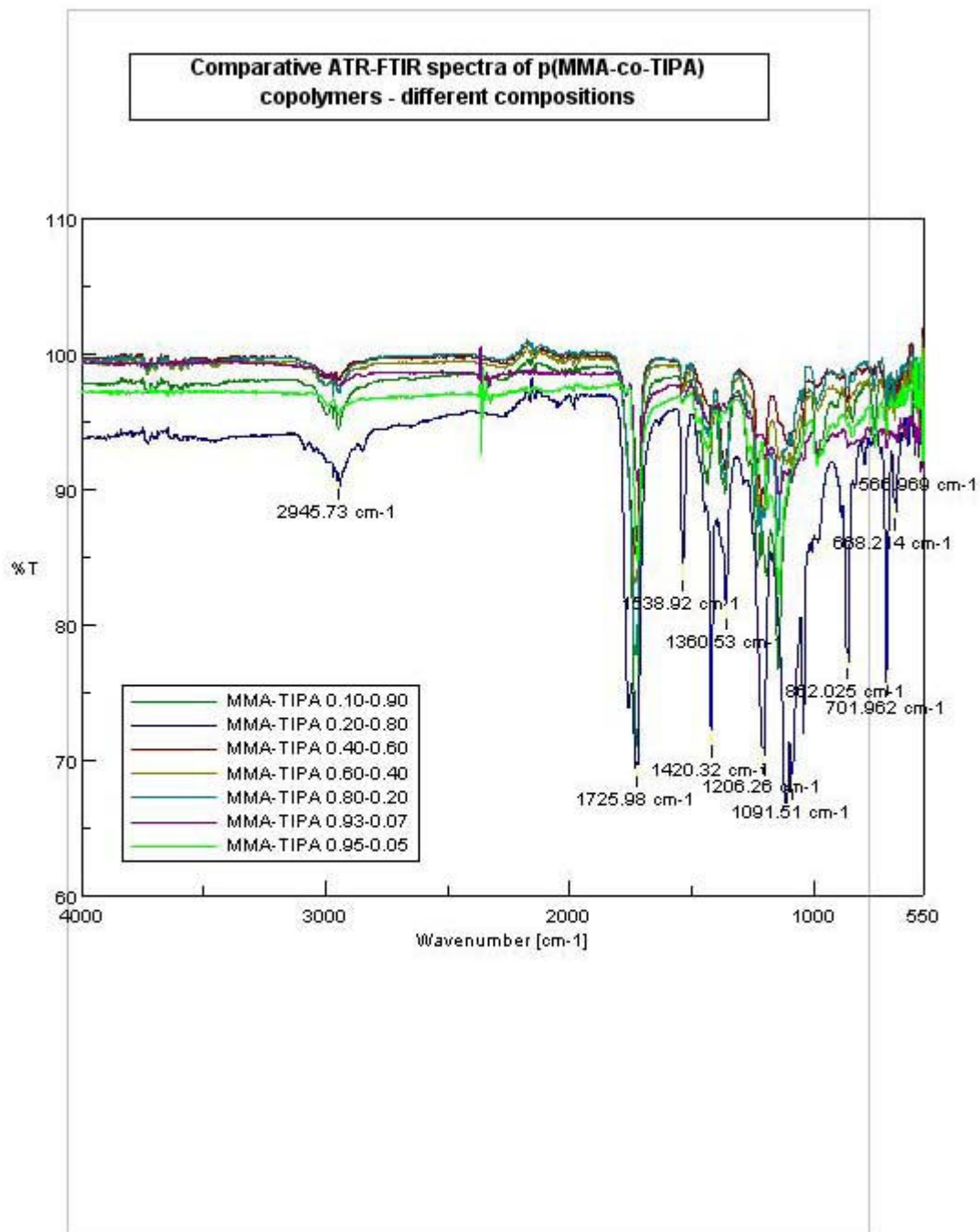


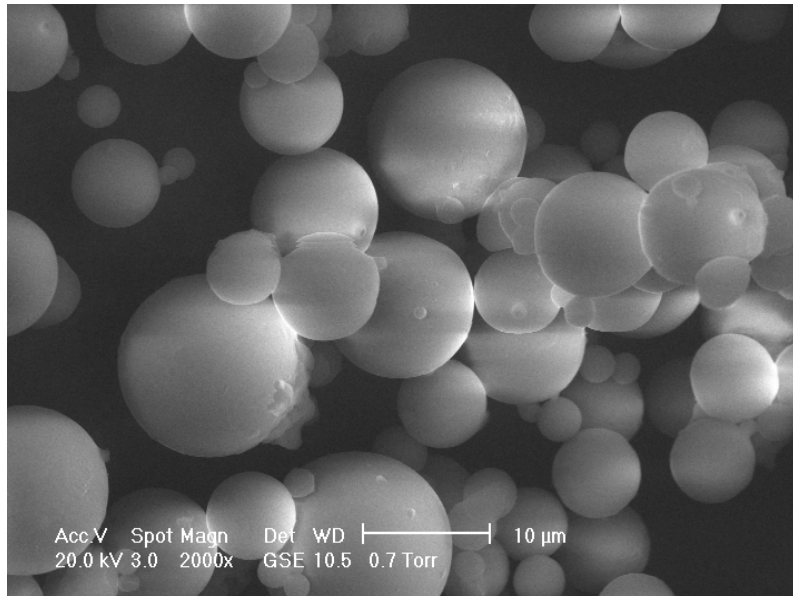
Fig. 3-4. FT-IR spectra of p(MMA-co-TIPA) with different molar ratios

3.3.2. SEM and EDX analyses of the obtained p(MMA-co-TIPA) microbeads

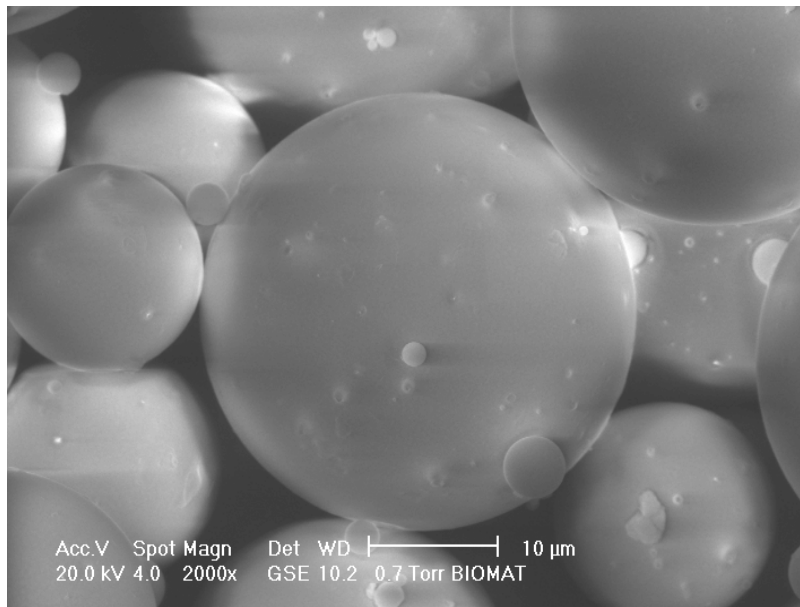
Morphological characterisation of the polymeric microbeads obtained was performed on a Philips XL30 - ESEM Turbo Molecular Pump (TMP), at 20 keV, equipped with an Energy Dispersive X-

rays (EDX) modulus, Detector Type: UTW-Sapphire, and a JEOL 6301F equipped with an EDX microanalysis system, model Link ISIS. The samples were first carbon-coated.

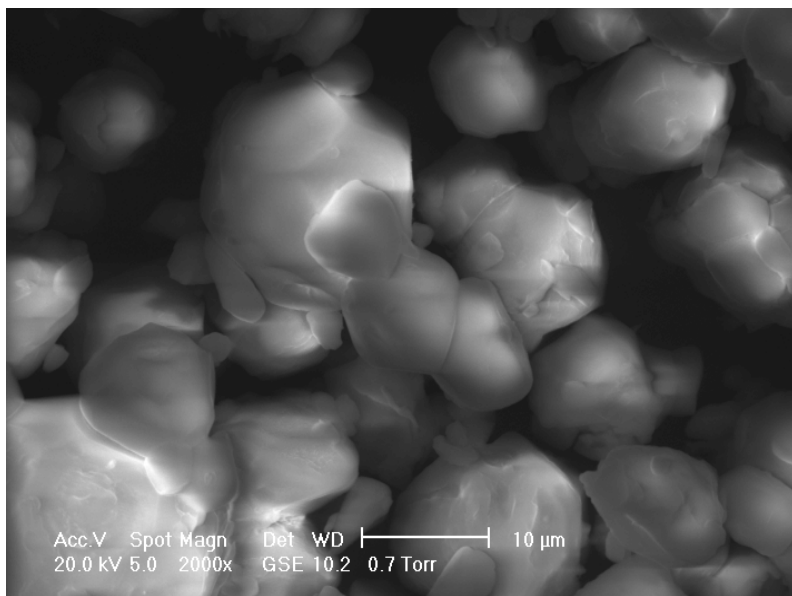
In Fig. 3-5 there are presented SEM microphotographs for the p(MMA-co-TIPA) copolymers obtained.



a)



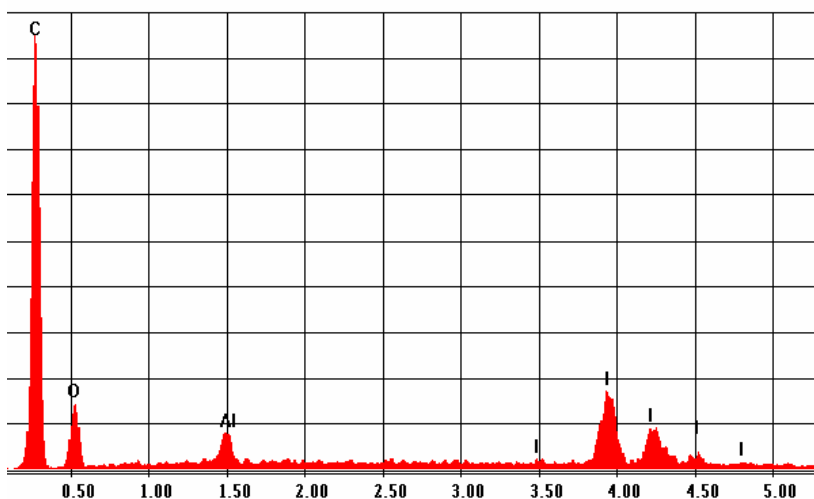
b)



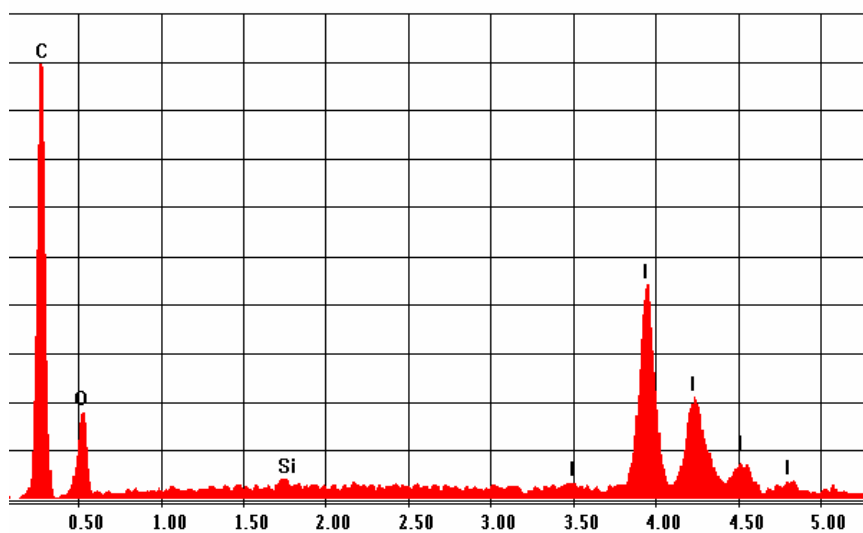
c)

Fig. 3-5. SEM microphotographs of p(MMA-co-TIPA) copolymers obtained: a) 95:5; b) 93:7; c) 90:10, molar ratios in the feed.

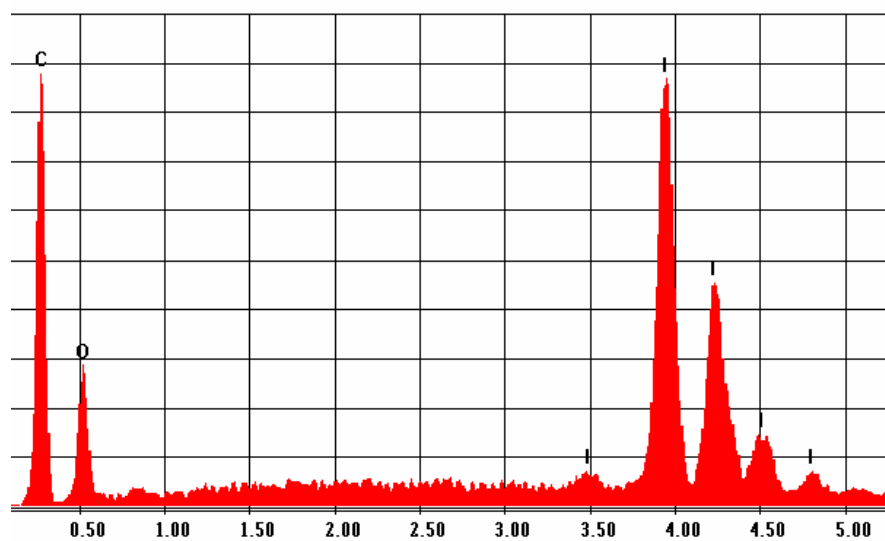
The Fig. 3-6 and Table 3-2 give the EDX weight measurements of the elemental distribution in the copolymers obtained. The results prove also that a linkage among MMA-TIPA has occurred and the iodine ratio in the copolymer increases with the TIPA ratio from the feed.



a)



b)



c)

Fig. 3-6. EDX of p(MMA-co-TIPA) copolymers obtained: a) 95:5; b) 93:7; c) 90:10, molar ratios in the feed.

Table 3-2

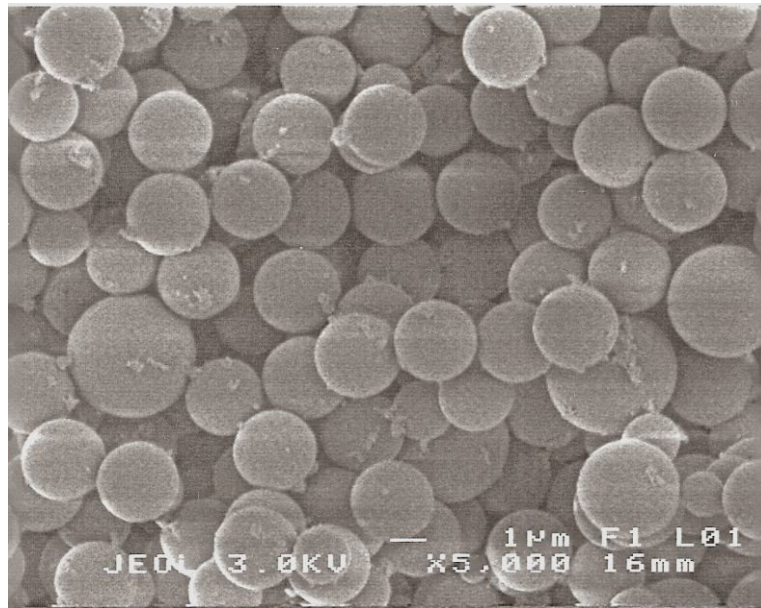
EDX results of p(MMA-co-TIPA) copolymers obtained: a) 95:5; b) 93:7; c) 90:10, molar ratios in the feed.

Element	Wt % (in function of the MMA:TIPA molar ratio in the feed)		
	95:5	93:7	90:10
C	71.64	59.61	47.44
O	14.35	12.32	11.67
I	12.72	27.73	40.89
Others (Si, Al)	1.29	0.35	-
Total	100	100	100

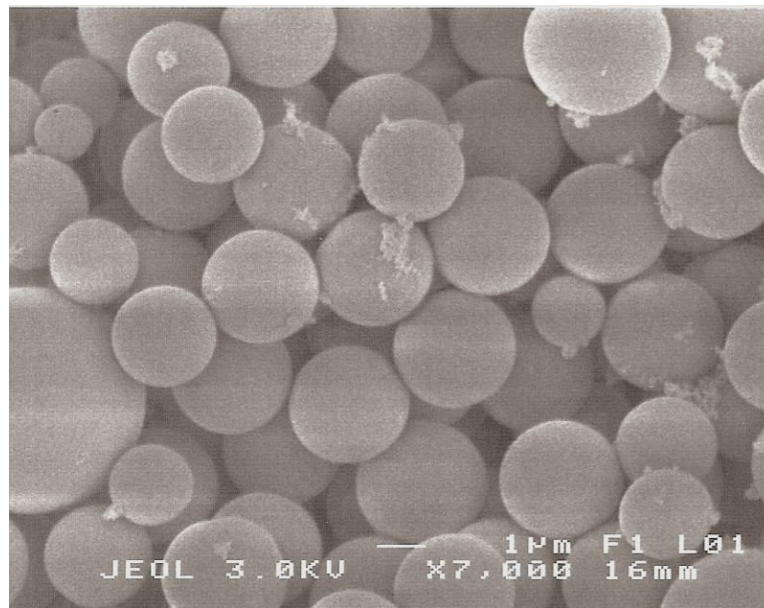
The first target of the study was to obtain 5 μm -microbeads of copolymer containing a high content of TIPA. From Fig. 3-6 one may notice a round shape of the copolymer only for 5% and 7% TIPA (in the feed)-containing copolymer, but in the latter case of a greater diameter, > 10 μm . Moreover, there is not observed a narrow distribution of the microbeads. The form of microbead disappears for a higher molar ratio. The copolymer tends to become an agglomerated amorphous mass, unavailable for the application desired.

Further, the synthesis of 95:5 and 93:7 copolymers was improved by changing the initiator, BPO, with a specific water-in-oil emulsion polymerisation initiator, potassium persulfate ($\text{K}_2\text{S}_2\text{O}_8$). $\text{K}_2\text{S}_2\text{O}_8$ initiator was introduced in the reaction as 0.5% vs. water (w/v), and the stirring rate was increased to 1000 rpm, for 6 hours. The other parameters of the reaction remained unchanged.

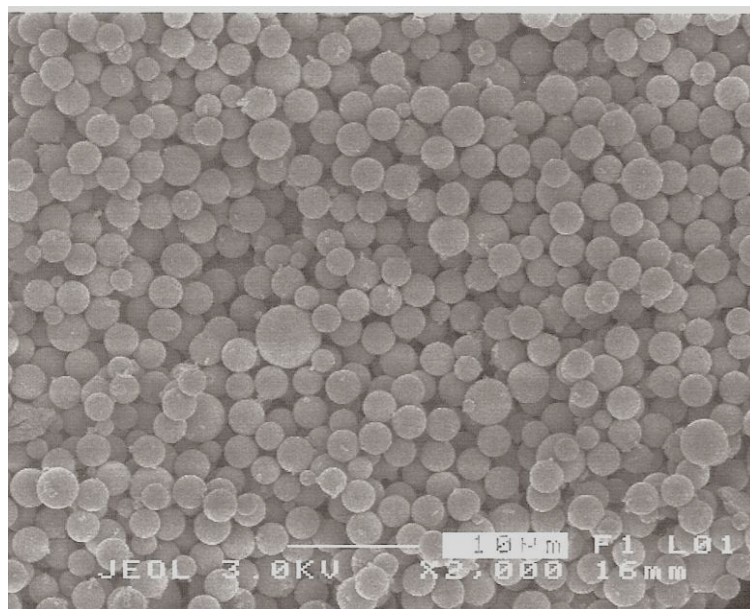
The result, presented in Fig. 3-7, proves that the initiator used highly improves the quality of the microbeads obtained: microbeads of 2-3 μm (in case of 95:5 ratio – Fig. 3-7 a)), 4-5 μm (for the 93:7 ratio – Fig. 3-7 b)), and a narrower distribution of the microbeads diameter, in case of 93:7 copolymer (Fig. 3-7 c)).



a)



b)



c)

Fig. 3-7. SEM microphotographs of p(MMA-co-TIPA) copolymers obtained: a) 95:5; b) 93:7; c) 93:7 as panoramic view of homogenous-size distribution, molar ratios in the feed.

3.3.3. Determination of reactivity ratios of the monomers in the binary system MMA-TIPA – a kinetic study

In the view of determination the reactivity ratios of the binary system MMA-TIPA, copolymerisations were performed at different compositions in the feed (Table 3-3). For each feed composition, there were extracted samples at different reaction time periods and conversions were determined.

Table 3-3

Feed compositions of the binary systems

Composition	Monomer 1	Monomer 2
1	0.2	0.8
2	0.4	0.6
3	0.6	0.4
4	0.8	0.2

The copolymers obtained were submitted to elemental analysis, in order to determine their molar composition. The results are given in Table 3-4.

Table 3-4

Results of the elemental analysis for the binary system MMA-TIPA

Binary system MMA-TIPA	Conversion (%)	Δt (min.)	Elemental analysis		
			N (%)	C (%)	H (%)
MMA:TIPA 0.2:0.8 conv. 1	0.3470	15	0	26.967	2.187
MMA:TIPA 0.2:0.8 conv. 2	0.6924	35	0	26.447	2.185
MMA:TIPA 0.2:0.8 conv. 3	0.7892	60	0	25.329	2.244
MMA:TIPA 0.4:0.6 conv. 1	0.2781	20	0	28.692	3.181
MMA:TIPA 0.4:0.6 conv. 2	0.4778	40	0	25.287	3.670
MMA:TIPA 0.4:0.6 conv. 3	0.56	60	0	27.190	3.826
MMA:TIPA 0.6:0.4 conv. 1	0.2028	20	0	41.710	4.442
MMA:TIPA 0.6:0.4 conv. 2	0.4529	50	2.190	52.320	0
MMA:TIPA 0.6:0.4 conv. 3	0.6135	120	0	31.431	3.530
MMA:TIPA 0.8:0.2 conv. 1	0.2036	20	0	39.773	5.443
MMA:TIPA 0.8:0.2 conv. 2	0.3963	40	0	40.501	5.248
MMA:TIPA 0.8:0.2 conv. 3	0.4933	60	0	40	5.680

Table 3-5

Calculated molar ratios for the binary system MMA-TIPA

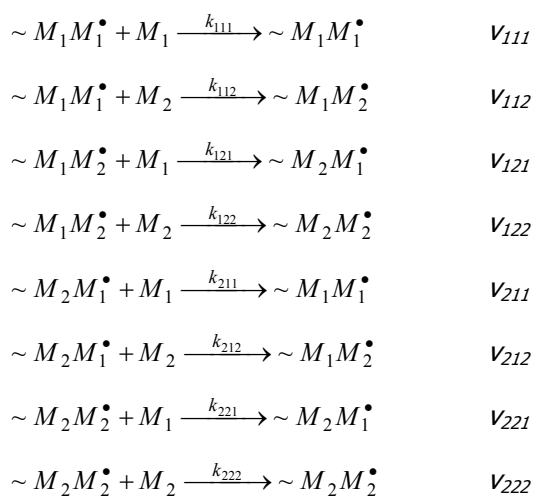
X_{MMA}^*	X_{TIPA}^*	%C	%H	X_{MMA}^{**}	X_{TIPA}^{**}
0.2	0.8	58.297	9.056	0.5454	0.4545
0.2	0.8	49.112	9.144	0.5633	0.4367
0.2	0.8	32.397	8.791	0.6296	0.3734
0.4	0.6	28.692	3.181	0.8379	0.1621
0.6	0.4	41.710	4.442	0.8016	0.1984
0.6	0.4	31.431	3.530	0.8500	0.1500
0.8	0.2	40.501	5.248	0.9753	0.0247

*composition of the monomers in the feed

**composition of the copolymer determined from elemental analysis

The composition in the feed is known, as well as the composition of the copolymers obtained and the correspondent conversions; therefore, the PROCOP software allowed the determination of the reactivity ratios. In the kinetic model the penultimate model was considered (8 types of propagation reactions) due to sterical effects (volume of TIPA comonomer), which affects the macroradicals' reactivity.

The kinetic scheme is presented below (where $M_1=[MMA]$ and $M_2=[TIPA]$, k_i = reactivity constants; v_i = reactivity rates).



The consumption rates of the two monomers being known, respectively admitting that the concentration of each type of propagating radical is constant, we obtain:

$$\frac{dM_1}{dM_2} = \frac{1+r_{21} \frac{M_1}{M_2} \cdot \frac{r_{11}M_1 + M_2}{r_{21}M_1 + M_2}}{1+r_{12} \frac{M_2}{M_1} \cdot \frac{r_{22}M_2 + M_1}{r_{12}M_2 + M_1}} \quad (1)$$

where $r_{11} = \frac{k_{111}}{k_{112}}$, $r_{21} = \frac{k_{211}}{k_{212}}$, $r_{12} = \frac{k_{122}}{k_{121}}$, $r_{22} = \frac{k_{222}}{k_{221}}$ (r_i = reactivity ratios).

The values obtained using the software were:

$r_{11}=4.89$

$r_{22}=0.051$

$r_{21}=31.83$

$r_{12}=0.053$

Following the reactivity ratios obtaining, the composition diagram for the binary system MMA-TIPA can be drawn (Fig. 3-8), using equation (1).

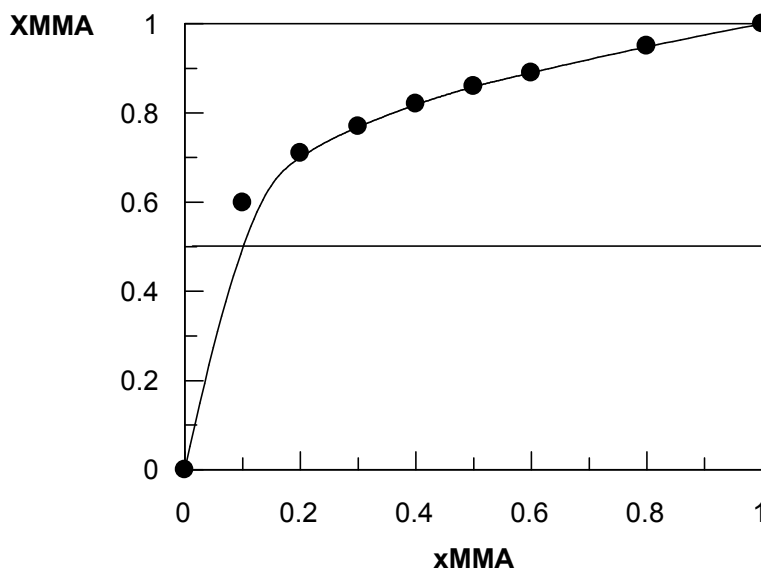


Fig. 3-8. Composition diagram of the binary system MMA-TIPA

The conclusion drawn from the analysis of the diagram above is that its' evolution is typical for a system where $r_1 > 1$ and $r_2 < 1$. Therefore, MMA-radicals present a higher reactivity during homopropagation against TIPA-radicals. The differential equation of Mayo-Lewis for copolymer composition describes the instantaneous composition (X_{MMA}) of the copolymer in function of the instantaneous feed composition (x_{MMA}) and relative reactivities. The equation shows that the two

monomers are being consumed at different rates. As a consequence, the feed composition continuously changes, enriching itself in the monomer less reactive.

For supplementary information (the integral form of the Mayo-Lewis equation giving a correlation among composition and conversion) the average values of r_1 and r_2 should be calculated in the composition interval analysed, using the equations of M. Berger and J. Kunz.

$$\bar{r}_1 = \frac{r_{21} \int_{f_1}^{f_2} \frac{r_{11}f + 1}{r_{21}f + 1} df}{\int_{f_1}^{f_2} df} \quad \text{and} \quad \bar{r}_2 = \frac{r_{12} \int_{f_1}^{f_2} \frac{r_{22} + f}{r_{12} + f} d\left(\frac{1}{f}\right)}{\int_{f_1}^{f_2} d\left(\frac{1}{f}\right)}$$

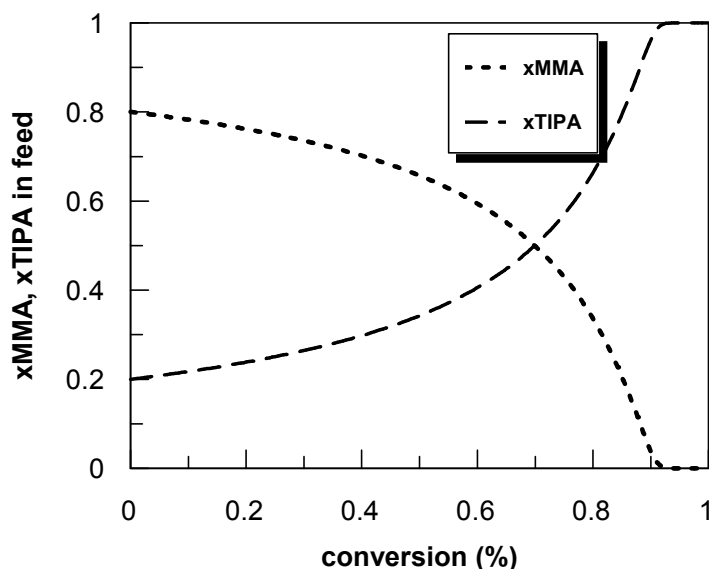
where $f = \frac{M_1}{M_2}$.

The average values obtained are:

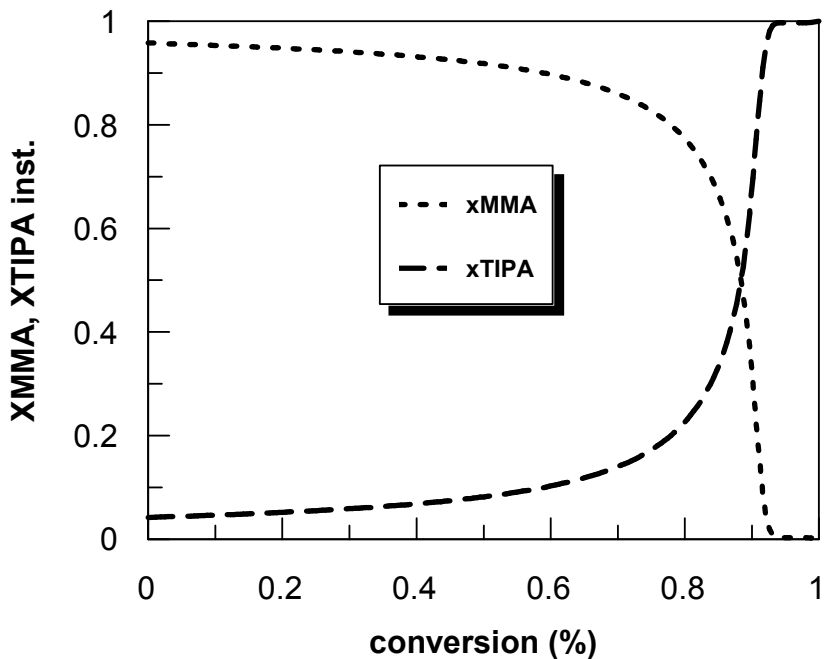
$$\bar{r}_1 = 5.49$$

$$\bar{r}_2 = 0.053$$

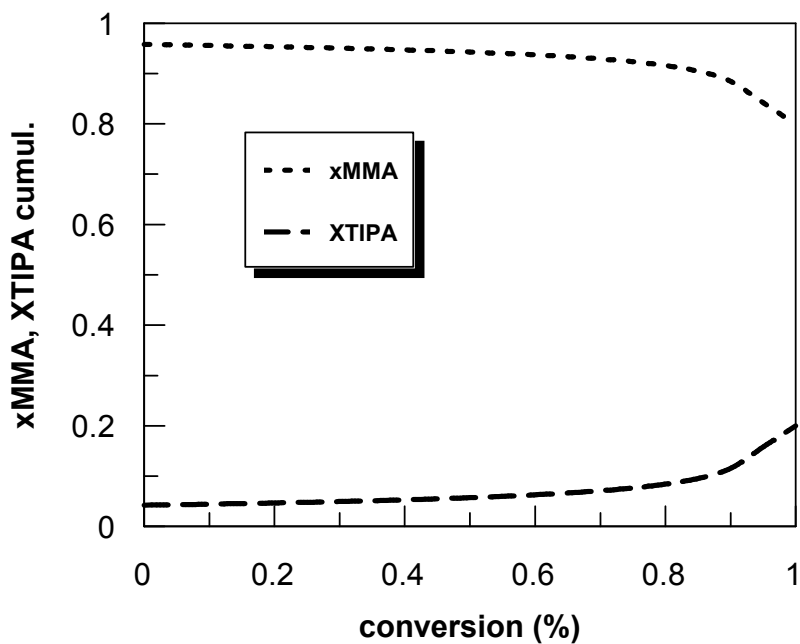
Integrating the Mayo-Lewis equation in the conversion interval [0...1], the following dependences for the $x_{\text{MMA}} = 0.8$ and $x_{\text{TIPA}} = 0.2$ defined feed were obtained. This feed composition was chosen due to the fact that this one has the composition the closest to 10% molar TIPA, which gave the best results from the synthesis and radioopacity point of view.



a) Feed composition versus conversion



b) Instantaneous copolymer composition versus conversion



c) Cumulative copolymer composition versus conversion

Fig. 3-9. Feed composition and copolymer compositions versus conversion

The analysis of the graphs above gives an increased reactivity of MMA-radicals towards homopropagation, comparatively with TIPA-radicals. This resolution is sustained by the values calculated for numerical average lengths of the two sequences.

$$l_{M1} = \frac{1}{P_{12}} = \frac{1}{0.42} = 2.38$$

$$l_{M2} = \frac{1}{P_{21}} = \frac{1}{0.82} = 1.21$$

In the following graph (Fig. 3-10), the evolution conversion vs. time is presented for the feeds analysed. It is noticed a decrease of the rate as the feed enriches in MMA.

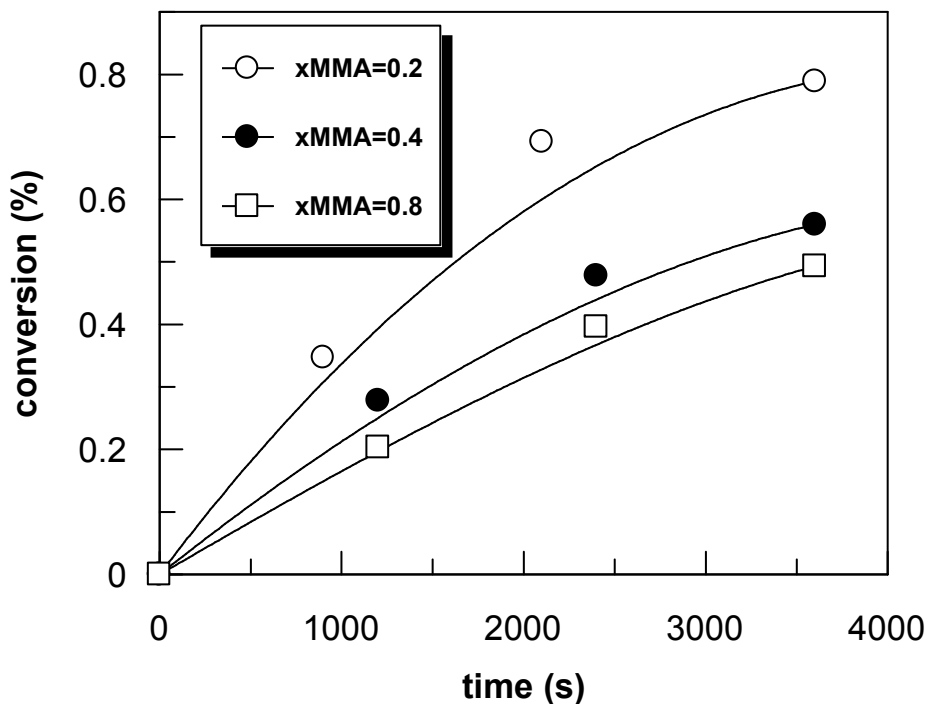


Fig. 3-10. Conversion versus time for the binary system MMA-TIPA

The molar composition of the copolymers obtained being calculated, initial copolymerisation rates can be also calculated (and expressed in mol/L·s). Although MMA-radicals reactivity is obviously superior to TIPA-radicals, a decrease of initial copolymerisation rate is noticed as the feed enriches in MMA. This unusual behaviour can be due to diffusion control on the interruption stage, accentuated by radical chains rigidisation because of TIPA units. Most likely, the rate determination stage for interruption is represented by segmental diffusion.

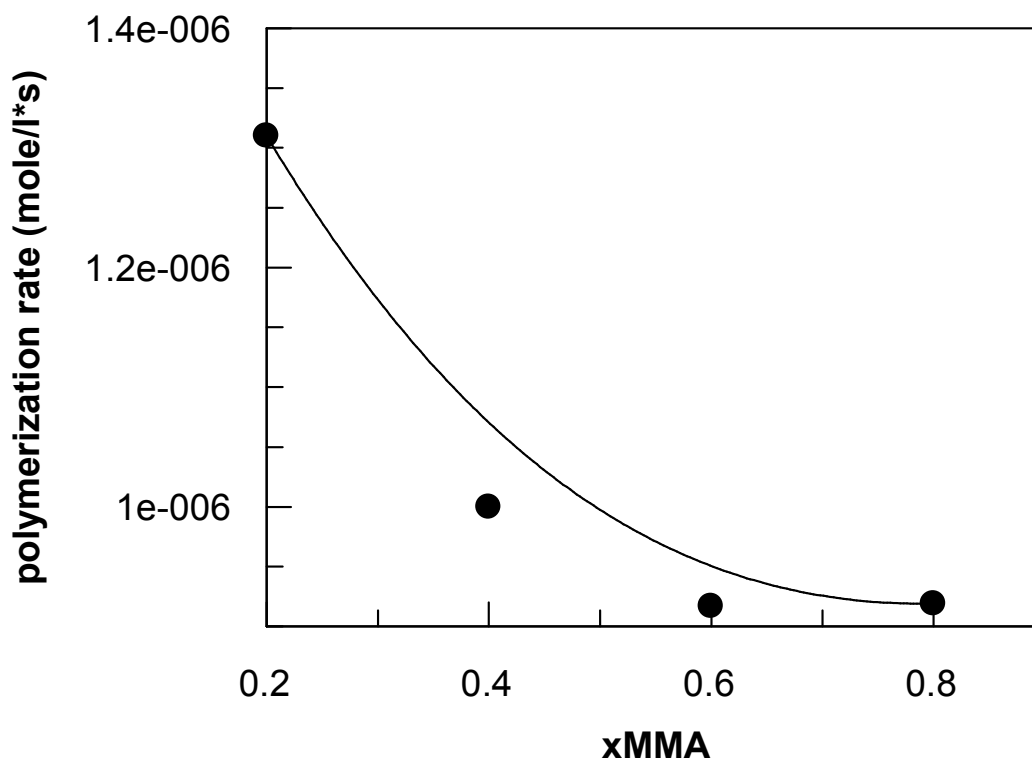


Fig. 3-11. Copolymerisation initial rate versus feed composition

3.3.4. *In vitro* mineralisation potential of the p(MMA-co-TIPA) copolymers

Mineralisation potential is a very important property of polymeric biomaterials, which greatly influences their application field. As stated before, the purpose of the iodine-containing microbeads would be used for tumoral detection. Therefore, calcification following tests should not occur.

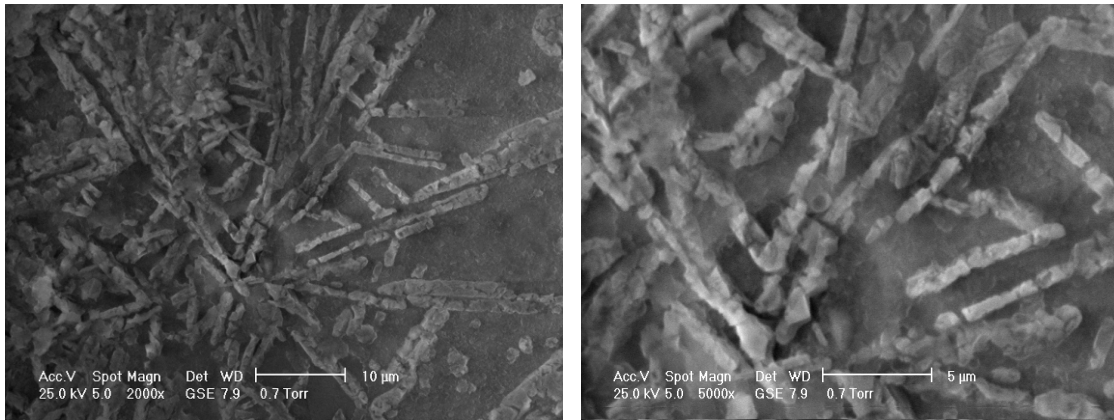
The Kokubo et al. (1990, 2006) method of *in vitro* evaluation was chosen. The procedure involves samples incubation in synthetic body fluid (SBF) in different concentrations. For the present test 1x SBF solution was chosen (Table 3-6).

Cylinder samples of p(MMA-co-TIPA) with TIPA 5 and 7% molar ratio in the feed were incubated in fresh solutions of 50 mL 1x SBF, at 37°C for 2 weeks, changing the medium every two days. After the test was finished, samples were washed with demineralised water and dried in an oven at 40°C. There were performed SEM and EDX analysis in order to quantify the results obtained (Fig. 3-12 and Fig. 3-13 and Table 3-7).

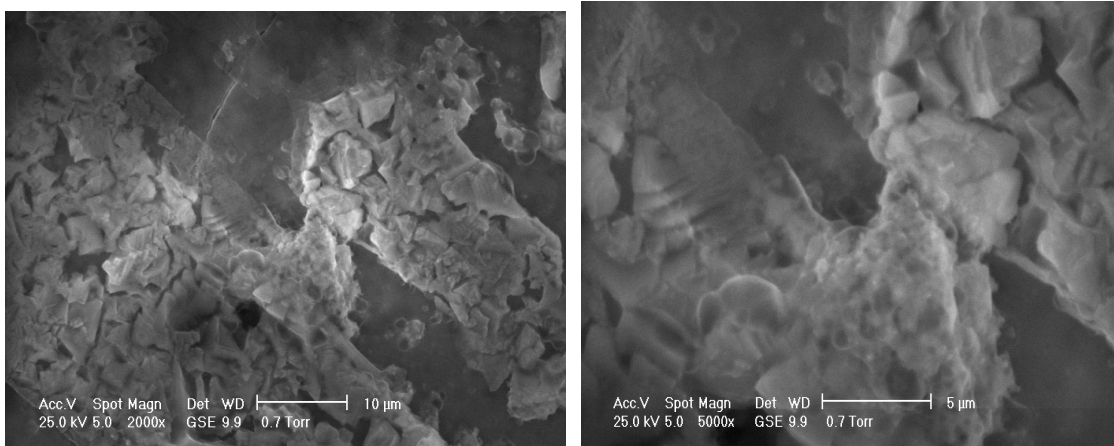
Table 3-6

Composition of the SBF in ions concentration (mM) versus human body plasma

Ion	SBF 1x (mM)	Human body plasma (mM)
Na ⁺	142.19	142.0
K ⁺	4.85	5.0
Mg ²⁺	1.5	1.5
Ca ²⁺	2.49	2.5
Cl ⁻	141.54	103.0
HCO ₃ ⁻	4.2	27.0
HPO ₄ ²⁻	0.9	1.0
SO ₄ ²⁻	0.5	0.5
pH	7.4	7.2-7.4

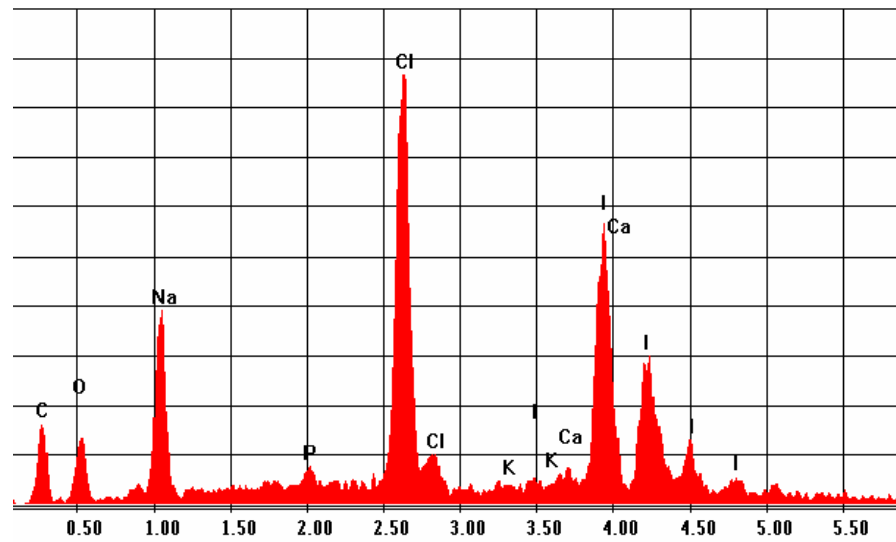


a)

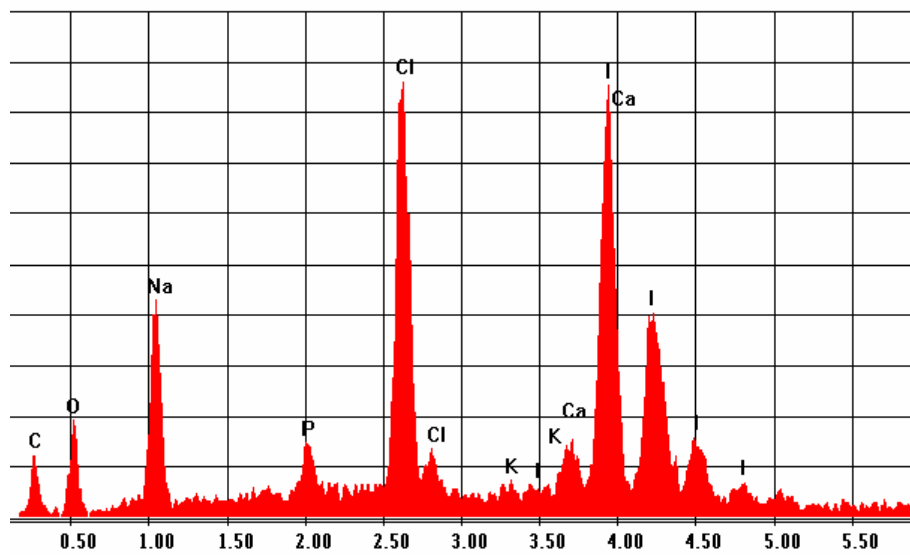


b)

Fig. 3-12. SEM microphotographs of p(MMA-co-TIPA) copolymers incubated in 1x SBF: a) 95:5; b) 93:7, molar ratios (views at 5 and 10 µm).



a)



b)

Fig. 3-13. EDX of p(MMA-co-TIPA) copolymers incubated in 1x SBF for 2 weeks: a) 95:5; b) 93:7, molar ratios.

From Fig. 3-12 one may observe that cylinder copolymers were obtained from bulk polymerisation. Mineral deposits of hydroxyapatite are not noticed and defective calcium phosphate-like minerals are slightly present. In this case, this is a positive result, otherwise possible obstruction of blood vessels might occur.

Table 3-7

Results of EDX analysis for p(MMA-co-TIPA) copolymers incubated in 1x SBF for 2 weeks

Element	Wt % (in function of the MMA:TIPA molar ratio in the feed)	
	95:5	93:7
C	37.59	24.7
O	10.55	11.18
Na	11.82	12.69
P	0.67	1.77
Cl	11.53	11.19
K	0.28	0.33
Ca	0.83	1.93
I	26.72	36.21
Total	100	100
Ca/P ratio*	1.09 <<1.67	1.24<1.67

*Ca/P ratio in hydroxyapatite ($\text{Ca}_{10}(\text{PO}_4)_6(\text{OH})_2$) is 1.67.

3.3.5. *In vitro* cytotoxicity evaluation of p(MMA-co-TIPA) copolymers

The materials tested in order to determine their biocompatibility were p(MMA-co-TIPA) copolymers with 95:5 and 93:7 molar ratios of the comonomers in the feed. In this view, an adapted method of *in vitro* cytotoxicity testing was used, on the L929 murine fibroblast cell line.

Indirect contact supposes interposition of a solid medium of DMEM (Dulbecco's Modified Eagle's Medium) containing 0.75% agar between cells and polymer. Cells were cultivated in DMEM culture medium supplemented with 10% bovine foetal serum, 1% L-Glutamine and antibiotics (penicillin and streptomycin). In order to obtain a homogenous distribution, cells were cultivated at a confluence of 25% of the surface in plates of 24 places in 1000 μ L/place and incubated for 72h at 37°C, in humidified atmosphere containing 5% CO₂, until necessary experimental density is attained. At a 95% microscopically observed confluence, the culture medium was replaced with 1000 μ L DMEM containing 0.75% agar, 10% bovine foetal serum, 1% L-Glutamine and antibiotics (penicillin and streptomycin) at a temperature of 40°C (in order to maintain it as a liquid). After agar polymerisation, samples were put on its surface, negative witness consisting in a polypropylene fragment for cellular cultures. Cells were incubated for 24 h at 37°C, in humidified atmosphere and 5% CO₂.

Due to the solid status of the samples and mechanical damage risk onto the cells, the indirect contact method was used. In order to eliminate the infection risk of the cellular cultures, polymers were first sterilized overnight under UV light.

Cellular viability was determined with 3-(4,5-dimethylthiazol-2-yl)-2,5-diphenyltetrazolium bromide (MTT). This test is based on the capacity of dehydrogenases in viable cells mitochondria of converting the soluble yellow tetrazolium salt (MTT) in insoluble formazan, which accumulates as violet crystals in the viable cells.

After incubation in the presence of the polymers, cells were microscopically examined in order to detect visible signs of cytotoxicity, such as modification of external shape, membrane disruption (cellular lysis) or cellular components aspect or dimensions. Afterwards, MTT was added (100 μ L/place from a 5 mg/mL solution in TFS) and plates were incubated for 3h.

Further there are presented representative images of the samples (Fig. 3-14).

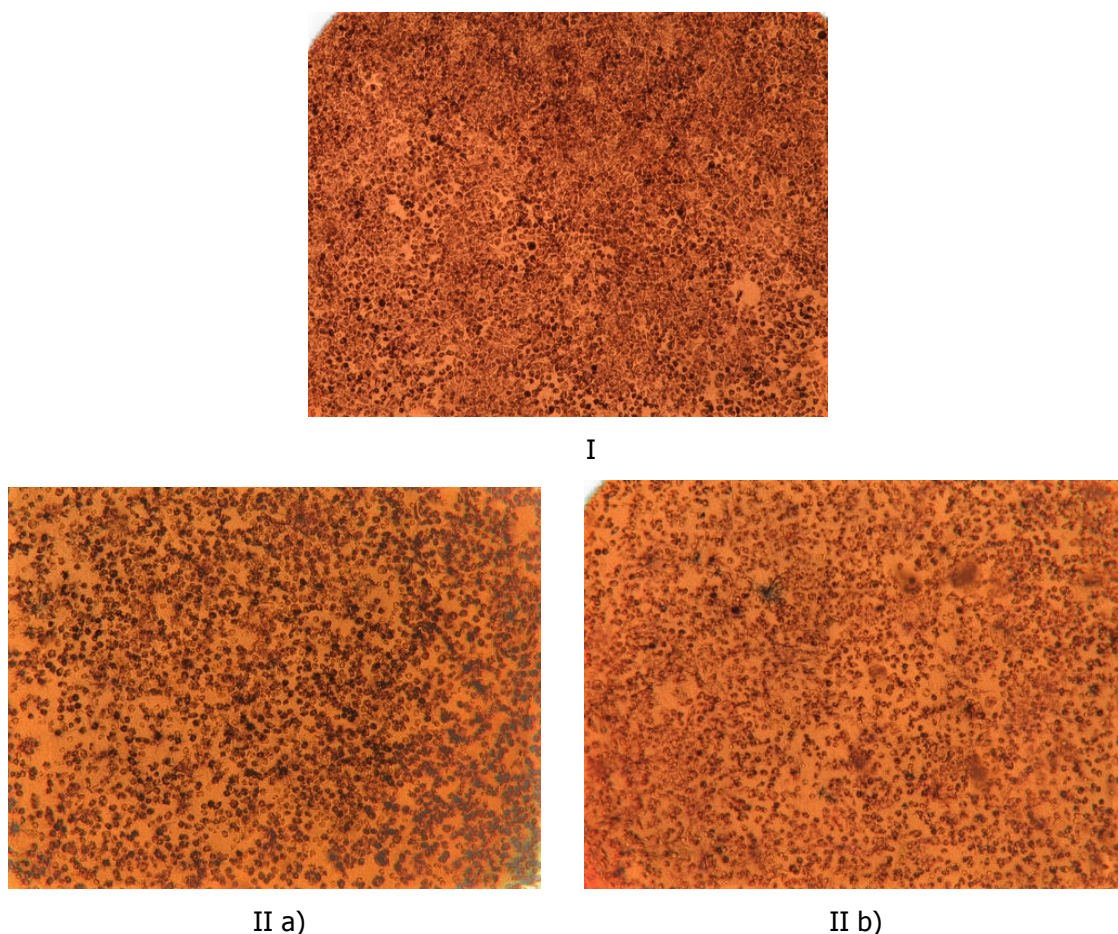


Fig. 3-14. Microscopic image of L929 cells in culture after MTT adding: I) negative control; II) positive control, incubated with: a) 95:5; b) 93:7, molar ratios p(MMA-co-TIPA).

The *in vitro* tests of cytotoxicity made on fibroblast murine L929 cell line gave adequately results for both of the compositions tested, presenting minimal adverse effects on cell morphology and viability. It is easy to remark that L929 cell line of mouse fibroblasts maintains its initial morphology, the polymers tested not presenting toxic effects.

3.4. Conclusions and perspectives

Different compositions of p(MMA-co-TIPA) were synthesised and physico-chemically and biologically characterised through: FT-IR, SEM, EDX, elemental analysis, *in vitro* biocompatibility and calcification tests. There were obtained microbeads of 2-3 μm for a monomer composition in the feed of 95:5, and of 4-5 μm for 93:7. Reactivity ratios of the comonomers were determined. MMA reactivity is obviously superior to TIPA, and a decrease of initial copolymerisation rate is noticed as the feed enriches in MMA. p(MMA-co-TIPA) is not appropriate for preparing drug loading matrices because TIPA presents low reactivity. Moreover, such a matrix could block the capillary vessels due to their big dimensions.

Their biocompatibility, low-calcification potential, shape and narrow distribution, good radio-opacity of the microbeads make p(MMA-co-TIPA) very good micro-carrier systems for tumoral detection and imaging.

Chapter 4

HEMA-based microbeads for drug delivery systems: optimisation of the synthesis and *in vitro* tests

Data presented in:

T. Zecheru, C. Zaharia, G. Mabillean, D. Chappard, C. Cincu, *New HEMA-based polymeric microbeads for drug delivery systems*, Journal of Optoelectronics and Advanced Materials, Vol.3, No.8, 2006, p. 1312-1316.

Teodora ZECHERU, Catalin ZAHARIA, Guillaume MABILLEAN, Daniel CHAPPARD, Corneliu CINCUI, *New micron ad nano-sized polymer particles for controlled drug release*, The 4th National Conference „New Research Trends in Material Science ARM-4” – Proceedings, Volum II, September 4-6 2005, Constanta, Romania.

Teodora Zecheru, Aurora Salageanu, Corneliu Cincu, Daniel Chappard, Amar Zerroukhi, Poly(HEMA-co-MOEP) microparticles: optimisation of the preparation method and *in vitro* tests, UPB Sci. Bull., Series B, Vol. 70, No. 1 (2008) 45-54.

4.1. Introduction

Efficient drug delivery remains an important challenge in medicine: continuous release of therapeutic agents over extended time periods in accordance with a predetermined temporal profile; local delivery at a constant rate to the tumour microenvironment to overcome much of the systemic toxicity and to improve antitumour efficacy; improved ease of administration, and increasing patient compliance required are some of the unmet needs of the present drug delivery technology. Microfabrication technology has enabled the development of novel controlled-release microchips with capabilities not present in the current treatment modalities.

Biopolymers involvement in the cellular metabolism and the possibility of a certain structural, electronic and sterical physiological effect achievement between the drug and the macromolecular structure explain the use of polymeric compounds in therapeutics.

Macromolecular compounds, characterised by a functional optimal combination meant to satisfy the enormous amount of biocompatibility, solubility, biological pH, catalytically stimulation or low toxicity requests, might offer valuable solutions.

Without elucidating all the biological active polymers mechanisms and improved technologies, without a great number of substances disposals, clinical experimental results show the great value of some natural and synthetic macromolecular compounds as drugs and as drug conditioning additives. In this way, polymer use in pharmacology leads to decreased toxicity, better physiological effects, controlled position effects, etc.

There were also recorded some remarkable results in the polymer synthesis with biopolymer-like structure, as polypeptides, polynucleotides, thiol- and imidazol- containing polymers, showing different physiological effects.

Micro and nanotechnologies and micro and nanostructured materials develop applications in different areas of interest, the most important being in medicine and biology, as drug delivery systems in the damaged tissue or organ.

This chapter presents the obtaining of some micropolymeric beads for further use as containers for physically or chemically bound drugs, in order to obtain the drug orientation to certain organs. When these particles reach the damaged tissue or organ, drugs are slowly released at a certain rate by diffusion or splitting (enzymatically or chemically).

An area of interest is that of the ligatures functionalised nanocontainers for cellular receptors. A drug-containing polymeric particle will be surface functionalised by a ligature attached to a specific surface receptor, followed by endocytosis. The proof of the nanocontainers endocytosis is given by the

introduction of a fluorescent dye into the polymeric particle and the observation of the cell fluorescence after the nanocontainers endocytosis.

In the last few years, 2-hydroxyethyl methacrylate (HEMA) has been considered one of the most interesting synthetic monomers for general biopolymer purposes. HEMA-based compounds are very well tolerated by the human organism. Conjugation with some specific drugs would increase the accumulation of these microbeads into tumours and would decrease the drug toxicity for other organs.

In recent papers, there have been presented opposite opinions concerning the copolymer system p(2-hydroxyethyl methacrylate-co-methacryloyloxyethyl phosphate) (p(HEMA-co-MOEP)). The incorporation of negatively charged groups, such as phosphate, into the structure of biopolymers has been widely proved to be a method for inducing mineralization or, on the contrary, in a more recent paper, that this system presents an inhibitory effect of the phosphate ions on the deposition of calcium and phosphate phases on methacrylic-based copolymers. The reason for choosing p(HEMA-co-MOEP) as a possible drug delivery matrix is based exactly on this idea.

Another polymer system tackled is p(HEMA-co-GuaMA), where GuaMA is 2-methacrylic acid 3-guanidinopropyl ester. The guanidinium group is highly basic ($pK_a = 12.5$), and fully protonated at physiological pH. Therefore, synthetic polymers (e.g., poly(meth)acrylates) bearing guanidinium side chains should be able to complex and condense drugs, proteins, DNA into small particles. When compared to polymethacrylates, other polymers, such as polypeptides, have a much lower transfection efficiency, thus changing the backbone of poly(arginine) to a methacrylate may be advantageous. This may result in increased transfection levels.

In this respect, the aim of the present study was to obtain copolymer microbeads using the dispersive polymerisation. Microbeads obtained were further analysed for potential biomedical application.

4.2. Experimental

4.2.1. Synthesis of 2-Methacrylic Acid 3-Guanidinopropyl Ester (GuaMA) monomer (Funhoff et al., 2004)

Materials. The following materials were used as received: 3-amino-1-propanol (Fluka), 2-ethyl-2-thiopseudourea hydrobromide 98% (Aldrich), methacryloyl chloride 97% (Sigma), acetonitrile and ethyl acetate (Merck).

2-Guanidinopropanol was synthesized as follows (Fig. 4-1 a)). 3-aminopropanol (0.641 g = 8.54 mmol) was added dropwise to 2-ethyl-2-thiopseudourea hydrobromide (1.58 g = 8.54 mmol) in a 10 mL flask. After 5 min. of stirring, 1 mL demineralised water was added. The resulting solution was stirred overnight at room temperature. Next, water was removed under reduced pressure to obtain a

white solid, which was further dried. Yield of the guanidinopropanol obtained was 1.67 g, 8.43 mmol, 99.8%.

2-Methacrylic acid 3-guanidinopropyl ester (GuaMA) was synthesized as follows (Fig. 4-1 b)). Methacryloyl chloride (0.892 g = 8.50 mmol) was added to guanidinopropanol (1.67 g = 8.43 mmol) dissolved in acetonitrile (10 mL) and stirred at room temperature for 48 hours. Acetonitrile was removed under reduced pressure, resulting in a white solid. The solvent was removed under reduced pressure, resulting in a light yellow solid, the HCl salt of the monomer, which was recrystallized in ethyl acetate, yielding 1.04 g (46%).

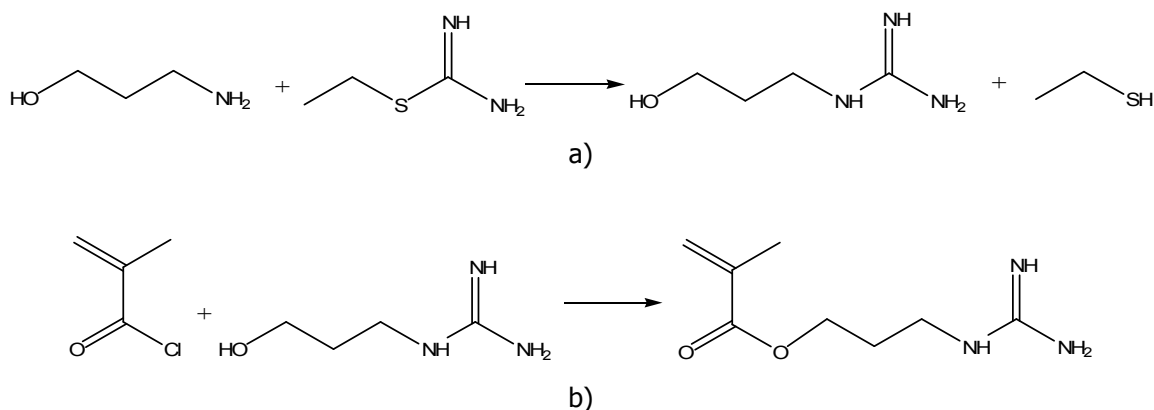


Fig. 4-1. Chemical reactions for GuaMA synthesis: a) intermediary reaction – synthesis of guanidinopropanol; b) synthesis of GuaMA.

4.2.2. Synthesis of the polymers

Materials. 2-hydroxyethyl methacrylate (HEMA), methacryloyloxyethyl phosphate (MOEP), benzoyl peroxide (BPO), 2-butanol, ethylenglycol dimethacrylate (EGDMA), ethyl eosin were used, all these reagents being purchased from Sigma-Aldrich. 2-methacrylic acid 3-guanidinopropyl ester (GuaMA) was prepared as previously described. Chemical structures of the monomers are presented in Fig. 4-2.

The solvents, toluene and diethyl ether, were provided from Chimopar, Bucharest, polybutadiene (pBu) and three star copolymers styrene-butadiene (pBuSt): 40% styrene, 48% in the 1,2 pBu block (901), 40% styrene, 30% in the 1,2 pBu block (902), and 45% styrene, 9% in the 1,2 pBu block (905) as stabilising agents, from ICECHIM Bucharest. Ethyl eosin was purchased from Merck.

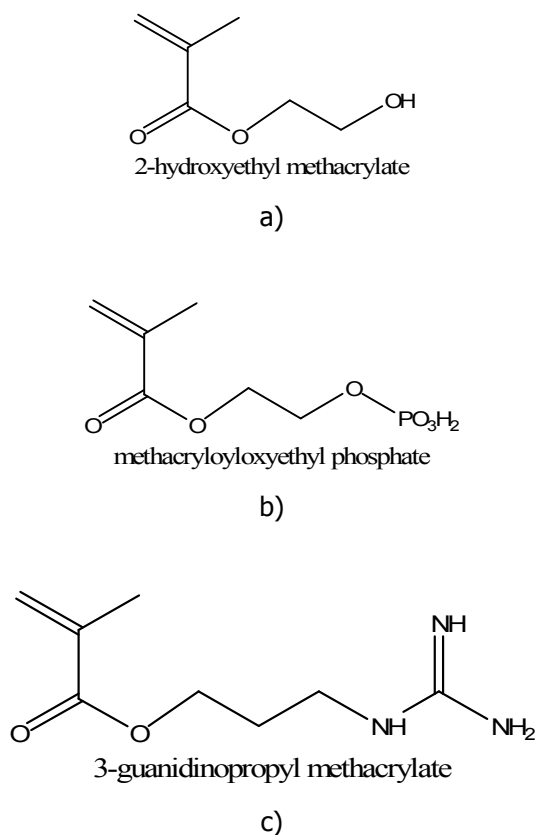


Fig. 4-2. Chemical structures of the comonomers used: a) HEMA; b) MOEP, and c) GuaMA.

The emulsifiers used, Brij 35 (Polyoxyethylene(23) lauryl ether, HLB Number (Hydrophilic-Lypophilic Balance): 16.9), Tween 60 (Polyoxyethylene(20) sorbitan monostearate, HLB: 15.0), Tween 80 (Polyoxyethylene(20) sorbitan monooleate, HLB: 14.9) and sodium dodecyl sulfate (DDSNa, HLB: 40), were purchased from Sigma-Aldrich.

The initiator BPO was purified by recrystallisation from ethanol and the comonomers were distilled under reduced pressure before use.

Ethyl eosin. Fluorescence stains and dyes are frequently used in biology and medicine to highlight structures in biological tissues for viewing with the aid of different microscopes.

Ethyl eosin, $C_{22}H_{11}O_5Br_4Na$ or tetrabromo derivate of fluorescein, is a fluorescent red or brown potassium or sodium salt dye resulting from the action of bromine on fluorescein, used as a biological stain and in pharmaceuticals for examination under the microscope (Fig. 4-3).

There are actually two very closely related compounds commonly referred to as eosin. Most often used is eosin Y (also known as eosin Y ws, eosin yellowish, Acid Red 87, bromoeosine, bromofluoresceic acid); it has a very slightly yellowish cast. The other eosin compound is eosin B (eosin bluish, Saffrosine, Eosin Scarlet, or imperial red); it has a very faint bluish cast. The two dyes

are interchangeable, and the use of one or the other is a matter of preference and tradition. Eosin is an acidic dye and is observed in the basic parts of the cell, i.e. the cytoplasm.

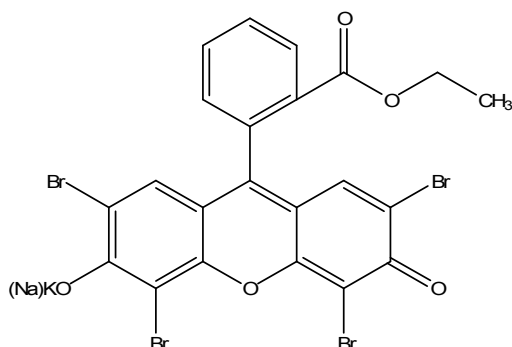


Fig. 4-3. Chemical structure of ethyl eosin.

Ethyl eosin was introduced in the polymer in order to be able to track the microbeads and their distribution inside body organs.

Synthesis procedure. The general method used for the synthesis of HEMA-containing microparticles was described previously (Takahashi et al., 1996), and improved by our group.

A 0.5% (w/v) solution of stabilising agent (5% (w/w) vs. monomer) in toluene was introduced into a three-neck reactor. At 40°C and while stirring, the 2-butanol was slowly introduced (toluene/2-butanol vol. ratio variations around 40/60 were chosen). Separately, a solution containing the monomer or the comonomers was prepared (HEMA:MOEP/GuaMA = 95:5 and 90:10 (mol/mol)), initiator (BPO) (5×10^{-3} mol/L in the solution), and cross-linking agent (EGDMA) (2% vs. comonomers), fluorescent dye (ethyl eosin) (0.25% (w/w) vs. monomer). This second solution was added dropwise to the first one, under stirring, increasing the temperature to 70°C and the stirring rate to 800 rpm. Polymerisations were performed in a water-bath and under nitrogen atmosphere. Installation used is presented in Fig. 4-4. An optimal result of the reaction was noticed after 6 hours.

The homopolymer and the copolymers obtained were washed twice with toluene and with diethyl ether, in order to remove any traces of unreacted monomer or other organic residue with low molecular weight. The microbeads were then dried at 37-38°C for 24 hours and sieved.

For the dispersion of the microbeads in water, several emulsifiers for the beads dispersion were verified: Brij 35, Tween 60, Tween 80 and DDSNa. Saline solutions of 20 g NaCl / L distilled water and of 9 g NaCl / L distilled water were also verified.



Fig. 4-4. Installation used for suspension polymerisation.

Characterisation of the microbeads. In order to characterise the microbeads obtained by dispersive polymerisation, Fourier Transform Infrared Spectroscopy (FT-IR), Scanning Electron Microscopy (SEM) and Fluorescence Optic Microscopy (FOM) were used.

FT-IR analysis was performed with a Shimadzu spectrophotometer. All samples were mixed and ground with spectroscopic grade potassium bromide prior to being placed in the sample cell, and the diffuse reflectance spectra were scanned over the range of $400\text{-}4000\text{ cm}^{-1}$.

SEM was performed on a Philips XL30 - ESEM Turbo Molecular Pump (TMP), at 20 keV. The samples were first carbon-coated.

Fluorescence imaging was carried with a Zeiss fluorescence microscope.

Elemental analysis was performed in order to establish the chemical structure of the copolymer, using a LECO CHN2000, MI, USA instrument.

Swelling rate was carried out on samples of copolymers obtained by bulk polymerisation, in triplicate, using a solution of 9 g/L NaCl in distilled water, for three days at 37°C.

In vitro cytotoxic effect of the polymers obtained was evaluated. For the *in vitro* tests, the microbeads were first exposed to UV light (long wave UV, 360 nm, 12W) for 8 hours.

It was used a murine fibroblasts L929 cell line, which was cultivated in culture medium (DMEM), supplemented with calf fetal serum and antibiotics. The cells culture was incubated in thermostat at 37°C, for a few days in the presence of 5% CO₂ and was examined daily during three days.

In both of the methods the cells were microscopically examined for detecting cytotoxicity visible signs, cellular lysis or cellular components dimensions and conformation.

For cytotoxicity evaluation, besides microscopically examination, the cellular viability it was also quantified, using a Multiskan MCC/340 P Version 2.32, in absorbance mode, continuous movement. All tests were performed in triplicate.

In vivo tests. The research was approved by the University Animal Care Committee. Wistar rats were used (18-19 weeks old, from Charles River, Cléon, France, 300 ± 52 g weight), conditioned to local vivarium for two weeks (24°C and 12h/12h light/dark cycles). The animals received standard test food (UAR, Villemoison sur Orge, France) and water *ad libitum*.

For the injection into rats, a 0.005 g/ml emulsifying agent concentration was used. The following recipe was used: carboxymethyl-cellulose 1.25%, mannitol 4%, humectation and emulsifier agent Tween 80 1%, normal saline solution (9 g/L NaCl diluted in distilled water) 93.75%. For an optimal use, this solution was diluted 10 times. All the reagents used had pharmaceutical purity.

4.3. Results and discussion

pHEMA, p(HEMA-co-MOEP) and p(HEMA-co-GuaMA) microparticles with 5 and 10 molar ratio of the comonomers in the feed were synthesised by suspension polymerisation and were characterised by several specific methods. For easiness, these copolymers will be mentioned as p(HEMA-co-MOEP5%), respectively 10%, and p(HEMA-co-GuaMA5%), respectively 10%.

The behaviour of several solvent/non-solvent ratios and of the different stabilising agents chosen was verified, in order to obtain homogenous 1 µm-pHEMA particles with a narrow size distribution (Table 4-1). The results obtained for pHEMA conducted to further use in the optimisation synthesis study only pBu, pBuSt 902 and pBuSt 905 as stabilising agents.

4.3.1. SEM analysis

SEM was used to confirm the quality, size diameter and distribution of the polymers obtained. Microphotographs of p(HEMA), p(HEMA-co-MOEP) 5 and 10% and p(HEMA-co-GuaMA) 5 and 10% are presented in Fig. 4-5 to 4-7.

Table 4-1

Experimental data for the synthesis of pHEMA microbeads

No. sample	Toluene/2-butanol (vol. ratio)	Stabilising agent (g/100 mL toluene)	Conclusions
1.	40/60	0.5 pBu	2- μ m agglomerates of smaller particles
2.	40/60	0.5 pBuSt 901	Agglomerated particles
3.	40/60	0.5 pBuSt 902	4-5 μ m particles
4.	40/60	0.5 pBuSt 905	3 μ m well-defined particles
5.	35/65	0.5 pBu	1.5- μ m agglomerates of smaller particles
6.	42.5/57.5	0.5 pBuSt 905	1.1 μ m average diameter of the particles
7.	45/55	0.5 pBuSt 905	0.95 μ m average diameter of the particles; very good distribution of the particles

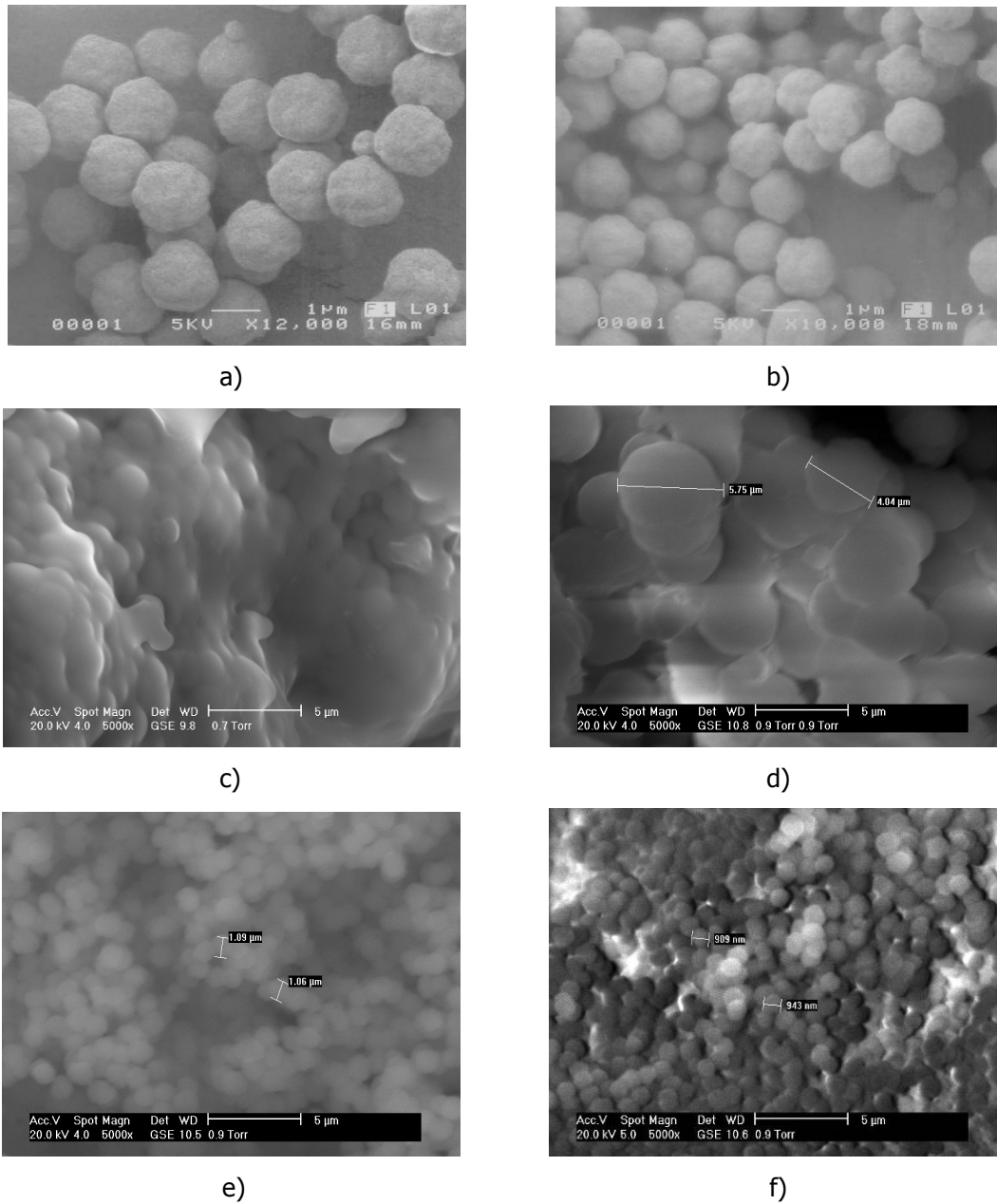


Fig. 4-5. SEM for pHEMA obtained using: a) pBu and 40/60 toluene/2-butanol ratio; b) pBu and 35/65 toluene/2-butanol ratio; c) pBuSt 901 and 40/60 toluene/2-butanol ratio; d) pBuSt 902 and 40/60 toluene/2-butanol ratio; e) pBuSt 905 and 42.5/57.5 toluene/2-butanol ratio; f) pBuSt 905 and 45/55 toluene/2-butanol ratio.

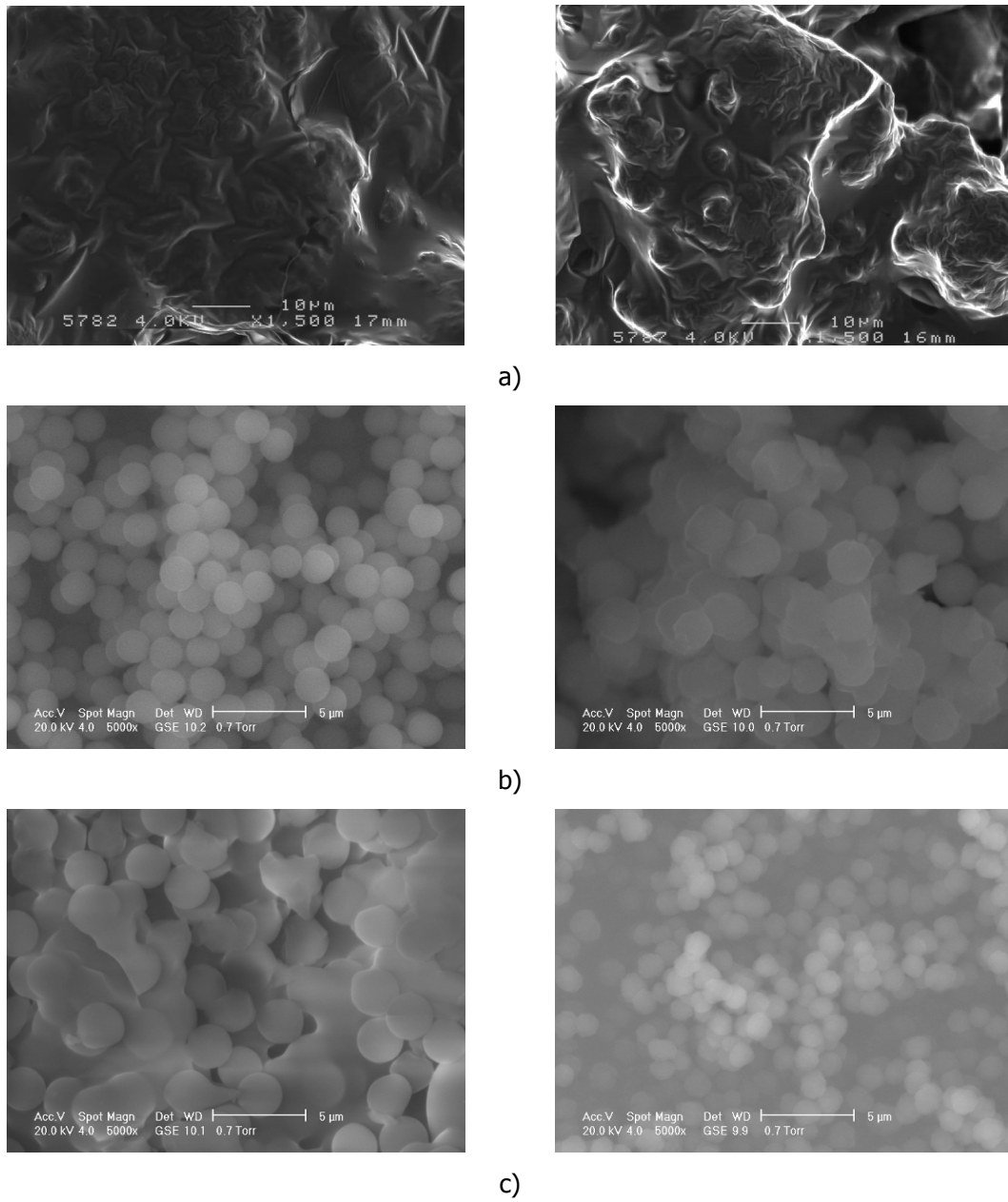


Fig. 4-6. SEM for p(HEMA-co-MOEP) 5% (left side) and 10% (right side) obtained using: a) pBu and 40/60 toluene/2-butanol ratio; b) pBuSt 905 and 42.5/57.5 toluene/2-butanol ratio; c) pBuSt 905 and 45/55 toluene/2-butanol ratio.

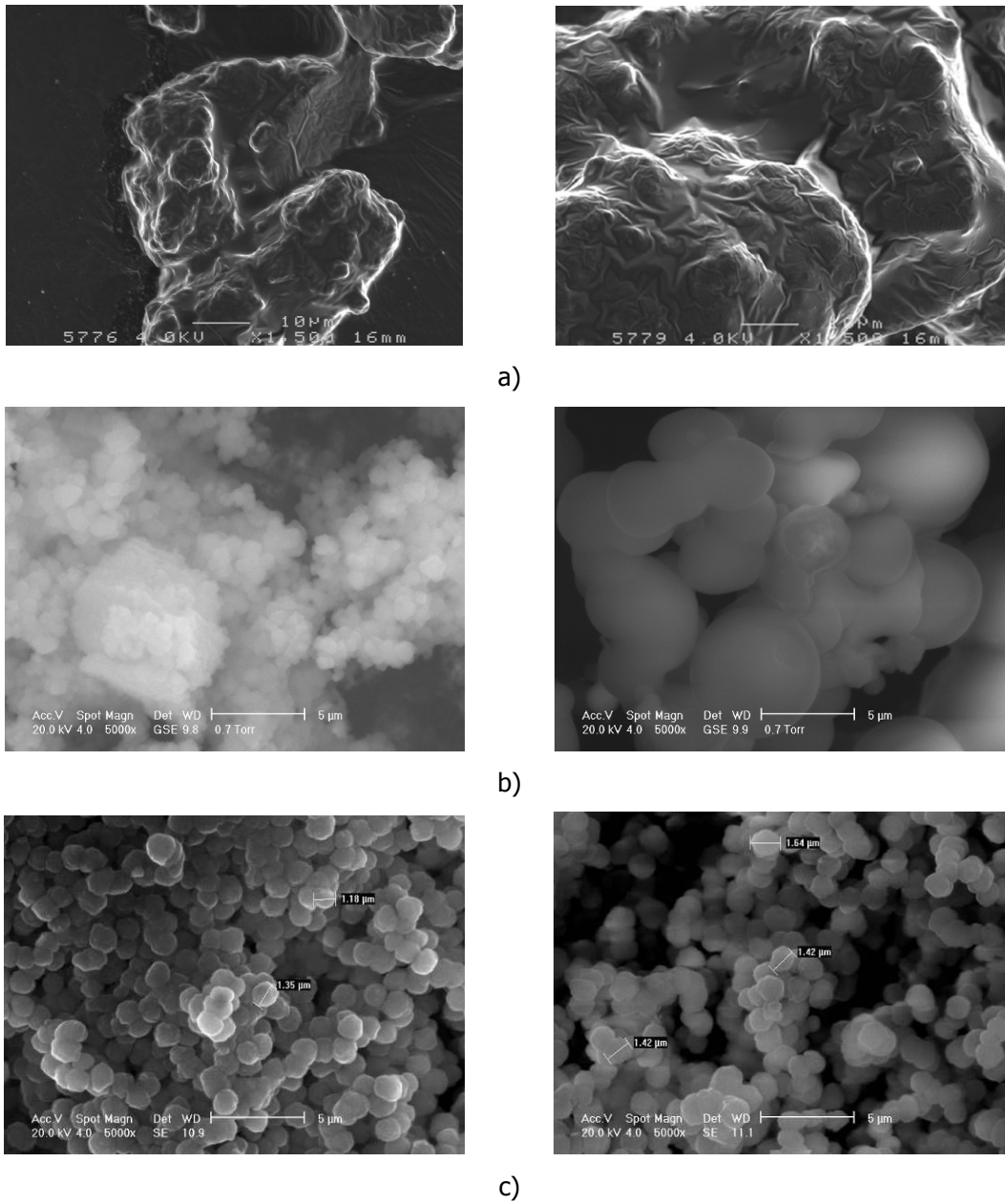


Fig. 4-7. SEM for p(HEMA-co-GuaMA) 5% (left side) and 10% (right side) obtained using: a) pBu and 40/60 toluene/butanol ratio; b) pBuSt 902 and 40/60 toluene/butanol ratio; c) pBuSt 905 and 45/55 toluene/butanol ratio.

An average polymer diameter distribution versus toluene-2-butanol ratio, where pBuSt 905 was employed, is presented in Fig. 4-8.

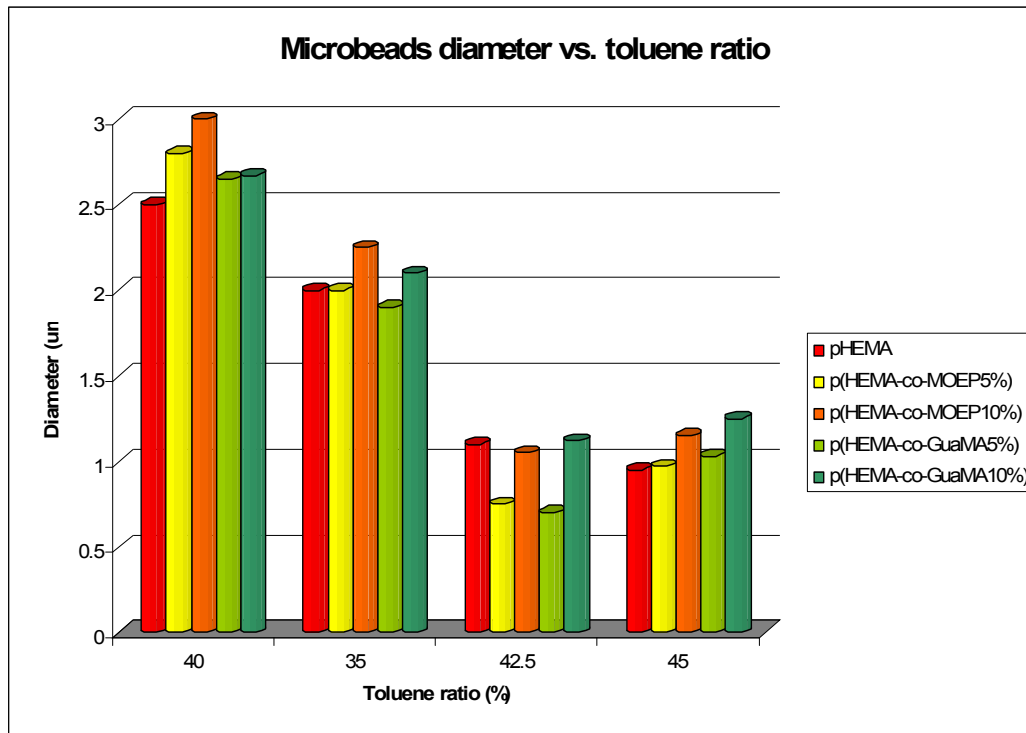


Fig. 4-8. Microbeads average diameter (μm) versus toluene ratio in the mixture toluene-2-butanol for: a) pHEMA; b) p(HEMA-co-MOEP5%); c) p(HEMA-co-MOEP10%); d) p(HEMA-co-GuaMA5%); e) p(HEMA-co-GuaMA10%).

The best results, meaning $\sim 1\text{-}\mu\text{m}$ average diameter well-defined particles, were obtained using pBuSt 905, for a toluene/2-butanol volume ratio of:

- 42.5/57.5 and 45/55 in case of pHEMA;
- 42.5/57.5 in case of p(HEMA-co-MOEP5%) and p(HEMA-co-GuaMA5%);
- 45/55 in case of p(HEMA-co-MOEP10%) and p(HEMA-co-GuaMA10%).

4.3.2. FT-IR analysis

FTIR spectra present specific absorption bands of polymer functions: pHEMA (3435, 2989, 1733, 1267, 1164 cm^{-1}), p(HEMA-co-MOEP) (3488, 3100, 2924, 2864, 1742, 1240, 1081, 802, 685 cm^{-1}), p(HEMA-co-GuaMA) (3410, 3161, 2947, 2885, 1728, 1666, 1454, 1280, 1159, 1074, 748 cm^{-1}).

4.3.3. Swelling behaviour

The swelling rate of the copolymers obtained is a very useful parameter in the field of the controlled release, being noticed the fact that cross-linked microparticles swell to a certain extent (Fig. 4-9). Also, in comparison with pHEMA microparticles (55% molar water uptake ratio), the copolymers swell less ($\sim 48\%$ in case of p(HEMA-co-MOEP10%)), which gives us information about the cross-links created in the copolymer and the hydrophobicity of the comonomers used.

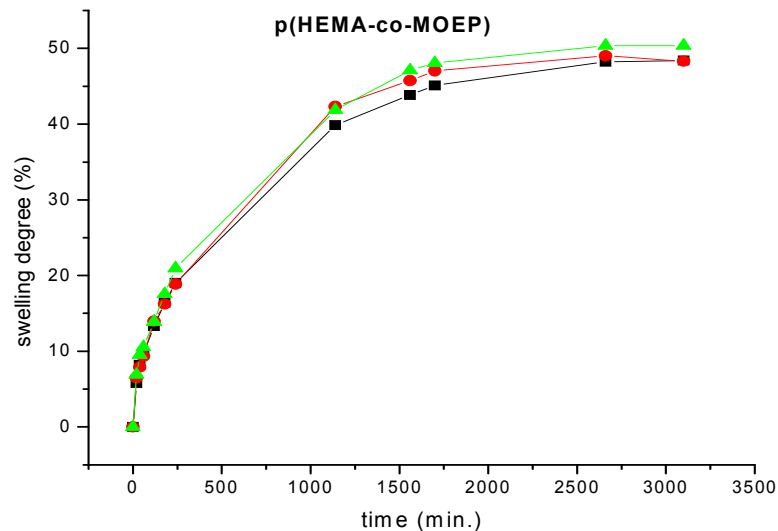
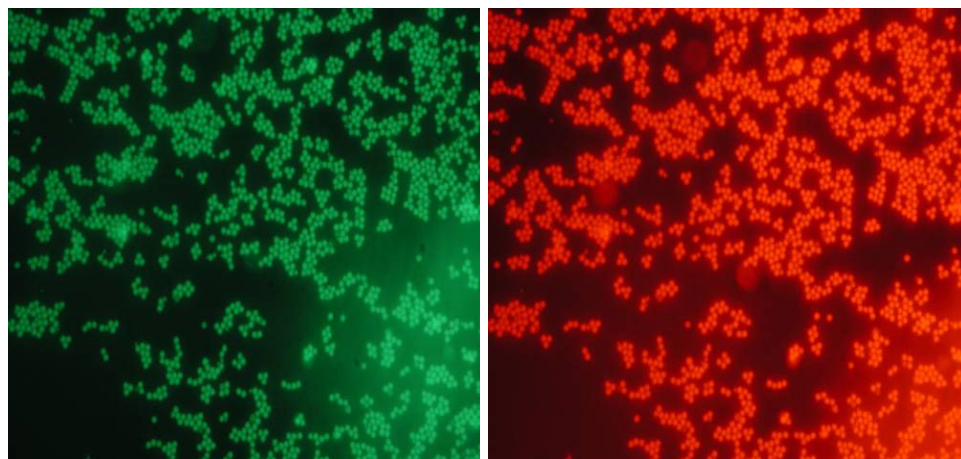


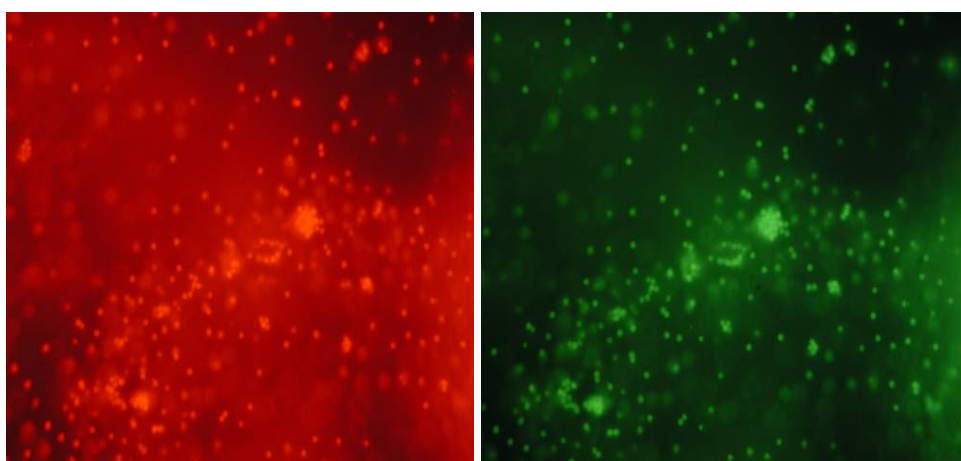
Fig. 4-9. Swelling rate of p(HEMA-co-MOEP10%).

4.3.4. FOM analysis

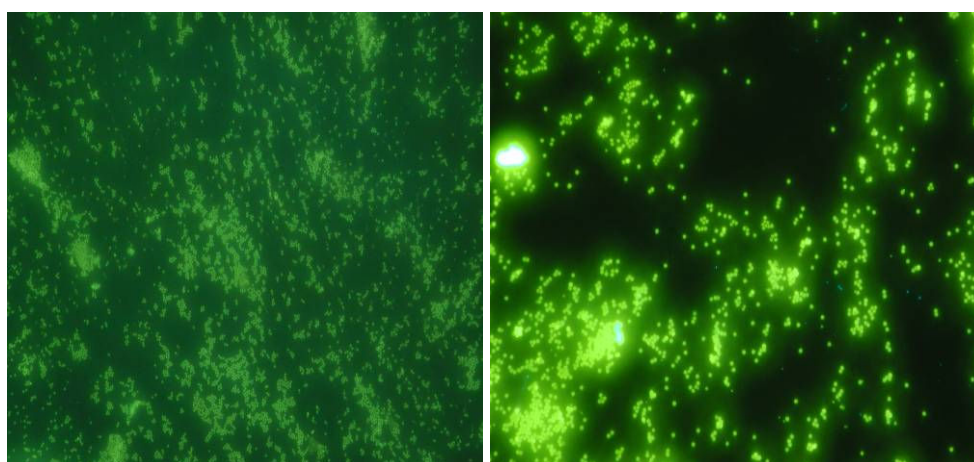
The FOM gives the microbeads localisation and the distribution into the main organs (liver, spleen, lungs). In Fig. 4-10 there are presented fluorescent microbeads before actually using them in *in vivo* tests.



a)



b)



c)

Fig. 4-10. FOM appearance for microbeads containing ethyl eosin: a) pHEMA; b) p(HEMA-co-MOEP); c) p(HEMA-co-GuaMA).

4.3.5. *In vitro* tests

The cells were examined by inversion microscopy, before and after the incubation with the samples. There were not observed cytotoxic effects, the morphologic characteristics and the adherence being similar for the cells incubated in the presence or in the absence of the samples. In the same time, after the addition of the dye, MTT, both the cells incubated with the samples and those untreated reduced the MTT and formed formazan crystals (Fig. 4-11 to 4-13).



Fig. 4-11. Microscopic image of L929 cells in culture, in the absence of samples and before the addition of MTT

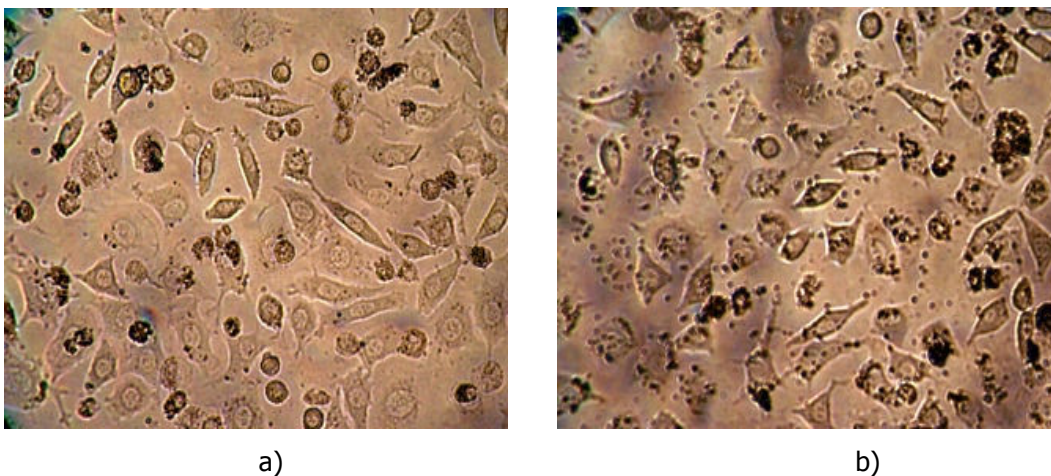


Fig. 4-12. Microscopic image of L929 cell line in culture, incubated for 24h with: a) p(HEMA-co-MOEP10%); b) p(HEMA-co-GuaMA10%).

After the solubilisation of formasan crystals, the optic density at 570 nm was measured and the cellular viability was calculated in percentage versus the control sample (cells incubated in the same conditions and volume) (Table 4-2).

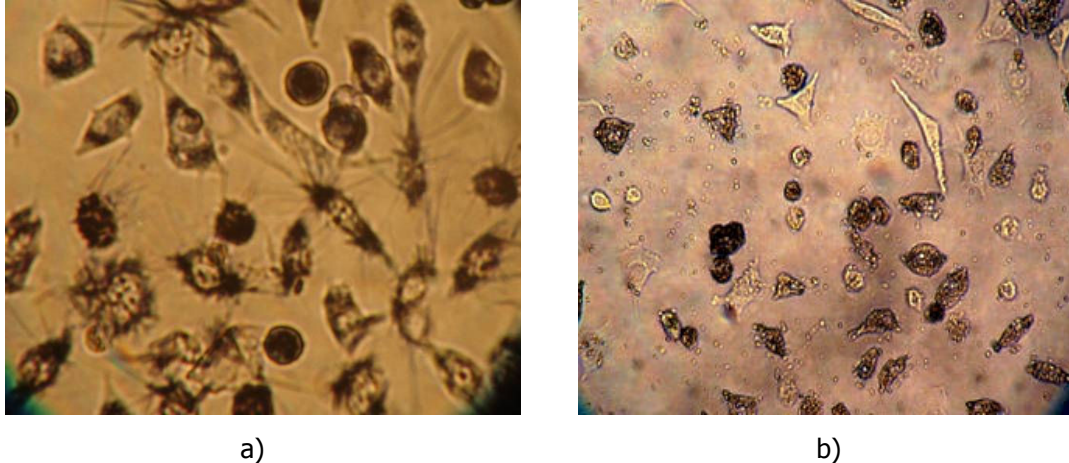


Fig. 4-13. Microscopic image of L929 cells in culture after incubation for 24h in the presence of: a) p(HEMA-co-MOEP10%); b) p(HEMA-co-GuaMA10%), after the addition of MTT.

The *in vitro* tests of cytotoxicity and viability made on fibroblasts murine L929 line cell gave adequately results for all compositions obtained.

4.3.6. *In vivo* tests. Organs distribution analysis

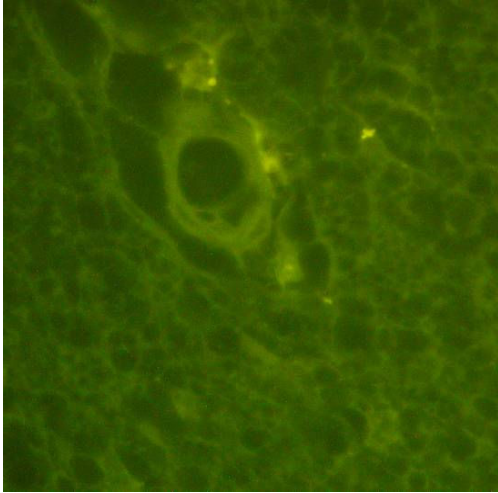
Among all the emulsifiers tested for the dispersion of the microbeads in water, in order to inject them into rats, only Tween 80 and saline solution (9 g NaCl / 1000 mL demineralised water) performed satisfactorily.

The results presented in Fig. 4-14 prove that the microbeads are homogeneously distributed into the injected organs: brain, lung and spleen.

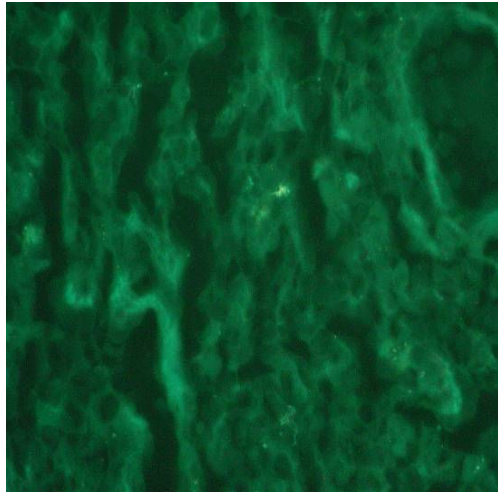
Table 4-2

Viability of the polymers obtained versus a blank control

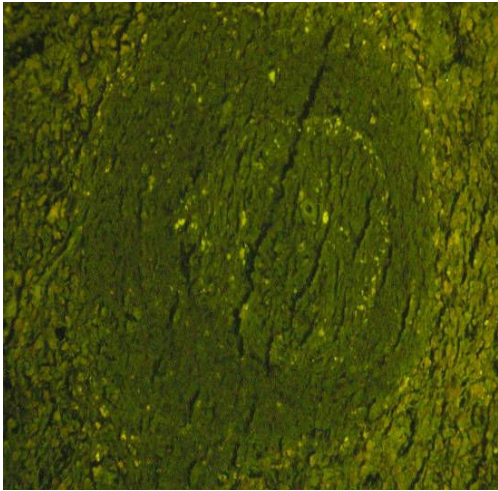
Sample	10 μ l TFS	Viability versus blank (%)	25 μ l TFS	Viability versus blank (%)	50 μ l TFS	Viability versus blank (%)
Blank	0.1187	100	0.11	100	0.146	100
pHEMA	0.105	88.46 \pm 3.66	0.097	88.18 \pm 4.03	0.144	98.63 \pm 1.13
p(HEMA-co-MOEP5%)	0.117	98.57 \pm 3.66	0.108	98.18 \pm 4.03	0.142	97.26 \pm 1.13
p(HEMA-co-MOEP10%)	0.113	95.20 \pm 3.66	0.102	92.73 \pm 4.03	0.141	96.57 \pm 1.13
p(HEMA-co-GuaMA5%)	0.112	94.47 \pm 3.66	0.107	97.27 \pm 4.03	0.144	98.63 \pm 1.13
p(HEMA-co-GuaMA10%)	0.111	93.51 \pm 3.66	0.105	95.45 \pm 4.03	0.145	99.32 \pm 1.13



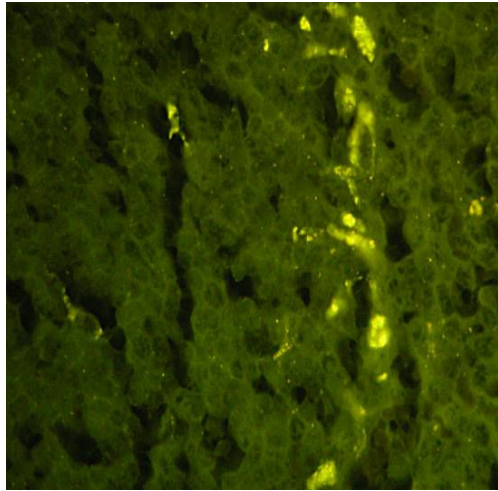
a)



b)



c)



d)

Fig. 4-14. Microbeads injected into rats and distributed within organs after 24h: a) brain; b) lung; c),d) spleen.

4.4. Conclusions

The need and the growing interest in polymers as biomaterials have led to the synthesis of new polymers with a variety of physico-chemical properties. Biomedical application of such materials not only depends on their physical properties but also on biocompatibility and biodegradability.

In the experimental part of this work, polymeric microbeads were obtained using the chemical synthesis. The influence of the solvent and stabilising agent was outlined, in terms of beads diameter and polydispersity. Even a very small variation of solvent/non-solvent ratio implies important variations in average diameter of the microbeads. The optimum values were determined experimentally in order to obtain uniform microbeads.

Polymeric microbeads of pHEMA, p(HEMA-co-MOEP) and p(HEMA-co-GuaMA) were obtained. SEM microphotographs gave a narrow distribution of the beads dimensions ($\sim 1 \mu\text{m}$) and uniform surface for 45/55 toluene/2-butanol vol. ratio, when pBuSt 905 was employed. The swelling rate confirmed our belief that the copolymers obtained are available as drug carriers.

In vitro tests gave satisfactory results in terms of cytotoxicity and viability of the cells submitted to tests. FOM analyses lead to the conclusion that the microbeads are homogeneously distributed into the injected damaged organs: brain, lung and spleen (*in vivo* tests). Also, the beads do not block the capillary vessels ($d_{\text{capillary}} = 5 - 7 \mu\text{m}$) and do not affect other cells or tissues.

These microbeads are expected to be used as injectable controlled drug release (see EPR effect) after drug binding to microbeads and afterwards traceable agents. This expectation is based on the combined physical properties of the copolymers, their noncytotoxicity and their cell sufficient anchoring in the soft tissues of the implantation site.

Chapter 5

Polymeric biocompatible structures for controlled drug release obtained by precipitant polymerisation

Beneficiary of research funds from:

Novel types of micro and nanostructured materials for new products in constructions, bioengineering and food safety, CEEX Research contract No. 11/03.10.2005 (2005-2008);

Data presented in:

T. Zecheru, C. Zaharia, A. Sălăgeanu, C. Țucureanu, E. Rusen, B. Mărculescu, T. Rotariu, C. Cincu, *Polymeric biocompatible structures for controlled drug release*, Journal of Optoelectronics and Advanced Materials, Vol. 9, Iss. 9, 2007, p. 2917-2920;

T. Zecheru, C. Zaharia, A. Salageanu, C.Tucureanu, E.Rusen,B.Marculescu, T.Rotariu, C.Cincu, *Polymeric biocompatible structures for controlled drug release*, 2nd International Conference on Biomaterials and Medical Devices - BiomMedD'06, 9-11 November 2006, Iasi, Romania.

5.1. Introduction

The goal of controlled drug delivery is to provide a specified drug concentration within the body for an extended period of time. A device that provides a sustained release of drug can maintain desired drug concentrations in the blood with reduced number of doses, while also minimising the concern of undesirable, sometimes toxic, side effects. Controlled release is, also, a more cost-effective way of delivering expensive medication. With less drug wasted, costs can be reduced. The first design concepts for controlled release were passive delivery systems.

In passive delivery, unassisted diffusion of solvent and solute is the only means of modulating the rate of drug delivery. Typically, there is a depot of drug contained within a polymer matrix which releases over time. However, this is just a subset of the actual goal of controlled release. The primary aim of controlled drug delivery is complete optimisation therapeutic delivery; that is the ability to deliver to the desired location, a precise dose for a finite period of time. With this ideal system, one could achieve high bioavailability with minimal side effects and drug exposure. To achieve this idealisation, systems must be responsive to fluctuations in the patient's needs. The advantage of implantable drug delivery devices is that they can be designed to meet these aims by providing a means of continually monitored and administered drug delivery.

The purpose of the present study was to obtain new copolymers in order to create a membrane-like barrier that would control the delivery of the active agent for an extended period.

Cross-linked poly(2-hydroxyethyl methacrylate) (pHEMA) swells to a significant extent. Hence, it was thought necessary to determine its swelling degree when incorporating methyl methacrylate (MMA), which is a hydrophobic monomer that is expected to restrain the water uptake in pHEMA. In order to be able to bind drugs, functionalised polymers should be inserted, this being the reason for using the acrylic acid (AA). Polymeric microbeads of pHEMA and p(HEMA-co-MMA) and functionalised biopolymers of p(HEMA-co-AA) and p(HEMA-co-MMA-co-AA) were prepared by precipitant polymerisation. There were obtained different types of micro-polymeric beads, which were characterised by measuring the swelling degree, scanning electron microscopy (SEM), elemental analysis and *in vitro* tests.

5.2. Experimental

Materials. MMA (Merck) was purified by *in vacuo* distillation ($T = 47^{\circ}\text{C}$, $p = 100$ mmHg), and HEMA (Aldrich) at 65°C and 100 mmHg, and AA (Sigma) was filtered through a 20-mm column full of basic Al_2O_3 (Merck). Azo-bis isobutyronitrile (AIBN) was purchased from Merck. Toluene was provided by Chimopar. The microbeads were obtained by precipitant polymerisation in the presence of AIBN as initiator.

Methods. A mixture of the monomer HEMA, respectively the comonomers (HEMA and MMA), (HEMA and AA), (HEMA, MMA and AA), with the initiator AIBN 0.5 % (w/v) and the solvent, toluene, was made just before the reaction. Mixtures of different compositions in the feed (Table 5-1) were then poured into 10 mL vials, while keeping the total volume of the solvent in the mixture (9 mL). Nitrogen was bubbled through the solutions, in order to remove the oxygen in it. A rich nitrogen atmosphere was enabled for polymerisation to occur.

The reactions were performed in a water-bath at 60-65°C, during 5 hours. The resulting solutions were washed three times with toluene in order to remove the residual monomer(s); afterwards, diethyl ether was used to extract the organic residues. The white precipitates formed were sieved in the oven at 40°C for 24 hours.

Table 5-1

Compositions of the monomers in the feed mixture

Polymer	Monomer(s)	Molar ratio
pHEMA	HEMA	-
p(HEMA-co-AA)	HEMA/AA	95/5, 90/10, 85/15, 80/20
p(HEMA-co-MMA)	HEMA/MMA	95/5, 90/10, 85/15, 80/20, 70/30, 60/40
p(HEMA-co-MMA-co-AA)	HEMA/MMA/AA	75/20/5, 70/20/10, 65/20/15, 60/20/20

Different types of polymeric microbeads of p(HEMA), p(HEMA-co-MMA), p(HEMA-co-AA) and p(HEMA-co-MMA-co-AA) were prepared by varying the ratios of the comonomers.

5.3. Results and discussion

The different polymer compositions prepared with this procedure were characterised by elemental analysis, measure of the water uptake capacity, in addition to examination of their topography in terms of homogeneity and distribution of the polymers with scanning electron microscopy (SEM).

5.3.1. Elemental analysis

The p(HEMA-co-MMA-co-AA) terpolymers structures were confirmed by the elemental analysis. The results are given in Table 5-2. The amount of nitrogen is due to AIBN residues.

Table 5-2

Elemental analysis results

Comonomers ratios (v/v)	N (%)	C(%)	H (%)
75:20:5	0.36	54.02	7.21
70:20:10	0.16	54.91	4.51
65:20:15	0.00	52.12	7.20
60:20:20	0.36	53.41	6.96

The formulas of the polymers obtained are given below, in Fig. 5-1:

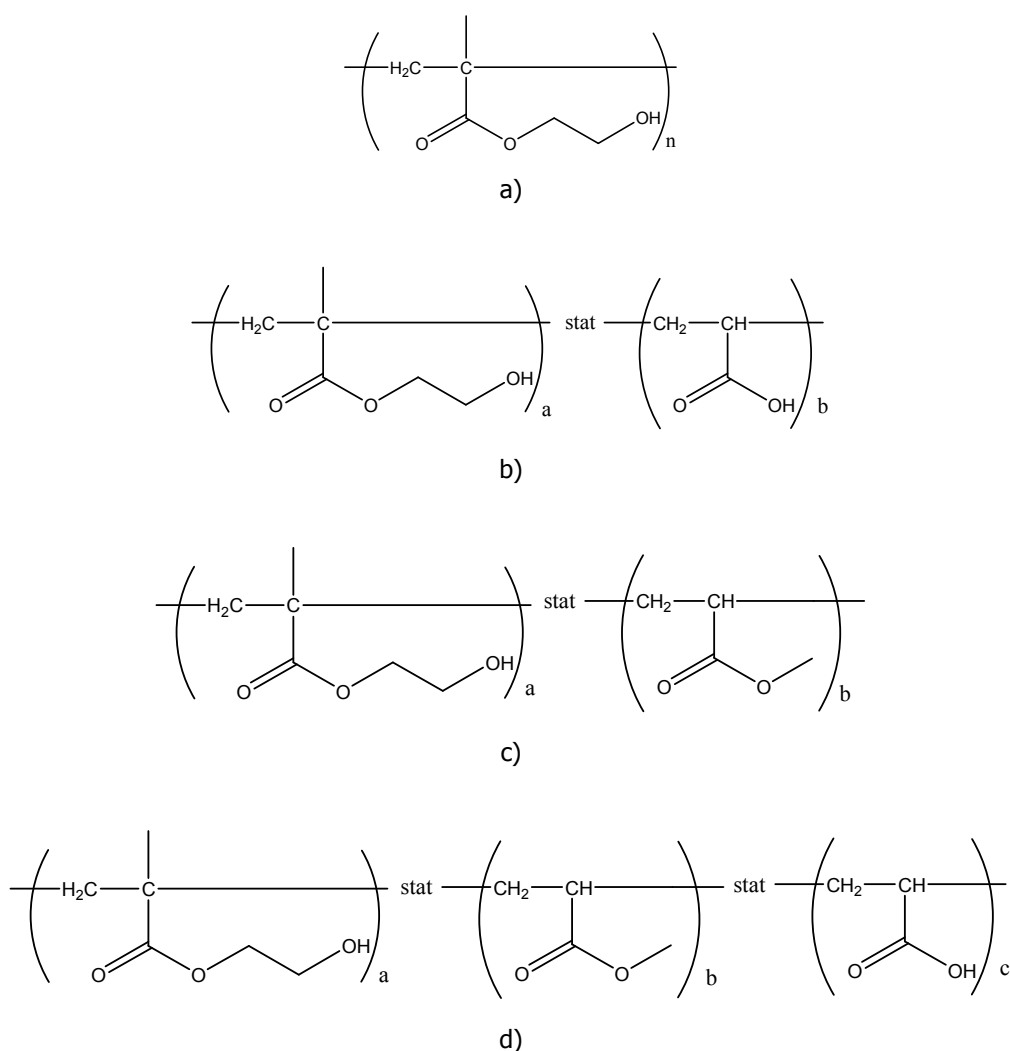


Fig. 5-1. Polymers obtained:

a) p(HEMA); b) p(HEMA-co-AA); c) p(HEMA-co-MMA); d) p(HEMA-co-MMA-co-AA).

5.3.2. Swelling tests

The swelling tests were made in triplicate on samples containing HEMA and MMA.

Bulk polymerisation was performed for polymeric samples in order to be used for the swelling tests, which were carried out in triplicate, in saline solution (9% NaCl (g/L distilled water) for three days (Fig. 5-2).

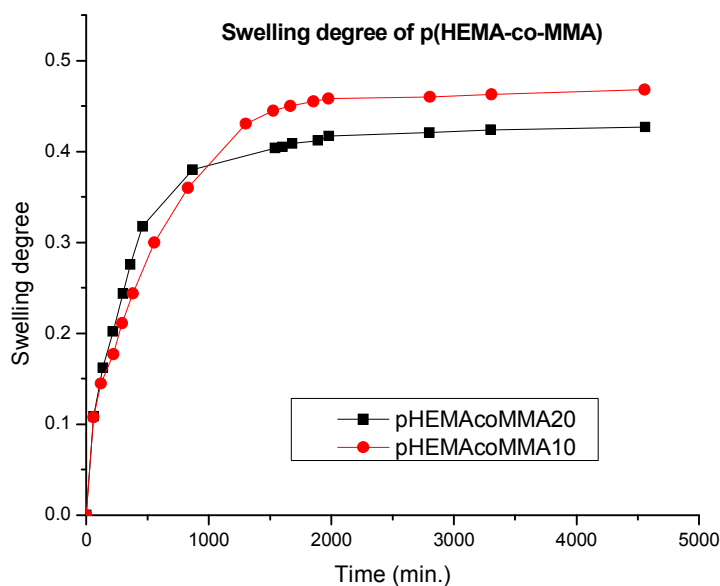


Fig. 5-2. Average swelling rate (g/g) versus time (min.) for p(HEMA-co-MMA) 90:10 and 80:20 molar ratio in the feed.

As expected, after testing the MMA-containing samples, it was concluded that a higher content of MMA would decrease microbeads swelling. This means that choosing a higher MMA:HEMA ratio would be the best approach in the construction of a controlled drug release system because with a lower swelling the release rate is expected to be lower.

5.3.3. Scanning electron microscopy

Moreover, from SEM it can be observed that a higher percent of MMA comparative with HEMA gets to micro-beads agglomeration. This is the reason for using a 20% ratio of the MMA in the terpolymer (Fig. 5-3 to 5-5).

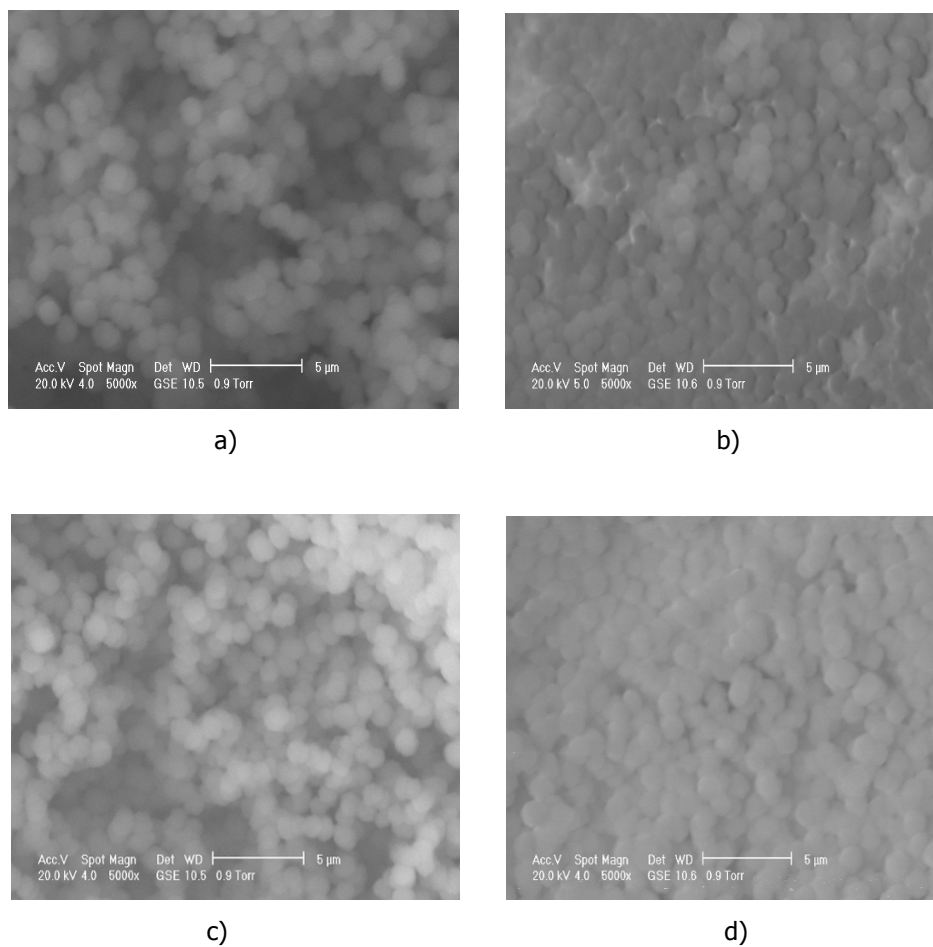


Fig. 5-3. Micro-beads distribution of: a) p(HEMA); and p(HEMA-co-AA) in molar ratios: b) HEMA:AA=95:5; c) HEMA:AA=90:10; d) HEMA:AA=85:15.

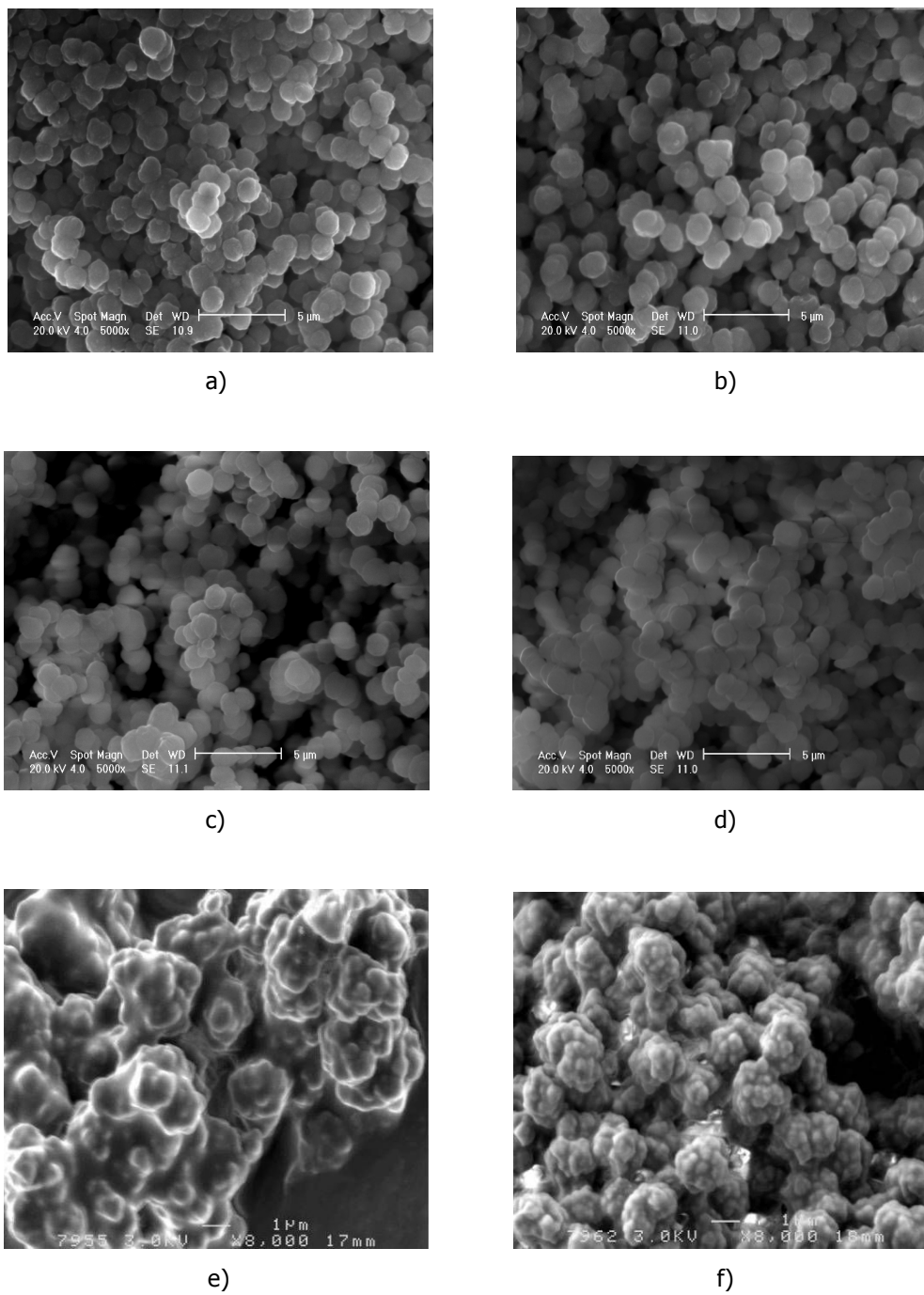


Fig. 5-4. Micro-beads distribution of p(HEMA-co-MMA) in molar ratios: a) HEMA:MMA=95:5; b) HEMA:MMA=90:10; c) HEMA:MMA=85:15; d) HEMA:MMA=80:20; e) HEMA:MMA=70:30; f) HEMA:MMA=60:40.

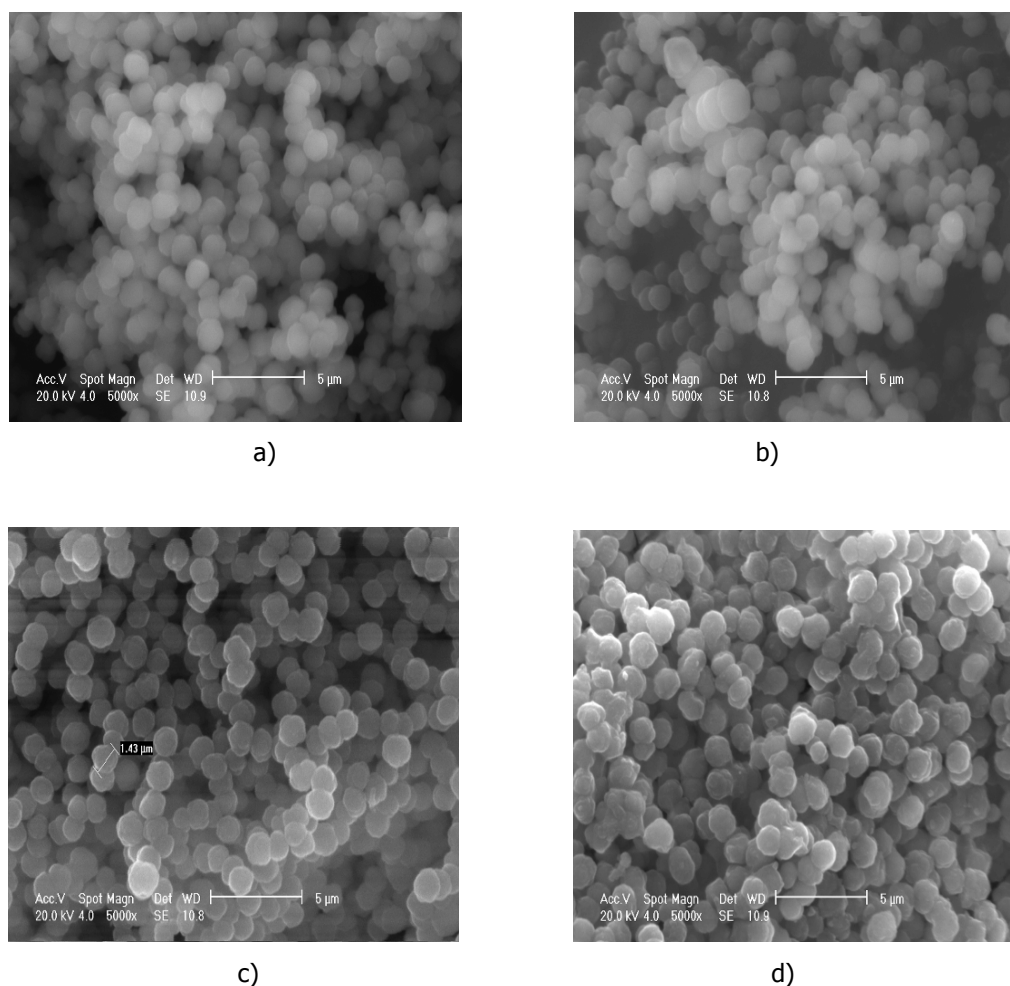


Fig. 5-5. Micro-beads distribution of p(HEMA-co-MMA-co-AA) in molar ratios:
 a) HEMA:MMA:AA=75:20:5; b) HEMA:MMA:AA=70:20:10; c) HEMA:MMA:AA=65:20:15;
 d) HEMA:MMA:AA=60:20:20.

SEM microphotographs gave adequately results for all compositions obtained and relevant from dimensionally point of view (1.2-1.5 μm).

5.3.4. Biocompatibility tests

Polymers biocompatibility was verified by testing their *in vitro* cytotoxicity. Microbeads were compacted in 10-mm round disks in appropriate matrices, at 100 bars and were exposed to UV light (long wave UV, 360 nm, 12W) overnight.

Murine fibroblasts L929 cell line was employed, which was cultivated in culture medium (DMEM), supplemented with calf fetal serum and antibiotics. Two specific methods were used: a) direct testing method; b) elution method.

In the first method, the polymers took contact with an adhered culture monolayer of cells in microplates of different cultures. In the second method the testing material was maintained in culture medium in standard conditions for 24-48 hours, at 37°C, in 5% CO₂ atmosphere. The culture medium where the testing material was maintained took contact with cells monolayer, replacing the medium in which the cells were raised until that moment. Thus, the cells culture took contact with fresh medium containing all the substances extracted from testing material. The cells culture was afterwards incubated in thermostat at 37°C, for a few days in the presence of 5% CO₂ and was examined daily during three days.

In both of the methods the cells were microscopically examined for detecting cytotoxicity visible signs, cellular lysis or cellular components dimensions and conformation.

For cytotoxicity evaluation, besides microscopically examination, it was also used the cellular viability. For this purpose, after incubation the cells were incubated with a tetrazolium soluble salt (MTT), 3-(4,5-dimethyliazol-2-il)-2,5-diphenyl tetrazolium bromide. This one is converted by dehydrogenases present in viable cells mitochondria in insoluble formasan which appears as violet crystals. 10 µL of MTT (5 mg/mL in buffer saline phosphate) sterile solution were added over 100 µL in every microplate sample where cells with testing material were incubated.

The microplates were incubated at 37°C, in a 5% CO₂ atmosphere, for 3-4 hours, until violet crystals of formasan appeared. For their solubility it was used a buffer prepared as following: for 12.5 mL SDS solution 5% in 50% dimethylformamide there were added 12.5 mL of 80% acetic acid solution containing 2.5% HCl 1N. There were added in every sample 100 µL of lysis buffer, the microplates were incubated for 24 hours at 37°C. Using an automatic well-reader (ELISA), the optical density was read at 570 nm. Optical density at 570 nm is proportional with viability. Viable cells percent contained by incubated samples with testing material was evaluated versus a blank test where only cells are incubated (Fig. 5-6 and 5-7, Table 5-3).

In vitro cytotoxicity and viability tests of made on murine fibroblast L929 line cell gave adequately results for all compositions obtained.

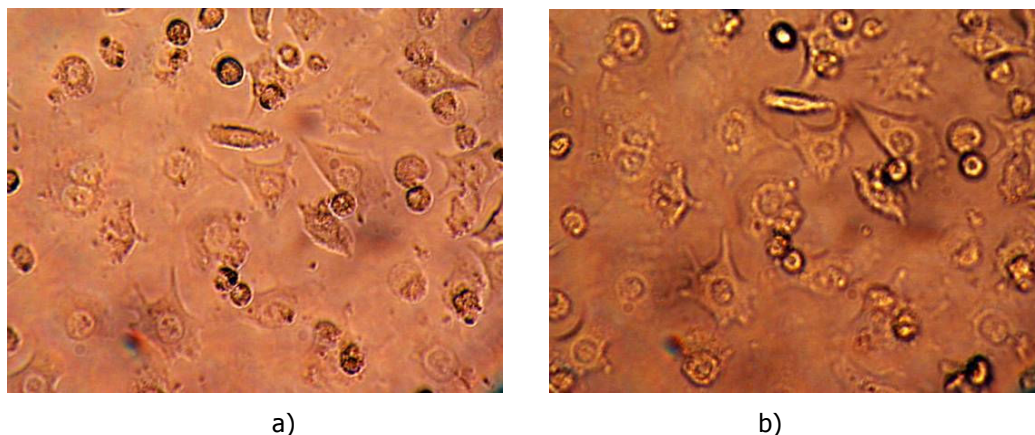
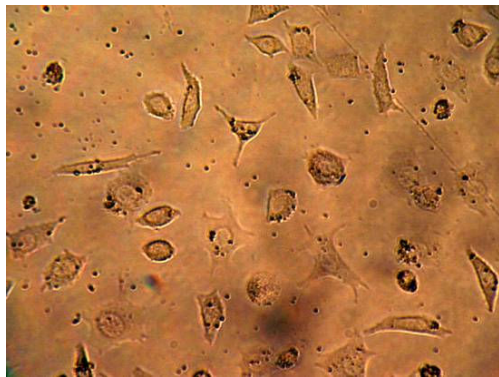
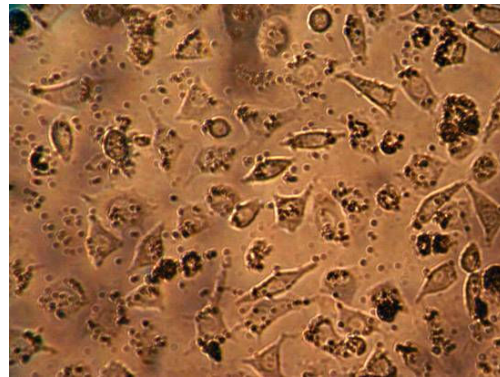


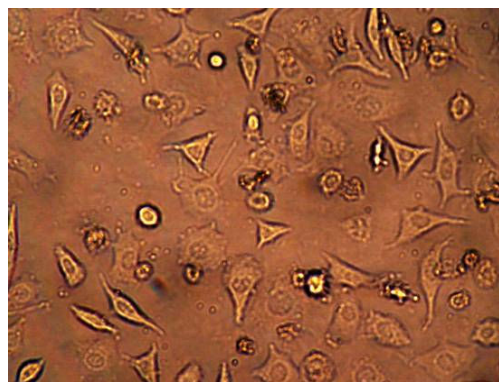
Fig. 5-6. Murine fibroblast L929 cell line: a) Blank 1; b) Blank 2.



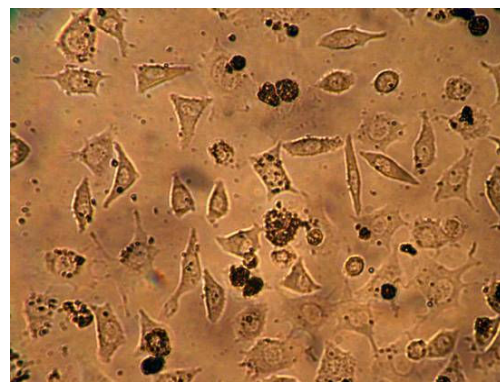
a)



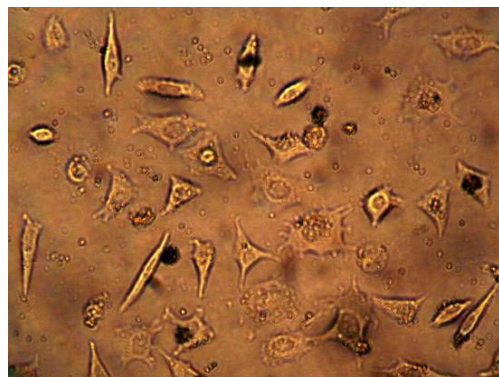
b)



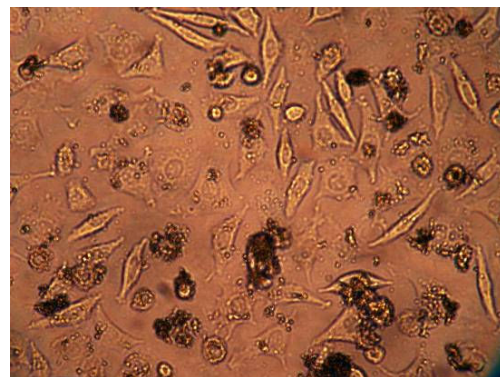
c)



d)



e)



f)

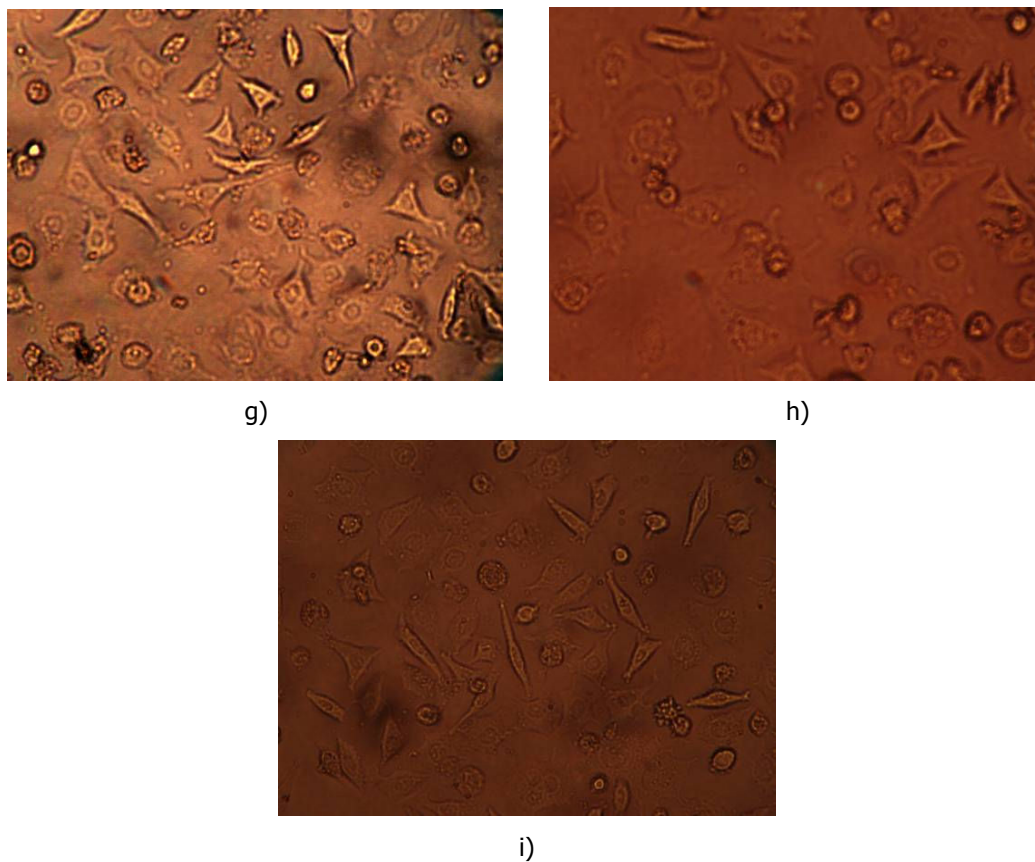


Fig. 5-7. Murine fibroblast L929 cell line with: a) p(HEMA-co-MMA5%); b) p(HEMA-co-MMA10%); c) p(HEMA-co-MMA15%); d) p(HEMA-co-MMA20%); e) p(HEMA-co-AA5%); f) p(HEMA-co-AA15%); g) p(HEMA-co-MMA20%-co-AA15%); h) p(HEMA-co-MMA20%-co-AA10%); i) p(HEMA-co-MMA20%-co-AA20%).

Table 5-3

Viability of the polymers obtained versus a blank control

Sample	10 μ l TFS	Viability versus blank (%)	25 μ l TFS	Viability versus blank (%)	50 μ l TFS	Viability versus blank (%)
Blank 1	0.1187	100	0.11	100	0.146	100
p(HEMA-co-MMA5%)	0.116	97.72 \pm 1.29	0.109	99.09 \pm 0.52	0.144	98.63 \pm 0.4
p(HEMA-co-MMA10%)	0.117	98.57 \pm 1.29	0.108	98.18 \pm 0.52	0.145	99.32 \pm 0.4
p(HEMA-co-MMA15%)	0.114	96.04 \pm 1.29	0.108	98.18 \pm 0.52	0.144	98.63 \pm 0.4
Blank 2	0.1395	100	0.1093	100	0.138	100
p(HEMA-co-MMA20%)	0.125	89.61 \pm 3.09	0.103	94.24 \pm 1.86	0.136	98.55 \pm 1.08
p(HEMA-co-AA5%)	0.131	93.91 \pm 3.09	0.105	96.07 \pm 1.86	0.1345	97.46 \pm 1.08
p(HEMA-co-AA15%)	0.133	95.34 \pm 3.09	0.108	98.81 \pm 1.86	0.137	99.27 \pm 1.08
p(HEMA-co-MMA20%-co-AA15%)	0.134	96.06 \pm 3.09	0.1073	98.17 \pm 1.86	0.1347	97.61 \pm 1.08
p(HEMA-co-MMA20%-co-AA10%)	0.137	98.21 \pm 3.09	0.1083	99.08 \pm 1.86	0.134	97.10 \pm 1.08
p(HEMA-co-MMA20%-co-AA20%)	0.136	97.49 \pm 3.09	0.107	97.89 \pm 1.86	0.1377	99.78 \pm 1.08

5.4. Conclusions

The capacity of water uptake of polymeric microbeads is a highly important property in the view of using them as controlled delivery devices. These experiments have allowed to conclude that choosing a higher MMA:HEMA ratio would be the best approach in the construction of a controlled drug release system. From the swelling tests it was observed that a high content of MMA decreases the micro-bead swelling rate, and also it decreases more, but in adequate parameters for use in drug delivery systems, when used both MMA and AA.

SEM spectra proved that homogeneously distributed polymer microbeads were obtained, with the diameter of 0.5-1.5 μm .

In vitro tests show that all the compositions submitted to tests are biocompatible and non-toxic for the cells.

Chapter 6

Comparative studies on different HEMA-based polymeric compositions and thalidomide-loading

Beneficiary of a research scholarship SOCRATES-ERASMUS (31.01-30.06.2007) at University of Angers, Laboratory of Histology-Embryology, France (co-tutelle)

Data presented in:

Hervé Nyangoga, **Teodora Zecheru**, Robert Filmon, Michel-Félix Baslé, Corneliu Cincu, Daniel Chappard, Synthesis and use of pHEMA microbeads with human EA.hy 926 endothelial cells. Journal of Biomedical Materials Research: Part B - Applied Biomaterials, in press;

Nyangoga H., **Zecheru T.**, Filmon R., Cincu C., Chappard D., *Use of pHEMA microbeads with human endothelial cells*, International Conference on Chemistry and Chemical Engineering RICCE 15, 19-22 September 2007, Sinaia, Romania.

6.1. Introduction

6.1.1. Systems and methods

In the present chapter a comparison among physico-chemical and biological *in vitro* and *in vivo* behaviour of different HEMA-based and functionalised-containing polymers is performed. In this study there were used several methacrylate derivatives with negative and positive functionalities: glycidyl, acetoacetate, carboxyl, tetrahydrofurfuryl and ammonium chloride (Table 6-1).

Table 6-1

Comonomers used in the study

No.	Principal comonomer	Second comonomer, containing different functions	Cross-linking agent
1.	HEMA	DADMAC	EGDMA
2.	HEMA	GlyMA	EGDMA
3.	HEMA	MAA	EGDMA
4.	HEMA	MOEAA	EGDMA
5.	HEMA	MOETAC	EGDMA
6.	HEMA	THFMA	EGDMA

6.1.2. Staining

The dye chosen for the present study is Nile Red (9-diethylamino-5H-benzo-(a)phenoxazine-5-one), presented in Fig. 6-1, a phenoxazone that fluoresces intensely, and in varying colour, in organic solvents and hydrophobic lipids. Nile red is a lipophilic stain; it will accumulate in lipid globules inside cells, staining them red. Nile red can be used with living cells. It fluoresces strongly when partitioned into lipids, but its fluorescence is fully quenched in water.

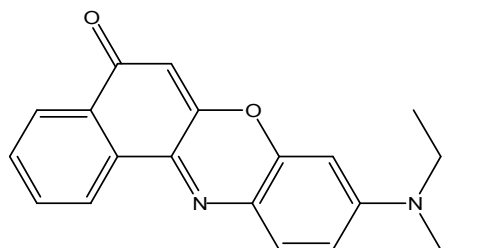


Fig. 6-1. Chemical structure of Nile Red

This dye acts, therefore, as a fluorescent hydrophobic probe. As it concerns the dye incorporation, from experience it was decided that, even it is about a physical bond, it is better to

include the dye during the polymerisation procedure. Otherwise, the dye will only create a layer on the microparticles, but it will also be found non-linked into the final solution, in crystalline form. Taking into the consideration that Nile Red is not water-soluble, it would be very difficult to separate the dye-polymer from the solution. That is the reason for choosing the dye addition right from the beginning of the synthesis.

6.1.3. Calcification studies

The interest in obtaining new biocompatible materials for bone recovery has consistently gained interest in the last few decades. Though, there are still a lot of questions to answer before actually implant such a biomaterial in the human body. Conditions to be achieved regard several aspects, such as: biocompatibility, degradability, swellability, osteoinduction or osteoconduction ability.

In order to manufacture biomaterials with calcification ability, it is very important to be aware of the factors that influence this complex process. The description of calcification mechanisms begins with the idea that, although all the tissues are sunk by extracellular fluids rich in calcium and phosphate ion, their mineralization takes place only in hard tissues rich in collagen fibers.

Normal (non-pathologic) mineralization processes in the body are controlled by the complex physicochemical and cellular regulation of substances that promote and inhibit hydroxyapatite (HA) formation. Significant magnesium concentrations and proteins in plasma effectively inhibit HA precipitation in tissues exposed to that body fluid.

There are two general processes by which mineralization can be initiated: (1) by the removal and/or degradation of HA inhibitors at a particular site and (2) through nucleation and growth of a calcium phosphate layer at the surface of the biomaterial, which further leads to a direct bone-binding.

As local inhibitors of mineralization we can number: pyrophosphates, proteoglycans, glycosaminoglycans, serum proteins, phosphoproteins, metals (such as aluminum and magnesium), metal-citrate complexes (Fe^{3+} , Al^{3+} , Cr^{3+}). As local stimulators of calcification, which were proven to increase calcium and phosphate local concentrations, there are known: collagen I, acidic molecules charged and containing important quantities of aminoacid, polysaccharide, carboxylate or sulfate groups (proteins, glycoproteins, phospholipids, proteolipids rich in aminoacids with high aspartate and serine content, and polysaccharide units), but with no useful information upon nucleation for HA formation.

All these ideas led to new studies regarding the role of these substances upon mineralization.

The calcification phenomenon is an important and desired process for orthopedic applications. HA, the main inorganic component of bone and calcified materials is an inorganic biocompatible and biofunctional material with osteoconductivity. The normal calcification processes

inside the organisms are controlled by many physico-chemical factors that act both as initiators and inhibitors for HA.

Many research teams studied the calcification phenomenon onto various HA-polymer composite materials. These biomaterials would improve both the mechanical properties of orthopedic implants and their tolerance by the neighboring tissues and interface reactions with the healthy bone tissue. Some materials show bioactivity only when they are mixed with molecules that stimulate nucleation and growth of hydroxyapatite. In all the cases, improved performance of the implantable materials was reported: better bone-implant interface, superior mechanical behaviour etc.

Calcification phenomenon induced by such materials takes place through successive immobilization of Ca^{2+} and PO_4^{3-} from physiological medium on/in the material. Once the nuclei are formed, HA crystals grow leading to the transformation of the implanted graft into a polymeric composite reinforced with HA. In this way a direct bone-bonding link is achieved. The benefits are easily observed from the point of view of mechanical stability of the graft and its tolerance by the organism.

It is well known that the presence of different functionalities, such as inorganic phosphates, plays a very important role in the nucleation stage of biomineralization. Therefore, the calcium phosphate-polymer composites became an interesting subject as bone substitutes. Due to polymeric component, these materials show a higher affinity for bone than the classical bioactive ceramics.

Poly(2-hydroxyethyl methacrylate) (pHEMA) is one of the most interesting biocompatible material that has been studied in the field, along with different copolymers, basically containing negatively charged groups, such as phosphate, carboxyl and sulfonic groups. Not enough information upon *in vivo* HA nucleation was reported yet. This fact led to new studies regarding the role of these substances upon mineralization and the synthesis of new materials. Special attention was given to the materials that contain special chemical functions, in order to initiate HA formation.

Filmon et al. (2000, 2002) have demonstrated that due to carboxyl groups' fixation on pHEMA by carboxy-methylation with bromoacetic acid, the polymer that was initially incapable of calcification becomes able to deposit spontaneously HA when it is immersed in a synthetic liquid having a similar composition with that of human plasma.

In order to favor a phenomenon similar to the one described above, a possibility would be to introduce in the polymer certain functional groups that would attract calcium. Taking into account all these considerations, mineralisation tests were conducted in order to evaluate the capability of *in vitro* HA induction of the new polymer structures.

6.1.4. Thalidomide

Thalidomide has been shown to inhibit angiogenesis induced by fibroblast growth factor and vascular endothelial growth factor. It has also been shown to cause apoptosis of established tumor-associated angiogenesis in experimental models (Singhal et al., 1999). The bone marrow of

patients with hematologic cancers shows extensive vascularity, which has prognostic implications in myeloma. The apparent lack of a consistent decrease in the microvascular density of bone marrow in patients in whom thalidomide had a marked antitumor effect requires further study. The antitumor properties of thalidomide are being evaluated in various malignant diseases, although only limited efficacy data are available so far. Prolonged responses to thalidomide in some patients with advanced refractory disease suggest that the mechanism of action of thalidomide is distinctly different from that of the other agents active against myeloma.

This drug is now being reassessed because it has been shown to be clinically useful in a number of situations through its ability to selectively inhibit TNF- α synthesis. Thalidomide is the drug of choice in the treatment of erythema nodosum leprosum, an acute inflammatory complication often seen in patients with lepromatous leprosy, and it has also been used to treat patients with rheumatoid arthritis, HIV-associated aphthous ulceration, chronic tuberculosis, and chronic graft-vs-host disease. Also, a number of double blind, placebo-controlled trials have indicated that thalidomide may be effective in the treatment of chronic diarrhea and wasting associated with HIV disease. However, reliable birth control methods must be used by women taking thalidomide, and monitoring for neurologic effects is required in all patients.

Thalidomide appears to have multiple effects that may account for its activity against myeloma. These include:

- ✦ Inhibition of angiogenesis (the growth of new blood vessels that feed tumor cells) by blocking basic fibroblast growth factor (bFGF) and vascular endothelial growth factor (VEGF)
- ✦ Inhibition of the growth and survival of stromal cells, tumor cells and cells in the bone marrow
- ✦ Altering production/activity of cytokines (chemical messengers) involved in the growth and survival of myeloma cells through various mechanisms: Inhibition of Cyclooxygenase-2 (COX-2); Inhibition of Tumor necrosis factor-alpha (TNF- α); Downregulation of Interleukin 6 (IL-6); Increased Production of Interleukin 10 (IL-10); Enhancement of Interleukin 4 (IL-4), Interleukin 5 (IL-5), and Interleukin 12 (IL-12); Inhibition of TNF- α -induced Interleukin-8 (IL-8)
- ✦ Altering the expression of adhesion molecules located on the surface of tumor cells and bone marrow stromal cells, which trigger the release of cytokines that induce tumour cell growth. Adhesion molecules may also be involved in drug resistance.
- ✦ Stimulation of T-cells, which help the immune system to attack tumour cells directly.

These effects are summarized in Fig. 6-2 and 6-3.

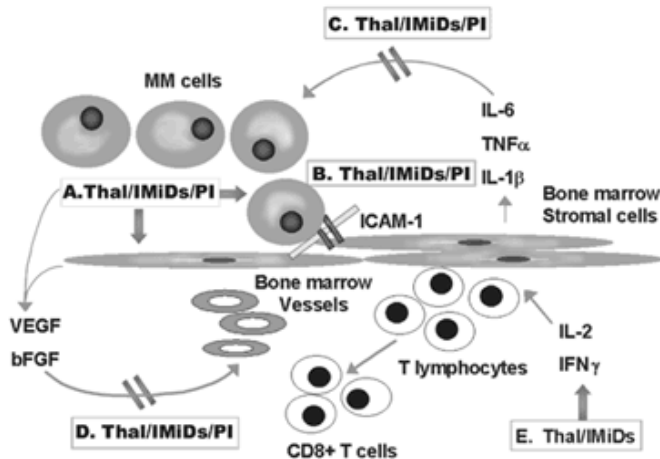


Fig. 6-2. Thalidomide's Various Effects in Myeloma (www.thalomid.com).

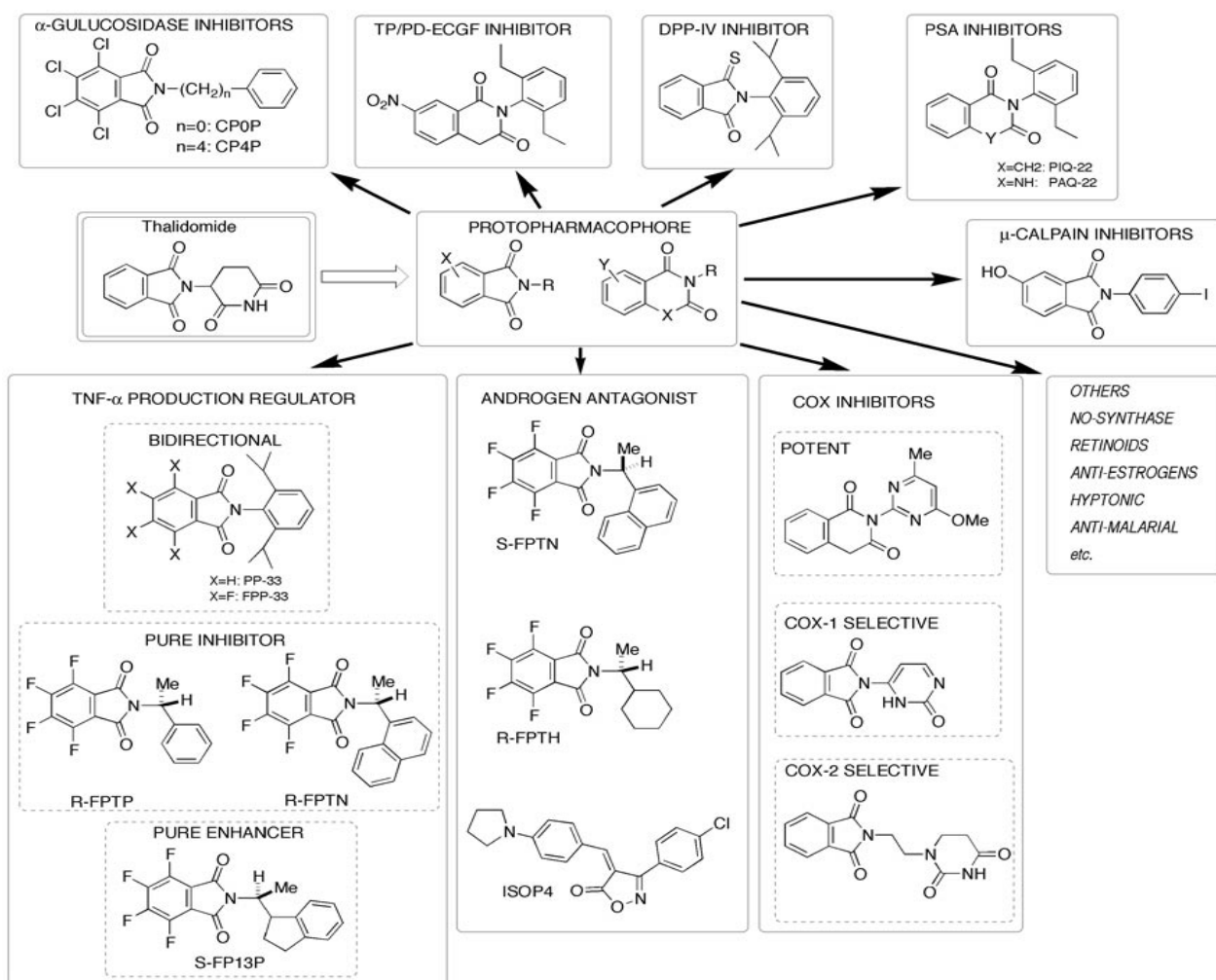
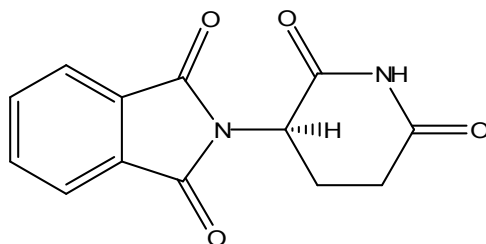


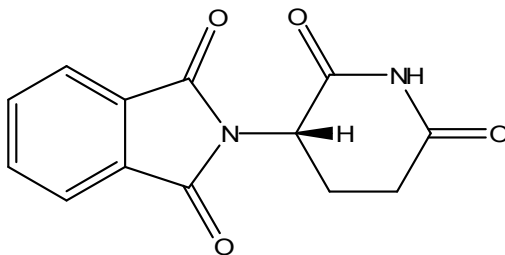
Fig. 6-3. Pharmacogenic utilities and behaviour of thalidomide (www.iam.u-tokyo.ac.jp/chem/theme/thalidomide.jpg).

Single-agent thalidomide may be particularly appropriate for the following patient types: patients who relapse following transplantation and patients who cannot tolerate steroids.

Thalidomide occurs as a racemic mixture of *S* and *R* enantiomers (Fig. 6-4). The *R* enantiomer is responsible for the drug's anti-inflammatory activity, whereas the *S* enantiomer is responsible for its teratogenic activity. Why not just purify the racemic mixture and give the patient only the *R* enantiomer? Unfortunately, the answer is not that simple. The liver contains an enzyme that converts the *R* to the *S* enantiomer. More than 30 mechanisms have been proposed to explain in detail this teratogenic action of thalidomide. Discovering thalidomide's various mechanisms may ultimately lead to new drugs that possess only its therapeutic benefits, without its harmful side effects.



(R) Thalidomide desirable properties: sedative and antinausea drug



(S) Thalidomide teratogenic: causes birth defects

Fig. 6-4. Chemical structures of Thalidomide and consequences of stereoisomerism

In 1999, Barlogie's group reported the results of studies of 84 patients with advanced multiple myeloma, an incurable and usually fatal cancer of the bone marrow. Enhanced angiogenesis is one of the characteristic symptoms. Treatment with thalidomide gave some interesting results: about a third of patients showed a significant reduction in cancer progression. Two of the patients achieved complete remission. The exact mechanism was unknown, but it was likely that thalidomide was working as an anti-angiogenic agent.

Thalidomide (also known as (\pm) -N-(2,6-Dioxo-3-piperidyl)phthalimide, or α -*N*-phthalimidoglutaramide) was chosen therefore for studies of evaluation of tumour necrosis. Its use, as presented above, is restricted by potentially serious side effects, including teratogenicity and neurotoxicity; furthermore, insolubility may present problems in terms of systemic bioavailability. Solubility is an important consideration in terms of systemic drug bioavailability, since insolubility

further limits drug efficacy and the subsequent need for increased dosage compromises patient tolerance.

Thalidomide is at present a capsule taken orally, usually once a day at bedtime. The daily dose is tailored to the individual patient and is dependent on each patient's tolerance. The side effects of thalidomide appear to be dose related, and as doses of thalidomide above 400 mg are less frequently used, the incidences of these side effects are generally decreasing.

The mean elimination half life of thalidomide following single 200 mg/dose ranges from 3-6.7 hr, and the elimination half life appears to be similar following multiple doses of the drug. In a study in healthy adults who received a single 50, 200 or 400 mg/dose of thalidomide, the mean elimination half life of thalidomide was 5.5, 5.5 or 7.3 hr.

Therefore, polymer systems were designed as possible matrices for controlled and sustained delivery of thalidomide.

6.2. Synthesis procedures

6.2.1. Synthesis of the copolymers

Materials. 2-Hydroxyethyl methacrylate (HEMA) was distilled under reduced pressure (65°C and 10⁻² mmHg) and stored at 4°C until use. Diallyldimethylammonium chloride (DADMAC), glycidyl methacrylate (GlyMA), methacrylic acid (MAA), 2-methacryloyloxymethyl acetoacetate (MOEAA), 2-methacryloyloxyethyltriethylammonium chloride (MOETAC), tetrahydrofurfuryl methacrylate (THFMA) were used without further purification. All the monomers were purchased from Sigma-Aldrich (Fig. 6-5).

Initiators benzoyl peroxide (BPO) and azo-bis-isobutyronitrile (AIBN) were obtained from Sigma, and were recrystallized from methanol at 40°C. Ethylene glycol dimethacrylate (EGDMA) was used as a cross-linking agent without further purification (Sigma). Other substances, as methyl ethyl ketone (MEK), toluene - refluxing agents, ethanol - extracting agent for copolymers, and others were used as received (Fluka).

Thalidomide was obtained from Merck and used as such.

Substances for the *in vitro* tests were: Roswell Park Memorial Institute (RPMI) - culture medium (Sigma-Aldrich), Phosphate Buffered Saline (PBS) - ensuring a pH of 7.2-7.4, (Faculty of Medicine of Angers, France), Dulbecco's Modified Eagle Medium (DMEM) - culture medium

(Eurobio, France), 3-4,5dimethylthiazole-2-yl)-2,5-diphenyltetrazolium bromide (MTT) - labeling agent, penicillin and streptomycin - antibiotics (Sigma).

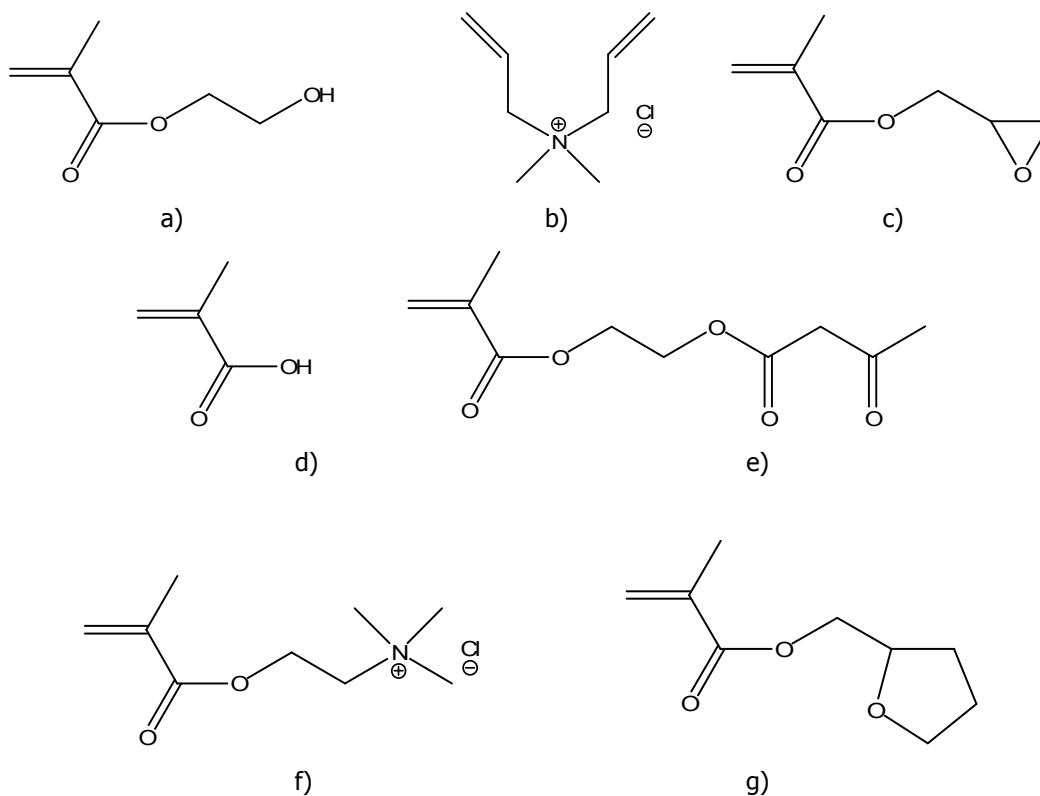


Fig. 6-5. Chemical structures of the monomers: a) HEMA, b) DADMAC, c) GlyMA, d) MAA, e) MOEAA, f) MOETAC, g) THFMA.

6.2.1.1. Synthesis of microbeads

In order to obtain HEMA-containing microbeads, the procedure followed was:

In a three-neck reactor, as shown in Fig. 6-6, the comonomers, HEMA versus function-containing comonomer in 90:10 molar ratio, the initiator (10^{-2} mol/L), the solvent (toluene), where the (monomers : solvent) volume ratio is (1 : 5), and, where the case, Nile Red (0.5% w/w) were mixed together.

Under continuous mechanical stirring, at 400 rpm, and nitrogen atmosphere (for the first half an hour), the temperature is increased to 70°C. A full conversion is obtained after 6 hours.

Possible residual monomers are washed away from the white precipitate obtained with toluene and a diethyl ether : 2-propanol (1 : 1 v/v) solution, in order to eliminate any other organic traces. Microbeads are allowed to dry in an oven at 35°C.

For further use, microbeads are introduced in a 20 ‰ NaCl saline aqueous solution, sonicated for a good dispersion for 5 min., and this solution is afterwards diluted to a 9 ‰. The

concentration of the final solution is observed using a Malassez cell and diluted with demineralised water or concentrated for the obtaining of a microbeads concentration of 10^8 - 10^9 particles/ mm^3 (no./v).



Fig. 6-6. Polymerisation reactor

6.2.1.2. Synthesis of pellets

Copolymers of p(HEMA-co-DADMAC), p(HEMA-co-GlyMA), p(HEMA-co-MAA), p(HEMA-co-MOETAC), p(HEMA-co-MOEAA) and p(HEMA-co-THFMA) were obtained by bulk polymerisation (the installation is presented in Fig. 6-7) as pellets with flat shape and maximum surface.

The reaction mixtures consisted in: monomers (HEMA : comonomers = 90 : 10 molar), initiator (5×10^{-3} mol/L) and cross-linking agent, EGDMA (3% molar concentration with respect to the monomers). The mixtures were stirred for 30 minutes at 500 rpm, then degassed for 5 minutes and finally poured into cylindrical polyethylene moulds (3x10 mm).



Fig. 6-7. Installation for bulk polymerisation

Polymerisations were conducted at 80°C for 12 hours; the post-polymerisation took place at 110°C.

There were obtained polymeric pellets, which were extracted in soxhlet for 12 hours with distilled water to remove any traces of the residual monomer that could negatively influence the *in vitro* assays.

6.2.2. Drug loading for bone methastases

0.45 g/L thalidomide is dissolved in a 60% aqueous solution of 2-hydroxypropyl- β -cyclodextrin (w/v). Fluorescent microbeads are added (20:1 weight ratio versus thalidomide) under stirring. The pH is adjusted to 7.4 at 37°C with a 0.5 M NaOH solution. 400 rpm magnetic stirring is set at room temperature for 48 hours. Particles are gently washed with demineralised water, dried and stored at 4-7°C. This procedure conducted to physically bonded thalidomide to the microbeads.

6.3. Characterisation studies

The first stage in the present work consisted in the synthesis of HEMA-based copolymers. Taking into account that methacrylic comonomers were used, which are capable of homopropagation, and that polymerisations were conducted to total conversion, in bulk, the final copolymers composition is identical with the composition in the feed. In case of DADMAC, radical polymerisation of "polar" monomers is substantially accelerated by heating. Moreover, conventional radical cyclo-polymerisation gives also an important cross-linking degree (Moad et al., 2008). Therefore, in this case also, the copolymerisation reached the maximum conversion.

The functionalization of biomaterials with functional groups that may act as nucleating sites has been one of the most frequently attempted methods of enhancing the deposition of Ca-P phases on biomaterial substrates.

In the present literature these polymer systems are not mentioned, therefore studies regarding availability for either drug delivery matrices or HA-induction are performed.

6.3.1. Fluorescence study

Fluorescence studies were performed on thin slices of bulk copolymer samples, regarding the influence of the polymerisation temperature, of the comonomers, and of the initiation system on the Nile Red (Fig. 6-8 and 6-9).



Fig. 6-8. Confocal fluorescence microscope

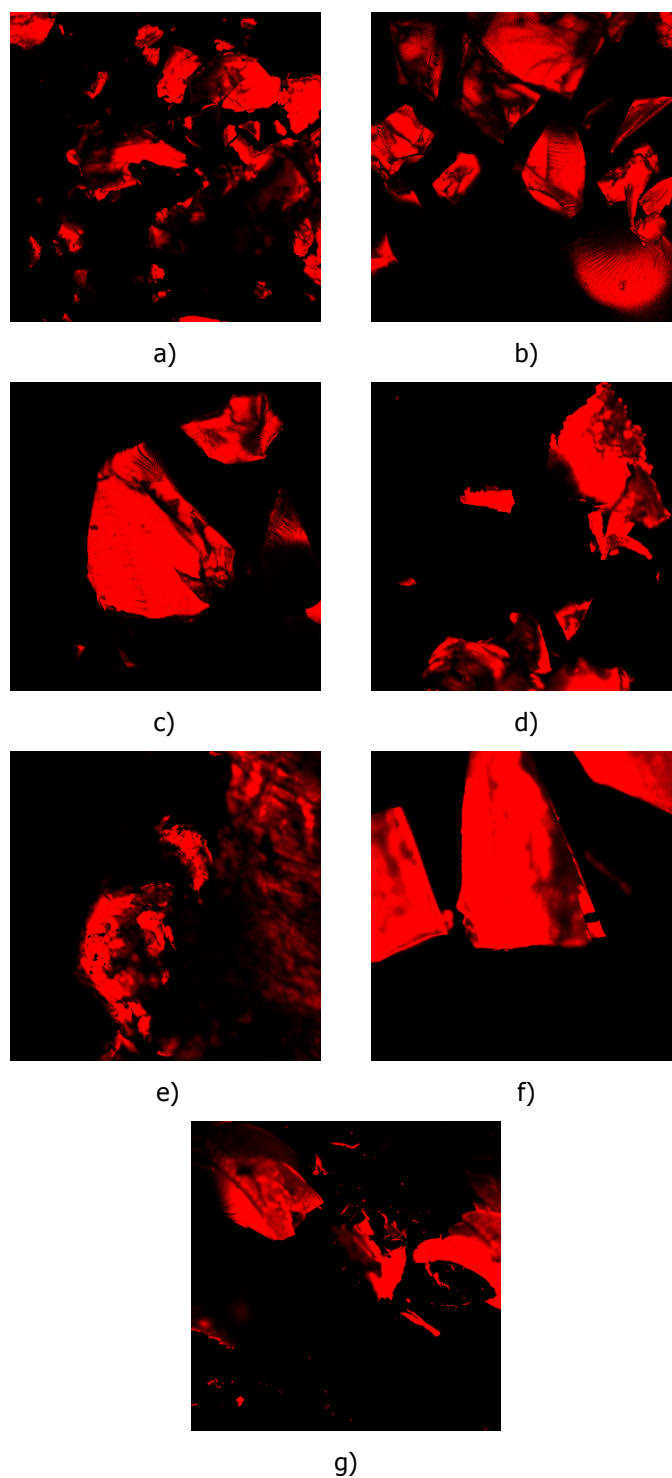


Fig. 6-9. Fluorescence microphotographs: a) GlyMA (AIBN, 60-65°C), b) GlyMA (PBO, 70-75°C), c) MOEAA (AIBN, 60-65°C), d) MOEAA (PBO, 70-75°C), e) MOETAC (PBO, 70-75°C), f) DMA (PBO, 70-75°C), g) DADMAC (PBO, 70-75°C).

The temperature used for polymerisation does not destroy the dye and does not influence negatively the fluorescence of the dye, neither the comonomers' structure nor the use of AIBN or BPO.

Moreover, fluorescence tests on microbeads doped with Nile Red gave satisfactory results (Fig. 6-10).

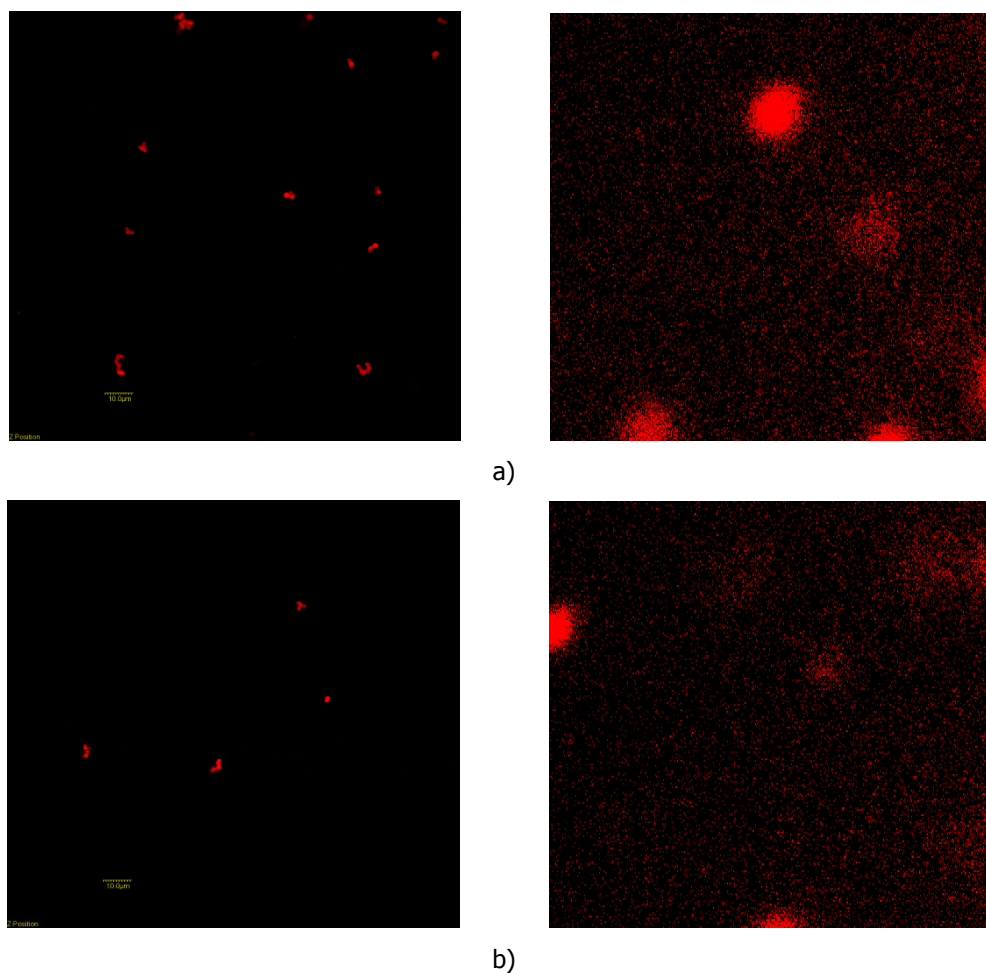


Fig. 6-10. FOM for: a) p(HEMA-co-MOEAA); b) p(HEMA-co-DADMAC), microbeads stained with Nile Red, in two concentrations.

6.3.2. Fourier Transform Infra Red (FT-IR) and RAMAN Spectroscopy

These methods of analysis were used in order to confirm the presence of functional groups in the copolymers.

ATR-FTIR spectra of the copolymers were obtained at 20°C and constant 40% relative humidity by coupling ATR modulus to a Bruker Vertex 70 spectrophotometer (Fig. 6-11). Spectra were obtained over the range of 4000–350 cm^{-1} at 4 cm^{-1} resolution and the number of scans 50.

Raman analysis was performed on a Senterra microscope (Fig. 6-12) with OPUS 5.5 software (Bruker Optik, Germany). The excitation laser wavelength was 785 nm. Spectra were recorded over the range 3500-250 cm^{-1} for 50 scans.



Fig. 6-11. Bruker Vertex 70 spectrophotometer

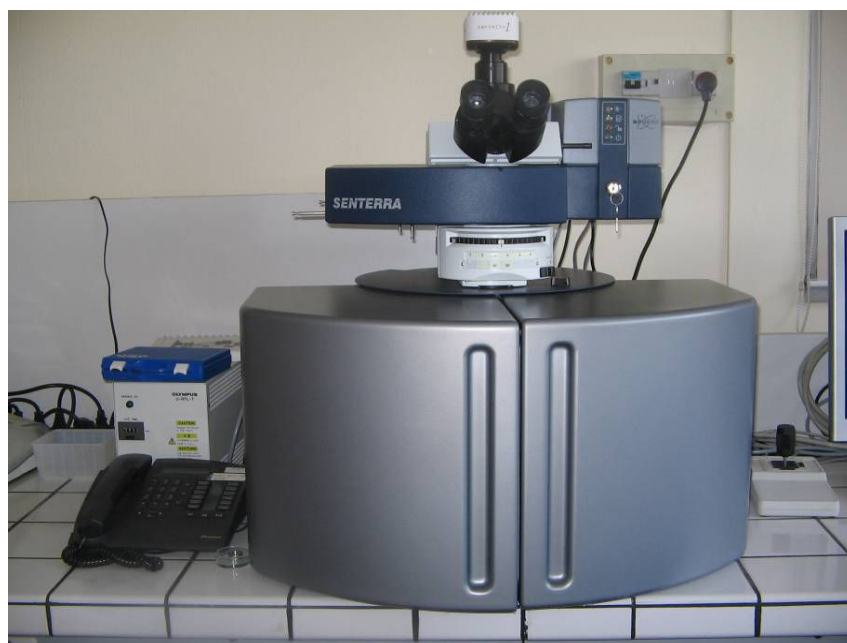


Fig. 6-12. Senterra microscope

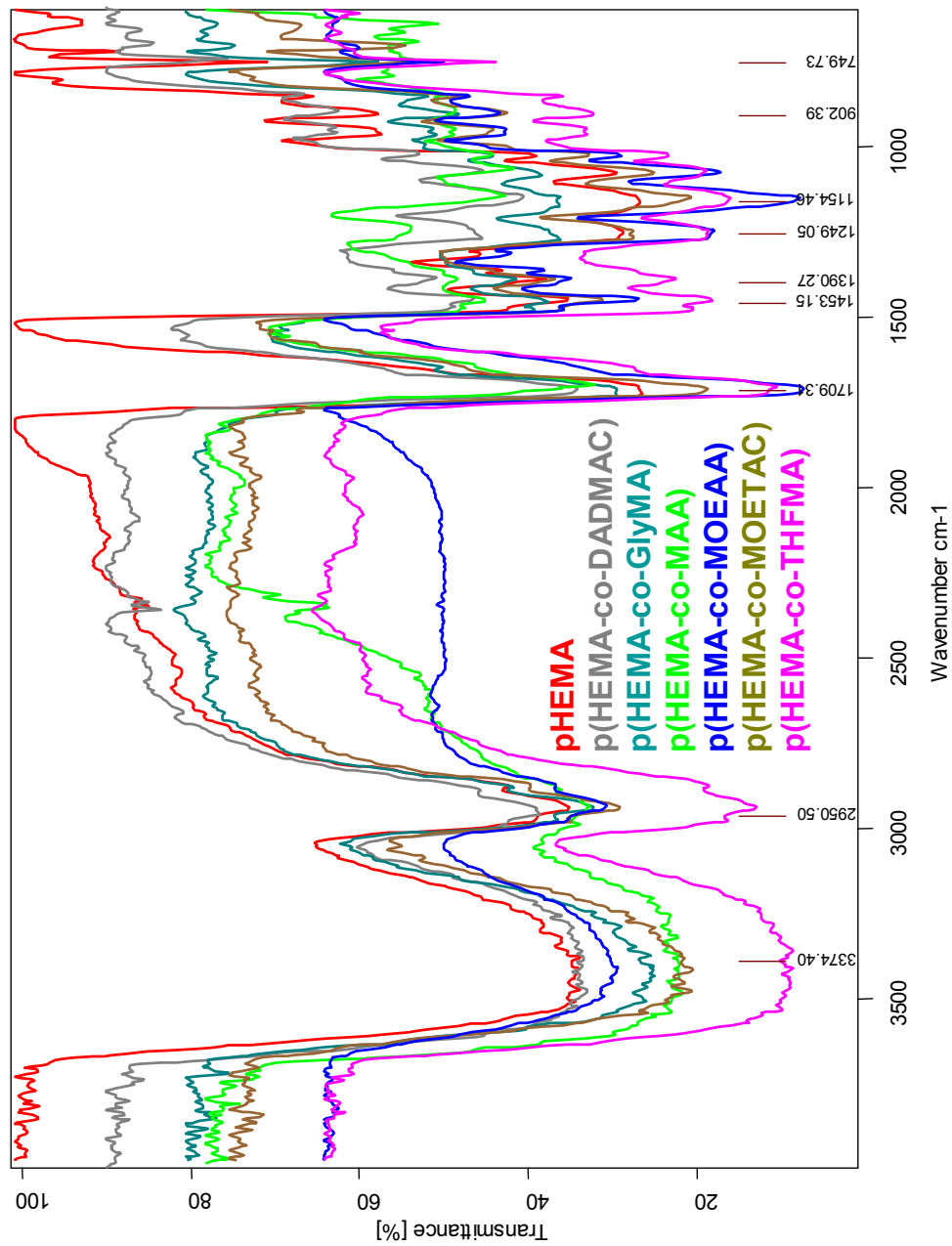


Fig. 6-13. Comparative FT-IR spectra of the copolymers obtained

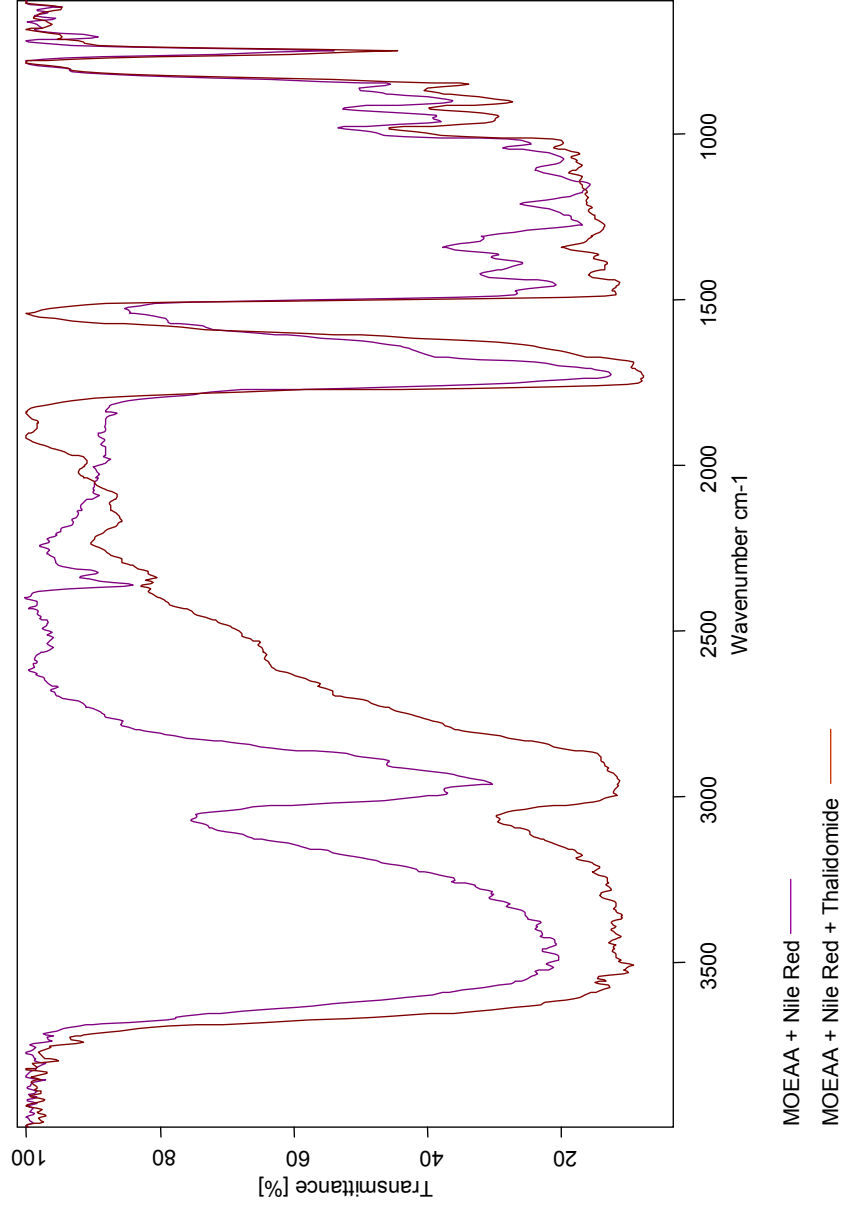


Fig. 6-14. Comparative FT-IR spectra of p(HEMA-co-MOEAA) and p(HEMA-co-MOEAA) loaded with thalidomide

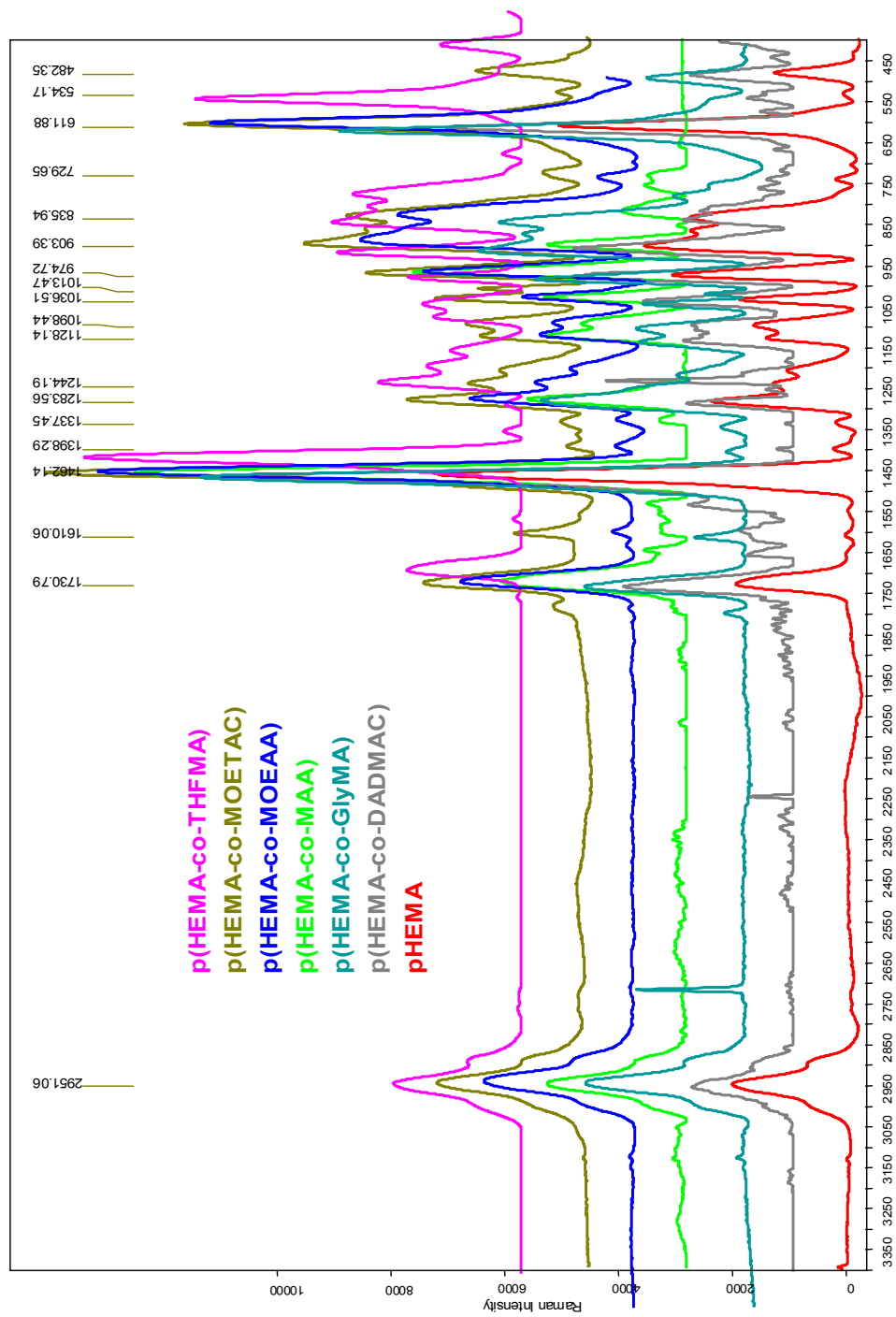


Fig. 6-15. Comparative Raman spectra of the copolymers obtained

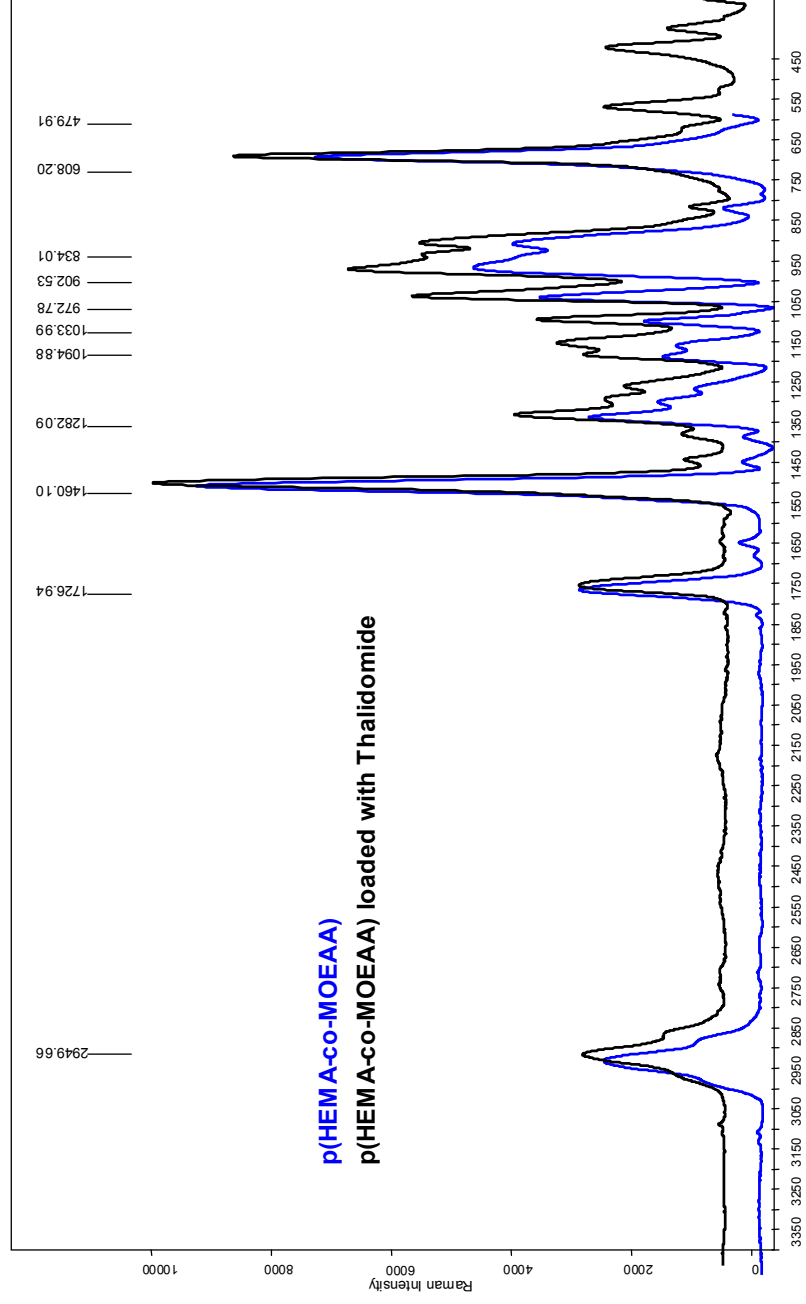


Fig. 6-16. Comparative Raman spectra of p(HEMA-co-MOEAA) and p(HEMA-co-MOEAA) loaded with Thalidomide

FT-IR and Raman spectroscopy represent the best techniques available for the quick identification and characterisation of specific bonds attached to new copolymers. The results of the spectra gave us the absorbance wavelengths of the specific bonds which appeared in the polymers obtained (Table 6-2 and Fig. 6-13 to 6-16), in comparison with a standard pHEMA spectrum, confirming the structure of the new materials.

Table 6-2

Wavelengths of specific functional groups in the copolymers obtained

Copolymer	Specific bonds	Peak wavelength (cm⁻¹)
p(HEMA-co-DADMAC)	R ₃ N (quaternary ammonium salt)	1359
p(HEMA-co-GlyMA)	3 ring ether C-O-C	1272, 904
p(HEMA-co-MAA)	COOH	1697
p(HEMA-co-MOEAA)	C=O	1716
p(HEMA-co-MOETAC)	R ₃ N (quaternary ammonium salt)	1356
p(HEMA-co-THFMA)	5 ring ether C-O-C	1074

One may also notice modifications of the initial spectrum of p(HEMA-co-MOEAA), so that the drug is expected to have been loaded.

6.3.3. Swelling tests

The polymers obtained are cross-linked hydrophilic matrices, especially due to the high HEMA ratio. Therefore, they do not dissolve in aqueous media, but they swell, in function of the degree of cross-linking and of the hydrophilicity of the comonomers in the matrix.

The swellability of the copolymers obtained is important in order to verify the compatibility of these structures with the physiological fluids. Also, the water uptake capability could be useful in promoting the fixation of Ca-P crystals onto the polymers' surface.

Water uptake ratios of the polymeric structures were determined in saline solution (concentration of 9 g NaCl / 1 L distilled water). The experiment was performed as follows: three pellet samples of each copolymer were dried up to constant mass and weighted before being poured into 50 mL vials containing saline solution. The vials were put in an oven at 37 °C. The samples were allowed to swell and they were weighted every 30 min., up to constant mass. The weights of dry and wet pellets were recorded. The swelling degree was determined gravimetrically, by using the following expression:

$$x(\%) = \frac{m_i - m_0}{m_0} \cdot 100$$

where: x is the swelling degree (%), and m_0 and m_i are the weights of the dry and wet samples, respectively (expressed in grams).

The evolution of the swelling degree enables also the calculus of the swelling constant, accordingly to the equations for swelling degree of first order:

$$\frac{dx}{dt} = k \cdot (A - x)$$

$$\ln\left(\frac{A}{A-x}\right) = kt$$

where: k is the swelling constant, and $A = x_{max}$ (the maximum swelling degree, %).

The swelling degree of the polymers obtained versus time is presented in Fig. 6-17.

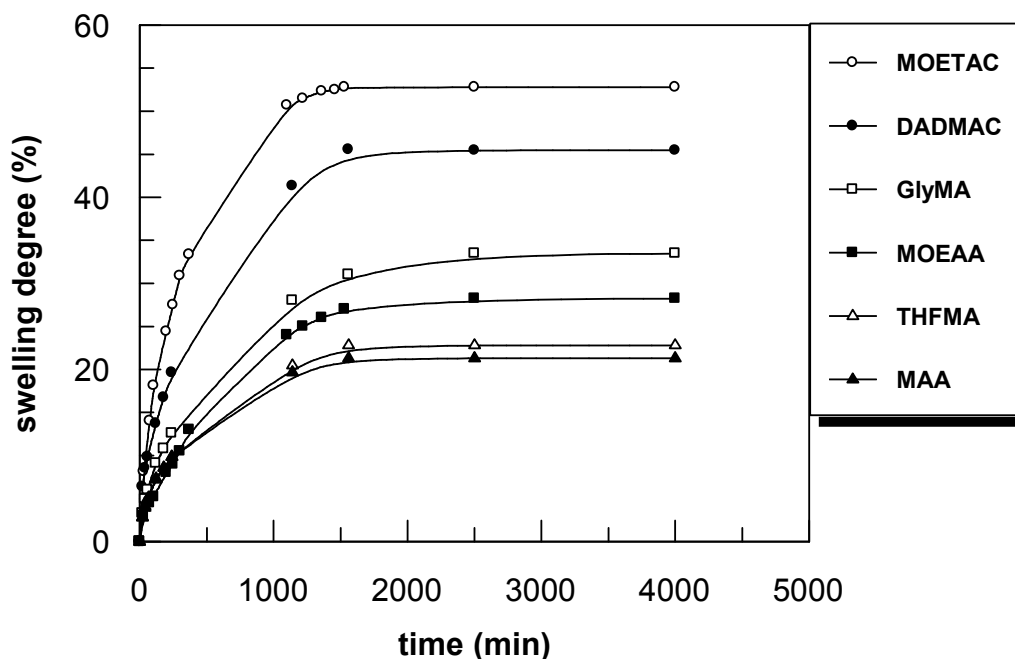


Fig. 6-17. Evolution of the swelling degree versus time (for simplification, it was only mentioned the name of the comonomer)

The swelling process follows a 1st order kinetic, and as a consequence the k parameter measures the diffusion rate of the water phase in the polymer matrix (kinetic compatibility) and the maximum value of the swelling coefficient A measures the thermodynamic equilibrium compatibility of the two substances. The results are presented in Table 6-3.

The high values for A parameter represent a smaller cross-linking ratio (due to the feed composition). In case of MOETAC and DADMAC-containing copolymers, the value of the swelling degree is higher than for the others, which is explained by the monomers' structure (quaternary

ammonium salt) which increases greatly the compatibility with the aqueous media. Taking into account all these considerations, one may conclude that all the structures investigated present thermodynamic and kinetic compatibility with the physiological serum.

Table 6-3

A and k values

Copolymers	A (%)	k (min ⁻¹)
p(HEMA-co-MOETAC)	52.78	0.0019
p(HEMA-co-DADMAC)	45.56	0.0020
p(HEMA-co-GlyMA)	29.20	0.0016
p(HEMA-co-MOEAA)	28.20	0.0029
p(HEMA-co-THFMA)	22.79	0.0019
p(HEMA-co-MAA)	21.30	0.0022

The water uptake ratio of the polymers slightly decreases in case of p(HEMA-co-MOETAC) ($\approx 53\%$) versus pHEMA ($\approx 55\%$). Incorporating ammonium-containing comonomers (such as MOETAC and DADMAC) actually increases the hydrophilicity potential of the polymer chain, in comparison with the other structures proposed.

In function of the drug release rate needed, all the systems are available for use as such, or even to incorporate a hydrophobic monomer to decrease the swelling potential.

6.3.4. Mineralization tests

The next step of the study consisted in the *in vitro* evaluation of HA induction capacity on the polymers' surface. In this respect, three samples of each copolymer, as pellets and microbeads, were incubated in 1x and 1.5x synthetic body fluid (SBF) (Table 6-4) (Kokubo et al., 1990 and 2006) adjusted with tris(hydroxy-methyl) aminomethane (Tris) and hydrochloric acid HCl to pH = 7.4. Sterile containers with 50 mL of the incubation medium were maintained at 37°C in an atmosphere composed of 5% CO₂ and 95% O₂ for 14 days.

Microbeads were continuously stirred in a Rotatest (Bioblock Scientific) (Fig. 6-18), while pellets were shaken at 400 rpm (Fig. 6-19).

The medium was changed every 48 hours. After incubation, the pellets were rinsed with distilled water, in order to remove any traces of inorganic salts from the polymers surface, and dried overnight at room temperature, followed by drying at 40°C for 24 hours.

Table 6-4

Composition of the SBF in ions concentration (mM) versus human body plasma

Ion	SBF 1x (mM)	SBF 1.5x (mM)	Human body plasma (mM)
Na ⁺	142.19	144.785	142.0
K ⁺	4.85	7.275	5.0
Mg ²⁺	1.5	2.25	1.5
Ca ²⁺	2.49	3.735	2.5
Cl ⁻	141.54	143.31	103.0
HCO ₃ ⁻	4.2	6.3	27.0
HPO ₄ ²⁻	0.9	1.35	1.0
SO ₄ ²⁻	0.5	0.75	0.5
pH	7.4	7.4	7.2-7.4



Fig. 6-18. Installation for microbeads homogenous turning – calcification tests.



Fig. 6-19. Installation for pellets stirring – calcification tests.

6.3.5. Scanning electron microscopy (SEM) and Energy Dispersive X-rays (EDX)

The surface morphology before and after the calcification tests was examined using SEM coupled with EDX. It was used a JEOL JSM-6301F (JEOL Paris, France), equipped with an EDX microanalysis system, model Link ISIS (Oxford, Anglia) (Fig. 6-20). Samples were dried at 40°C up to constant mass before analysis. The samples were then mounted on Pb plots and covered with a thin layer of carbon using a MED 020 Baltec (Balzers, Lichtenstein). After carbon-coating, the samples were introduced in the microscope and scanned at 3 kV. Quality and dimensions of the microbeads obtained and morphology of the crystals on the surfaces after incubation were studied.



Fig. 6-20. SEM coupled with EDX apparatus

Particles of approximately 1 μm were obtained. They are dispersible in aqueous saline solution of 9 ‰ NaCl (g/L) in demineralised water. The microphotographs did not show any mineral activity in case of polymers incubated in 1x SBF, but presented mineral deposits on all the surfaces of materials incubated in 1.5x SBF (Fig. 6-21 to 6-26).

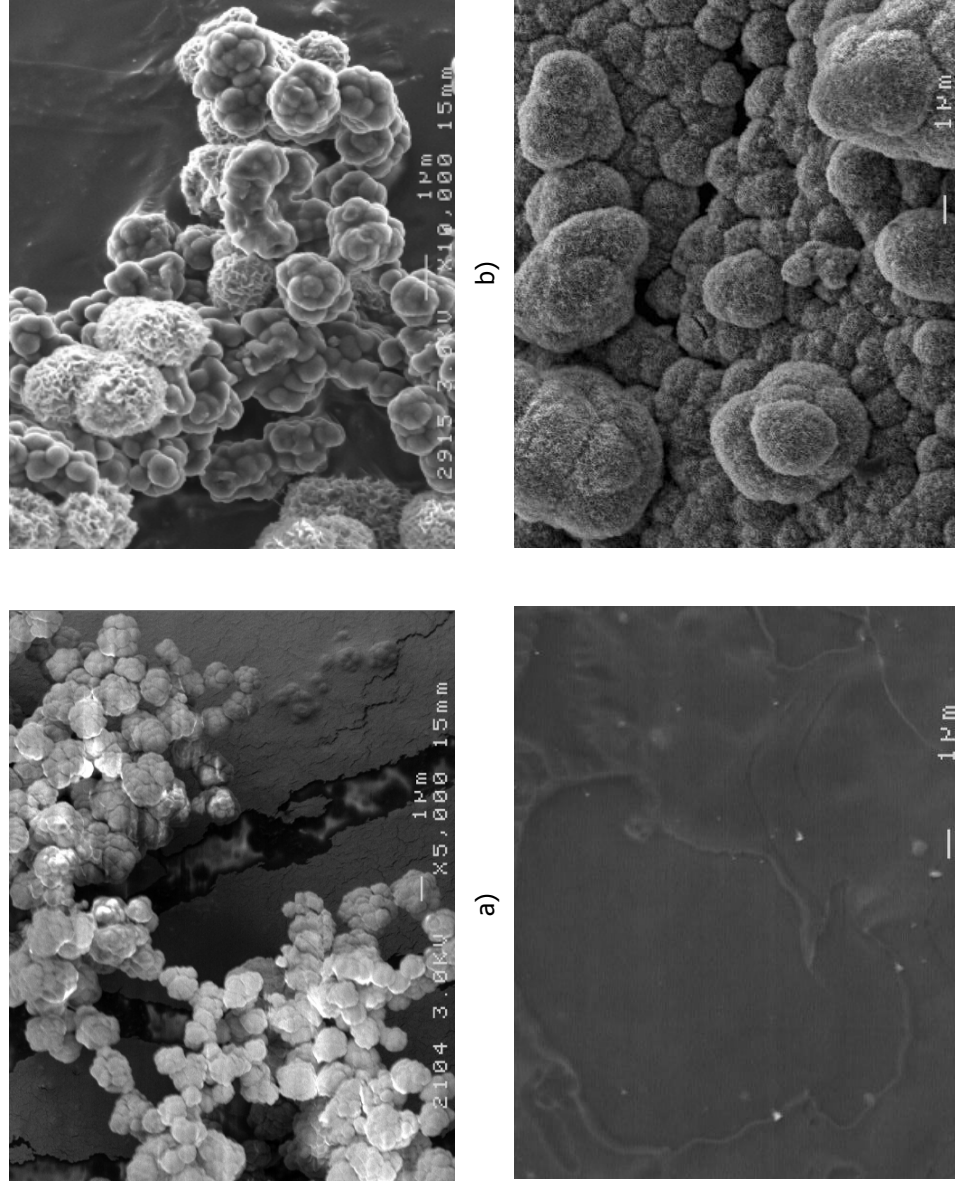


Fig. 6-21. p(HEMA-co-DADMAC) microbeads before (a) and after (b) incubation in 1.5x SBF and pellets before (c) and after (d) incubation in 1.5x SBF.

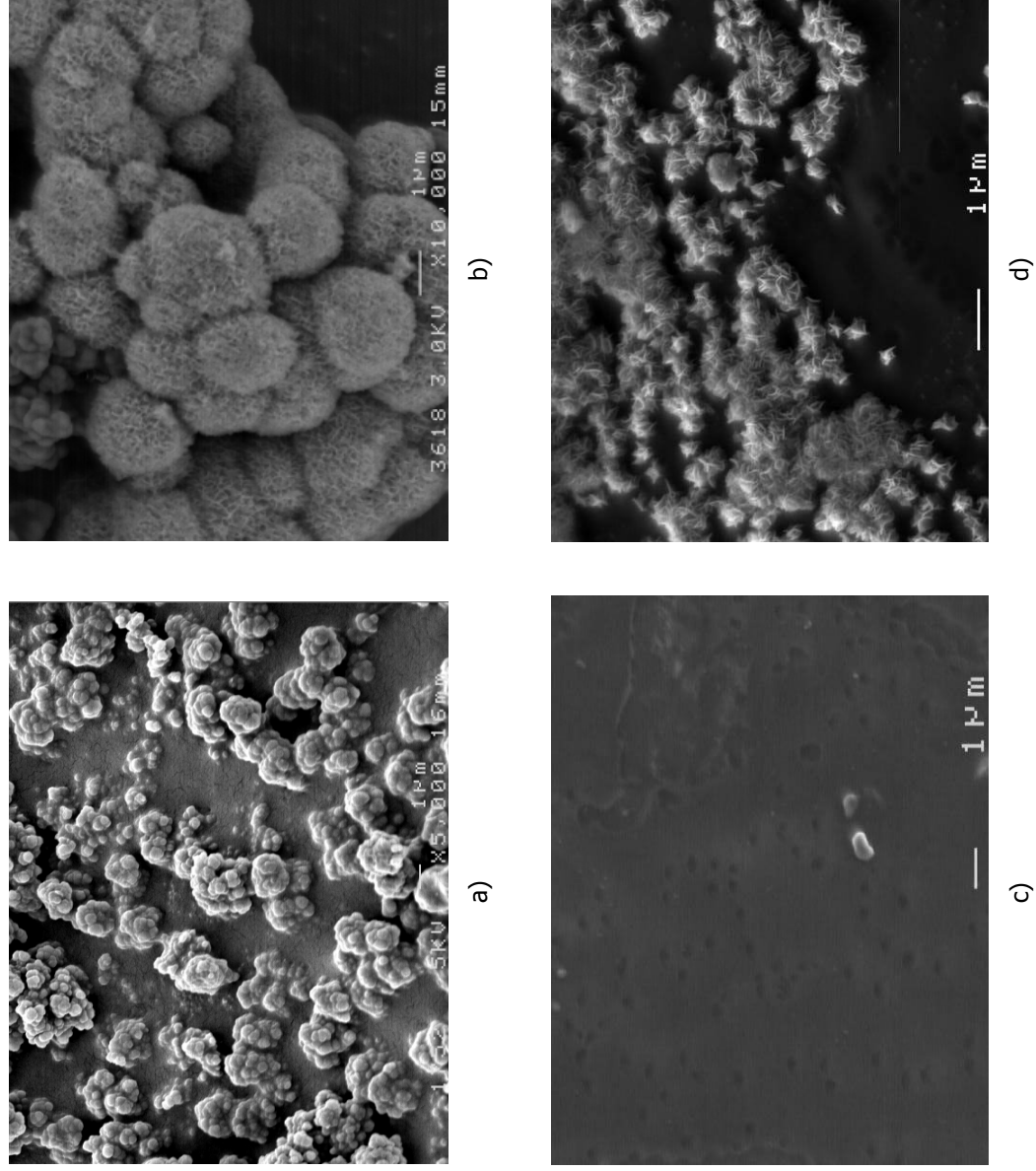


Fig. 6-22. p(HEMA-co-GlyMA) microbeads before (a) and after (b) incubation in 1.5x SBF and pellets before (c) and after (d) incubation in 1.5x SBF.

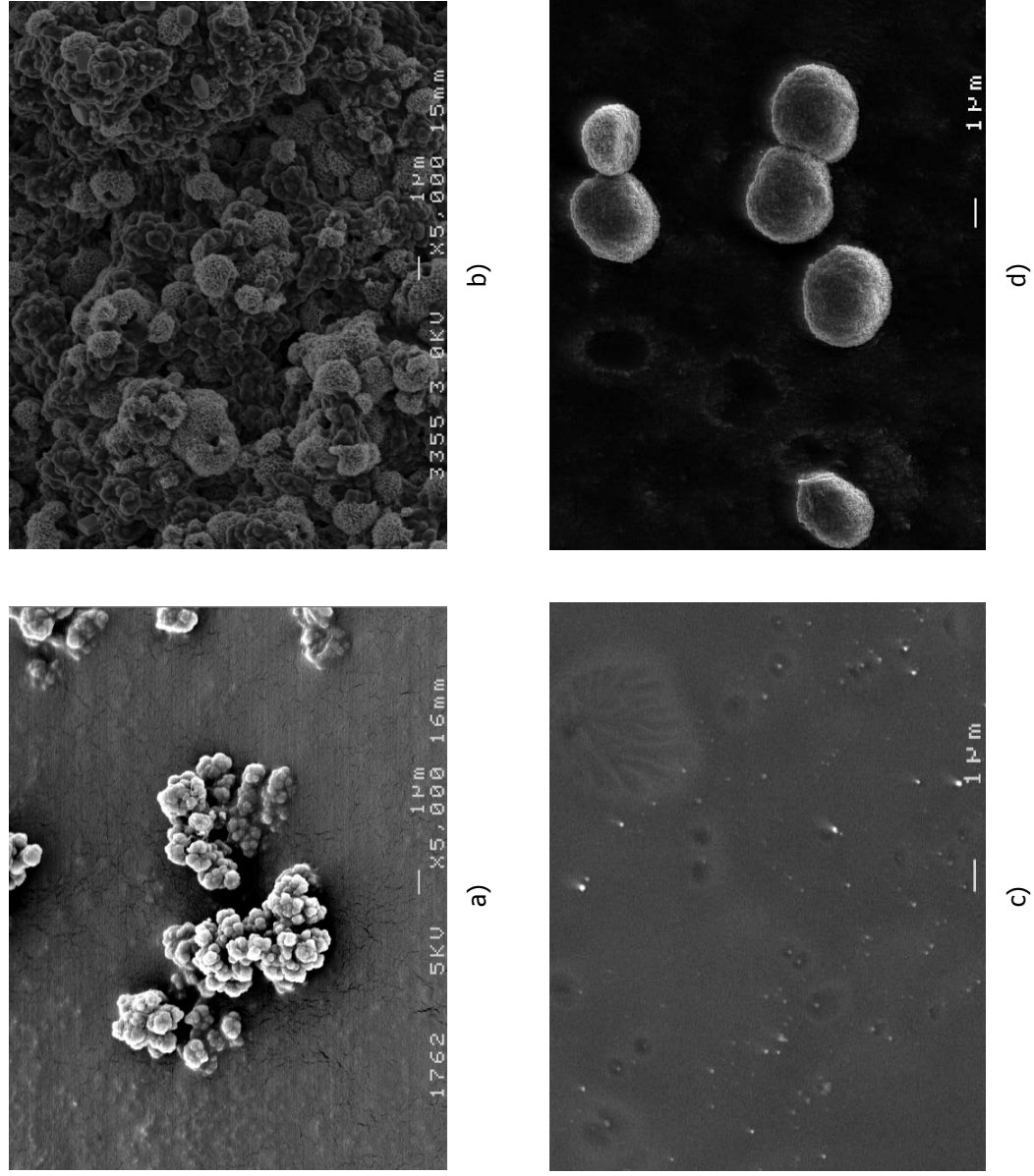
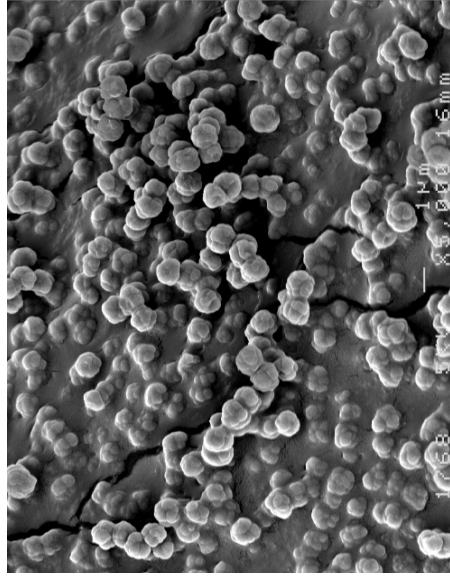
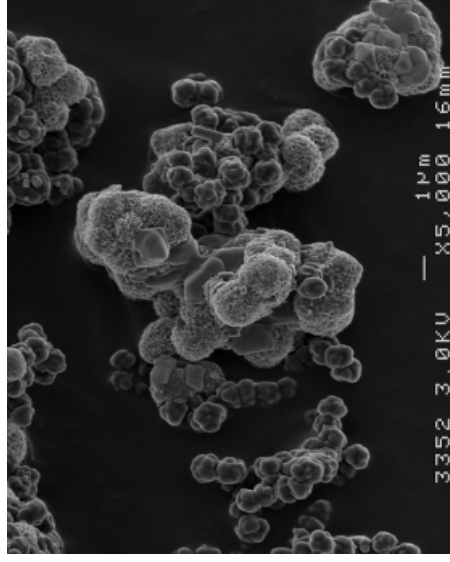


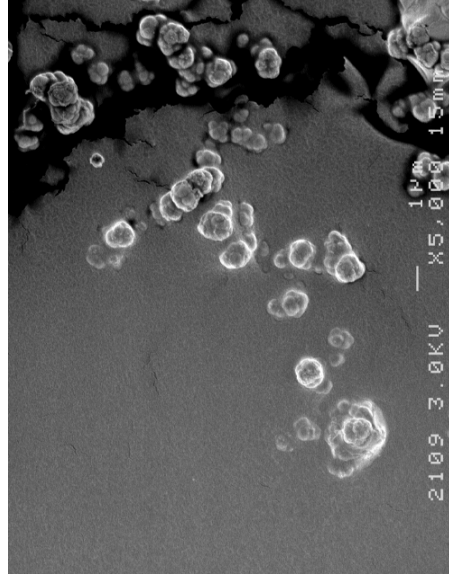
Fig. 6-23. p(HEMA-co-MAA) microbeads before (a) and after (b) incubation in 1.5x SBF and pellets before (c) and after (d) incubation in 1.5x SBF.



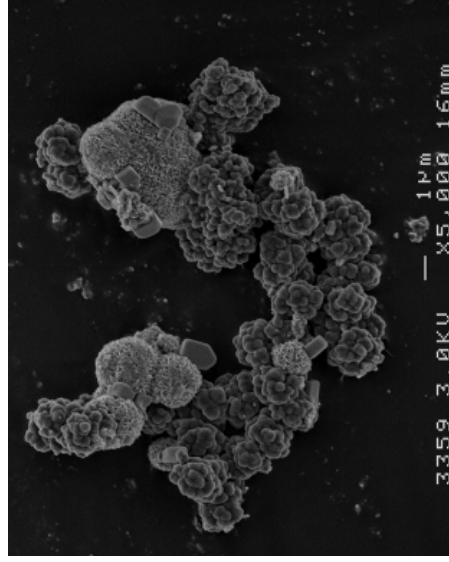
a)



b)



c)



d)

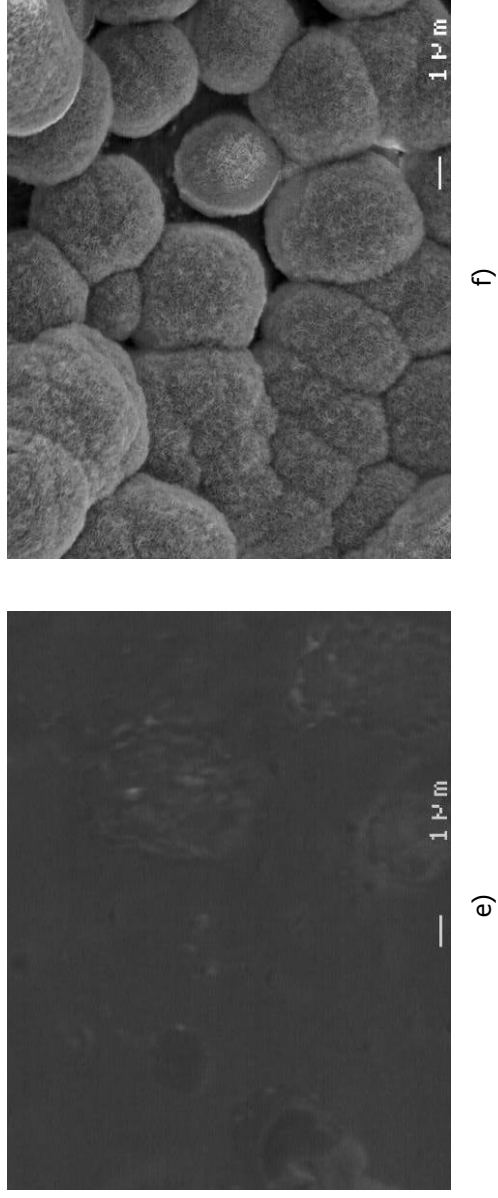


Fig. 6-24. p(HEMA-co-MOEAA) microbeads before (a) and after (b) incubation in 1.5x SBF, Nile Red-containing microbeads before (c) and after (d) incubation in 1.5x SBF, and pellets before (e) and after (f) incubation in 1.5x SBF.

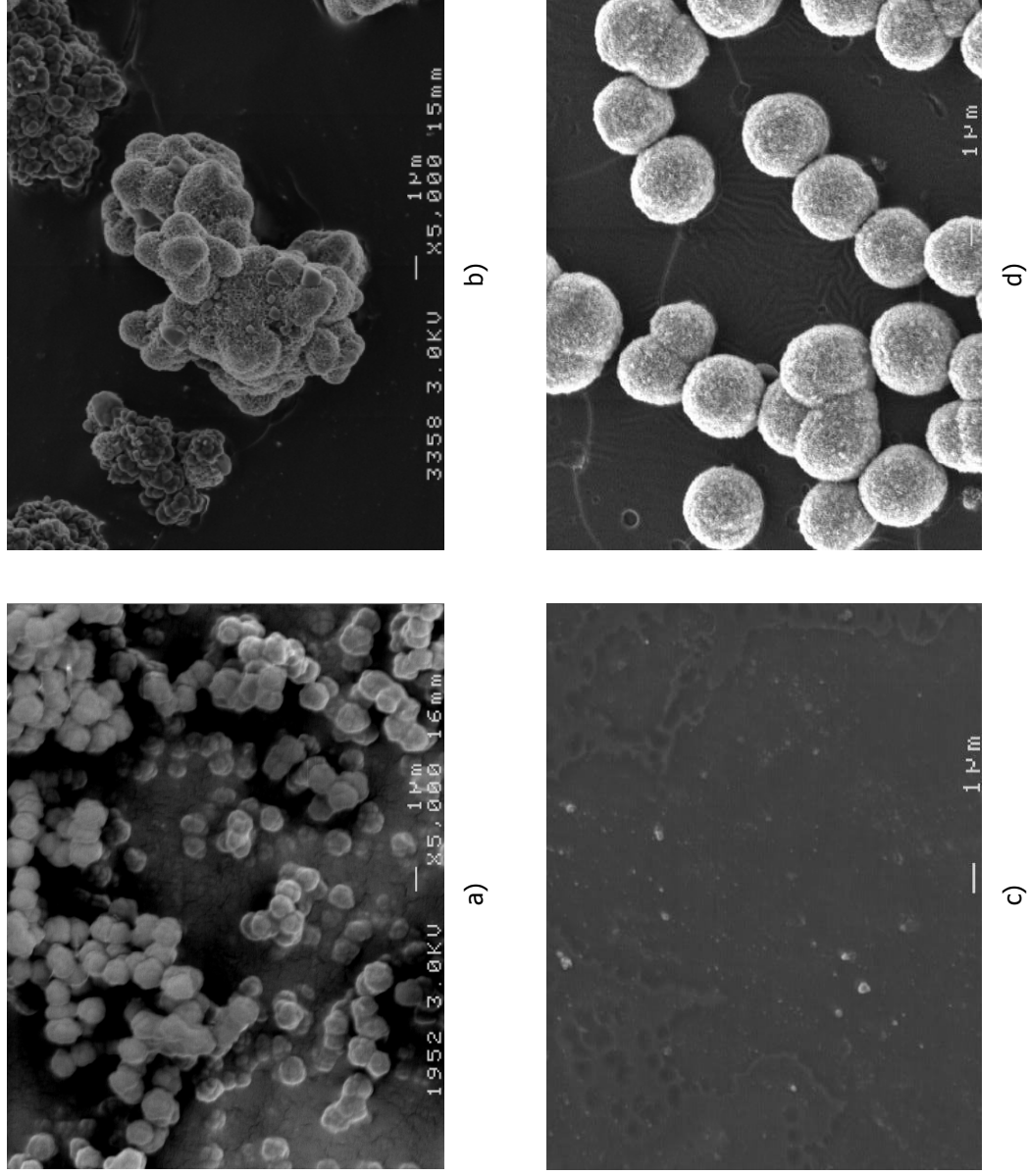


Fig. 6-25. p(HEMA-co-MOETAC) microbeads before (a) and after (b) incubation in 1.5x SBF and pellets before (c) and after (d) incubation in 1.5x SBF.

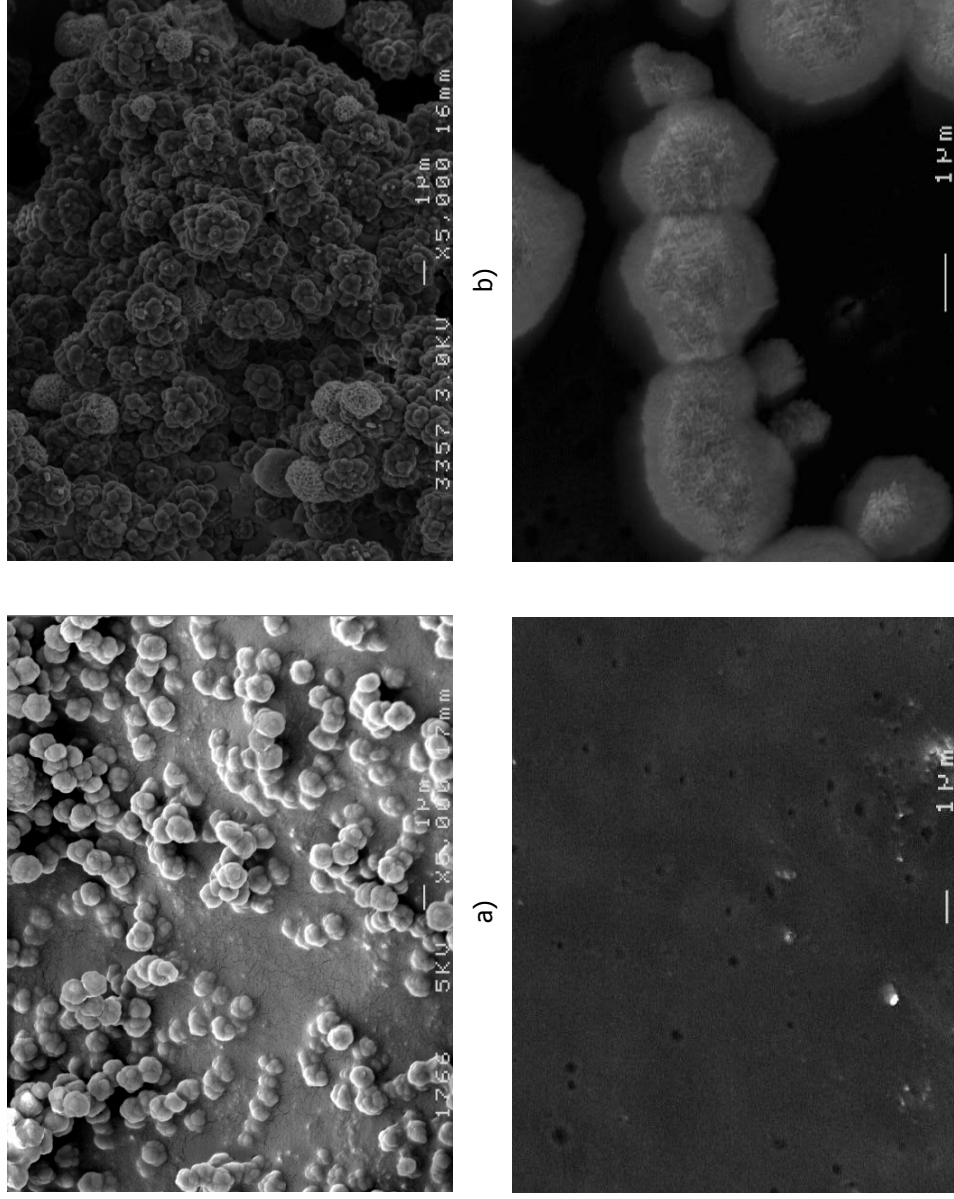


Fig. 6-26. p(HEMA-co-THFMA) microbeads before (a) and after (b) incubation in 1.5x SBF and pellets before (c) and after (d) incubation in 1.5x SBF.

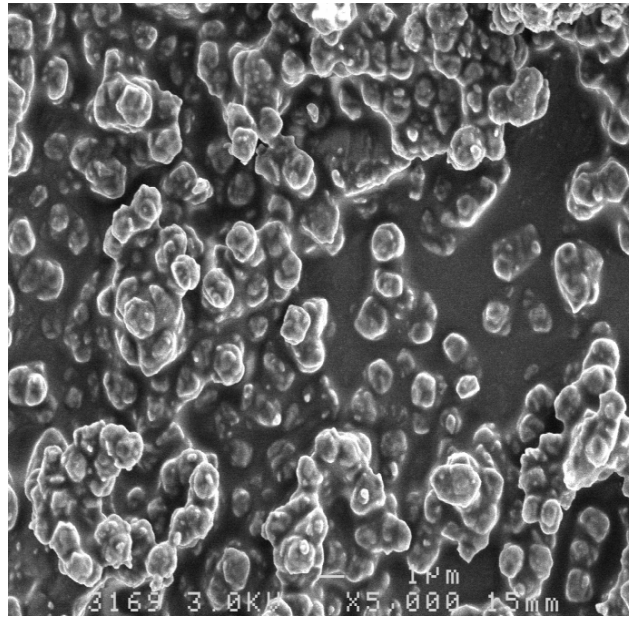


Fig. 6-27. Microbeads of p(HEMA-co-MOEAA) loaded with thalidomide.

There were obtained $\sim 1\mu\text{m}$ microbeads, the best shaped and individualised being MOEAA and DADMAC-containing polymers. Consequently, p(HEMA-co-MOEAA) microbeads loaded with thalidomide were analysed (Fig. 6-27) and the results obtained confirmed that this polymer is available for *in vivo* tests.

As regarding the pellets obtained, they present a flat shape and homogenous surface. The solution 1x SBF does not initiate the calcification neither in case of the pellets, nor of the microbeads. Consequently, a further study using 1.5x SBF was performed. From the microphotographs one may observe that p(HEMA-co-GlyMA) and p(HEMA-co-MOETAC) give the best shaped calcospherites, while p(HEMA-co-DADMAC) gives mineral agglomerates, but which appear not to be calcospherites. The other do not seem to induce HA formation.

The results are sustained by EDX spectra that give also an expression of the Ca/P molar ratio of the mineral deposits found on the polymeric surfaces (Fig. 6-28). In Table 6-5 there are shown the Ca/P ratios found for the copolymers incubated.

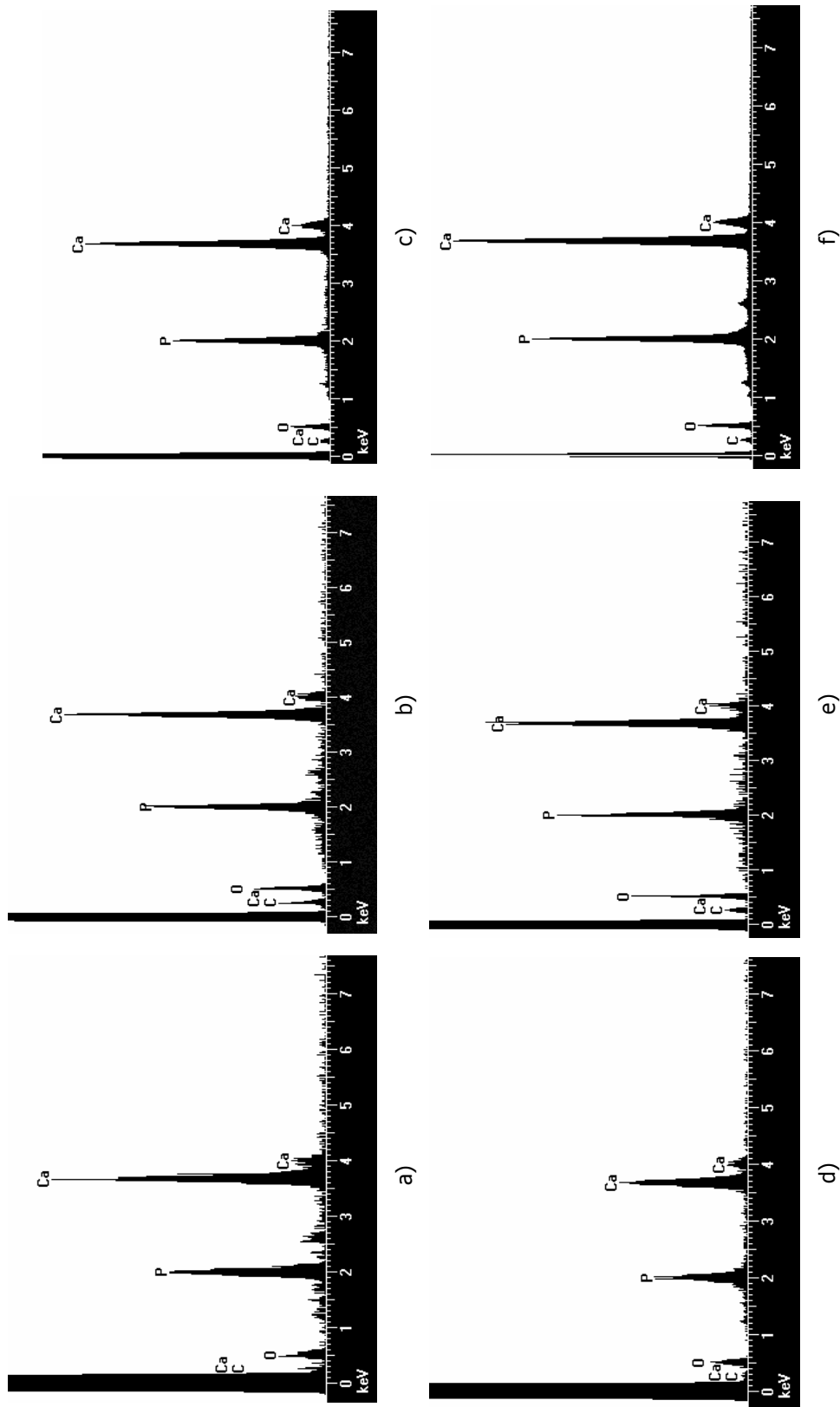


Fig. 6-28. EDX graphs of the copolymers after incubation in 1.5x SBF: a) p(HEMA-co-DADMAC), b) p(HEMA-co-GlyMA), c) p(HEMA-co-MAA), d) p(HEMA-co-MOEAA), e) p(HEMA-co-MOETAC), f) p(HEMA-co-THFMA).

Table 6-5

Ca/P ratios obtained from EDX

Ca/P values in copolymers found by EDX	
p(HEMA-co-DADMAC)	1.729
p(HEMA-co-GlyMA)	1.683
p(HEMA-co-MAA)	1.850
p(HEMA-co-MOEAA)	1.740
p(HEMA-co-MOETAC)	1.687
p(HEMA-co-THFMA)	1.633

In case of p(HEMA-co-GlyMA), Ca/P ratio is 1.683 and, for p(HEMA-co-MOETAC), 1.687 that are the closest values to the one in HA, $\text{Ca}_{10}(\text{PO}_4)_6(\text{OH})_2$ (where Ca/P molar ratio is 1.67). A preliminary conclusion that can be drawn from SEM and EDX spectra is that GlyMA and MOETAC-containing polymers represent potential apatite crystal growth stimulators.

6.3.6. Spectrophotometrical dosage of calcium and phosphorus

Spectrophotometrical dosage of Ca^{+2} and PO_4^{-3} ions was used in order to determine quantitatively the Ca/P ratio at polymers' surface (comparatively with 1.67 from HA) and to clarify the nature of salts inducted, after having obtained the specific shape of HA clusters only for p(HEMA-co-GlyMA) and p(HEMA-co-MOETAC). There were used three samples of each polymer. The samples were washed, treated with 2 ml of a 0.2 M HCl solution in order to dissolve eventual calcium and phosphate mineral deposits. After 24 hours the solution was filtered and recovered. Calcium and phosphate ions dosage from these solutions was performed on a Hitachi 917 spectrophotometer (Roche, France). Finally, the Ca/P molar ratio was computed to see if it approaches or not the ratio of HA.

The study revealed important quantities of these elements onto the surfaces of the synthesized materials. The dosage results are given in Table 6-6.

Taking as reference the structure of HA, there were quantitatively established the polymer structures available for *in vitro* HA formation.

As expected from the previous results obtained from SEM and EDX, in case of p(HEMA-co-GlyMA) and p(HEMA-co-MOETAC) the Ca/P molar ratios are very close to 1.67. In the other cases, there were found calcium and phosphate quantities on the surface in ratios very different from the ratio in HA. The applicability of p(HEMA-co-GlyMA) and p(HEMA-co-MOETAC) films would be to induce osseous growth (osteinduction or osteoconduction) into osseous defects.

Table 6-6

Dosage results for Ca^{2+} and PO_4^{3-} ions

Polymers *		Ca^{2+} (mM)	PO_4^{3-} (mM)	Ca/P
pHEMA (control)	a	0.45	0.20	2.3
	b	0.26	0.10	2.6
	c	0.13	0.07	1.9
p(HEMA-co-DADMAC)	a	3.18	1.30	2.4
	b	3.30	1.10	3.0
	c	2.20	1.00	2.2
p(HEMA-co-GlyMA)	a	1.45	0.80	1.8
	b	1.80	1.00	1.8
	c	1.60	1.00	1.6
p(HEMA-co-MAA)	a	7.20	2.40	3.0
	b	5.10	2.30	2.2
	c	7.20	2.50	2.9
p(HEMA-co-MOEAA)	a	0.88	0.36	2.4
	b	0.55	0.12	4.6
	c	2.35	0.60	3.9
p(HEMA-co-MOETAC)	a	3.86	2.40	1.6
	b	3.27	2.10	1.6
	c	1.57	1.20	1.3
p(HEMA-co-THFMA)	a	3.00	1.50	2.0
	b	3.50	1.70	2.1
	c	3.37	1.50	2.2

*for each type of polymer there were submitted to dosage three samples, for reproducibility

Also, taking into account the analyses made until this moment, (water uptake capacity, fluorescence, and surface properties), further there were used MOEAA and DADMAC-containing copolymers.

6.3.7. Size distribution report by volume

The present test is not an ordinary characterisation method for the size distribution determination and it was used for the first time in the literature, as far as we know, for polymeric particles, due to the reproducibility and accuracy of the method.

Microbeads were analysed by flow cytometry with a BD-FACS Aria flow cytometer (Becton Dickinson, Le Pont-De-Claix, France) equipped with an octagon laser (488nm) (Fig. 6-29), for a number of events of 30000. Microbeads signal was detected by the band pass filter (575/26 nm) of Phycoerythrin (PE), for fluorescence homogeneity (PE and Nile Red have similar absorption peaks (545/566 nm and 553 nm, respectively)).

Samples were also investigated for dimension homogeneity by Forward Scattering (FSC). Obtained data were computed with the WinMDI 2.8 software (Scripps Research Institute, La Jolla, CA).



Fig. 6-29. BD FACS Aria Flow Cytometer

FACS analysis of microbead polymers showed that microbeads are homogenous in size (narrow peaks on logarithmic scale) and fluorescence. Nile Red was successfully attached to all the polymeric samples during polymer synthesis (Fig. 6-30 and 6-31).

FSC-A = dimension, SSC-A = granulometry, PE-A = fluorescence, A = surface, H = height, W = width

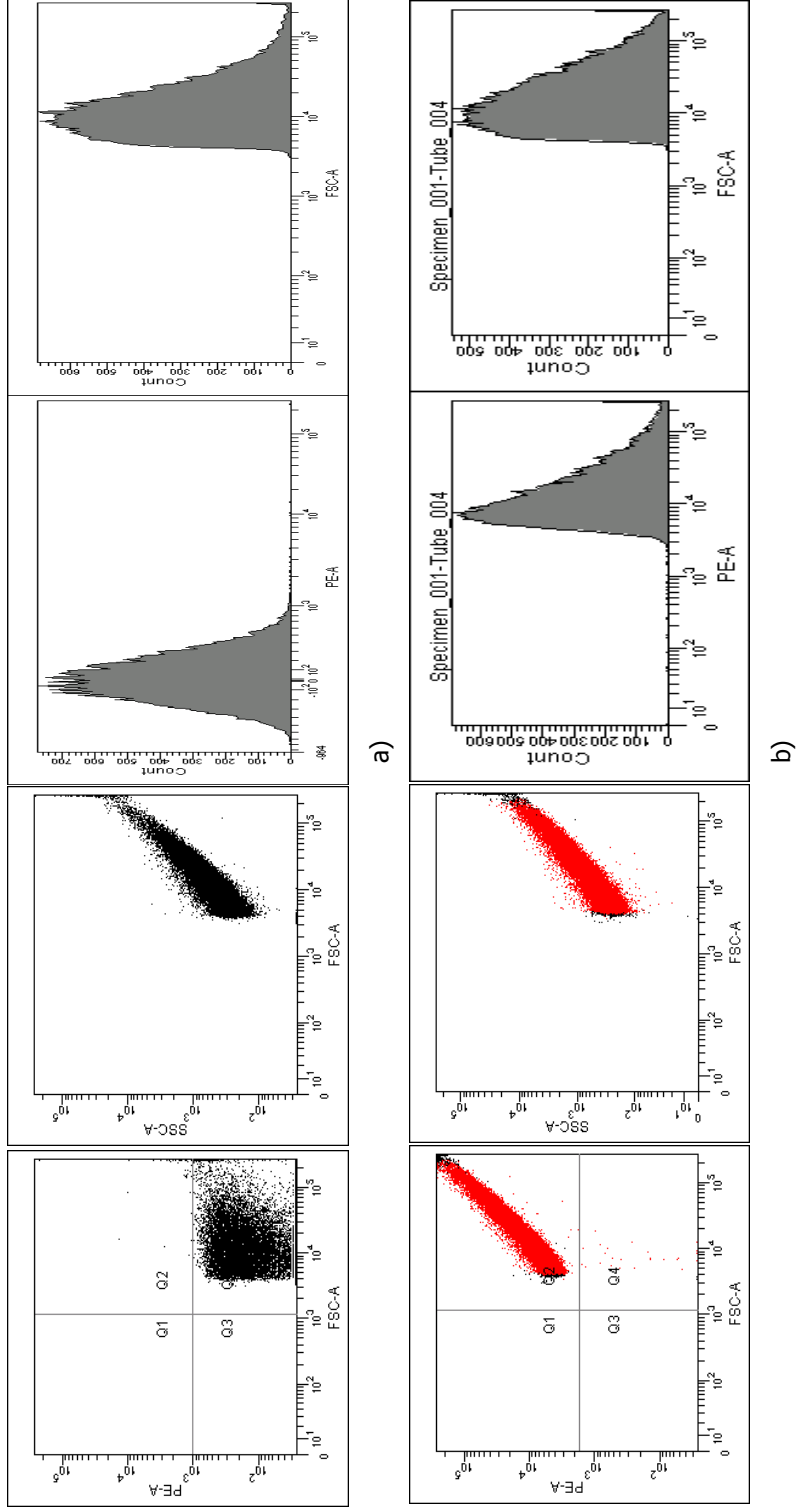


Fig. 6-30. Flow cytometry results for: a) p(HEMA-co-MOEAA) microbeads; b) p(HEMA-co-MOEAA) microbeads stained with Nile Red.

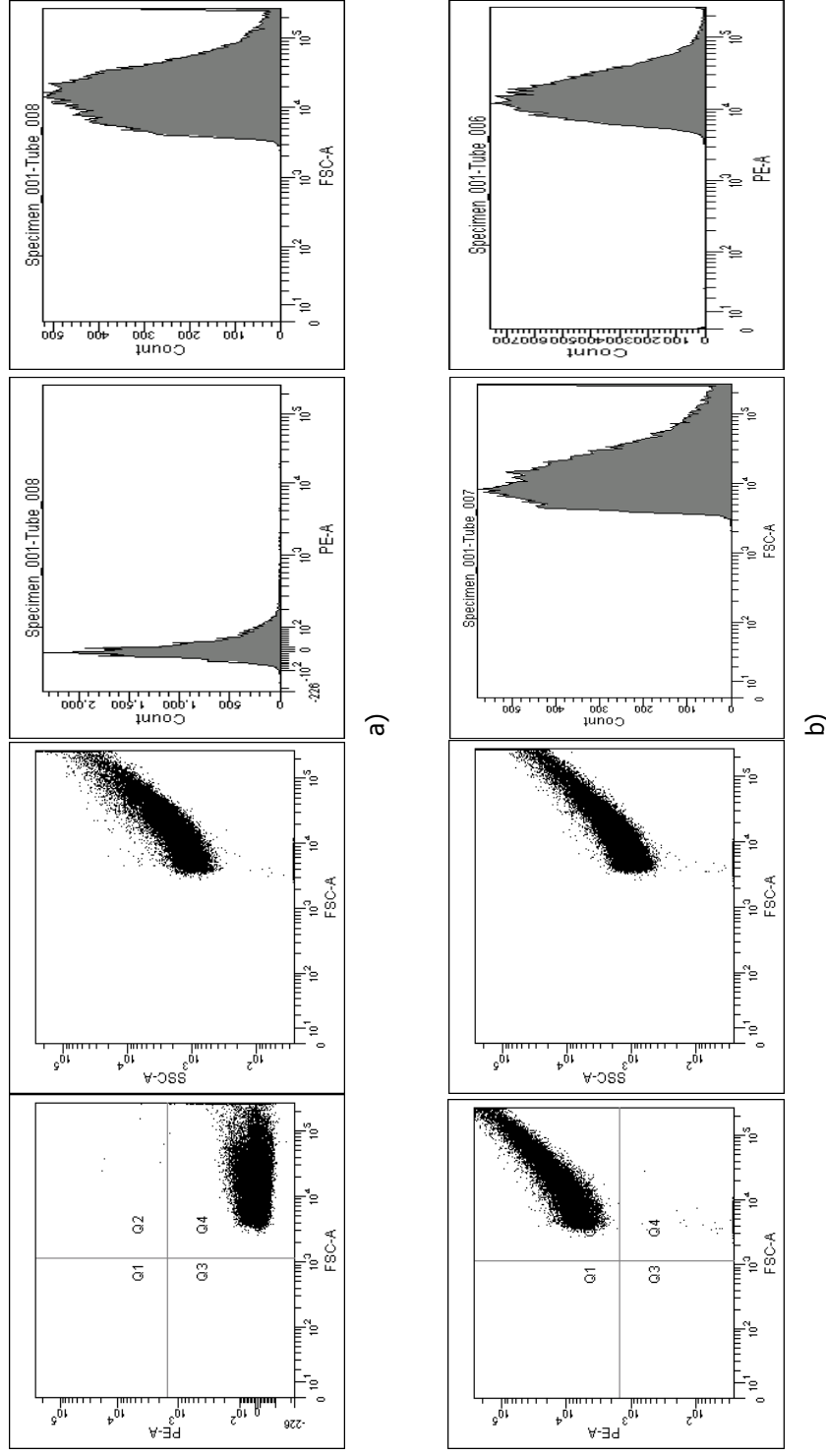


Fig. 6-31. Flow cytometry results for: a) p(HEMA-co-DADMAC) microbeads; b) p(HEMA-co-DADMAC) microbeads stained with Nile Red.

6.3.8. Cytotoxicity evaluation

6.3.8.1. *In vitro* evaluation with L929 line cell

Polymers biocompatibility was verified by testing their *in vitro* cytotoxicity and viability. The pellets were first exposed for 8 hours to UV light, at 360 nm and 12 W, for sterilization. It was used a murine fibroblast L929 cell line, which was cultivated in culture medium (DMEM), supplemented with calf fetal serum and antibiotics. The cultures were incubated in standard conditions, for 24-48 hours at 37 °C, in the presence of 5% CO₂ and were examined daily during three days. Cells were microscopically examined with an Olympus inverted microscope for detecting cytotoxicity visible signs, cellular lysis or cellular components dimensions and conformation.

For cytotoxicity evaluation, besides microscopically examination, it was also performed a cellular viability test. For this purpose, after transfection the cells were incubated in well plates with a tetrazolium soluble salt, MTT. This one is converted by dehydrogenases present in viable cells mitochondria in insoluble formazan which appears as violet crystals. The pellets were incubated at 37 °C and 5% CO₂ for 4 hours, until violet crystals of formazan appeared. The optical density was read at 570 nm using an automatic multi-well reader (ELISA).

There were not observed cytotoxic effects, the morphologic characteristics and the adherence being similar for the cells incubated in the presence or in the absence of the samples (Fig. 6-32 and 6-33).

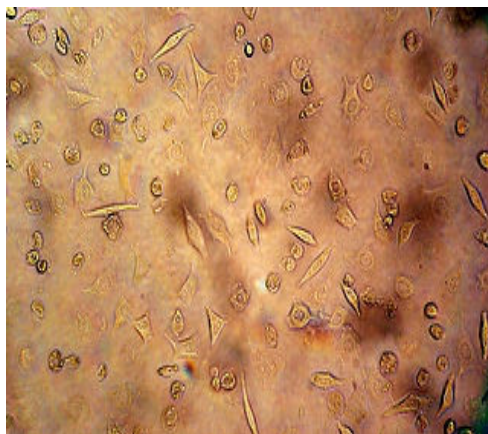


Fig. 6-32. Microscopic image of L929 cells in culture, in the absence of samples and before the addition of MTT

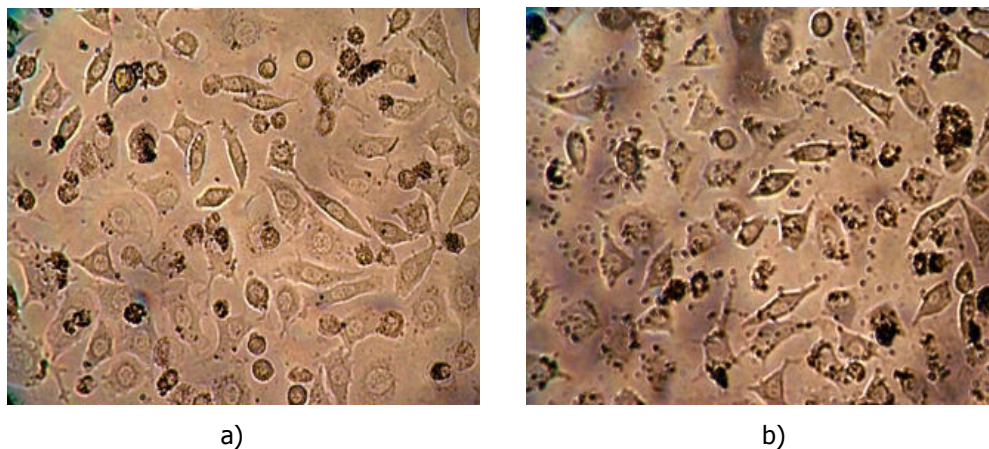


Fig. 6-33. Microscopic image of L929 cell line in culture, incubated for 24h with: a) p(HEMA-co-GlyMA), b) p(HEMA-co-MOETAC).

In the same time, after the addition of the MTT dye, both the cells incubated with the samples and those untreated reduced the MTT and formed formazan crystals (Fig. 6-34).

After the formazan crystals dissolution, optic density, which is proportional with the viability, was measured at 570 nm. Cellular viability was calculated in percentage versus a blank control test (with cells incubated in the same conditions and volume). Viability of L929 cell line is given (Fig. 8) as average \pm standard deviation of viability ratios obtained from three experiments (on abscise is given the sample suspension ratio in the entire volume) (Fig. 6-35).

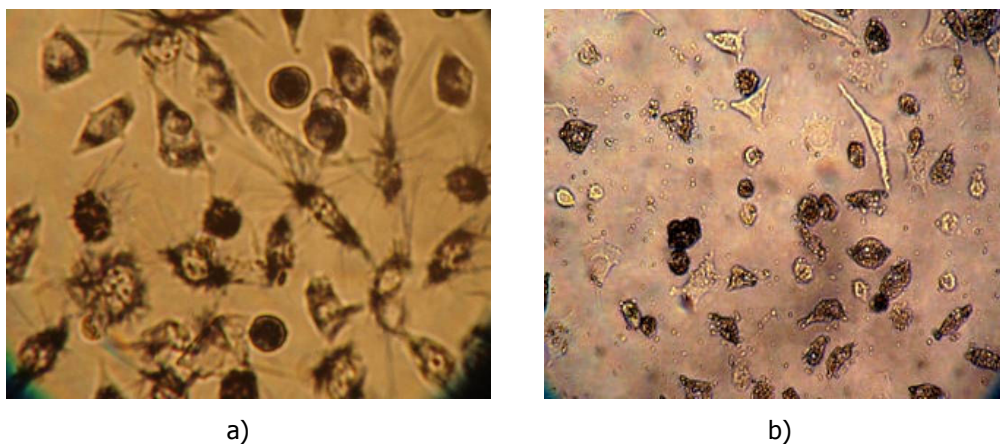


Fig. 6-34. Microscopic image of L929 cells in culture after incubation for 24h in the presence of: a) p(HEMA-co-GlyMA), b) p(HEMA-co-MOETAC), after the addition of MTT.

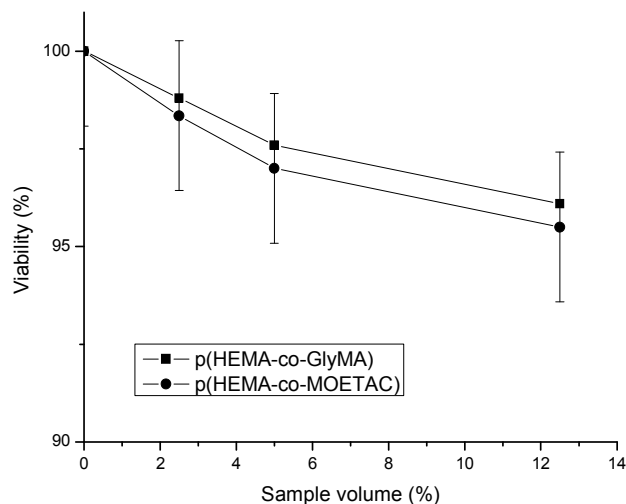


Fig. 6-35. L929 cell line viability measured by MTT assay performed 4 h after transfection in the presence of polymeric samples (average \pm standard deviation).

From the data presented, one can observe that polymeric samples present only a very slight cytotoxic effect. Calculated values of cellular viability versus the control sample, incubated in the same conditions in the absence of polymeric samples, were found to be 96.1 ± 1.65 % for p(HEMA-co-GlyMA) and 95.5 ± 1.89 % for p(HEMA-co-MOETAC) in case of maximum stimulation volume. Attenuation of cell viability curves is noticed as stimulation suspension volume increases.

The *in vitro* tests of cytotoxicity made on fibroblast murine L929 cell line gave adequately results for the compositions tested, presenting minimal adverse effects on cell morphology and viability.

6.3.8.2. *In vitro* evaluation with EA.hy 926 cells

There were also performed *in vitro* tests for the evaluation of the cells capability to incorporate microbeads of p(HEMA-co-MOEEA) and p(HEMA-co-DADMAC) stained with Nile Red.

Endocytosis is a complex pathway, its mechanisms depend on membrane receptors present on endothelial cells, and caveolar-mediated uptake is the most frequently observed process in endothelial cells. The optimal selection of surface determinants of endothelial cell is necessary in designing and functionalizing drug delivery systems. The role of surface charges in the endocytic process of particles remains poorly understood and the effect charge interactions is limited compared to steric interactions.

Human endothelial EA.hy 926 cells (INSERM U922, Angers, France) were cultured in a mixture medium (1:1) containing DMEM and HAM F12 medium. The mixture was supplemented with 10% of fetal calf serum, with HAT (100 μ M hypoxanthine, 0.4 μ M aminopterin, and 16 μ M thymidin) and penicillin/streptomycin. EA.hy 926 cells were seeded at the concentration of 5×10^4

cells in 1ml of complete medium, on cover glass. Cell culture was maintained in a humidified atmosphere of 5% CO₂ at 37°C. All experiences were performed in triplicate.

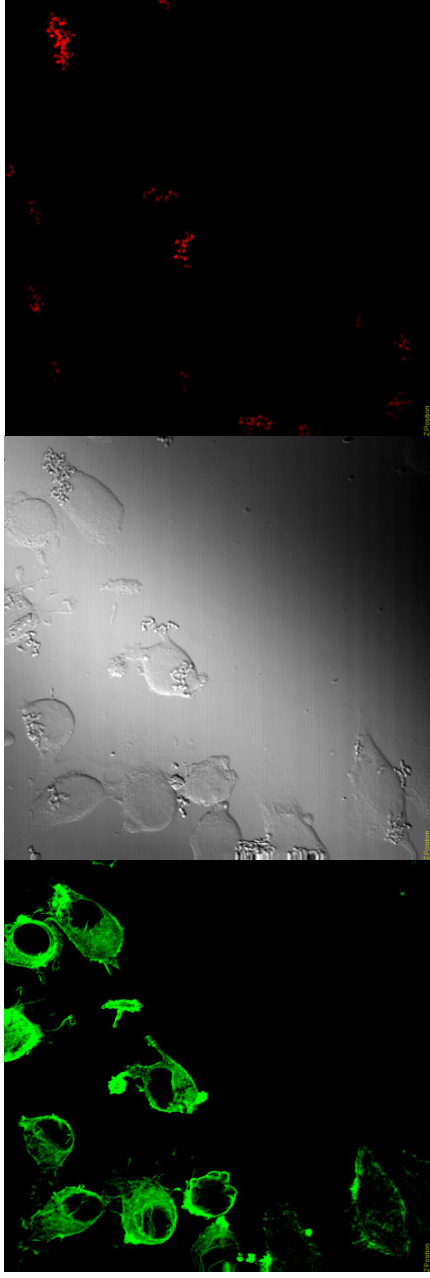
After 24 hours, when cells had well attached on cover glass, about 10⁷ microbeads were added in the medium. Cells and microbeads were incubated for 1, 2, 3, and 6 hours. Cells were washed three times to eliminate non-adherent microbeads.

EA.hy 926 cells were fixed in paraformaldehyde 4% and stained with phalloidin-FITC (Sigma-Aldrich), an F-actin fluorescent marker of the cell cytoskeleton. Analyses were performed on a confocal microscope (BX 50 Olympus, equipped with two laser beams). A 488 nm band was used to analyze cells while the 543 nm band was used to visualize microbeads. Images were taken, section by section, on an average of 10 µm in depth, from the top of cell to the bottom, with a 0.25 µm of distance between two focal planes.

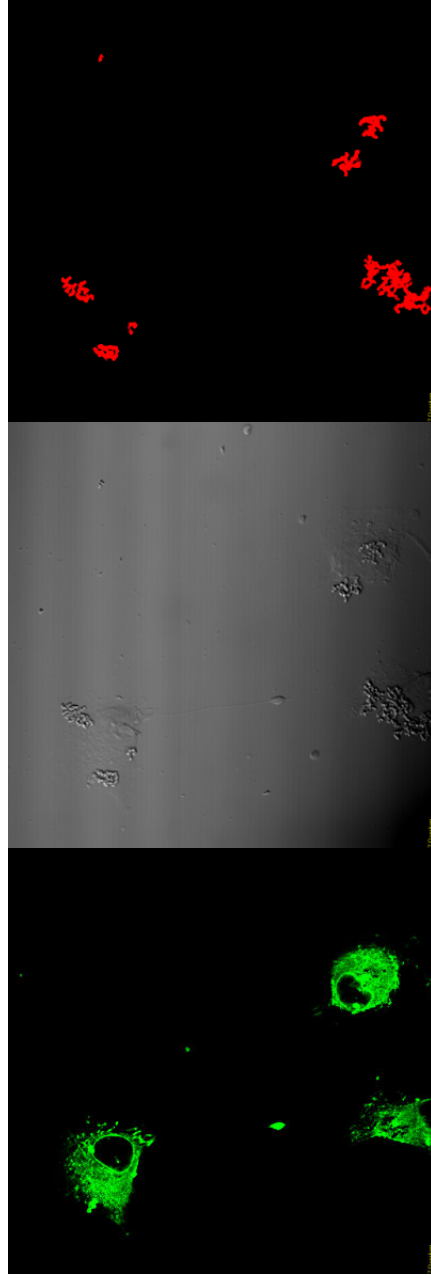
Endothelial cells grew as monolayer with irregular shape and cytoplasm extensions. Microbeads were visualized at the outer surface and photographs taken indicated that microbeads were internalized by cells (Fig. 6-36 and 6-37). At all incubation times ranging from 1 to 6 hours, microbeads were found inside cells, internalization progressing in time.

Microbeads appear randomly inside the cytoplasm, even near the nucleus, but not inside it, and the uptake of MOEAA-containing microbeads seems to be higher than in case of DADMAC-containing ones.

In the present model, no cell damage was observed whatever the type of microbead. p(HEMA-co-MOEAA) microbeads were less aggregated and better uptaken by endothelial cells; they will further be used in *in vivo* tests, for carrying compounds targeting endothelial cells in tumor models.



a)



b)

Fig. 6-36. p(HEMA-co-DADMAC) microbeads stained with Nile Red with EA.hy 926 cells: a) after 3 hours; b) after 6 hours.

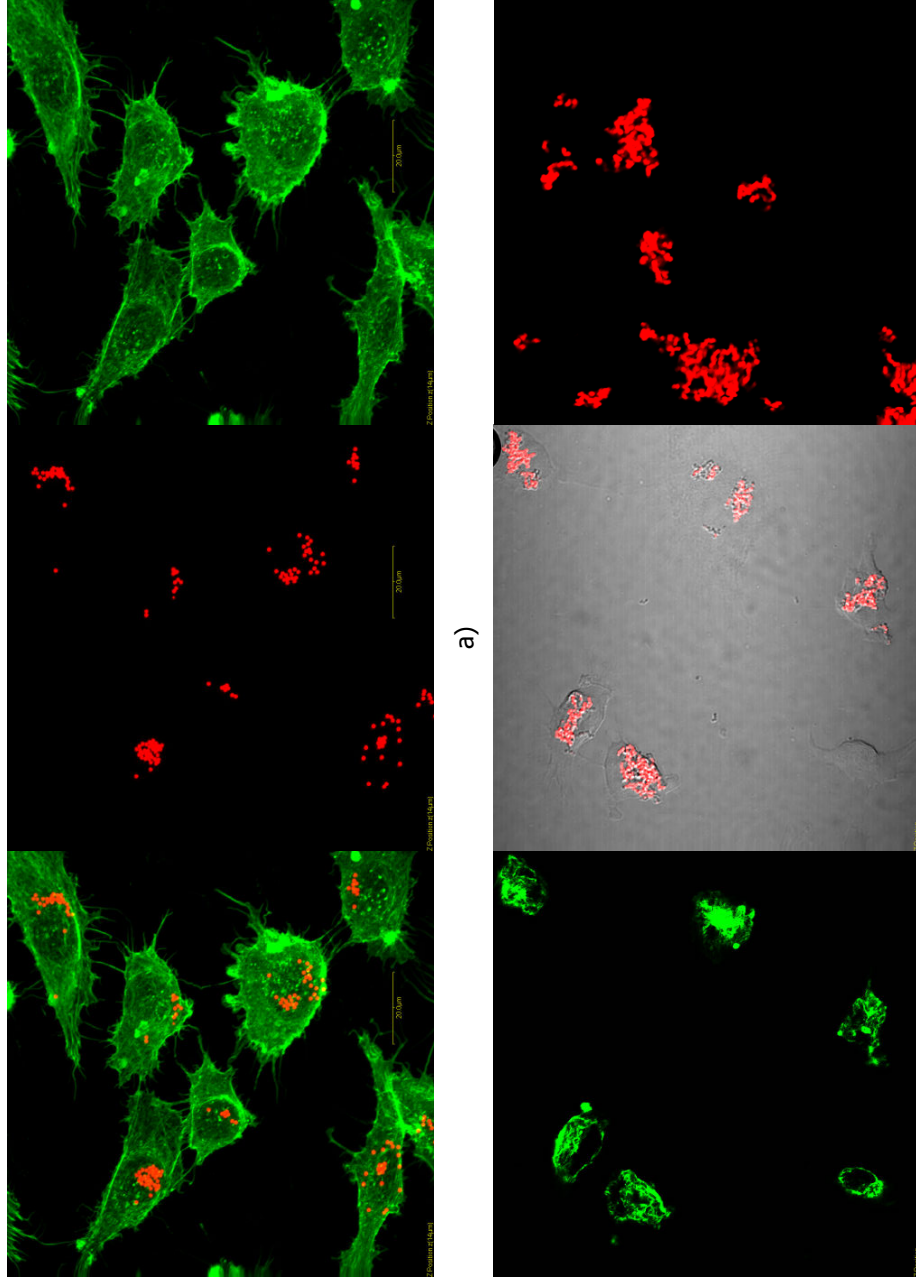


Fig. 6-37. p(HEMA-co-MOEAA) microbeads stained with Nile Red with EA.hy 926 cells: a) after 3 hours; b) after 6 hours.

6.4. Use of p(HEMA-co-MOEAA) microbeads loaded with thalidomide, in a rat methastases model

For the drug delivery for bone methastases, there were first obtained the tumour methastases, accordingly to the method of S. Blouin et al. (2006). The purpose of the study was to study antiangiogenic-containing (thalidomide) microbeads behaviour against tumour development.

Walker Swiss Cells 256 in 2nd ascite are injected intraosseous (10 000 cells) into Sprague-Dawley rats (University of Angers, France), divided into three groups (Table 6-7).

- Group 1: Walker cells and no microparticles (8 animals) (tumour control)
- Group 2: Walker cells + microparticles thalidomide-containing (8 animals)
- Group 3: No Walker cells + microparticles thalidomide-containing (thalidomide control)

The injection containing Walker cells is intraosseously performed. There is created a hole in the femurus with a screw and afterward waxed. With a microsyringe, 256 Walker Swiss cells are injected and afterwards wax-glued.

Table 6-7

Protocol of *in vivo* injection

Sample	Group 1 (control) W256 + PBS	Group 2 W256 + thalidomide-containing microbeads
J ₀	Intraosseous injection (IO) with 10 ⁷ Walker cells/animal	Intraosseous injection with 10 ⁷ Walker cells/animal
J ₇	Injection IC PBS (250µl)/ animal	Injection of microparticles 2,5 10 ⁸ microparticles/mL/animal
J ₁₁	Injection IC PBS (250µl)/ animal	Injection of microparticles 2,5 10 ⁸ microparticles/mL/animal
J ₁₅	Injection IC PBS (250µl)/ animal	Injection of microparticles 2,5 10 ⁸ microparticles/mL/animal
J ₁₉	Injection IC PBS (250µl)/ animal	Injection of microparticles 2,5 10 ⁸ microparticles/mL/animal
J ₂₃	Animals euthanasia	Euthanasia

In function of the general status of the animals we may count 3 to 4 weeks for side effect. From the tested animals, bone recuperation (femurus, tibia, right and left) and brain, lungs, liver, spleen were prevealed.

Group 3 – same operation protocol as in case of Group 2 but without Jo, where there is no injection of Swiss Walker cells.

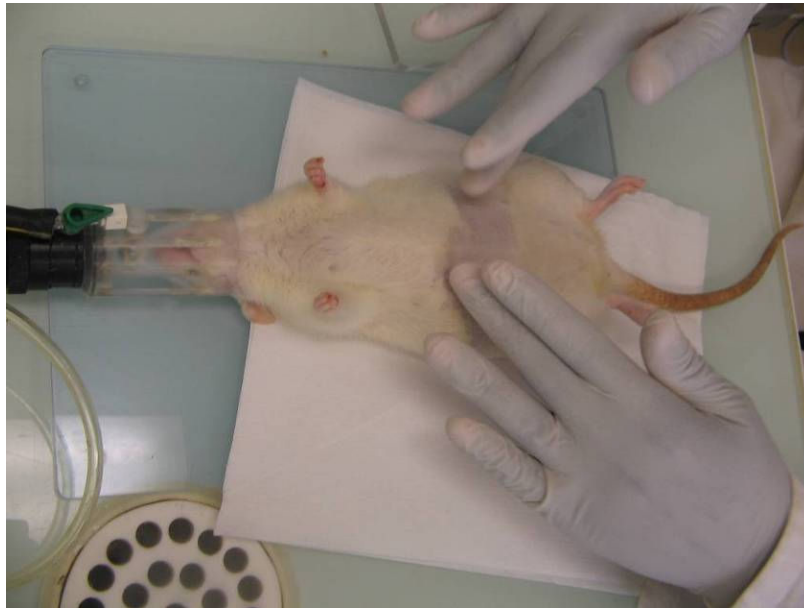


Fig. 6-38. Rat anaesthesia before injecting the suspension of microbeads



Fig. 6-39. Injection of the suspension of microbeads

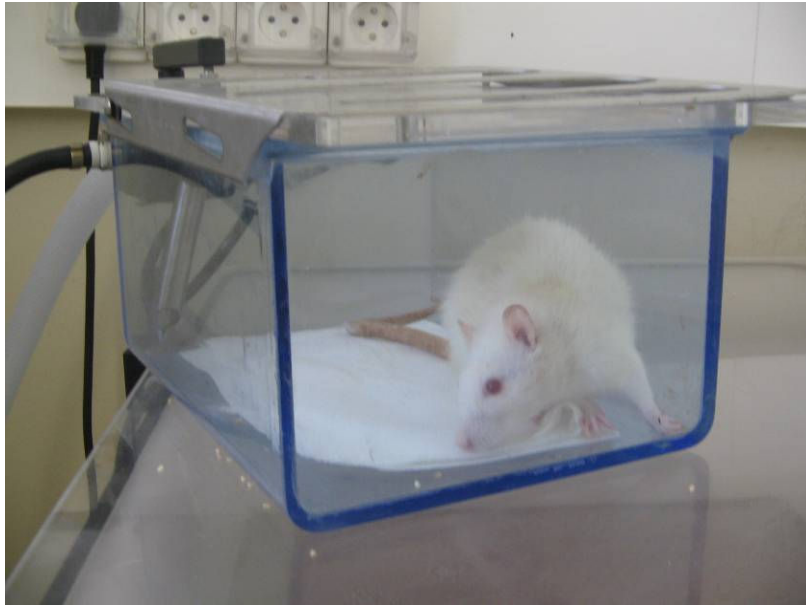


Fig. 6-40. Rat euthanasia for organs sampling



Fig. 6-41. Rat with metastatic tumours



Fig. 6-42. Organs sampling from a metastatic tumour rat

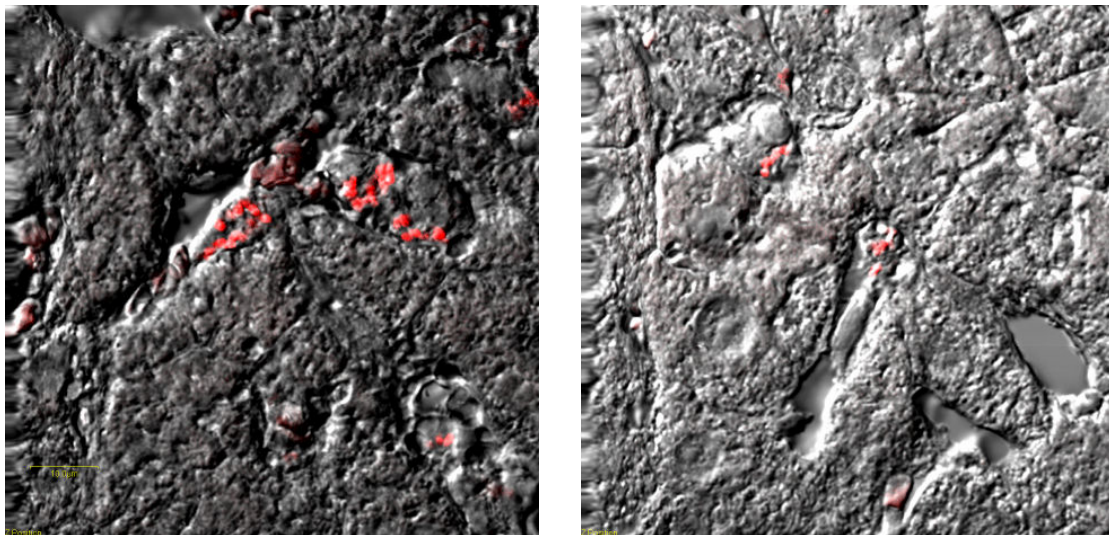


Fig. 6-43. Microbeads internalised into Sprague-Dawley rats (liver).

6.5. Conclusions

The purpose of the present work was to obtain new HEMA-based copolymers in order to be used as drug delivery matrices for bone metastases. A comparison among several copolymers was performed.

Copolymers of p(HEMA-co-DADMAC), p(HEMA-co-GlyMA), p(HEMA-co-MAA), p(HEMA-co-MOETAC), p(HEMA-co-MOEAA), and p(HEMA-co-THFMA) with 90:10 molar composition of HEMA:comonomers were synthesised by bulk polymerisation for the obtaining of pellets and by suspension polymerisation for the obtaining of microbeads.

The copolymers were physico-chemically and biologically characterised.

In vitro evaluation of the copolymers calcification capacity (incubation in SBF) conducted to some interesting conclusions. p(HEMA-co-GlyMA) and p(HEMA-co-MOETAC) could be used as a potential alternative to the classical bone grafts, as apatite crystal growth stimulators in bone tissue engineering.

Meanwhile, the other copolymers are usable in other biomedical applications, such as systems for controlled drug delivery, which specifically require that the calcification phenomenon does not occur.

Microbeads of p(HEMA-co-MOEAA) and p(HEMA-co-DADMAC) were submitted to *in vitro* tests with human endothelial cells. Polymers were successfully internalised by EA.hy 926.

Further, thalidomide was successfully loaded to p(HEMA-co-MOEAA) and *in vivo* behaviour of the microbeads was evaluated. All tests gave satisfactorily results. *In vivo* tests on methastatic tumours are still running, with positive results, which will continue with clinical tests.

Appendix**Protocol for endothelial cells staining by phalloidin**

Objective: Visualization of fluorescent microparticles of pHEMA. The microparticles were put on the endothelial cells at different times. The purpose was to see whether the polymers are localized or not inside the cells. Also, differences between microparticles negatively and positively charged were observed.

Endothelial cells EAHY 926 were employed.

Microparticles of p(HEMA-co-MOEAA) and p(HEMA-co-DADMAC) of 1 μm diameter were used.

Cellular staining: actinic filaments (F-actinic polymers): Alexa Fluor 488 Phalloidin, Phalloidin TRITC

1) Microparticles deposition.

Culture experiences take place on P24 well-plates. Clean round plates are placed on a P24 and sterilized for 1 hour. Cells in suspension are added.

Cells are numbered and placed in the cavity: 25000 cells contained in 100 μL of full milieu, on the round plates, are allowed to adhere for at least 3 hours. 1 mL full milieu EAHY926 was completed. Once the cells are stacked on the plate, a concentration of a known number of microparticles (10^7 microparticles) was inserted.

2) Cells staining by phalloidin

Once ended the adherence time, the wells were carefully washed, in order to eliminate the microparticles which have not binded or internalised by the cells. 3 times washing with sterile PBS 1x are enough.

Cells fixation is performed with 1mL of 4% paraformaldehyde for 20 minutes at room temperature.

Away from light, 75 μL phalloidin diluted from the stock solution* were added.

The reaction was allowed to take place for 20 minutes, with samples covered.

We dissolve the phalloidin in 0.1mL methanol; we add 2mL PBS 1X and 21 μL DMSO. Aliquots are made in Eppendorf tubes, 100 μL /tube. Once coloration appeared, we dilute to 1/3 with 200 μL 1x PBS the aliquot of 100 μL .

** Solution stock **Phalloidin TRITC**: Phalloidin : 0.1 mg; Methanol : 0.1 mL; DMSO : 21 μL ; PBS 1X : 2mL.*

Chapter 7

p(HEMA-co-dDMA-co-AA) and p(HEMA-co-dDMA-co-DEAEMA) microbeads and nafcillin loading

Beneficiary of research funds from:

Grant for young scientists, PN II-RU-TD-I No. 21/2007 received from Romanian Ministry of Education and Research, CNCSIS

Data presented in:

T. Zecheru, C. Zaharia, E. Rusen, F. Miculescu, C. Cincu, *Synthesis, Physico-Chemical Properties and Biological Evaluation of two new copolymer systems*, World Biomaterials Congress 28 May – 01 June 2008, Amsterdam, The Netherlands – rewarded with ***Student Travel Award WBC 2008***.

7.1. Introduction

In the last few years, polymeric materials have been designed and proposed as matrices or depot systems for injectable or implantable systems or devices. A particular approach towards an improved use of drugs for therapeutic applications is the design of polymeric prodrugs or polymer–drug conjugates. Polymer chemists started to link drugs to polymers to improve their efficiency early in the 1950s and 1960s. At that time, they were mainly concentrating on the chemistry itself, and almost any class of polymers was covalently combined with any class of drugs. The biological aspects for the design of polymeric prodrugs were hardly taken into account.

For the first time in 1975, a rational model for pharmacologically active polymers was proposed. Ringsdorf was the first to recognize the immense potential of polymeric prodrugs, if only polymer chemists and biologists would work together in the field. The proposed model consists mainly of five components: the polymeric backbone, the drug, the spacer, the targeting group, and the solubilizing agent (Fig. 7-1). This model, though still oversimplified, is an important milestone in the history of polymeric prodrug design. The polymeric carrier can be either an inert polymer or a biodegradable polymer. The drug can be fixed directly or via a spacer group onto the polymer backbone. The proper selection of this spacer opens the possibility of controlling the site and the rate of release of the active drug from the conjugate by hydrolytic or enzymatic cleavage.

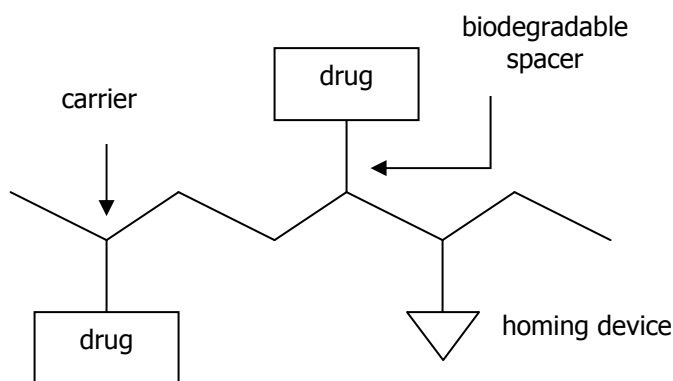


Fig. 7-1. Model for polymeric prodrugs proposed by Ringsdorf.

Treatment of osteomyelitis in most patients requires a lengthy regimen of parenteral antibiotic therapy and surgical removal of all necrotic, avascular, infected bone and soft tissue. Optimally, culture-directed antimicrobial therapy should be initiated after complete surgical debridement and after microbial confirmation of the diagnosis by biopsy. Generally, antibiotic therapy is maintained for at least 6 weeks. Inadequate debridement is a frequent underlying factor in therapy failure in patients with chronic osteomyelitis.

In recent years, rising hospital costs have compelled the search for new approaches to extended parenteral antibiotic regimens in patients who do not otherwise require hospitalization. Oral antibiotic therapy (often following initial parenteral therapy) and parenteral therapy on an outpatient basis are gaining acceptance for use in patients with osteomyelitis (Fig. 7-2).

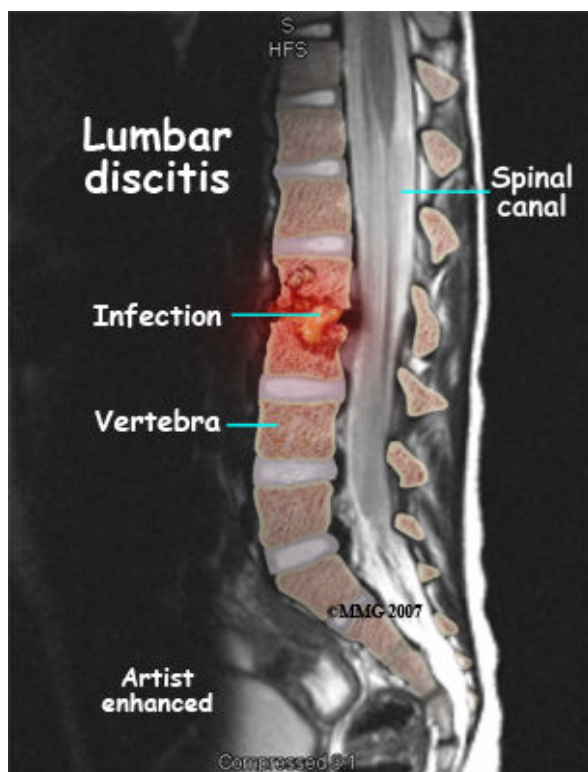


Fig. 7-2. Osteomyelitis (www.eorthopod.com).

The most common pathogen involved in osteomyelitis is *Staphylococcus aureus*; however, other organisms, including gram-negative pathogens and coagulase-negative staphylococci, may be found. Often, bone infections may be polymicrobial. The penicillin family of antibiotics has bacterial activity, low toxicity, excellent distribution throughout the body, and efficacy against infections caused by susceptible bacteria.

It is generally accepted that antibiotics incorporated in methacrylate-cements are released to some extent, but the mechanism by which these drugs are released is still debated. Several observations indicate that antibiotic release is a surface phenomenon. There is no consensus that antibiotic release is an exclusive surface phenomenon and theories favoring a bulk diffusion model have been proposed as well. The diffusion model relies heavily on the availability of pores and connecting capillaries, through which fluids can penetrate and dissolve the antibiotics that slowly diffuse outwards. Although in vitro studies suggest that antibiotics are released from acrylic bone

cements, it is of some concern that various *in vitro* studies show adherence and growth of bacteria on antibiotic-loaded bone cement.

Nafcillin is an anti-infective drug (antibiotic), which belongs to the drug class of beta-lactam antibiotics. Such antibiotics, for incorporation in bone or dental cements, should have a broad antibacterial spectrum, including Gram-positive and Gram-negative pathogens, sufficient bactericidal activity, high special antibacterial potency, low rate of primary resistant pathogens, minimal development of resistance during therapy, low protein binding, low sensitizing potential, marked water solubility facilitating its release from the bone cement, and last, but not least, chemical and thermal stability. Over the years various antibiotics have been evaluated in *in vitro* studies regarding their suitability for incorporation. In general, it was shown that aminoglycosides, especially gentamicin, are suitable antibiotics from a bacteriological and physico-chemical point of view.

Nafcillin sodium, or 4-Thia-1-azabicyclo[3.2.0]heptane-2-carboxylic acid, 6-[[[(2-ethoxy-1-naphthalenyl)carbonyl]amino]-3,3-dimethyl-7-oxo-, monosodium salt, monohydrate, [2S-(2^α, 5^α, 6^β)] or Nafcillin (Fig. 7-3), is a semi-synthetic antistaphylococcal penicillin, highly effective in penicillinase-producing staphylococcal infections, in which activity is conferred mainly by steric hindrance. Unlike penicillin, ampicillin, or the extended-spectrum penicillins, nafcillin resists hydrolysis by penicillinase. As a result, nafcillin, along with other agents in the same group (e.g., oxacillin, dicloxacillin), is active against penicillinase-producing *Staphylococcus aureus*. Nafcillin, because of its side chain, resists destruction by beta-lactamases. This makes it useful for treating bacteria that resist penicillin due to the presence of penicillinase. Nowadays, Nafcillin is employed in invasive diseases due to *Enterobacter cloacae* and *Serratia marcescens*.

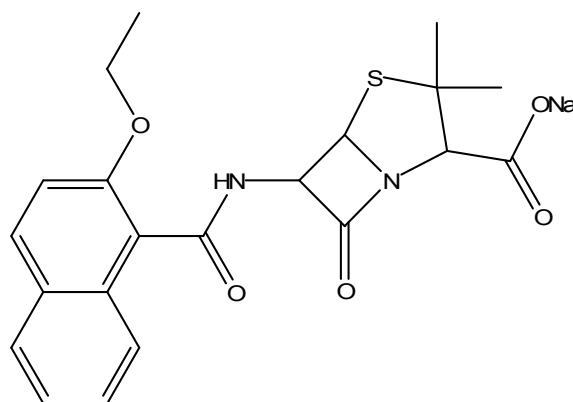


Fig. 7-3. Nafcillin sodium

In recently years, polymer-nafcillin conjugates were synthesized as hydrogels or beads, and their *in vitro* behaviour properties were studied, such as pMMA, p(MMA-co-AA), poly(N-isopropylacrylamide-co-itaconic acid), but the influence of some factors such as, the synthesis method, the

crosslinking agent, the solvent and others, in the structure of the hydrogel, make difficult to compare the diffusion coefficients either hydrogels or particles.

Nafcillin works by binding penicillin-binding proteins and inhibiting cross-linking of cell wall peptidoglycan. Nafcillin is especially useful to treat infections caused by methicillin-sensitive penicillinase-producing staphylococci. The offending bacteria can be successfully treated anywhere including bone, joint, urinary tract, respiratory tract, skin, endocarditis, meningitis. However with serious infections such as those just described intravenous administration is recommended.

Polymeric beads of p(HEMA-co-dDMA-co-AA) and p(HEMA-co-dDMA-co-DEAEMA) were synthesised, and characterised by scanning electron microscopy (SEM), swelling behaviour for different monomer compositions, elemental analysis, a kinetic study and *in vitro* tests. The most appropriate compositions were nafcillin-loaded, in order to evaluate their *in vitro* release capacity.

7.2. Synthesis of the polymers

Free-radical polymerisation was used for the microparticles obtaining, following the methods established in previous studies (Zecheru et al., 2006 and 2007).

2-hydroxyethyl methacrylate (HEMA), dodecyl methacrylate (dDMA), acrylic acid (AA), diethylaminoethyl methacrylate (DEAEMA), benzoyl peroxide (BPO), 2-butanol, and ethylenglycol dimethacrylate (EGDMA) were purchased from Sigma-Aldrich. The solvents, toluene and diethyl ether, were provided from Chimopar, Bucharest, and the star copolymer styrene-butadiene (pBuSt), as stabilising agent, from ICECHIM Bucharest.

The initiator BPO was purified by recrystallisation from ethanol, HEMA was distilled under reduced pressure, and the other comonomers were passed before use through a column packed to a height of 20 cm with basic Al₂O₃ (Merck).

The synthesis had into the view the obtaining of 1 µm-size particles, using precipitant polymerisation procedure at a conversion over 90%.

A solution of stabilising agent (w/v) in toluene (95:5 (w/w) vs. monomer) was introduced into a three-neck reactor. At 40°C and while stirring, the 2-butanol (45:55 (v/v) ratio of solvent vs. non-solvent solution) was slowly introduced. Separately, a solution containing the comonomers (Table 7-1), initiator (BPO) (5×10^{-3} mol/L in the solution), and cross-linking agent (EGDMA) (2% vs. comonomers) was prepared. This second solution was added dropwise to the first one, under mechanical stirring, increasing the temperature to 75°C and the stirring rate to 800 rpm. Polymerisations were performed in a water-bath and under nitrogen atmosphere. An optimal result of the reaction and a high conversion was noticed after 6-7 hours.

Table 7-1

Molar composition of the initial mixture of monomers

Sample	HEMA	dDMA	AA
A1	90	5	5
A2	85	5	10
A3	80	5	15
A4	85	10	5
A5	80	10	10
A6	75	10	15
Sample	HEMA	dDMA	DEAEMA
D1	90	5	5
D2	85	5	10
D3	80	5	15
D4	85	10	5
D5	80	10	10
D6	75	10	15

The copolymers obtained were repeatedly washed with toluene and diethyl ether and extracted under centrifugation, in order to remove any traces of unreacted monomer and other organic residue with low molecular weight. The microparticles were then dried in the oven at 37°C for 24 hours.

7.3. Characterisation studies

In order to characterise the microparticles obtained by heterogeneous polymerisation, Scanning Electron Microscopy (SEM), Fourier Transform Infrared Spectroscopy (FT-IR), and Elemental Analysis were used. The water uptake capacity and the cytotoxic effect were determined.

7.3.1. Swelling tests

Swelling test was carried out on samples of copolymers obtained by bulk polymerisation, in triplicate, using a solution of 9 g/L NaCl in distilled water, for three days at 37°C. p(HEMA-co-dDMA-co-AA) and p(HEMA-co-dDMA-co-DEAEMA) terpolymers should be capable to swell to a significant extent, because of the presence of the 2-hydroxyethyl methacrylate (HEMA) monomer units, but in the

same time to a controlled rate (the reason for including dodecyl methacrylate (dDMA)), the linkages towards drugs being made by acrylic acid (AA) or diethylaminoethyl methacrylate (DEAEMA). The water uptake capacity of the microbeads represents a very important property, which should be considered especially in case of drug delivery studies, taking into account that pHEMA presents a significant swelling rate, of 55% (Denizli et al., 2005). The introduction of a hydrophobic monomer, dDMA, should lead to a decreased swelling degree for a higher dDMA ratio in the terpolymer.

The polymers obtained are cross-linked hydrophilic matrices. Therefore, they do not dissolve in aqueous media, but they swell, in function of the degree of cross-linking and of the hydrophilicity of the comonomers in the matrix. The swellability of the copolymers obtained is important in order to verify the compatibility of these structures with the physiological fluids (Fig. 7-4). The swelling process follows a 1st order kinetic, and as a consequence the *k* parameter measures the diffusion rate of the water phase in the polymer matrix (kinetic compatibility) and the maximum value of the swelling coefficient *A* measures the thermodynamic equilibrium compatibility of the monomers in the copolymers. The results are presented in Table 7-2.

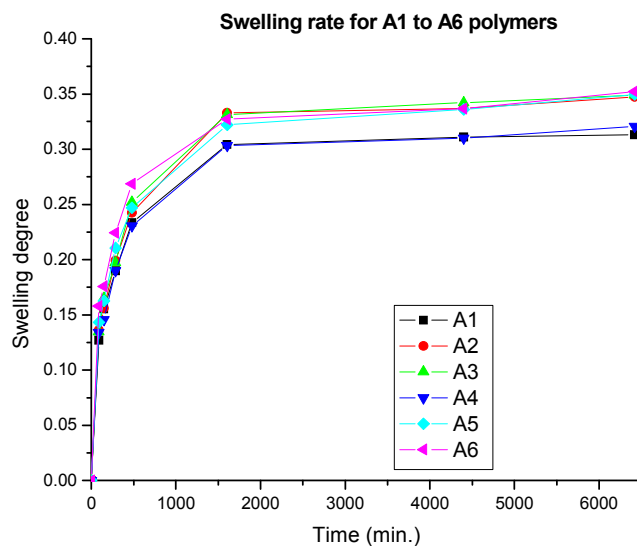
Table 7-2

k and A constants

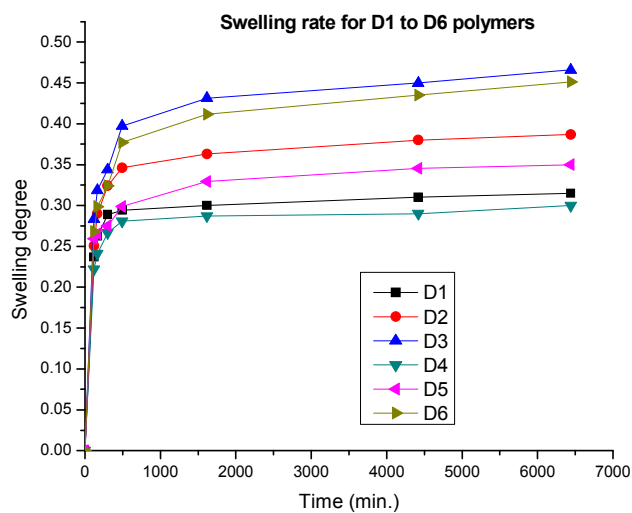
Sample	A (%)	k (min⁻¹)
A1	31.29	0.0013
A2	34.73	0.0010
A3	34.91	0.0010
A4	32.09	0.0009
A5	34.94	0.0009
A6	35.22	0.0009
D1	31.50	0.0012
D2	38.71	0.0011
D3	46.60	0.0009
D4	30.02	0.0010
D5	35.00	0.0011
D6	45.12	0.0009

The high values for the parameter *A* correspond to a smaller cross-linking ratio (due to the feed composition). The water uptake ratio of the polymers decreases in comparison to a standard pHEMA ($\approx 55\%$). Incorporating either AA or DEAEMA actually increases the hydrophilicity potential of

the polymer chain, but dDMA presents a strong hydrophobic behaviour, which decreases the water uptake in the copolymers. In case of A series, k values are very close, due also to reactivity ratios of the comonomers. Therefore, all the structures investigated present thermodynamic and kinetic compatibility with the physiological serum.



a)



b)

Fig. 7-4. Swelling rate for the copolymers obtained: a) A1 to A6; b) D1 to D6.

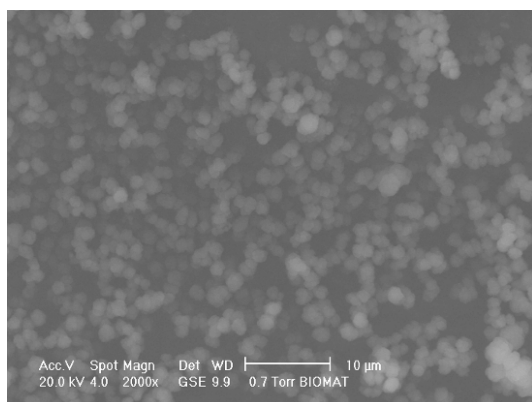
Among polymers in A series, A1 and A4 present the weakest water uptake capacity. In the meanwhile, A1 swells significantly faster than all the others. In case of D series, a similar behaviour is

observed, where D1 and D4 swell less, and D1 swells faster. Even though both AA and DEAEMA cannot be considered as hydrophobic monomers, the presence of dDMA strongly influences the swelling behaviour of the polymers obtained. This fact leads to the possibility of imaging different molar compositions of the copolymers, in function of the cross-linking and releasing rate needed.

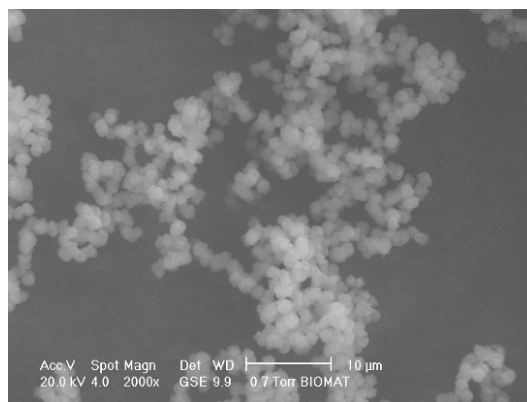
7.3.2. Scanning Electron Microscopy

Scanning Electron Microscopy (SEM) was performed on a Philips XL30 - ESEM Turbo Molecular Pump (TMP), at 20 keV. The samples were first carbon-coated.

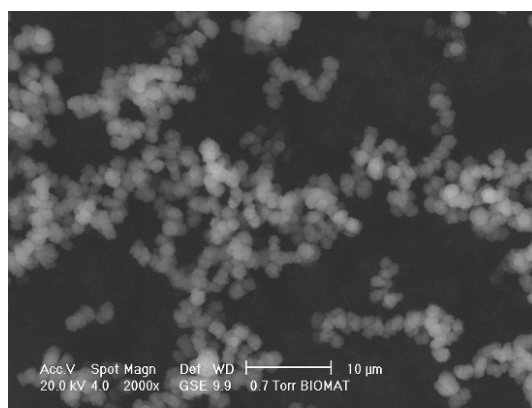
The results in Fig. 7-5 show that all the compositions obtained present desired round shape and dimensions of $\sim 1\mu\text{m}$, and appropriate to be used as drug delivery matrices.



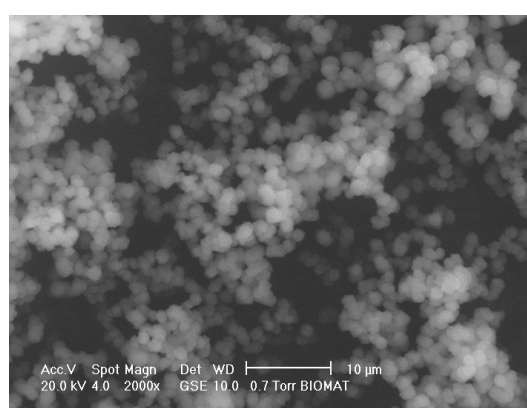
A1



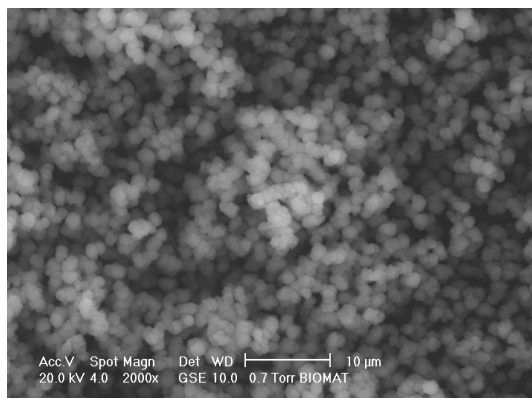
A2



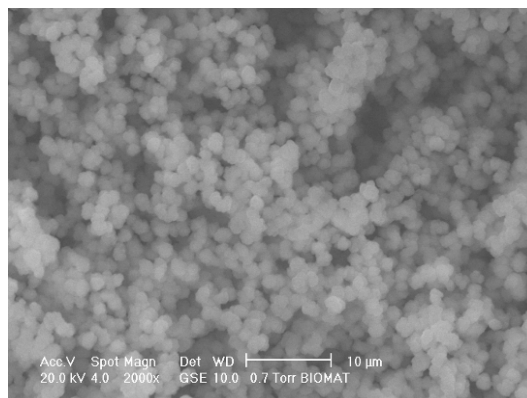
A3



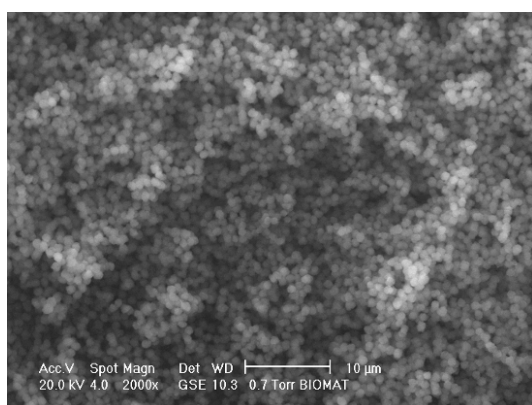
A4



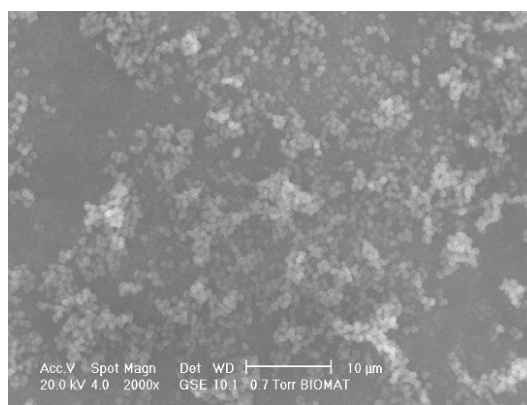
A5



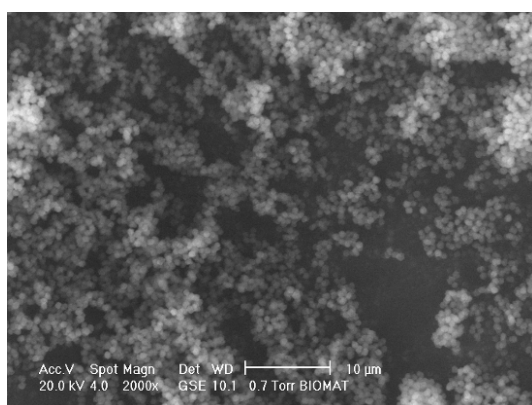
A6



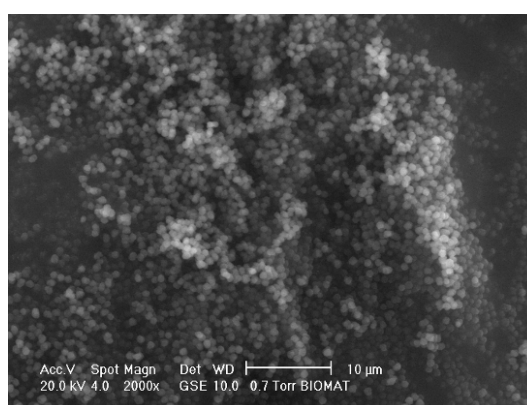
D1



D2



D3



D4

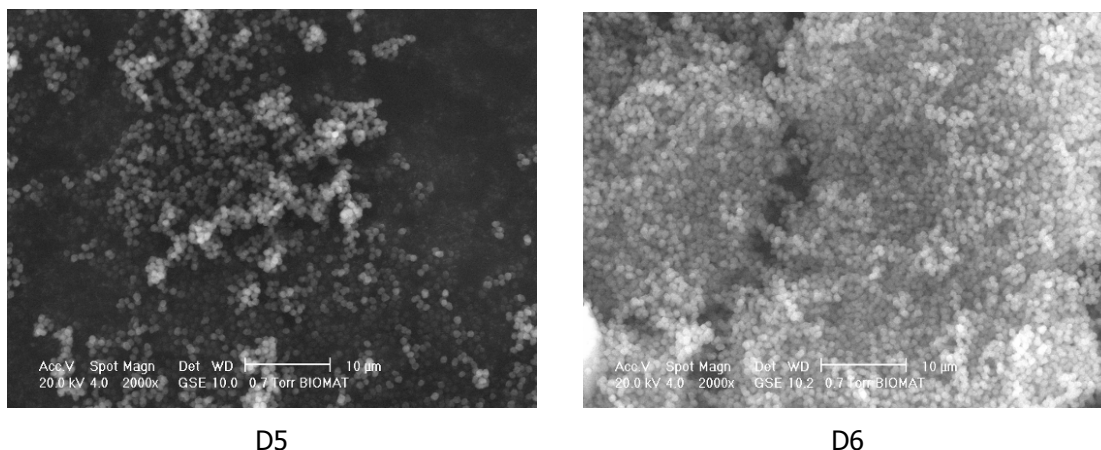


Fig. 7-5. Microphotographs of the copolymers obtained (A1 to A6 and D1 to D6).

7.3.3. FT-IR analysis

The FT-IR analysis was performed with a Jasco FT-IR 6200 with a ATR modulus SPECAC Golden Gate apparatus. The results proved that the obtaining compounds have the chemical structures presented in Fig. 7-6.

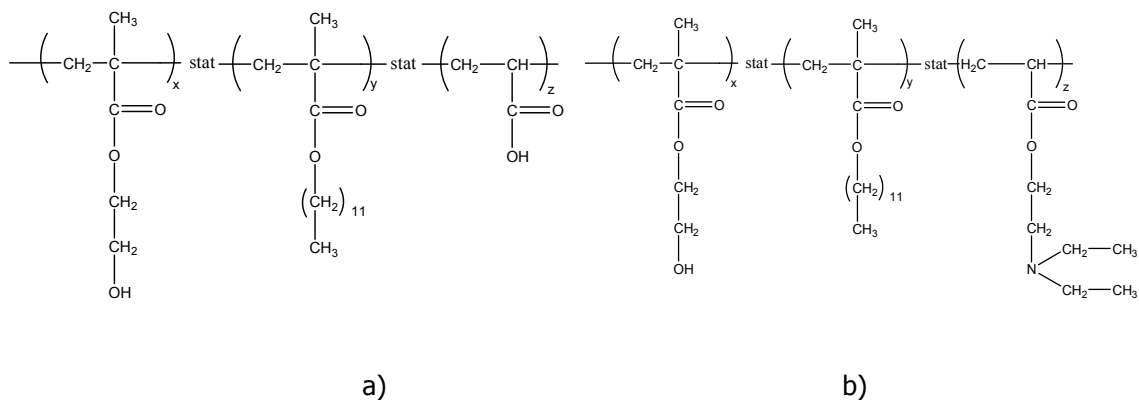
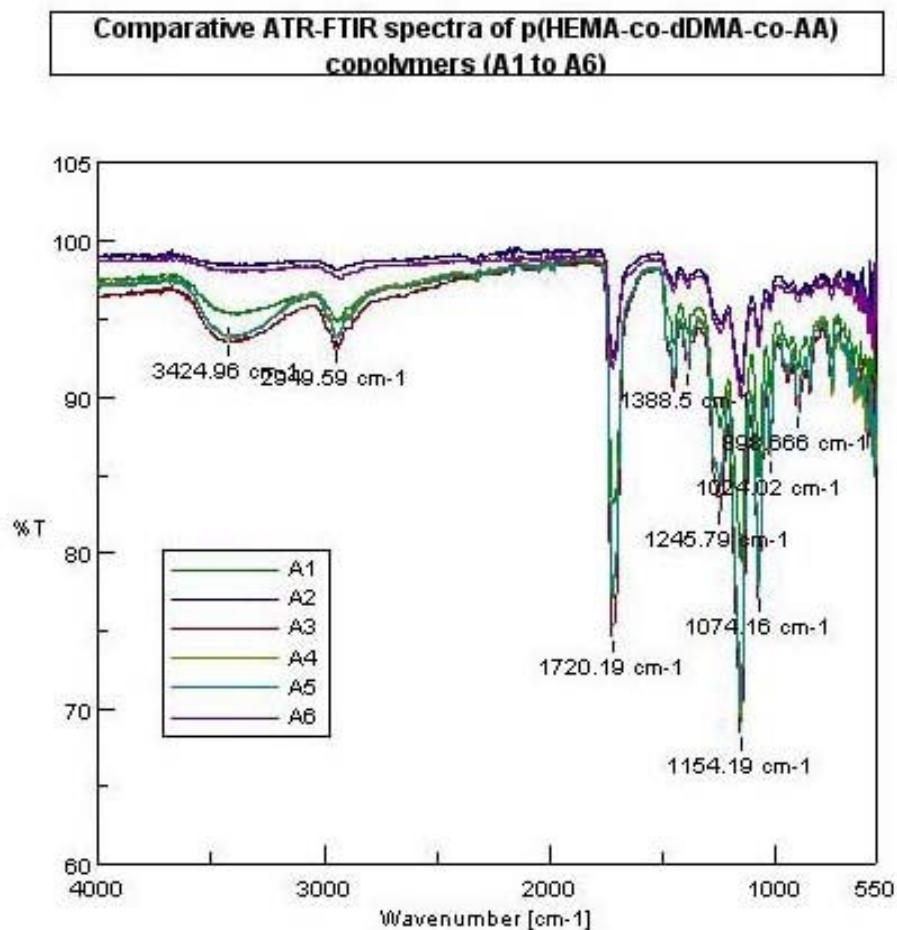


Fig. 7-6. Chemical structures of the copolymers obtained: a) p(HEMA-co-dDMA-co-AA); b) p(HEMA-co-dDMA-co-DEAEMA).

Spectra were scanned over the range of 4000-400 cm^{-1} . In the range 550-400 cm^{-1} noise was too strong and, therefore, the interval was eliminated from the presentation (Fig. 7-7).

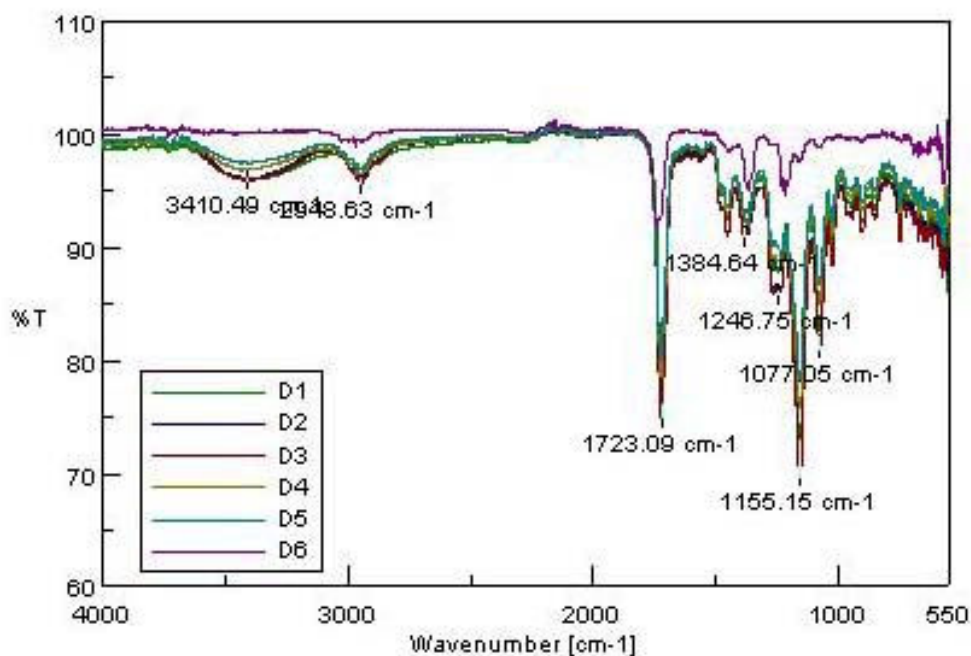


[Data Information]	
Creation Date	30.07.2008 14:29
Data array type	Linear data array
Horizontal	Wavenumber [cm-1]
Vertical	%T
Start	399.193 cm-1
End	4000.6 cm-1
Data pitch	0.964233 cm-1
Data points	3736

[Measurement Information]	
Model Name	FT/IR-6200typeA
Serial Number	A007661022
Light Source	Standard
Detector	TGS
Accumulation	20
Resolution	4 cm-1
Zero Filling	On
Apodization	Cosine
Gain	Auto (16)
Aperture	Auto (7.1 mm)
Scanning Speed	Auto (2 mm/sec)
Filter	Auto (10000 Hz)

a)

**Comparative ATR-FTIR spectra of
p(HEMA-co-dDMA-co-DEAEMA) copolymers (D1 to D6)**



[Data Information]	
Creation Date	30.07.2008 15:52
Data array type	Linear data array
Horizontal	Wavenumber [cm-1]
Vertical	%T
Start	399.193 cm-1
End	4000.6 cm-1
Data pitch	0.964233 cm-1
Data points	3736

[Measurement Information]	
Model Name	FT/IR-6200typeA
Serial Number	A007661022
Light Source	Standard
Detector	TGS
Accumulation	20
Resolution	4 cm-1
Zero Filling	On
Apodization	Cosine
Gain	Auto (16)
Aperture	Auto (7.1 mm)
Scanning Speed	Auto (2 mm/sec)
Filter	Auto (10000 Hz)

b)

Fig. 7-7. Comparative spectra of copolymers obtained: a) A1 to A6; b) D1 to D6.

In case of A series, in the spectra presented above, there is seen an increasing peak for the –OH bond at 3424.96 cm^{-1} , in function of the HEMA comonomer introduced in the feed. The same, in the case of –COOH bond, at 2949.59 cm^{-1} , the spectra shows that the composition enriches in AA.

In case of D series, a broad peak is observed at 3410.49 cm^{-1} , which is responsible for secondary amine bond N-H; the peak increased with composition enriching in DEAEMA.

7.3.4. Kinetic study of HEMA-AA and AA-dDMA binary systems

Elemental analysis was performed in order to establish the reactivity ratios of the comonomers, and the chemical structure of the copolymer, using a LECO CHN2000, MI, USA instrument.

Solution polymerisation was used as procedure for the kinetic study. The following pairs of comonomers were studied: HEMA-AA and dDMA-AA.

Comonomer solution of [1.5 mol/L] concentration are prepared with the molar ratio among the comonomers given in Table 7-3.

Table 7-3

Feed compositions of the binary systems

Composition	Monomer 1	Monomer 2
1	0.2	0.8
2	0.4	0.6
3	0.6	0.4
4	0.8	0.2

The polymer solution is constituted by the two comonomers, the solvent and the initiator AIBN ($5 \times 10^{-3}\text{ mol/L}$). 4 polymerisation test tubes are used for each composition, in order to determine different conversions. The polymer obtained is precipitated using an adequate non-solvent (Table 7-4).

The solid products obtained are washed several times with the same non-solvent, in order to remove residual monomers, dried in a vacuum oven up to constant mass and weighted. The resulting products are sent to elemental analysis. The results are given in Table 7-5 and Table 7-6.

Table 7-4.

Non-solvents for the binary compositions studied

Binary system	Composition	Solvent	Nonsolvent
HEMA-AA	1	DMF	2% NaOH in demineralised water
	2		
	3		
	4		
dDMA-AA	1	Dioxane	DMF : glacial acetic acid (1:1 v/v)
	2		NH ₃ aqueous solution 25%
	3		Formamide
	4		NH ₃ aqueous solution 25%

Table 7-5

Results of the elemental analysis for the binary system HEMA-AA.

Binary system HEMA-AA	Conversion (%)	Δt (min.)	Elemental analysis		
			N (%)	C (%)	H (%)
HEMA:AA 0.2:0.8 conv. 1	40.09	0	5.94	58.297	9.056
HEMA:AA 0.2:0.8 conv. 2	45.05	75	0	49.112	9.144
HEMA:AA 0.2:0.8 conv. 3	60.4	105	0	32.397	8.791
HEMA:AA 0.2:0.8 conv. 4	64	135	0.009	37.825	7.615
HEMA:AA 0.4:0.6 conv. 1	46.56	0	0	54.330	7.687
HEMA:AA 0.4:0.6 conv. 2	58.22	75	0	49.808	9.274
HEMA:AA 0.4:0.6 conv. 3	70.17	105	0.968	49.543	8.857
HEMA:AA 0.4:0.6 conv. 4	76.44	135	0	40.798	5.287
HEMA:AA 0.6:0.4 conv. 1	37.28	0	2.154	66.809	9.884
HEMA:AA 0.6:0.4 conv. 2	55.22	75	2.453	49.498	0
HEMA:AA 0.6:0.4 conv. 3	68.01	105	2.160	51.596	0
HEMA:AA 0.6:0.4 conv. 4	72.25	135	2.703	44.479	0
HEMA:AA 0.8:0.2 conv. 1	45.26	0	0.480	48.328	7.727
HEMA:AA 0.8:0.2 conv. 2	61.99	75	2.179	52.062	0
HEMA:AA 0.8:0.2 conv. 3	63.32	105	0.076	63.719	5.450
HEMA:AA 0.8:0.2 conv. 4	71.59	135	0	50.580	8.842

Table 7-6

Results of the elemental analysis for the binary system AA-dDMA.

Binary system AA-dDMA	Conversion (%)	Δt (min.)	Elemental analysis		
			N (%)	C (%)	H (%)
AA:dDMA 0.2:0.8 conv. 2	17.31	132	0	50.179	8.772
AA:dDMA 0.2:0.8 conv. 3	23.20	152	0	46.886	7.306
AA:dDMA 0.2:0.8 conv. 4	24.59	182	0.747	66.606	0
AA:dDMA 0.4:0.6 conv. 3	48.67	145	0	94.706	13.401
AA:dDMA 0.4:0.6 conv. 4	55.74	180	0	46.009	7.170
AA:dDMA 0.6:0.4 conv. 1	48.89	75	0	47.170	7.593
AA:dDMA 0.6:0.4 conv. 2	72.40	105	0	41.489	6.151
AA:dDMA 0.6:0.4 conv. 3	89.18	125	0	63.933	11.207
AA:dDMA 0.6:0.4 conv. 4	94.74	150	0	59.560	13.397
AA:dDMA 0.8:0.2 conv. 1	30.81	30	2.158	66.953	9.906
AA:dDMA 0.8:0.2 conv. 2	43.60	60	0	34.969	2.609
AA:dDMA 0.8:0.2 conv. 3	58.27	90	0.077	63.959	5.470
AA:dDMA 0.8:0.2 conv. 4	59.33	120	0	34.456	2.571

7.3.4.1. Binary system HEMA-AA

The analysis of the binary system HEMA-AA began from experimental data, meaning from the elemental analysis results that gave quantifiable results.

Table 7-7

Results of the copolymerisation of HEMA-AA

X_{HEMA}^*	C%	H%	Conversion (%)	X_{HEMA}^{**}
0.2	49.112	9.144	45.05	0.2519
0.4	54.330	7.687	46.56	0.7636
0.4	49.808	9.274	58.22	0.3205
0.4	49.543	8.857	70.17	0.361
0.6	66.809	9.884	37.28	0.7748
0.6	49.498	0	55.22	0.2511
0.8	48.328	7.727	45.26	0.0755
0.8	50.580	8.842	71.59	0.361

*feed composition

**copolymer composition determined from elemental analysis

Reactivity ratios were determined using PROCOP software:

$$r_1=0.00029, M_1=[\text{HEMA}]$$

$$r_2=0.148, M_2=[\text{AA}]$$

These values enable plotting of the instantaneous composition diagram, for the system, which is characterised by $r_1 < 1, r_2 < 1$.

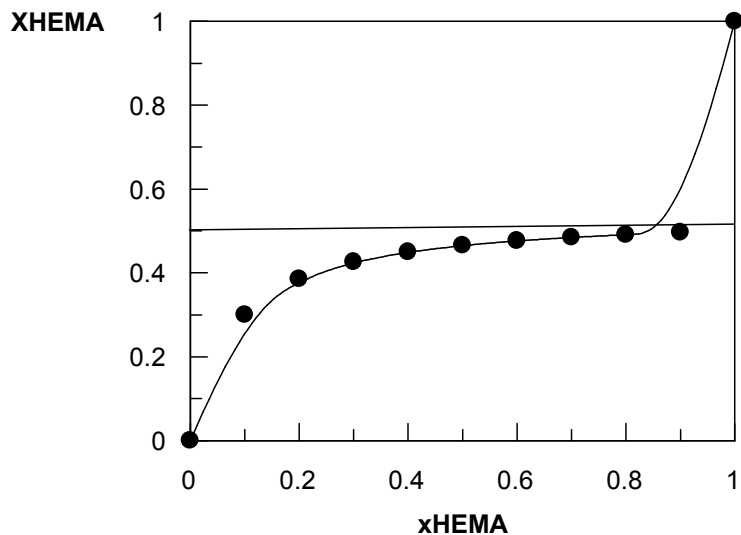
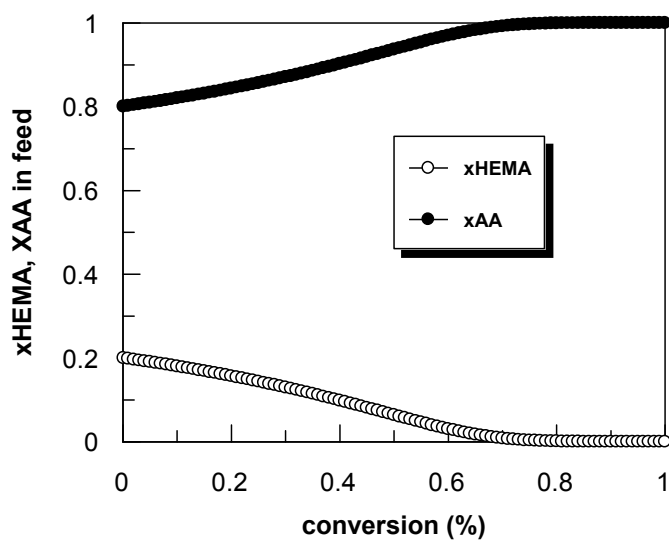
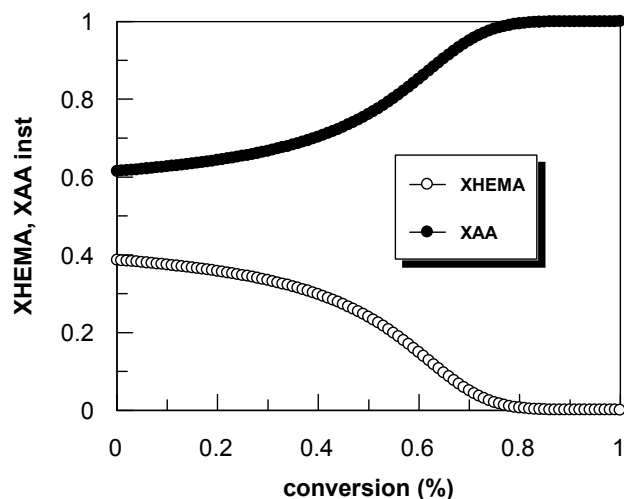


Fig. 7-8. The composition diagram for the binary system HEMA-AA

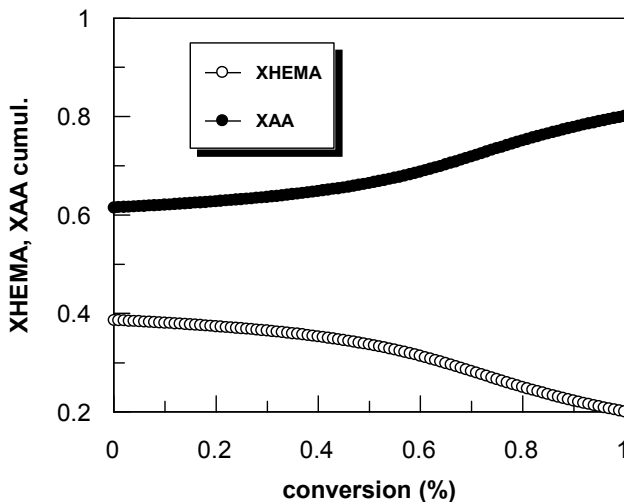
For the $x_{\text{HEMA}}=0.2$, $x_{\text{AA}}=0.8$ feed composition, the correlation composition versus conversion is given in Fig. 7-9.



a) Feed composition versus conversion



b) Instantaneous copolymer composition versus conversion



c) Cumulative copolymer composition versus conversion

Fig. 7-9. Feed composition and copolymer compositions versus conversion

An analysis of the graphs leads us to the conclusion that HEMA has a greater tendency versus cross-propagation than AA.

This affirmation is sustained by the calculated values for numerical average lengths of the two sequences.

$$l_{M1} = 1$$

$$l_{M2} = 1.61$$

Conversion-time dependence for HEMA-AA binary system copolymerisation is presented below (Fig. 7-10).

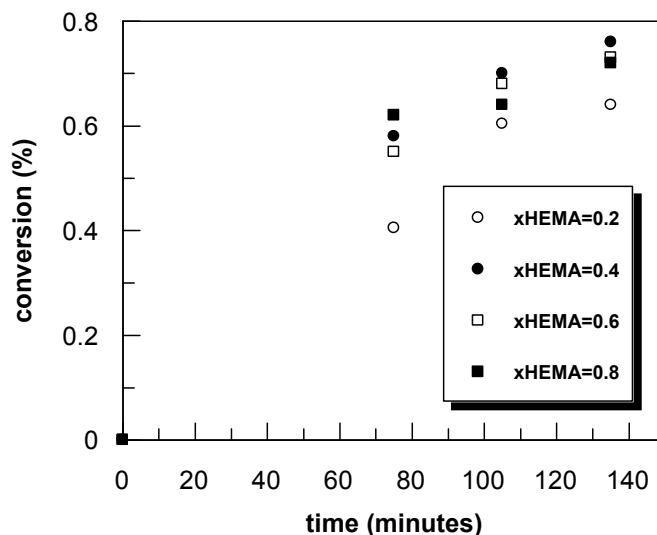


Fig. 7-10. Conversion versus time for HEMA-AA binary system

The analysis of the graph in figure 7 leads us to the conclusion that the ratio among the two monomers in the feed does not influence substantially the copolymerisation rate.

7.3.4.2. Binary system AA-dDMA

As in the other studies presented before, this system was analysed starting from the experimental data, given by elemental analysis (Table 7-8).

Table 7-8

Results of the copolymerisation of dDMA-AA

x_{AA}^*	%C	%H	Conversion (%)	X_{AA}^{**}
0.4	46.009	7.170	0.5574	0.9454
0.8	66.953	9.906	0.3081	0.4545
0.6	41.489	6.151	0.7240	0.4292
0.2	46.886	7.306	0.2320	0.9450

*feed composition

** copolymer composition determined from elemental analysis

There are known: feed composition, obtained copolymers compositions and conversions. PROCOP software helped us to determine the reactivity ratios. The penultimate effect was considered for the kinetic model (8 types of propagation reactions) due to steric effects (volume of dDMA), which affects the macroradicals' reactivity.

Notations: $M_1=[AA]$, $M_2=[dDMA]$

The values obtained using the software are:

$$r_{11}=0.02099$$

$$r_{22}=0.12933$$

$$r_{21}=0.13121$$

$$r_{12}=4.83283$$

The plotting of composition diagram for the AA-dDMA binary system is performed knowing the values of the reactivity ratios and using equation (1).

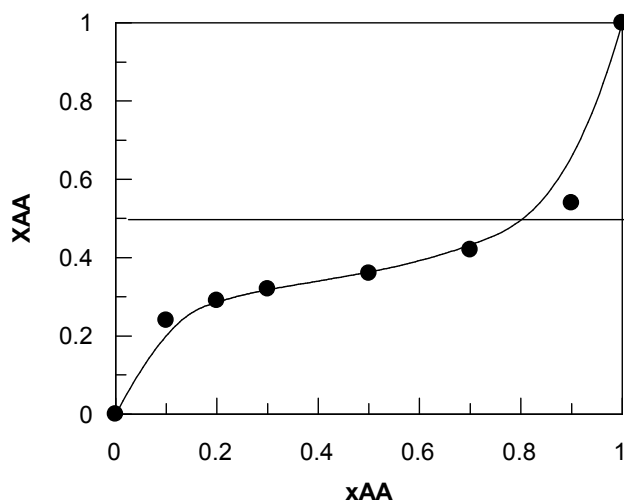


Fig. 7-11. Composition diagram of AA-dDMA binary system

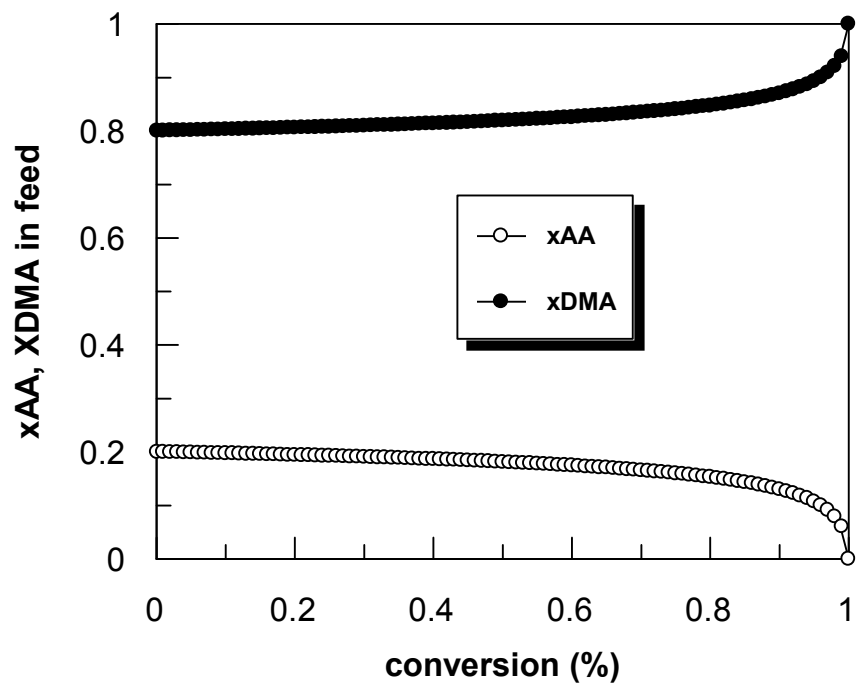
The analysis of the diagram above gives us a typical behaviour of a $r_1 < 1$ and $r_2 < 1$ system. For further information (integral form of Mayo-Lewis equation – giving a correlation composition versus conversion), and using M. Berger and J. Kunz equations, average values of r_1 and r_2 for the composition interval analysed.

The average values obtained are:

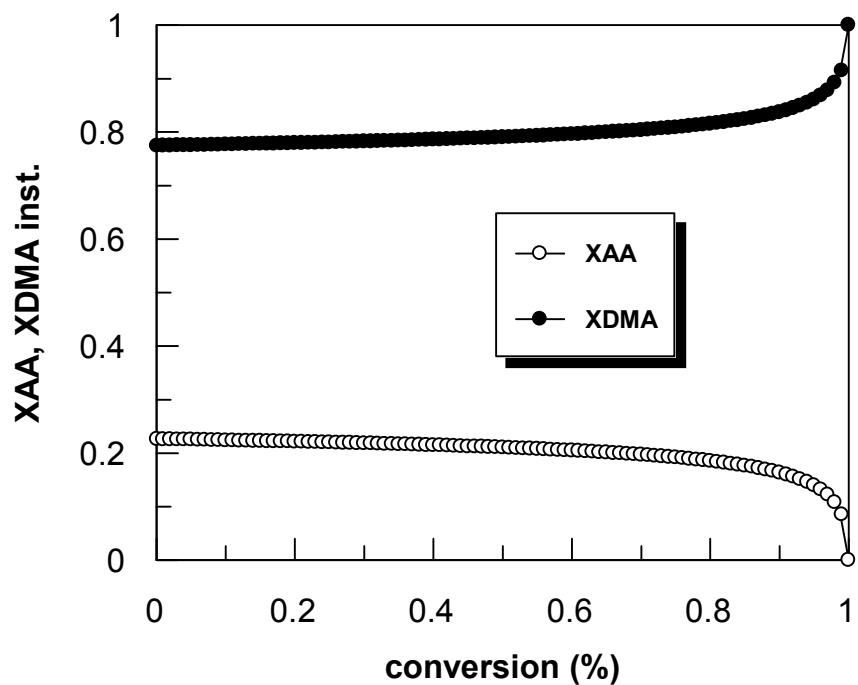
$$\bar{r}_1 = 0.108$$

$$\bar{r}_2 = 0.63$$

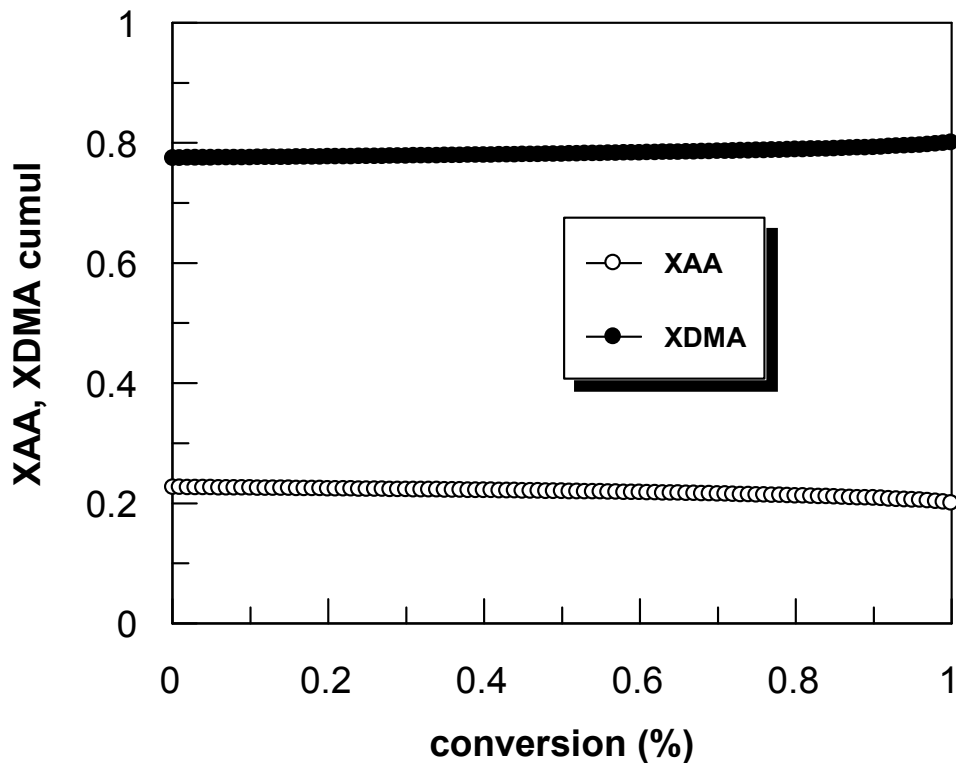
The integration of Mayo-Lewis equation on the conversion interval [0...1] gave the following dependences for the feed defined by $x_{AA}=0.2$ and $x_{DMA}=0.8$.



a) Feed composition versus conversion



b) Instantaneous composition of the copolymer versus conversion



c) Cumulative composition of the copolymer versus conversion

Fig. 7-12. Feed composition and copolymer compositions versus conversion

The analysis of the graphs presented above gives a feed composition quite constant, the same in case of instantaneous and cumulative composition of the copolymer versus conversion. The explanation comes from the similar values of the reactivity ratios. Although, a more intense tendency to homopropagation in case of dDMA it is observed. This affirmation is sustained by the calculated values of the numerical average lengths of the two sequences.

$$l_{M1} = 1.03$$

$$l_{M2} = 3.57$$

Conversion versus time dependence for the AA-dDMA binary system copolymerisation is presented in Fig. 7-13.

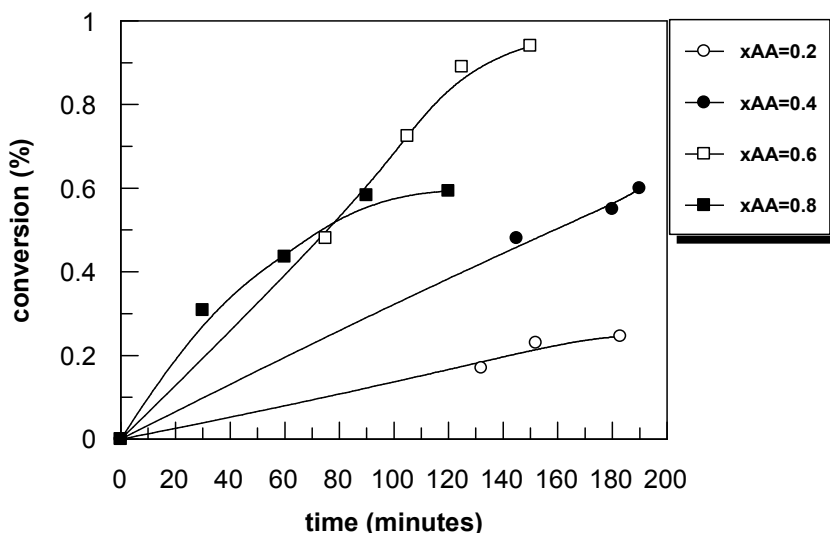


Fig. 7-13. Conversion versus time for the AA-dDMA binary system

Initial rates of copolymerisation can be calculated (in mol/L·s), knowing the molar composition of the copolymers obtained (Fig. 7-14).

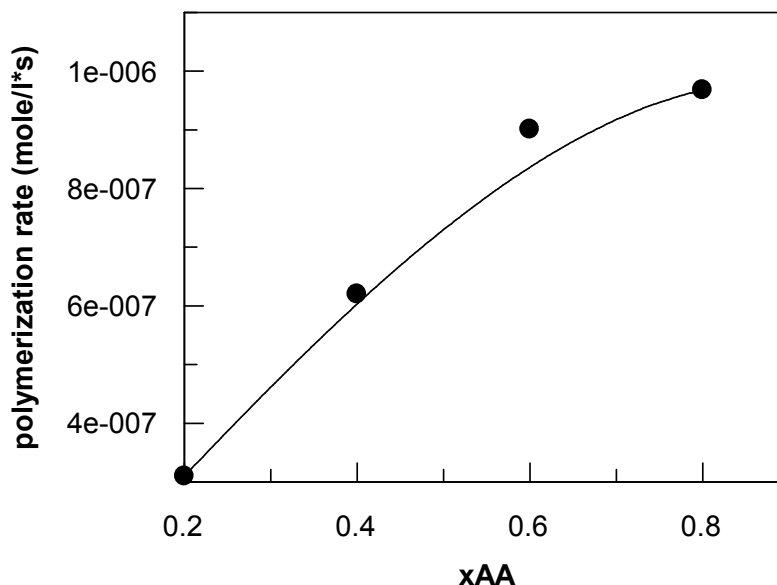


Fig. 7-14. Initial rate of copolymerisation versus feed composition

The copolymerisation rate increases monotonously with AA fraction in the feed. The global rate increase with AA fraction seems impossible to explain if it is correlated with the values of the copolymerisation ratios, which indicate a lower relative tendency for AA homopropagation. In fact, the AA accelerate effect seems to imply the "dilution" of the dDMA units responsible for mutual sterical repulsions, which increase the activation energy of dDMA homopropagation. This explanation is sustained by the relationships $r_{12} \gg r_{11}$ and $r_{12} \gg r_{22}$.

7.3.5. Kinetic study of HEMA-dDMA-AA ternary system

In order to elucidate kinetic aspects regarding ternary system HEMA-dDMA-AA, it was conceived a mathematical model of the reactivity ratios of the comonomers in the terpolymer.

Notations:

[HEMA]=M₁, [dDMA]=M₂, [AA]=M₃.

Instantaneous composition of the terpolymers depends of the six copolymerisations constants and of the three instantaneous concentrations of monomers in the feed.

The Alfrey-Merz-Goldfinger composition equations system is presented further:

$$\frac{d[M_1]}{d[M_2]} = \frac{[M_1] \left([M_1] + \frac{[M_2]}{r_{12}} + \frac{[M_3]}{r_{13}} \right) \left(\frac{[M_1]}{r_{21}r_{31}} + \frac{[M_2]}{r_{21}r_{32}} + \frac{[M_3]}{r_{31}r_{23}} \right)}{[M_2] \left(\frac{[M_1]}{r_{21}} + [M_2] + \frac{[M_3]}{r_{23}} \right) \left(\frac{[M_1]}{r_{12}r_{31}} + \frac{[M_2]}{r_{12}r_{32}} + \frac{[M_3]}{r_{32}r_{13}} \right)}$$

$$\frac{d[M_2]}{d[M_3]} = \frac{[M_2] \left(\frac{[M_1]}{r_{21}} + [M_2] + \frac{[M_3]}{r_{23}} \right) \left(\frac{[M_1]}{r_{12}r_{31}} + \frac{[M_2]}{r_{12}r_{32}} + \frac{[M_3]}{r_{32}r_{13}} \right)}{[M_3] \left(\frac{[M_1]}{r_{31}} + \frac{[M_2]}{r_{32}} + [M_3] \right) \left(\frac{[M_1]}{r_{13}r_{21}} + \frac{[M_2]}{r_{23}r_{12}} + \frac{[M_3]}{r_{13}r_{23}} \right)}$$

where: $r_{12} = \frac{k_{11}}{k_{12}}$; $r_{21} = \frac{k_{22}}{k_{21}}$; $r_{23} = \frac{k_{22}}{k_{23}}$; $r_{32} = \frac{k_{33}}{k_{32}}$; $r_{13} = \frac{k_{11}}{k_{13}}$; $r_{31} = \frac{k_{33}}{k_{31}}$.

The pairs of reactivity ratios r_{ij} and r_{ji} are actually r_i and r_j from binary copolymerisation M_i/M_j .

Therefore:

$r_{13}=0.00029$ [determined in chapter 3.10.4.1]

$r_{12}=2$ [K. Ito et al., 1985]

$r_{21}=1$ [K. Ito et al., 1985]

$r_{23}=0.63$ [determined in chapter 3.10.4.2]

$r_{31}=0.148$ [determined in chapter 3.10.4.1]

$r_{32}=0.108$ [determined in chapter 3.10.4.2]

With these values, respectively of the compositions in the feed, there are plotted ternary compositions diagrams. For the analysis there were considered only HEMA-containing feeds among the limits $[x_{HEMA} = 0.75...0.9]$ in order to maintain the terpolymer properties imposed by the medical application. In the next table the values of the feed composition and instantaneous values of terpolymers composition are given.

Knowing the reactivity ratios, respectively the feed composition ($x_{\text{HEMA}}=0.8$, $x_{\text{dDMA}}=0.1$, $x_{\text{AA}}=0.1$) we can plot the evolution of the feed composition, the instantaneous and cumulative composition, respectively versus conversion, using the PROCOP software.

The analysis of the monomers evolutions leads to the following conclusion: AA presents the highest reactivity during terpolymerisation, followed by HEMA, and dDMA, respectively.

Table 7-9

Compositions of the ternary system

xHEMA*	xdDMA	xAA	XHEMA**	XdDMA	XAA
0.9	0.05	0.05	0.48	0.0362	0.4832
0.85	0.05	0.1	0.47	0.039	0.48
0.8	0.05	0.15	0.47	0.04	0.48
0.85	0.1	0.05	0.46	0.07	0.466
0.8	0.1	0.1	0.45	0.07	0.47
0.75	0.1	0.15	0.447	0.07	0.47

*feed composition

**calculated terpolymer composition

Some of the data above were represented in the Gibbs diagram in Fig. 7-15. There is noticed an intensified tendency of accumulation of AA units in the copolymer, in spite of HEMA units, while dDMA conserves in the copolymer the fraction from the feed.

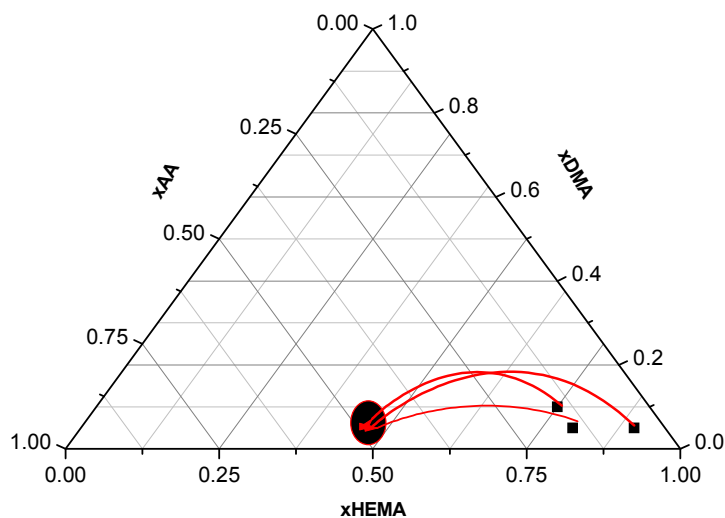
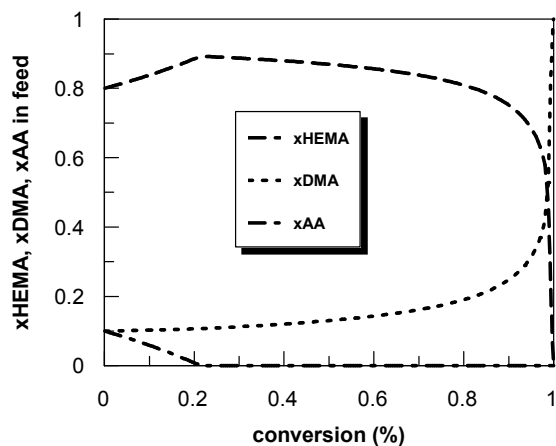
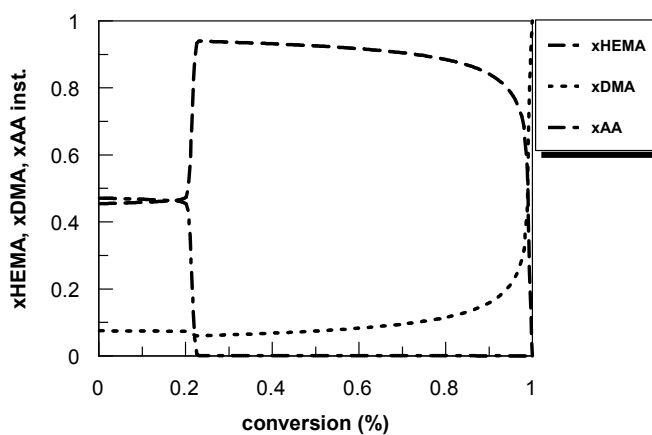


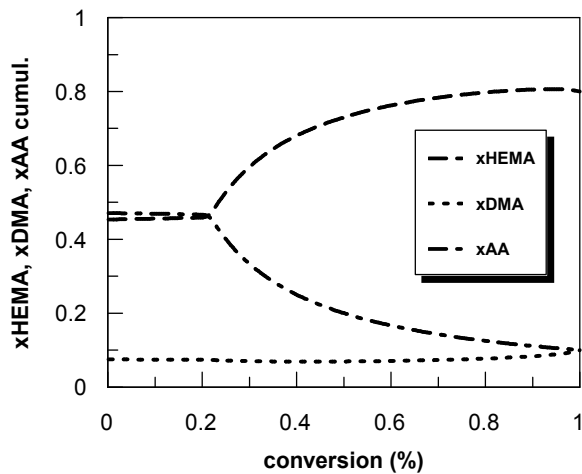
Fig. 7-15. Gibbs diagram



a) Feed composition versus conversion



b) Instantaneous composition of the copolymer versus conversion



c) Cumulative composition of the copolymer versus conversion

Fig. 7-16. Feed composition and copolymer compositions versus conversion

7.3.6. *In vitro* studies for polymers biocompatibility testing

The following materials were tested: A1, A2, A3, A4, A5, A6, D1, D2, D3, D4, D5 and D6, in order to determine their biocompatibility. In this view, an adapted method of *in vitro* cytotoxicity testing was used, on the L929 murine fibroblast cell line.

Indirect contact supposes interposition of a solid medium of DMEM containing 0.75% agar between cells and polymer. Cells were cultivated in DMEM culture medium (Dulbecco's Modified Eagle's Medium) supplemented with 10% bovine foetal serum, 1% L-Glutamine and antibiotics (penicillin and streptomycin). In order to obtain a homogenous distribution, cells were cultivated at a confluence of 25% of the surface in plates of 24 places in 1000 μ L/place and incubated for 72h at 37°C, in humidified atmosphere containing 5% CO₂, until necessary experimental density is attained. At a 95% microscopically observed confluence, the culture medium was replaced with 1000 μ L DMEM containing 0.75% agar, 10% bovine foetal serum, 1% L-Glutamine and antibiotics (penicillin and streptomycin) at a temperature of 40°C (in order to maintain it as a liquid). After agar polymerisation, samples were put on its surface, negative witness consisting in a polypropylene fragment for cellular cultures. Cells were incubated for 24 h at 37°C, in humidified atmosphere and 5% CO₂.

Due to the solid status of the samples and mechanical damage risk onto the cells, the indirect contact method was used. In order to eliminate the infection risk of the cellular cultures, polymers were first sterilized overnight under UV light.

Cellular viability was determined with 3-(4,5-dimethylthiazol-2-yl)-2,5-diphenyltetrazolium bromide (MTT). This test is based on the capacity of dehydrogenases in viable cells mitochondria of converting the soluble yellow tetrazolium salt (MTT) in insoluble formazan, which accumulates as violet crystals in the viable cells.

Taking into account that agar's presence would not allow cellular lysis, formazan dissolution and spectrophotometric reading, the cell number containing violet crystals of formazan was estimated through the analysis of images taken from an inverse microscope ZEISS Axiovert with a 5MP Canon photo camera through ImageJ software analysis (<http://rsb.info.nih.gov/ij/>). The number of living cells is directly proportional with the level of formazan obtained.

After incubation in the presence of the polymers, cells were microscopically examined in order to detect visible signs of cytotoxicity, such as modification of external shape, membrane disruption (cellular lysis) or cellular components aspect or dimensions.

Afterwards, MTT was added (100 μ L/place from a 5 mg/mL solution in TFS) and plates were incubated for 3h.

Further there are presented representative images for each sample (Fig. 7-17 to 7-19) and calculated cytotoxicity ratios (average and standard deviation for 3 images) (Table 7-10). Computed analysis results were in complete agreement with microscopic evaluation.

The standard deviation (SD) is calculated as follows:

$$SD = \sqrt{\frac{1}{n-1} \sum_{i=1}^n (X_i - \bar{X})^2}$$

where n is the sample size and \bar{X} is the mean.

The results obtained show that both A and D series present only slight toxicity. Calculated values of cellular viability versus the control sample, incubated in the same conditions in the absence of polymeric samples, were found to be $> 96.4 \pm 2.55$ % in case of A series and $> 95.3 \pm 3.32$ % for D series.

The *in vitro* tests of cytotoxicity made on fibroblast murine L929 cell line gave adequately results for both of the compositions tested, presenting minimal adverse effects on cell morphology and viability.



Fig. 7-17. Microscopic image of L929 cells in culture, after MTT addition – negative control

Table 7-10

Cellular mortality ratio, reported to negative witness (image analysis method)

Sample	Cytotoxicity (%)	SD
Negative witness	0	± 0
A1	2.3	± 1.63
A2	3.6	± 2.55
A3	3.1	± 2.19
A4	1.8	± 1.27
A5	1.9	± 1.34
A6	2.6	± 1.84
D1	2.8	± 1.98
D2	3.6	± 2.55
D3	1.3	± 0.92
D4	4.6	± 3.25
D5	1.1	± 0.78
D6	4.7	± 3.32

7.4. Conclusions of the synthesis

The microbeads obtained were homogenous in dimensions, 0.7-0.9 μm , their swelling rate suits the controlled drug delivery, and the *in vitro* tests, of biocompatibility and viability, show positive results. These results gave us the possibility to conclude that the beads could be used for controlled drug release.

Copolymers of 2-hydroxyethyl methacrylate (HEMA) with dodecyl methacrylate (dDMA) and acrylic acid (AA) were synthesized by free-radical polymerisation. For further studies, A4, A5 and A6 compositions were chosen, due to water uptake capacity, loading capacity and cytotoxicity behaviour.

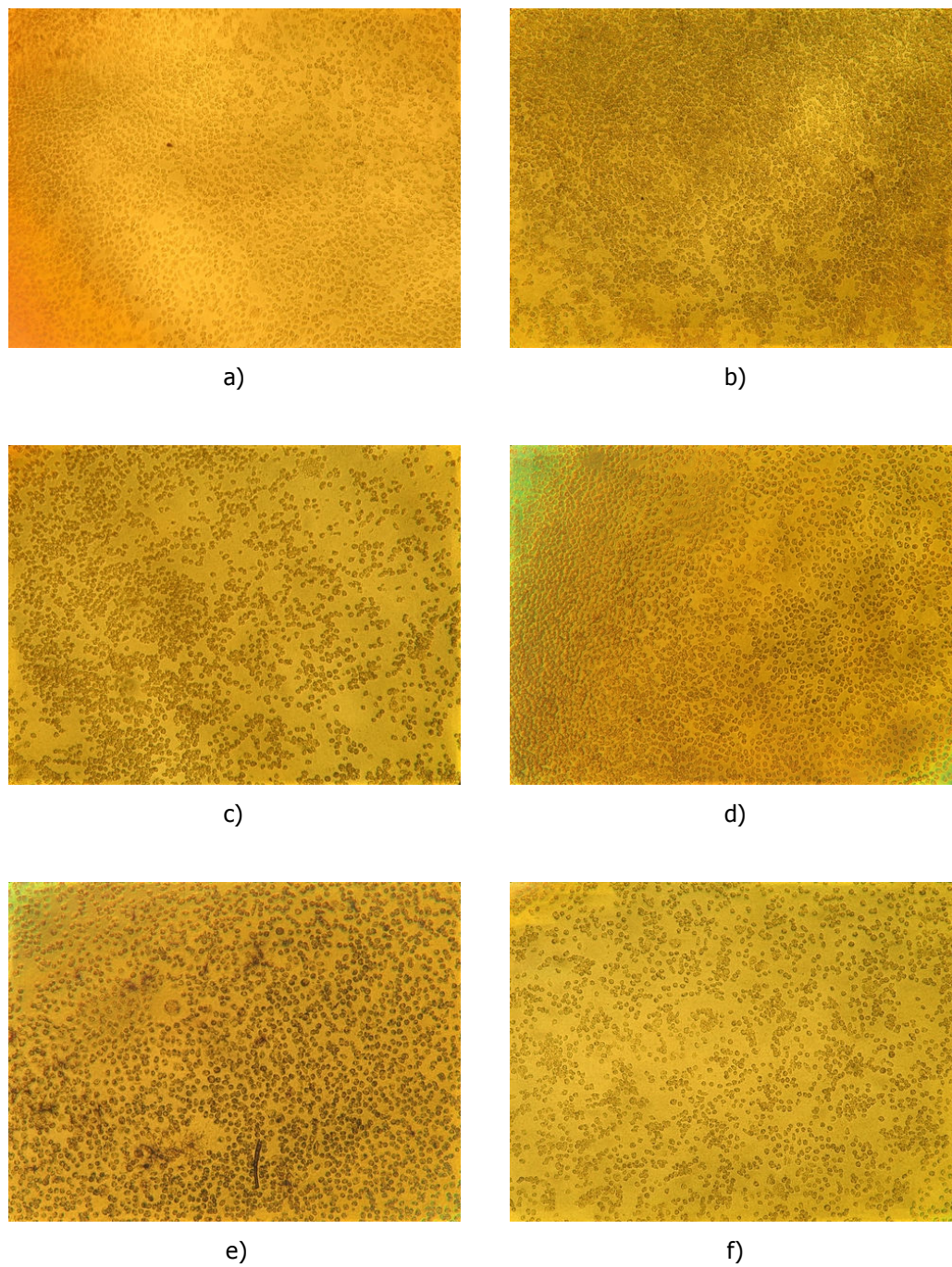


Fig. 7-18. Microscopic image of L929 cells in culture, after MTT addition – positive control, incubated with: a) A1, b) A2, c) A3, d) A4, e) A5, f) A6.

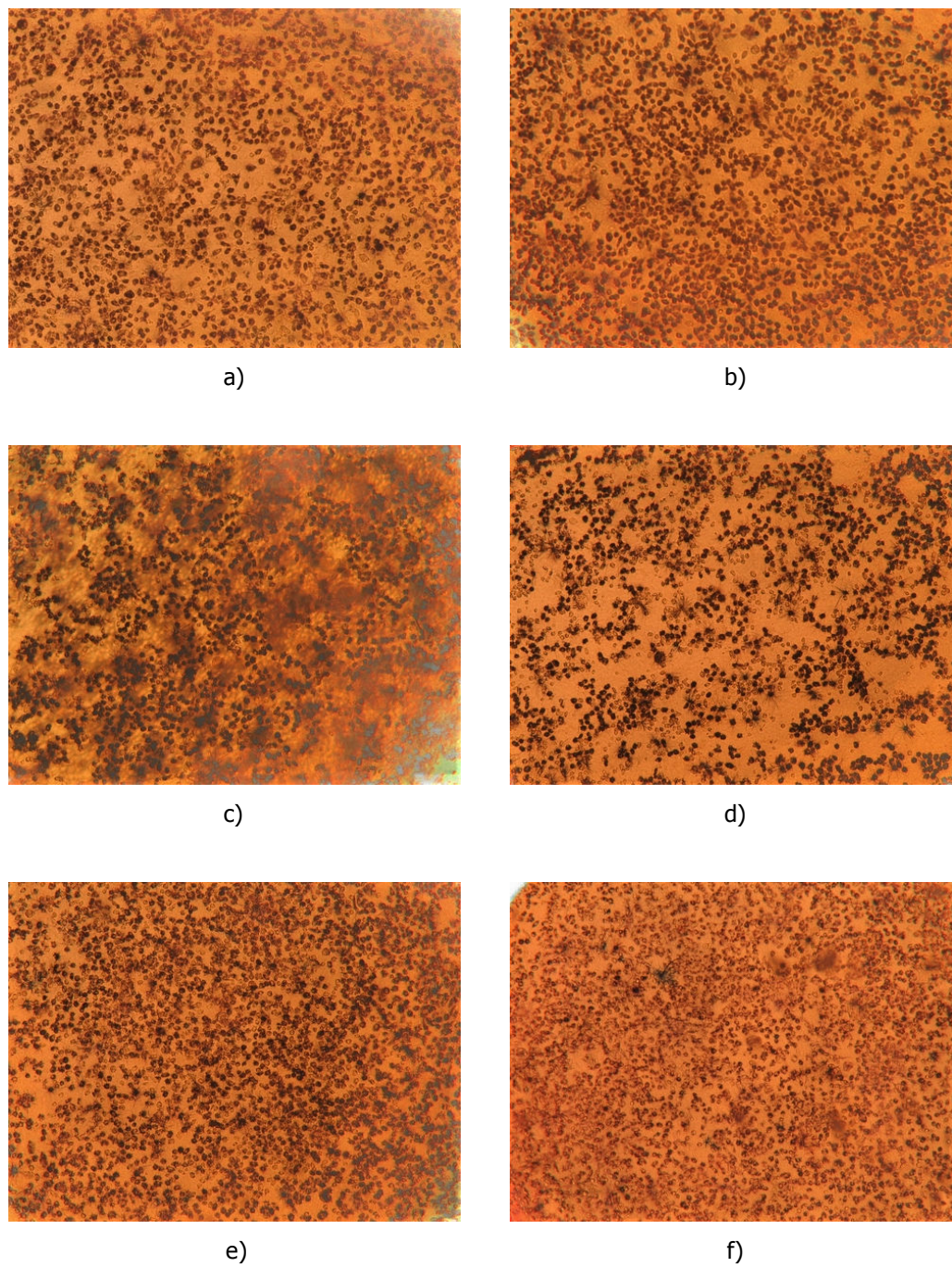


Fig. 7-19. Microscopic image of L929 cells in culture, after MTT addition – positive control, incubated with: a) D1, b) D2, c) D3, d) D4, e) D5, f) D6.

7.5. Nafcillin loading to the synthesized copolymers

The aim of this part of the thesis was to test the application of copolymeric p(HEMA-co-dDMA-co-AA) microparticles to nafcillin release. The drug release kinetics has been examined as a function of the copolymers composition. This part of the thesis reports the synthesis and hydrolytic behavior of acrylic-type polymeric prodrugs of nafcillin.

Nafcillin, a hydrophobic penicillin-derivative used both in orthopaedics and in dentistry, was attached to the resultant copolymers by hydrolyzable ester bonds, as presented further.

The majority of penicillins are not fluorescent compounds because the association of β -lactam and thiazolidine rings does not exhibit fluorescence by itself. Nafcillin contains a bound group in the 6-position, which can be used as a source of fluorescence emission when excited at appropriate wavelengths.

The hydrolysis of the polymer–drug adducts was studied under physiological conditions in saline solution (9 g/L NaCl in demineralised water). The pendent nafcillin group is hydrolyzed at 37°C, and the quantity of the released drug was detected by UV spectroscopy. Also, the influence of various ratios from the polymeric carriers on the release of the drug was studied.

The characterisation studies of the nafcillin-loaded microparticles concerned SEM microphotographs, FT-IR spectra, and UV *in vitro* studies of drug release evaluation.

7.5.1. Esterification procedure

1.54 g (3.4 mmol) of nafcillin were dissolved in 5 mL of dried DMF, in a two-necked flask containing two dropping funnels, and the flask was cooled to 0–5°C with an ice–water bath. Then, 0.72 g (3.5 mmol) of N,N'-dicyclohexyl carbodiimide (DCC) was dissolved in 5 mL of dried DMF and added dropwise to the solution of the flask through the first dropping funnel.

The resultant solution was stirred at 0–5°C for 10 min. In another dropping funnel, 1.0 g (6.8 mmol) of poly(HEMA-co-dDMA-co-AA) (accordingly to the kinetic study) were diluted in 5 mL of dried DMF and added dropwise under stirring to the solution of the flask. The mixture was vigorously stirred at room temperature for 24 h, and the white precipitate produced was filtered.

The precipitated polymer–drug conjugates were collected, washed several times with cooled ethanol, and dried *in vacuo* at room temperature for 24 h.

7.5.2. Hydrolysis and drug release procedures

Powdered polymer–drug adducts (100 mg) were poured into 10 mL of saline aqueous solution (9 g NaCl / 1000 mL distilled water) at 37°C, and the mixtures were placed in cellophane membrane dialysis tubes (50 feet, Sigma). The tubes were closed and transferred into flasks containing 200 mL of the saline solution maintained at 37°C. 3-mL samples were removed at selected intervals, and 3 mL of the saline solution were replaced. The quantity of the released drug

was detected with a UV spectrophotometer and determined from the calibration curve obtained under the same conditions.

7.5.3. Results

It is reported here a synthetic method for the preparation of polymers that contain pendent drug substituents. In this method, the drug agent is attached to preformed polymer backbones via degradable chemical bonds to produce polymeric prodrugs.

Nafcillin has a secondary amine group in its structure. When nafcillin is converted to a suitable polymerisable monomer, the obtained monomer is not polymerised by free-radical polymerisation because the amine group in the structure of nafcillin acts as an inhibitor and prevents radical polymerisation of the monomer. Therefore, for the preparation of polymeric prodrugs, nafcillin must be bound to preformed polymers by chemically links.

Nafcillin was attached to the synthesized copolymers by transesterification. Esterification reactions were carried out in the presence of DCC as a water absorber. The hydroxyl group from HEMA units in the copolymers reacted with the carboxyl group from nafcillin to give a new ester bond between the drug and copolymers (Fig. 7-20 a)). In these reactions, the obtained water is absorbed by DCC and produced N,N'-dicyclohexylurea as a white precipitate, which is removed from the resultant mixture by repeatedly washing with ethanol (Fig. 7-20 b)).

After the completion of the reactions, the white precipitate was isolated, and each solution was poured into the proper nonsolvent. The copolymers containing nafcillin were dried and collected in high yields (between 75 and 80%).

The FT-IR spectrum proves by comparison with polymer spectra that nafcillin was loaded, relevant being the medium peak at $\sim 1568\text{ cm}^{-1}$, of the N-H II band (2j-amide) (Fig. 7-21).

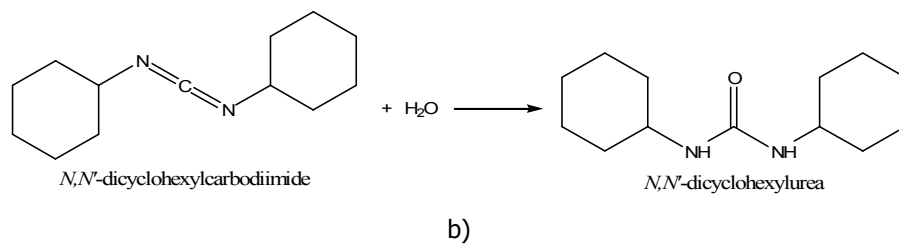
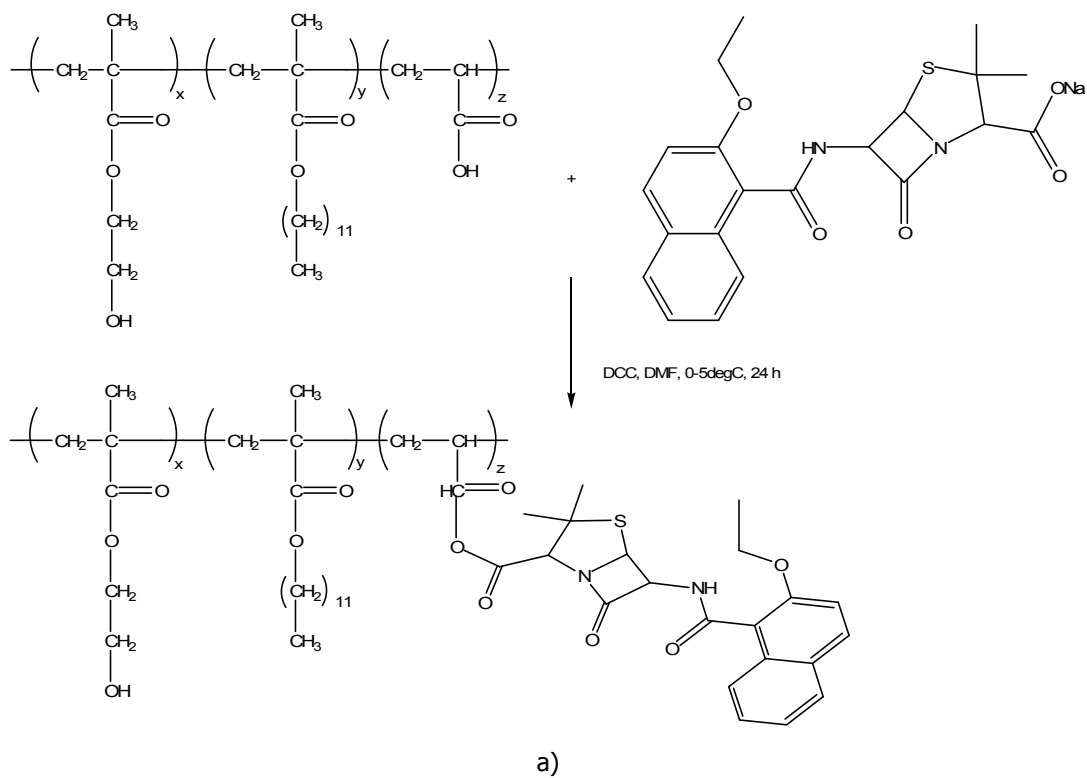


Fig. 7-20. Chemical reactions: a) esterification reaction; b) secondary reaction.

Notations:



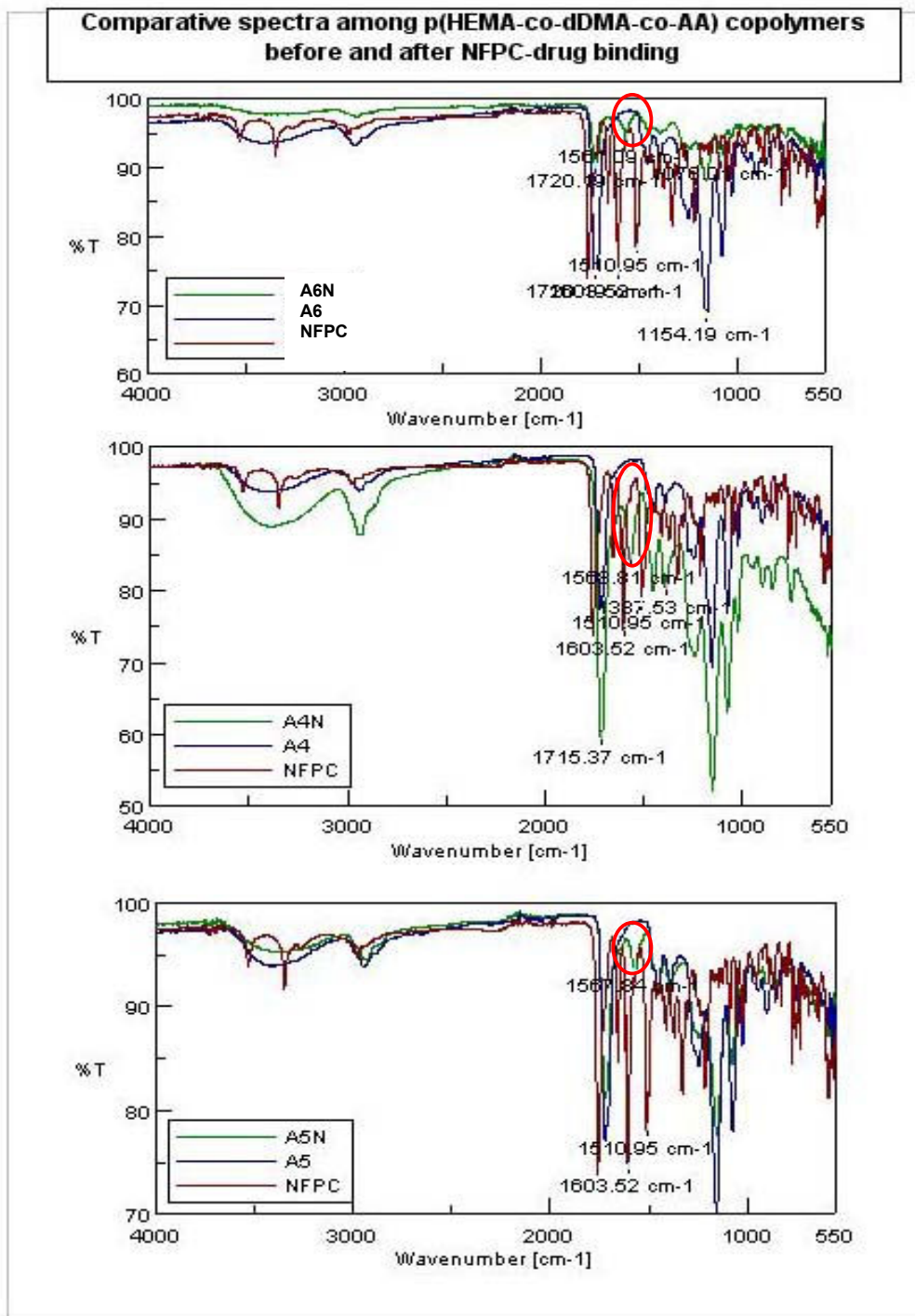
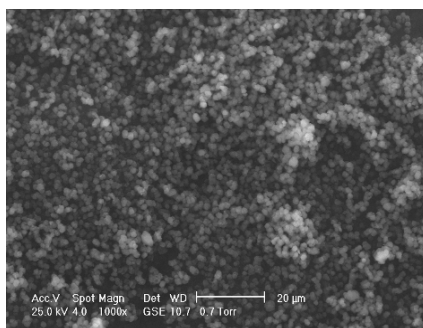


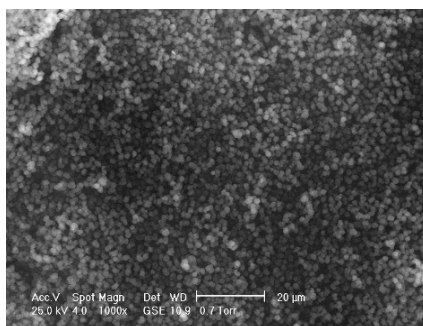
Fig. 7-21. Comparative spectra among A4, A5, A6 and A4N, A5N, A6N and NFPC

7.5.3.1. SEM analysis

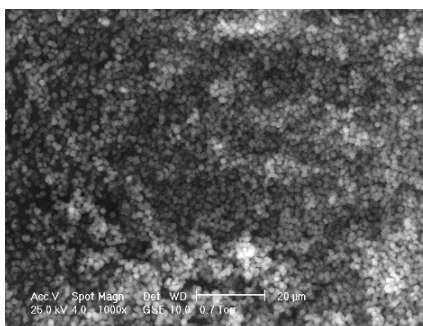
The SEM microphotographs were taken in order to observe whether the microparticles were damaged in shape or agglomerated during the procedure followed for drug loading. As it can be noticed from Fig. 7-22, the beads do not show any relevant modification in size or shape, remaining sharp in form and dimension, and presenting only very slight agglomeration in dry state, which is not the case in saline solution.



a)



b)



c)

Fig. 7-22. SEM microphotographs of: a) A4N; b) A5N; c) A6N.

7.5.3.2. Nafcillin loading efficiency

The measurement of nafcillin content in the copolymers was performed by UV-Vis spectroscopy, using a GBC Cintra 303 apparatus (Fig. 7-23) at a fixed wavelength of 330 nm. The reference cuvette was methanol. 0.02 g of drug-copolymer compounds were suspended in 8 mL methanol to destroy the chemical linkage between nafcillin and copolymer, releasing the drug into the solution. Subsequently the samples were vigorously vortexed and the copolymers were separated by centrifugation (4000 rpm for 10 min). Then the supernatant was used for absorbance measurement at 330 nm. Drug content was determined by comparing with the standard curve of nafcillin, which was achieved from nafcillin solutions in methanol with concentrations in the interval between 0.001 and 0.1 mg/mL.



Fig. 7-23. UV-VIS spectrometer GBC Cintra 303

Nafcillin concentrations calculated using the formula below are given in Table 7-11.

$$D(\%) = \frac{Abs_{sample}}{Abs_{ref}} \cdot \frac{m_{ref}}{m_{sample}} \cdot 100$$

Table 7-11

Drug loading efficiency in the polymer samples

Composition	Sample weight (mg)	Absorbance	Drug loading (%)	Drug loading efficiency (%)
A4N	20	1.2916	38.77	77.5
A5N	20	1.5411	46.26	92.5
A6N	20	1.7864	53.62	98

Nafcillin – polymer weight ratios in the feed were 1:2. Taking into consideration all the approximations and errors, we come to the conclusion that the whole amount of nafcillin was loaded into A6N, while into the other two samples the efficiency was of 77.5%, in case of A4N, and of 92.5% for A5N, respectively.

In vitro drug release experiments of nafcillin loaded copolymers were carried out in an oven at 37°C. The drug-loaded samples were enclosed in dialysis membrane and then incubated in medium of saline solutions.

The measurement of Nafcillin concentration was performed also by UV-Vis spectroscopy at the wavelength of 330 nm. The reference cuvette was saline solution (9 g/L NaCl in demineralised water). Drug content was determined by comparing with the standard curve, which was achieved from solutions in saline solution with concentration between 0.001 and 0.1 mg/mL. Each experiment was repeated three times.

7.5.3.3. *In vitro* study of nafcillin release

The amount of drug released at any time (M_t) was calculated from the calibration curve obtained with saline aqueous solutions of nafcillin from 0.001 mg/mL to 0.1 mg/mL (Table 7-12 and Fig. 7-24).

Nafcillin release kinetics using A4N, A5N and A6N microbeads are presented in Table 7-15 and Fig. 7-25, where M_t is the molar amount of drug released at time t and M_∞ is the maximum molar amount of drug released at equilibrium, which reached the values of 98, 92.5 and 77.5% efficiency of drug loaded in the microbeads.

Table 7-12

Calibration of the NFPC standard concentration

Mixture	Concentration (mg/mL)	Absorbance
1	0.1000	0.5315
2	0.0500	0.2633
3	0.0100	0.0586
4	0.0050	0.0230
5	0.0025	0.0210
6	0.0010	0.0047

The calibration coefficient obtained was 0.99986, with the max. error: 0.0014, and the linear expression of the calibration:

$$\text{Conc.} = + 0.188278 \times \text{Absorbance} - 1.34576e-011$$

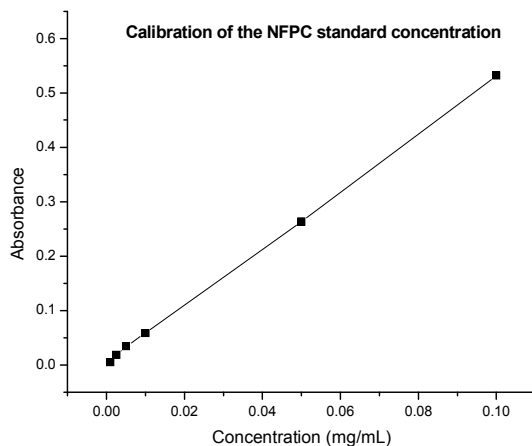


Fig 7-24. Calibration of NFPC using UV spectrophotometry

As presented in Fig. 7-25, nafcillin release is faster as the percentage of acrylic acid in the copolymer increases. Due to the hydrophobic character of this drug, as the content of the hydrophobic comonomer in the copolymer (dDMA) remains constant, the drug will be more released easier with an increase in acrylic acid.

Table 7-15

UV data for nafcillin release

Time (min.)	Concentration of NFPC released from polymer systems determined by UV (mg/mL)		
	A4N	A5N	A6N
0	0	0	0
60	0.0143	0.0201	0.0255
120	0.0186	0.0273	0.0346
180	0.0227	0.0307	0.0385
240	0.0245	0.0318	0.0407
300	0.0257	0.0332	0.0424
360	0.0264	0.0347	0.0442
420	0.0271	0.0351	0.0466
480	0.0279	0.0362	0.0486
540	0.0287	0.0372	0.0501
600	0.0295	0.0375	0.0522

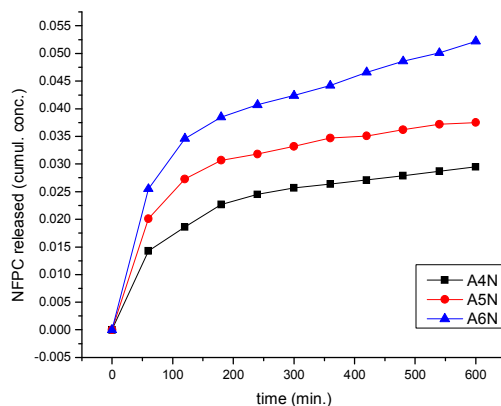


Fig. 7-25. Release kinetics of NFPC from p(HEMA-co-dDMA-co-AA) microbeads.

As Kortusuo (2001) described, in order to simplify the analysis of controlled release data from polymeric devices of varying geometry, an empirical, exponential expression was developed to relate the fractional release of drug to the release time:

$$\frac{M_t}{M_\infty} = kt^n$$

where M_t/M_∞ is the fractional solute release, t is the release time, k is a constant and n is the exponent characteristic of the release mechanism. This equation applies until 60% of the total amount of drug is released. It predicts that the fractional release of drug is exponentially related to the release time and it adequately describes the release of drug from slabs, spheres, cylinders and discs from both swellable and non-swallowable matrices (Table 7-16). The slope (n) of the $\log(\text{drug released})$ vs. $\log(\text{time})$ plot is 0.5 for pure Fickian diffusion.

Table 7-16

Diffusional exponent and mechanism of diffusional release from cylindrical and spherical non-swallowable and swallowable controlled release systems (Peppas, 1985).

Controlled release system	Diffusional exponent n	Drug release mechanism
Non-swallowable	<0.5	Release from porous material
	0.5	Fickian diffusion
	0.5-1.0	Anomalous (non-Fickian) transport
	1.0	Zero-order release
Swallowable	0.45	Fickian diffusion
	0.45-0.89	Anomalous (non-Fickian) transport
	0.89	Case-II transport
	>1	Super-Case II transport

An anomalous non-Fickian diffusion pattern ($n = 0.5-1$ or $n = 0.45-0.89$) is observed when the rates of the solvent penetration and drug release are in the same range. This deviation is due to increasing drug diffusivity in the matrix by the solvent induced relaxation of the polymers. Zero order drug release ($n = 0.89$ or $n = 1$) can be achieved when drug diffusion is rapid compared to the constant rate of solvent induced relaxation and swelling in the polymer (Case II transport for swellable polymers). Use of this equation to analyse data of drug release from a porous system will probably lead to $n < 0.5$, since the combined mechanisms (diffusion through the matrix and partially through water-filled pores) will shift the release exponent toward smaller values (Peppas, 1985). Fig. 7-26 describes the effect of exponent n on the release profile from controlled release systems.

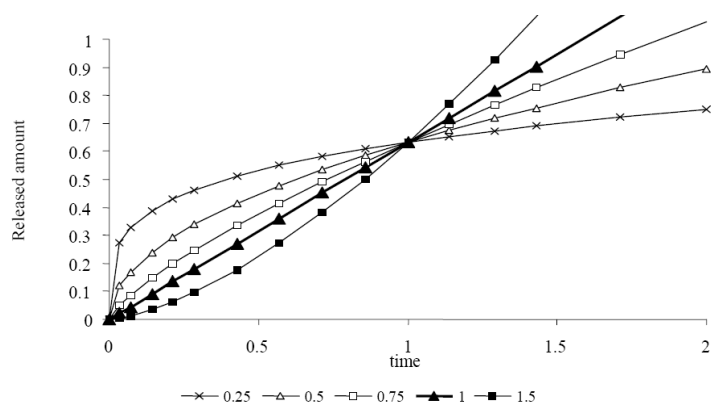
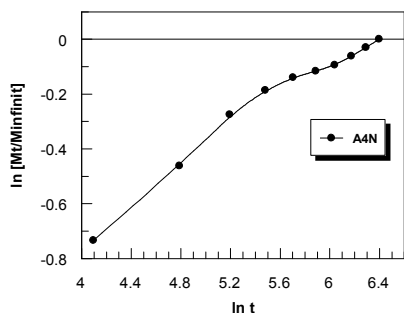


Fig. 7-26. Fractional drug release versus time curves with different values of exponent n (0.25-1.5) when the constant (k) in the equation (5) is 0.6 (Kortesuso, 2001).

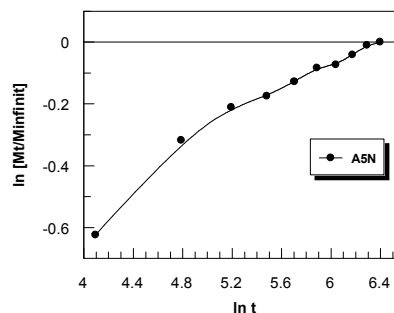
In consequence, graphs of $\ln(M_t/M_\infty)$ versus $\ln t$ were projected in order to obtain the slope (value of n). The study conducted to values of n close to 0.3 (Fig. 7-27), which means that, in this case, the mechanism followed is case " $n < 0.5$ ", where the release takes place from a porous material.

Accordingly to the USP Nafcillin Sodium Reference standard (USP30-NF25) in FARMACOPEEA, concentrations of about 0.4 mg of nafcillin sodium are used for patient treatment in doses every 6 hours. Consequently, doses of conjugates designed could be further used in *in vivo* tests, either 1000 mg of A5N or 800 mg of A6N, in order to be administered to patients for gradually releasing nafcillin during 10 hours.



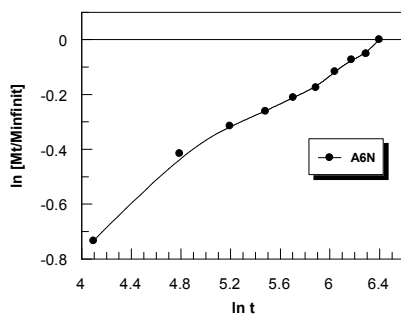
Intercept -1.9236 0.1151
Slope 0.3058 0.0204

a)



Intercept -1.5708 0.1121
Slope 0.2506 0.0198

b)



Intercept -1.8729 0.0878
Slope 0.2922 0.0155

c)

Fig. 7-27. Kinetic mechanism of the nafcillin release from: a) A4N; b) A5N; c) A6N.

7.6. Conclusions and perspectives

In the present chapter it was presented the synthesis of two series of copolymers, p(HEMA-co-dDMA-co-AA) and p(HEMA-co-dDMA-co-DEAEMA), as 1 μm -microbeads. They were physico-chemically characterised and were submitted to cytotoxicity tests. After obtaining positive results, three compositions of the acrylic acid-containing polymers were used for nafcillin loading.

The efficiency of the drug loading and the *in vitro* release were determined. Two of the compositions, 80:10:10 and 75:10:15 molar compositions, present valuable opportunities for further *in vivo* testing, in order to be used as drug delivery systems in treatment of different osseous diseases.

Chapter 8

General conclusions of the thesis

Polymers are becoming increasingly important in the field of drug delivery. The pharmaceutical applications of polymers range from their use as binders in tablets to viscosity and flow controlling agents in liquids, suspensions and emulsions. Polymers can be used as film coatings to disguise the unpleasant taste of a drug, to enhance drug stability and to modify drug release characteristics.

The present thesis focused on the use of pharmaceutical polymers for controlled drug delivery applications. The principles of controlled drug delivery are outlined and applications of polymers for controlled drug delivery are described.

The mechanism of delivery can be the difference between a drug's success and failure, as the choice of a drug is often influenced by the way the medicine is administered. Sustained (or continuous) release of a drug involves polymers that release the drug at a controlled rate due to diffusion out of the polymer or by degradation of the polymer over time.

Improving delivery techniques that minimize toxicity and maximise efficacy offers great potential benefits to patients, and opens up new markets for pharmaceutical and drug delivery companies. The ultimate goal in controlled release is the development of a microfabricated device with the ability to store and release multiple chemical substances on demand.

HEMA-based copolymers were the core materials used in this thesis. The interest in using these copolymers resides basically in their improved characteristics regarding hydrophilicity/hydrophobicity ratio and functionalisation ratio choice for drug incorporation. These two advantages, i.e. higher stability and drug binding and release led to two main research interests, which were addressed in this work: the use of microcarriers based on synthetic polymers as active targeting drug delivery systems and drug immobilization on surfaces.

The studies performed in this thesis started from these principles, developing from the synthesis to physical, chemical and biological characteristics.

Binding nano or microbeads with radio-opaque elements, such as iodine-based polymers, allow finding better diagnose methods. In the **3rd Chapter**, there was conceived a new copolymer system for tumour targeting. In this respect, the following steps were pursued:

1. synthesis and purification of a iodine-containing monomer, 2,4,6-triodophenyl acrylate (TIPA);
2. chemical characterisation through FT-IR of the monomer obtained;
3. synthesis of p(MMA-co-TIPA) as microbeads and pellets, with different comonomer ratios;
4. physico-chemical characterisation of the copolymers obtained through: FT-IR, SEM, EDX;
5. determination of the reactivity ratios of the comonomers in the binary system, in order to establish the microarchitecture of the MMA-TIPA copolymer. The reactivity ratios were evaluated by the penultimate model and integrated using the equations of M. Berger and J. Kunz. The average values obtained were $r_1=5.49$ and $r_2=0.053$. The analysis of the graphs above gives an increased reactivity of MMA-radicals towards homopropagation, comparatively with TIPA-radicals. This resolution is sustained by the values calculated for

numerical average lengths of the two sequences. Also, the rate determination stage for interruption is represented by segmental diffusion;

6. toxicity of the copolymers was evaluated by *in vitro* assays against murine fibroblast L929 line cells. The results of this tests show a good biocompatibility of the copolymer MMA-TIPA and no images of necrotic cell were evidenced at the surface of the polymer compositions;
7. evaluation of the calcification capacity of the copolymers *in vitro* (incubation in 1x SBF). SEM and EDX analysis showed the presence of calcium and phosphorus onto the surfaces of the materials, but the molar Ca/P ratio was far from the ratio found in hydroxyapatite (1.67).

Together with the other results obtained, the low-calcification potential represents an opportunity for using this copolymer in tumoral targeting and imaging systems.

Chapter 4 presents the obtaining of new HEMA-based micropolymeric beads as containers for physically or chemically bound drugs. The main purpose of this study was to optimise the method of microbeads synthesis. In this view, 2-hydroxyethyl methacrylate (HEMA) as principal comonomer, and methacryloyloxyethyl phosphate (MOEP) and 2-methacrylic acid 3-guanidinopropyl ester (GuaMA) as functionalised comonomers were considered. There were followed the stages:

1. synthesis and purification of the GuaMA monomer;
2. synthesis of the copolymers in different ratios by suspension polymerisation, by varying either the initiator or the ratio in the solvent/non-solvent system, followed by SEM analyses. Ethyl eosin, a fluorescent marker, was incorporated during synthesis for *in vitro* and *in vivo* detection;
3. characterisation studies: FT-IR, swelling behaviour, fluorescence microscopy, *in vitro* and *in vivo* tests

The results obtained prove the possibility of further use of such micropolymeric architectures in controlled delivery systems.

The purpose of the **5th Chapter** was to obtain new copolymers in order to create a membrane-like barrier that would control the delivery of the active agent for an extended period of time in the organism. Cross-linked pHEMA swells to a significant extent. Hence, it was thought necessary to determine its swelling degree when incorporating methyl methacrylate (MMA), which is a hydrophobic monomer that is expected to restrain the water uptake in pHEMA. In order to be able to bind drugs, we need functionalised polymers, this being the reason for using the acrylic acid (AA). The study consisted in:

1. preparation of polymeric microbeads of pHEMA and p(HEMA-co-MMA) and functionalised biopolymers of p(HEMA-co-AA) and p(HEMA-co-MMA-co-AA) by precipitant polymerisation;
2. characterisation of the different compositions of microbeads obtained by: swelling degree measurement, SEM, elemental analysis and *in vitro* tests.

The experiments allowed to conclude that a higher MMA:HEMA ratio would be the best approach in the construction of a controlled drug release system, but in adequate parameters for use in drug delivery systems.

In the **6th Chapter**, a comparison among physico-chemical and biological *in vitro* and *in vivo* behaviour of different HEMA-based and functionalised-containing polymers is performed. In this study there were used several methacrylate derivatives with negative and positive functionalities: glycidyl, acetoacetate, carboxyl, tetrahydrofurfuryl and ammonium chloride. The stages of the study were:

1. synthesis of the copolymers of p(HEMA-co-DADMAC), p(HEMA-co-GlyMA), p(HEMA-co-MAA), p(HEMA-co-MOETAC), p(HEMA-co-MOEAA) and p(HEMA-co-THFMA) were obtained as microbeads by suspension polymerisation and as pellets by bulk polymerisation. Nile Red was incorporated during synthesis for detection purposes;
2. physico-chemical characterisation studies: fluorescence microscopy, FT-IR, Raman, swelling tests, mineralization tests and spectrophotometrical dosage of calcium and phosphorus, SEM, EDX, flow cytometry;
3. thalidomide, a drug that has been shown to inhibit angiogenesis induced by fibroblast growth factor and vascular endothelial growth factor, was physically loaded to p(HEMA-co-MOEAA);
4. biological *in vitro* evaluation with murine fibroblast L929 line cell and endothelial EA.hy 926 cells;
5. *in vivo* evaluation of thalidomide-copolymer system, in a rat methastases model, with positive results, which would be continued with clinical tests.

In the 7th Chapter, another drug was considered for application in the field of dentistry and orthopedics, nafcillin, a drug active against penicillinase-producing *Staphylococcus aureus*. In this view, the steps of the polymeric systems obtaining were:

1. synthesis of p(HEMA-co-dDMA-co-AA) and p(HEMA-co-dDMA-co-DEAEMA) polymeric beads in different compositions;
2. characterisation of the systems obtained by: swelling tests, SEM, FT-IR, elemental analysis, *in vitro* behaviour with L929 line cell;
3. reactivity ratios of the binary system HEMA-AA were determined using PROCOP software: $r_1=0.00029$, and $r_2=0.148$. An analysis of the graphs lead to the conclusion that HEMA has a greater tendency versus cross-propagation than AA, but the ratio among the two monomers in the feed does not influence substantially the copolymerisation rate;
4. the penultimate effect was considered for the kinetic model in case of the binary system AA-dDMA, due to sterical effects (volume of dDMA), which affects the macroradicals' reactivity. The integral form of Mayo-Lewis equation and M. Berger and J. Kunz equations gave the average values of $r_1 = 0.108$ and $r_2 = 0.63$. The results imply a feed composition quite constant, the same in case of instantaneous and cumulative composition of the

copolymer versus conversion, due to the similar values of the reactivity ratios. Meanwhile, a more intense tendency to homopropagation in case of dDMA it is observed;

5. in order to elucidate kinetic aspects regarding ternary system HEMA-dDMA-AA, it was conceived a mathematical model of the reactivity ratios of the comonomers in the terpolymer, using the Alfrey-Merz-Goldfinger composition equations system. Analysing the Gibbs diagram, there is noticed an intensified tendency of accumulation of AA units in the copolymer, in spite of HEMA units, while dDMA conserves in the copolymer the fraction from the feed.
6. nafcillin was attached to three different compositions of p(HEMA-co-dDMA-co-AA) copolymers by hydrolyzable ester bonds, and the drug release kinetics has been examined as a function of the copolymers composition;
7. characterisation studies of nafcillin-loaded microbeads concerned SEM microphotographs, FT-IR spectra, and UV *in vitro* studies of drug release evaluation;
8. the efficiency of the drug loading and the *in vitro* release were determined.

Two of the compositions present valuable opportunities for further *in vivo* testing, in order to be used as drug delivery systems in treatment of different osseous diseases.

REFERENCES

A

- Abishek Singh Reports, MURJ Volume 2, 56-58, 2000.
- Agnihotri S.A., Mallikarjuna N.N., Aminabhavi T.M., *J. Ctrl. Rel.*, 100, 5-28, 2004.
- Alvarez-Lorenzo C., Concheiro A., *J. Chromatogr. B*, 804, 231-45, 2004.
- Am Ende, M.T., Diffusion-Controlled Delivery of Proteins from Hydrogels and Other Hydrophilic Systems, in *Protein Delivery: Physical Systems*, Sanders and Hendren, Editors. 1997, Plenum Press: New York.
- Anderson, A.R.A., Chaplain, M.A.J. *Bull Math Biol*, 60, 857-899, 1998.
- Anderson DG, Akinc A, Hossain N, Langer R. *Mol Ther*. 11(3): 426-34, 2005.
- Anderson, J.M. *Cardiovasc Pathol*, 2(3): p. 33-41, 1993.
- Anderson, J.M. *Trans Am Soc Artif Intern Organs*, 19: p. 101-107, 1988.
- ANSI/AAMI/ISO 10993-5:1999, Part 5: Tests for in vitro cytotoxicity, International Organization for Standardization, 1999
- Apicella, A., Cappello, B. and al, e., Poly(Ethylene Oxide)-Based Delivery Systems, *Acs Symposium Series*, in *Polymeric Drugs and Drug Administration*. 1994, ACS: Washington, DC.

B

- Babazadeh, M., *J. Appl. Polym. Sci.* 2007, Vol. 104, 2403–2409
- Badiger, M.V., McNeill, M.E., Graham, N.B., *Biomaterials*, 1993, 1993(14): p. 14.
- Bae Y., Fukushima S., Harada A., Kataoka K., *Angew. Chem. Int. Ed.*, 42, 4640-43, 2003.
- Baish, J.W., Gazit, Y., Berk, D.A., Nozue, M., Baxter, L.T., Jain, R.K. *Microvascular Research*, 1996, 51: p. 327-402.
- Balding, D., McElwain, D.L.S. *J Theor Biol*, 1985, 114: p. 53.
- Batycky RP, Hanes J, Langer R, Edwards DA. *J Pharm Sci*. 1997 Dec;86(12):1464-77.
- Benita S (ed), *Microencapsulation: Methods and Industrial Applications*, New York, Marcel Dekker, 1996.
- Bertolini, F., Mancuso, P., Gobbi, A., Pruneri, G. *Experimental Hematology*, 2000, 28: p. 993-1000.
- Bibby DC, Davies NM, Tucker IG., *Int J Pharm*. 2000 Mar 20;197(1-2):1-11.
- Bigi, A., Boanini, E., Panzavolta, S., Roveri, N., Rubini, K., *J. Biomed. Mater. Res*. 59, 709, 2002.
- Bigi, A., Panzavolta, S., Roveri, N., *Biomaterials* 19, 739, 1998.
- Blumenthal N.C., *Clin. Orthop. Relat. R*. 247, 279, 1989.
- Bosch, R.A. *SIAM Review*, 1999, 41(3): p. 594-604.
- Brauker, J.H., Carr-Brendel, V.E., Martinson, L.A., Crudele, J., Johnston, W.D. *J Bio Mat Res*, 1995, 29: p. 1517-1524.
- Breimer, D.D. *J Control Release*, 1992, 21: p. 5-10.
- Brockhurst R.J., Ward R.C., Lou P., Ormerod D., Albert D., *Am. J. Ophthalmol*. 115, 524, 1993.
- Burri, P.H., *Dev Dyn*. 231(3): 474-88, 2004.
- Byrne M. E., Park K., Peppas N., *Advanced Drug Delivery Reviews*, 54, 149-61, 2002.

C

- Carenza, M. Veronese, F.M. *J Control Rel*, 1994, 29: p. 187-93.
- Chaplain, M.A.J. Anderson, A.R.A. *Invasion Metastasis*, 1996, 16: p. 222-234.
- Charman W.N., Chan H.-K., Finin B.C. Charman S.A., *Drug Development Research*, 46, 316-27, 1999.
- Chasin M, Langer R (eds), *Biodegradable Polymers as Drug Delivery Systems*, New York, Marcel Dekker, 1990.
- Chien YW, *Novel Drug Delivery Systems*, New York, Marcel Dekker, 1982.
- Chirila, T.V., Higgins, B. Dalton, P.D. *Cellular Polymers*, 1998, 17(3): p. 141-162.
- Chirila T.V., Constable I.J., Crawford G.J., Vijayasekaran S., Thompson D.E., Chen Y.C., Fletcher W.A., Griffen B.J. (1993) *Biomaterials*, 14:26-38.
- Chirila T.V., Zainuddin, Hill D.J.T., Whittaker A.K., Kemp A., *Acta Biomaterialia* 3, 2007, p. 95–102
- Chirila T.V., Zainuddin, *React. Funct. Polym.* 67 (2007) 165.

-
- Chung J.E., Yokoyama M., Yamato M., Aoyagi T., Sakurai Y., Okano T., *J. Contr. Rel.* 62, 1999, p. 115–127
- Clayton, A.B., Chirila, T.V. Dalton, P.D. *Polym Int*, 1997, 42(1): p. 45-56.
- Clayton, A.B., Chirila, T.V. Lou, X. *Polym Int*, 1997, 44: p. 201-207.
- Cleary GW, *Cosmetics and Toiletries*, 106:97–107, 1991.
- Cleary GW, "Transdermal Delivery Systems: A Medical Rationale," in *Topical Drug Bioavailability, Bioequivalence, and Penetration*, Shah VP, and Maibach HI (eds), New York, Plenum, pp 17–68, 1993.
- Cleland JL. *Biotechnol Prog.* 1998 Jan-Feb;14(1):102-7.
- Cook, A. *J Biomed Mater Res*, 1997, 35: p. 513-23.
- Crank, J. and Park, G.S., *Diffusion in Polymers*. 1968, London, New York: Academic Press. xii, 452.
- Curry, F.E., Huxley, V.H. Adamson, R.H. *Am J Physiol*, 1983, 245: p. H495-H505.

D

- Dalton P.D., Flynn L., Shoichet M.S., (2002) *Biomaterials*, 23 (18):3843-3851.
- Daniel, T.O. Abrahamson, D. *Annu Rev Physiol*, 2000, 62: p. 649-71.
- Dash, A.K. Cudworth II, G.C. *J Pharm Tox Meth*, 1998, 40: p. 1-12.
- Denizli, A., Say, R., Pişkin, E., *Reactive & Functional Polymers* 2003, vol. 55, 99-107
- Desai T.A., Chu W.H., Tu J.K., Beattie G.M., Hayek A., Ferrari M., *Biotechnol. Bioeng.* 57, 118 (1998).
- Domb AJ (ed), *Polymeric Site-Specific Pharmacotherapy*, Chichester, UK, Wiley, 1994.
- Donbrow M (ed), *Microcapsules and Nanoparticles in Medicine and Pharmacy*, Boca Raton, FL, CRC Press, 1992.
- Dorski CM, Doyle FJ, Peppas NA, *Polym Mater Sci Eng Proceed*, 76:281–282, 1997.
- Duncan, R., Dimitrijevic, S., *Journal of Bioactive and Compatible Polymers* 1998, 13, 165-178.
- Dziubla, Thomas D., PhD Thesis : *Macroporous hydrogels as vascularizable soft tissue – implant interfaces: materials characterization, in vitro evaluation, computer simulations, and applications in implantable drug delivery devices*, 2003

E

- Edelstein, L. *J Theor Biol*, 1982, 18: p. 679.
- Eldridge JH. *Infec Immun.* 1991; 59: 2978–2986.
- Endo A., *J. Jap. Orthop. Assoc.* 61 (1987) 563.

F

- Filmon R., Grizon F., Basle M.F., Chappard D., *Biomaterials* 23 (2002) 3053.
- Filmon R., Chappard D., Montheard J.P., Basle M.F., *Cell. Mater.* 6 (1996) 11.
- Filmon R., Basle M.F., Barbier A., Chappard D., *J. Biomat. Sci. Polym. E.* 11 (2000) 849.
- Fischbein L., Gallagher J.A., *J. Am. Chem. Soc.* 76, 3217 (1954).
- Fleisch H., Russel R.G.G., Straumann F., *Nature* 212 (1966) 901.
- Freyman, T.M., Yannas, I.V. Gibson, L.J. *Progress in Materials Science*, 2001, 46(3-4): p. 273-82.
- Fung, L.K. Saltzman, W.M. *Advanced Drug Delivery Reviews*, 1997, 26: p. 209-230.
- Funhoff A.M., van Nostrum C.F., Lok M.C., Fretz M.M., Crommelin D.J.A., Hennink W.E., *Bioconjugate Chem.* 2004, 15, 1212-1220.

G

- Gallin, J., Goldstein, I.M. Snyderman, R., *Inflammation: Basic Principles and Clinical Correlates*. 1988, New York: Raven Press.
- Gander B. Pulsed Tetanus Toxoid Release from PLGA Microspheres and Its Relevance for Immunogenicity in Mice, *Proceedings International Symposium on Controlled Release and Bioactive Materials*, Washington, D.C.: Controlled Release Society, 1993: 65–66.
- Gentry, L.O., *Int. J. of Antimicrobial Agents* 1997, 9, 37-42

George PM, Lyckman AW, Lavan DA, Hegde A, Leung Y, Avasare R, Testa C, Alexander PM, Langer R, Sur M.. *Biomaterials* 2005 26(17): 3511-9.

Gerwins, P., Skoeldenberg, E. Claesson-Welsh, L. *Critical Reviews in Oncology/hematology*, 2000, 34: p. 185-194.

Glimcher M.J., *Calcified Tissue Res.*, Sup 1 (1968).

Glimcher M.J., *Clin. Orthop. Relat. R.* 61 (1968) 16.

Gombotz WR, Pettit DK. *Bioconjug Chem.* 1995 Jul-Aug;6(4):332-51.

Grayson AC, Cima MJ, Langer R. *Biomaterials.* 2005 26(14): 2137-45.

Griffith, L.G. NAughton, G. *Science*, 2002, 295: p. 1009-14.

Groves, M.J., *Parenteral Drug Delivery Systems*, in *Encyclopedia of Controlled Drug Delivery*, Mathoiwitz, E, Editor. 1999, John Wiley and Sons, Inc.: New York.

Gutman RL, Peacock G, Lu DR. *J Control Release.* 2000 Mar 1;65(1-2):31-41.

H

Haag R., *Angew. Chem. Int. Ed.*, 43, 278-82, 2004.

Haas, T. L., Milkiewicz, M., Davis, S. J., Zhou, A. L., Egginton, S., Brown, M. D., Madri, J. A., Hudlicka, O. *Am J Physiol Heart Circ Physiol* 279: H1540-H1547, 2000

Hanahan, D. *Science:Cell Biology*, 1997, 277(5322): p. 48-50.

Harris, J.M., *Poly(Ethylene Glycol) Chemistry, Biotechnical and Biomedical Applications.* 1992, New York: Plenum Press.

Heller J, Pangburn SH, Penhale DWH, "Use of Bioerodible Polymers in Self-Regulated Drug Delivery Systems," in *Controlled-Release Technology, Pharmaceutical Applications*, Lee PI, and Good WR (eds), Washington DC, ACS Symposium Series, pp 172–187, 1987.

Heller J, *J Controlled Release*, 2:167–177, 1985.

Heller J, Barr J, Ng SY, Shen HR, Schwach-Abdellaoui K, Emmahl S, Rothen-Weinhold A, Gurny R. *Eur J Pharm Biopharm.* 2000 Jul;50(1):121-8.

Henson, PAM *J Pathol*, 1980, 101: p. 494-511.

Hepp, K.D *Diabetologia*, 1994, 37(Suppl 2): p. S108-S111.

Hermanson, G.T., *Bioconjugate Techniques.* 1st ed. 1996: Acedemic Press. 785.

Hertzog, B.A., Thanos, C., Sandor, M., Raman, V., Edelman, E.R., *Cardiovascular Drug Delivery Systems*, in *Encyclopedia of Controlled Drug Delivery*, Mathoiwitz, E, Editor. 1999, John Wiley and Sons, Inc.: New York.

Horák, D., Boháček, J., Šubrt, M., *J. of Polym. Sci. Part A. Polymer chemistry* 2000, vol. 38, n°7, pp. 1161-1171

Hoshi K., Ejiri S., Ozawa H., *J. Bone Miner. Res.* 16 (2001) 289.

Hsieh P.C.H., Davis M.E., Gannon J., Mac-Gillivray C., Lee R.T. (2006) *Journal of Clinical Investig. Ann Arbor*, 116 (1):237-248.

Hubbel, J. *Ann NY Acad Sci*, 1992, 665: p. 253-8.

Hughes G.A., *Nanomedicine: Nanotechnology, Biology, and Medicine* 1, 22 (2005).

I

Ingber D.E., Folkman J. (1989) *J. Cell Bio*, 109: 317-330.

Ishihara K, Kobayashi M, Shinohara I, *Makromol Chem Rapid Commun*, 4:327, 1983.

Islas-Blancas M.E., Cervantes-UC J.M., Vargas-Coronado R., Cauich-Rodroquez J.V., Vera-Graziano R., Martinez-Richa A., *J. Biomat. Sci. Polym. E* 12 (2001)

Ito, K., Uchida, K., Kitano, T., Yamada, E., Matsumoto, T., *Polymer Journal*, Vol. 17, No. 6, pp. 761-766 (1985)

J

Jain R, Shah NH, Malick AW, Rhodes CT. *Drug Dev Ind Pharm.* 1998 Aug;24(8):703-27.

Jones David, *Queen's University, Belfast*, ISBN 1-85957-479-3, Published 2004, p. 124, *Pharmaceutical Applications of Polymers for Drug Delivery*

Jung A., Bisaz S., Fleisch H., *Calcified Tissue Res.* 11 (1973) 269.

K

- Kaga M, The in vitro cytotoxicity of eluates from dentin bonding resins and their effect on tyrosine phosphorylation of L929 cells. *Dental Materials*, 2001, 17 (4), 333-339
- Kang, H.W., Tabata, Y. Ikada, Y. *Biomaterials*, 1999, 20(14): p. 1339-1344.
- Kaparissides C., Alexandridou S., Kotti K., Chaitidou S., DOI : 10.2240/azojono0111, <http://www.azonano.com/oars.asp>, 2006
- Kataoka, K., Harada, A., Nagasaki, Y., *Advanced Drug Delivery Reviews* 2001, Vol. 47, Iss. 1, 113-131
- Katime, I., Sáez, V., Hernández, E., *Polym. Bull.* 2005, 55, 403–409
- Kefalides, Paul T. "New Methods for Drug Delivery." *Annals of Internal Medicine* June 15, 1998 www.acponline.org/journals/annals/15jun98/currdrug. 9 July 2001.
- Kier, L.B., Cheng, C.-K. Testa, B. *Future generation computer systems*, 1999, 16(273-289).
- Kim SW, Bae YH, Okano T. *Pharm Res.* 1992 Mar;9(3):283-90.
- Kliment, K., Stol, M., Fahoun, K., Stockar, B. *J Bio Mat Res*, 1968, 2: p. 237-243.
- Klomp, G.F., Hashiguchi, H., Ursell, P.C., Takeda, Y., Taguchi, T., Dobelle, W.H. *J Bio Mat Res*, 1983, 17: p. 865-871.
- Knatterud, G. Fisher, M. *ASAIO Transactions*, 1988, 34(2): p. 148-149.
- Kokubo, T., Kim, H.M., Kawashita, M., *Biomaterials* 24 (2003) 2161.
- Kokubo T., Kushitani H., Sakka S., Kitsugi T., Yamamuro T., *J. Biomed. Mater. Res.*, 24, 721-734 (1990).
- Kokubo T., Ito S., Huang Z.T., Hayashi T., Sakka S., Kitsugi T., Yamamuro T., *J. Biomed. Mater. Res.*, 24, 331-343 (1990).
- Kokubo, T., Takadama, H., *Biomaterials* 27 (2006) 2907.
- Konobil, E. *Recent Progr Horm Res*, 1980, 36: p. 53-88.
- Kopecek J., *European Journal of Pharmaceutical Sciences*, 20, 1-16, 2003.
- Kortesuo, P., *Academic Dissertation, Department of Pharmacy - University of Helsinki*, 2001.
- Kost J, Horbett TA, Ratner BD, et al., *J Biomed Mater Res*, 19:1117–1133, 1985.
- Kost J., Langer R., (2001) *Advanced Drug Delivery Reviews*, 46:125-148.
- Krukowski M., Simmons D.J., Summerfield A., Osdoby P., *J. Bone Miner. Res.* 3 (1988) 165.
- Krukowski M., Shively R.A., Osdoby P., Eppley B.L., *J. Oral Maxil. Surg.* 48 (1990) 468.
- Krukowski M., Snyders R.V.L., Eppley B.L., Simmons D.J., *Clin. Orthop. Relat. R.* 298 (1994) 266.
- Kydonieus A., *Treatise on Controlled Drug Delivery: Fundamentals, Optimization, Applications*. New York, NY: CRC Press: 1992.
- Kwon, G., Forrest, M.L., *Drug Development Research* 2006, Vol. 67 Iss. 1, 15 - 22

L

- Labbare D. (2001) *Trends Biomater. Artif. Organs*, 15 (1):1-3.
- Langer R. Bioavailability of Macromolecular Drugs and Its Control. *Controlled Drug Bioavailability*. 1985; 3: 307.
- Langer R.A, *J Pharm Sci.* 1997; 86(12): 1464.
- Langer R., *J Pharm Sci.* 1997; 86(1):1464.
- Langer R. *Nature.* 1998 Apr 30;392(6679 Suppl):5-10.
- Langer, R. Peppas, N.A. *J Macromol Sci, Rev Macromol Chem Phys*, 1983, C23(1): p. 61-126.
- Lavik EB, Klassen H, Warfvinge K, Langer R, Young MJ. *Biomaterials*. 2005 26(16): 3187-96.
- Leach, K., *Cancer, Drug Delivery to Treat - Local & Systemic*, in *Encyclopedia of Controlled Drug Delivery*, Mathoiwitz, E, Editor. 1999, John Wiley and Sons, Inc.: New York.
- Lieb, W.R. Stein, W.D. *Nature New Biol*, 1971, 234: p. 220-222.
- Lipsky, M.H., *J Bio Mat Res*, 1989, 23: p. 1441-1452.
- Liu D., Ichikawa H., Cui F. , Fukumori Y. (2006) *International Journal of Pharmaceutics*, 307:300-307.
- Liu, Q., Hedberg, E.L., Liu, Z., Bahulekar, R., Meszlenyi, R.K., Mikos, A.G. *Biomaterials*, 2000, 21(21): p.2163-2169.
- Liu Q., de Wijn J.R., van Blitterswijk C.A., *Biomaterials* 18 (1997) 1253.
- Lloyd, P. G., Prior, B. M., Yang, H. T., & Terjung, R. L. *Am J Physiol Heart Circ Physiol* 284: 1668-78, 2003.

-
- Low, L., Seetharaman, S., He, K., Madou, M.J. *Sensors and Actuators B*, 2000, 67: p. 149-160.
Lou, X., Dalton, P.D. Chirila, T.V. *J Mat Sci Mat Med*, 2000, 11(5): p. 319-325.
Lowman AM, Peppas NA, *Polym Preprints*, 38(2):566–567, 1997.
Lowman, A.M. Peppas, N.A., *Hydrogels*, in *Encyclopedia of Controlled Drug Delivery*, Mathoiwitz, E, Editor. 1999, John Wiley and Sons, Inc.: New York.
Lu Y., Chen S.C., *Adv. Drug Delivery Rev.* 56, 1621 (2004).

M

- Maeda H., *Adv. Drug Delivery Rev.* 6 (2), 181 (1991).
Maeda H., Wu J., Sawa T., Matsumura Y., Hori K., (2000) *Journal of Controlled Release*, 65:271.
Malech, H. and Gallin, J. *N Engl J Med*, 1987, 317: p. 687-694.
Manabe T., Okino H., Maeyama R., Mizumoto K., Nagai E., Tanaka M., Matsuda T., *J. Control. Rel.*, 100, 317-30, 2004.
Mann, B.K., Gobin, A.S., Tsai, A.T., Schmedlen, R.H., West, J.L. *Biomaterials*, 2001, 22(22): p. 3045-51.
Makonkawkeyoon, S., Limson-Pobre, R.N.R., Moreira, A.L., Schauf, V., Kaplan, G., *Proc. Natl. Acad. Sci. USA* 1993, vol. 90, pp. 5974-5978
Markus, M., Boehm, D. Schmick, *Mathematical Biosciences*, 1999, 156: p. 191-206.
Matsuda, T. Kurumantani, H. *ASAIIO Trans*, 1990, 36(M565-8).
Mikos AG, Murphy RM, Bernstein H, et al. (eds), *Biomaterials for Drug and Cell Delivery*, Pittsburgh, Materials Research Society, 1994.
Moad, G., Rizzardo, E., Thang, S.H., *Polymer* 49 (2008) 1079.
Mort, M., *Modern Drug Discovery*, 2000, 3(3) 30–32, 34.
Muller-Goymann C.C., *European Journal of Pharmaceutics and Biopharmaceutics*, 58, 343-56, 2004.
Murphy, W.L., Kohn, D.H. Mooney, D.J. *J Biomed Mater Res*, 2000, 50(1): p. 50-58.

N

- Nahar M., Dutta T., Murugesan S., Asthana A., Mishra D., Rajkumar V., Tare M., Jain N.K., *Critical Reviews in Therapeutic Drug Carrier Systems* 23, nr. 4, 2006, p. 259-318
Nasser-Eddine M., Delaite C., Hurtrez G., Dumas P., *Eur. Polym. J.* 41, 2005, p. 313–318
Nguyen, M., Akrell, J., Jackson, C.J. *Inter J Biochem cell Bio*, 2001, 33: p. 960-970.
Niculescu-Duvaz I., Springer C.J., *Advanced Drug Delivery Reviews*, 26, 151-72, 1997.
Nyangoga, H., **Zecheru, T.**, Filmon, R., Baslé, M.F., Cincu, C., Chappard, D., *J. of Biomed. Mater. Res.: Part B - Applied Biomaterials*, in press;
Nyangoga, H., **Zecheru, T.**, Filmon, R., Cincu, C., Chappard, D., *Use of pHEMA microbeads with human endothelial cells*, International Conference on Chemistry and Chemical Engineering RICCE 15, 19-22 September 2007, Sinaia, Romania.
Nuttelmana C.R., Benoit D.S.W., Tripodia M.C., Anseth K.S., *Biomaterials* 27 (2006) 1377.

O

- Oh, S.H. and Jhon, M.S. *J Polym Sci Polym Chem*, 1989, 27: p. 1731-1739.
Okada H, Toguchi H. *Crit Rev Ther Drug Carrier Syst.* 1995;12(1):1-99.
Okamura, M., Yamanobe, T., Arai, T., Uchara, H., Komoto, T., Hosoi, S., Kumazaki, T., *J. of Molec. Str.* 2002, 602-603, 17-28
Oxley, H., Corkhill, P.H., Fitton, J.H., Tighe, B.J. *Biomaterials*, 1993, 14: p. 1064-72.
Ozin G.A., Varaksa N., Coombs N., Davies J.E., Perovic D.D., Ziliox M., *J. Mater. Chem.* 7 (1997) 1601.

P

- Packhaeuser C.B., Schnieders J., Oster C.G., Kissel T., *European Journal of Pharmaceutics and Biopharmaceutics*, 58, 445-55, 2004.
Padera, R.F. Colton, C.K. *Biomaterials*, 1996, 17: p. 277-284.
Park, J.B., *Biomaterials: An Introduction*. 1979, New York: Plenum Press.

-
- Park K, Shalaby WSW, Park H, Biodegradable Hydrogels for Drug Delivery, Lancaster, PA, Technomic, 1993.
- Paschalakis P., Vynios D.H., Tsiganos C.P., Koutsoukos P.G., Inhibition of hydroxyapatite growth in vitro by glycosaminoglycans. The effect of size, sulphation and primary structure, Water soluble polymers, Amjad Plenum Press, New York, 1998.
- Patrick B. O'Donnell James W. McGinity, Advanced Drug Delivery Reviews 28(1) (1997) pp. 25-42.
- Payne LG, Jenkins SA, Andrianov A, Roberts BE. Pharm Biotechnol. 1995;6:473-93.
- Peppas NA (ed), Hydrogels in Medicine and Pharmacy, Boca Raton, FL, CRC Press, 1986.
- Peppas NA, Sahlin JJ. Biomaterials. 1996 Aug;17(16):1553-61.
- Peppas, N., Hydrogels in Medicine and Pharmacy, Vol. I: Fundamentals. 1986, Boca Raton: CRS Press. 180.
- Peracchia, M.T., Harnisch, S., Pinto-Alphandary, H., Gulik, A., Dedieu, J.C., Desmaele, D., d'Angelo, J., Mueller, R.H., Couvreur, P. Biomaterials, 1999, 20: p. 1269-1275.
- Prior, B. M., Yang, H. T., & Terjung, R. L. J App Physiol 97: 1119-28, 2004

R

- Raggio C.L., Boyan B.D., Boskey A.L., J. Bone Miner. Res. 1 (1986) 409.
- Ratner BD, Hoffman AS, Schoen FJ, et al. (eds), Biomaterials Science: An Introduction to Materials in Medicine, San Diego, Academic Press, 1997.
- Reed M.L., Wu C., Kneller J., Watkins S., Vorp D.A., Nadeem A., Weiss LE., Rebello K., Mescher M., Smith A.J.C., Rosenblum W., Feldman M.D., J. Pharm. Sci. 87, 1387 (1998).
- Reverchon E., Schiavo Rappo E., Cardea S. (2006) Polymer Engineering and Science Brookfield Center, 46 (2):188-197.
- Robinson JR, and Lee VHL (eds), Controlled Drug Delivery: Fundamentals and Applications (2nd ed), New York, Marcel Dekker, 1987.
- Ronel, S.H., D'Andrea, M.J., Hashiguchi, H., Klomp, G.F., Dobbelle, W.H. J Bio Mat Res, 1983, 17: p. 855-864.
- Rosengren, A., Danielsen, N. Bjursten, L.MJ Bio Mat Res, 1999, 46(4): p. 458-464.
- Rösler A., Vandermeulen G. W. M., Klok H.-A., Advanced Drug Delivery Reviews, 53, 95-108, 2001.
- Rossant, J. Howard, L. Ann Rev Cell Dev Biol, 2002, 18: p. 541-73.

S

- Saito N., Murakami N., Takahashi J., Horiuchi H., Ota H., Kato H., Okada T., Nozaki K., Takaoka K., Adv. Drug Deliv. Rev. 57, 1037 (2005).
- Saltzman, W.M., Cell Interactions with Polymers, in Principles of Tissue Engineering, Lanza, R, Editor. 1997, RG Landes Company: Austin, TX. p.228-46.
- Santiago, J.V., White, N.H. Skor, D.A., Mechanical Devices for Insulin Delivery, in Recent Advances in Diabetes, Natrass, M and Santiago, JV, Editors. 1984, Churchill Livingstone: Edinburgh. p. 145-63.
- Santini Jr, J.T., Richards A.C., Scheidt R., Cima M.J. Langer R., Angew. Chem. Int. Ed., 39, 2396-407, 2000.
- Saralidze K., Aldenhoff Y.B.J., Knetsch M.L.W., Koole L.H., iomacromol. 4, 793 (2003).
- Saudek, C.D. Diabetes Care, 1993, 16(Duppl 3): p. 122-132.
- Saudek, C.D. J Clin Endocrinol Metab North Amer, 1997, 26: p. 599-610.
- Scavini, M., Galli, L., Reich, S., Eaton, R.P., Charles, M.A., Dunn, F.L. Diabetes Care, 1997, 20: p. 610-613.
- Scharp, D.W., Mason, N.S. Sparks, R.E. World J. Surg., 1984, 8: p. 221-229.
- Schoen F.J., Harasaki K.M., Kim H.C., Anderson H.C., Levy R.J., J. Biomed. Mater. Res. 22 (1988) 11.
- Selam, J.L., Micossi, P., Dunn, F.L., Nathan, D.M. Diabetes Care, 1992, 15: p. 877-885.
- Shalaby SW, Ikada Y, Langer R, et al. (eds), Polymers of Biological and Biomedical Significance, Washington DC, ACS Symposium Series, 1994.
- Sharma S., Nijdam A.J., Sinha P.M., Walczak R.J., Liu X., Cheng M.M.-C., Ferrari M., Expert Opinion on Drug Delivery 3, nr. 3, 2006, p. 379-394
- Shieh L, Tamada J, Chen I, Pang J, Domb A, Langer R. J. Biomed. Mater. Res., 28, 1465-1475, 1994.

Shive MS, Anderson JM. *Adv. Drug Del. Rev.* 28, 5-24,1997.

Shwarkawy, A.A., Klitzman, B., Truskey, G.A., Reichert, W.M, *J Biomed Mater Res*, 1997, 37: p. 401-12.

Shwarkawy, A.A., Klitzman, B., Truskey, G.A., Reichert, W.M. *J Biomed Mater Res*, 1998, 40: p. 586-597.

Shwarkawy, A.A., Klitzman, B., Truskey, G.A., Reichert, W.M. *J Biomed Mater Res*, 1998, 40: p. 598-605.

Sieminski, A.L. Gooch, K.J. *Biomaterials*, 2000, 21: p. 2233-2241.

Siepmann J., Goepferich A. (2001) *Advanced Drug Delivery Reviews*, 48:229-247.

Simpson, B.J. *Biomed Eng*, 1969, 4: p.65-68.

Singhal, S., Mehta, J., Desikan, R., Ayers, D., Roberson, P., Eddlemon, P., Munshi, N., Anaissie, E., Wilson, C., Dhodapkar, M., Zeldis, J., Barlogie, B., *The New England Journal of Medicine* 1999, vol. 341, no. 21, 1565-1571

Sinha VR, Khosla L. *Drug Dev Ind Pharm.* 1998 Dec;24(12):1129-38.

Sood A. Panchagnula R., *Chemical Reviews*, 101, 3275-303, 2000.

Soppimath K.S., Aminabhavi T.M., Kulkarni A.R., Rudzinski W.E., *Journal of Controlled Release*, 70, 1-20, 2001.

Stancu I.C., Filmon R., Cincu C., Marculescu B., Zaharia C., Tourmen Y., Basle M.F., Chappard D., *Biomaterials* 25 (2004) 205.

Stancu I.C., Filmon R., Grizon F., Zaharia C., Cincu C., Basle M.F., Chappard D., *J. Biomed. Mater. Res.* 69A (2004) 584.

Stryer, L., *Biochemistry* 4th Ed. 1995, New York: W. H. Freeman and Company.

Suwanprateeb J., Turner S., Bonfield W., *J. Mater. Sci.-Mater.M.* 8 (1997) 469.

Suchanek W., Yoshimura M., *J. Mater. Res.* 13 (1998) 94.

Suzuki S., Grøndahl L., Leavesley D., Wentrup-Byrne E., *E., Biomater.* 26, 2005, p. 5303–5312

Szycher M., *Prosthetic and biomedical devices, Encyclopedia of Chemical Technology. Kirk-Othmer* 4th Ed., 1997, 351.

T

Takahashi K., Miyamori S., Uyama H., Kobayashi S., *J. Pol. Sci., Part A: Polymer Chemistry*, Vol. 34, nr. 2, 1996, p. 175-182

Talia, D., Sloot, P. "Cellular Automata: Promise and Prospects in Computational Science". *Future generation computer systems*, 1999, 16: p. vvii.

Tanguay JF, Zidar JP, Phillips HR 3rd, Stack RS. *Cardiol Clin.* 1994 Nov;12(4):699-713.

Termine J.D., Belcourt A.B., Conn K.M., *J. Biol. Chem.* 256 (1981) 10403.

Thomson, R.C., Mikos, A.G., Beahm, E., Lemon, J.C., Satterfield, W.C. *Biomaterials*, 1999, 20(21): p. 2007-18.

Thurston, G. *Annals of Biomedical Engineering*, 2000, 28: p. S72-73.

Tierney, M.J. Martin, C.R. *J Electrochem Soc*, 1990, 137(12): p. 3789-3793.

Tierney, M.J. Martin, C.R. *J Electrochem Soc*, 1990, 137: p. 2005-2006.

Torchilin V.P., *Journal of Controlled Release*, 73, 137-72, 2001.

Tsuchiya, T., *J. of Biomater. Appl.* 1994, 9 (2), 138-157

U

Ulbrich K, Pechar M, Strohalm J, Subr V, Rihova B. *Ann N Y Acad Sci.* 1997 Dec 31; 831:47-56.

V

Van de Belt, H., Neut, D., Schenk, W., Van Horn, J.R., Van der Mei, H.C., Busscher, H.J., *Acta Orthop. Scand.* 2001; 72 (6): 557–571

Vandermeulen G. W. M., Klok H-A., *Macromolecular Bioscience*, 4, 383-98, 2003.

Vasir J. K., Tambwekar K., Garg S *International Journal of Pharmaceutics*, 255, 13-32, 2003.

Vert M, Li S, Garreau H, *J Controlled Release*, 16:15–26, 1991.

Vert M, Schwach G, Engel R, Coudane J. *J Control Release.* 1998 Apr 30;53(1-3):85-92.

Voldrich, Z., Tomanek, Z., Vacik, J., Kopecek, J. *J Bio Mat Res*, 1975, 9: p. 675-685.

W

- Wake, M.C., Mikos, A.G., Sarakinos, G., Vacanti, J.P., Langer, R. *Cell Transplantation*, 1995, 4(3): p. 275-279.
- Wang, W. *Inter J Pharm*, 1999, 185: p. 129-188.
- Wang, Y., Yang, Z., Xie, H., Li, S. *Journal of Biomedical Engineering*, 2001, 285(1-3): p. 116-22.
- Weng J., Wang M., Chen J., *Biomaterials* 23 (2002) 2623.
- Werner A., Grunder W., *Magn.Reson. Med.* 41 (1999) 43.
- Wheeler JC, Woods JA, Cox MJ, Cantrell RW, Watkins FH, Edlich RF. *J Long Term Eff Med Implants.* 1996;6(3-4):207-17.
- Winterhalter M., Hilty C., Bezrukov S. M., Nardin C., Meier W., Fournier D *Talanta*, 55, 965-71, 2001.
- Wolfram, S., *A New Kind of Science*. 2002: Wolfram Media, Inc.
- Wuthier R.E., Bisaz S., Russel R.G.G., *Calcified Tissue Res.* 10 (1972) 198.
- Wyatt TL, Saltzman WM. *Pharm Biotechnol.* 1997;10:119-37.

Y

- York P., *Proceedings of Chemical aspects of drug delivery systems*, 2005, p. 1-4

Z

- Zaharia, C., **Zecheru, T.**, Moreau, M.F., Pascaretti-Grizon, F., Mabileau, G., Marculescu, B., Filmon, R., Cincu, C., Staikos, G., Chappard, D., *Acta Biomaterialia, In Press 2008*
- Zecheru T.**, Salageanu A., Cincu C., Chappard D., Zerroukhi A., *U.P.B. Sci. Bull., Ser. B*, 70 (2008) 45.
- Zecheru, T.**, Zaharia, C., Rusen, E., Miculescu, F., Cincu, C., *Synthesis, Physico-Chemical Properties and Biological Evaluation of two new copolymer systems*, World Biomaterials Congress 28 May – 01 June 2008, Amsterdam, The Netherlands
- Zecheru T.**, Zaharia C., Salageanu A., Tucureanu C., Rusen E., Marculescu B., Rotariu T., Cincu C., *J. Optoel. Adv. Mater.* 9 (7), 2007.
- Zecheru, T.**, Spulber, C., Zecheru, C.C., Chereches, T., *Advanced technologies and concepts used in diagnosis and treatment*, Fall session 2007 of Romanian Scientists Association (AOSR), 15-16 October, Constanta, Romania.
- Zecheru, T.**, Zaharia, C., Rusen, E., Miculescu, F., Mărculescu, B., Cincu, C., *Synthesis, characterisation and bioavailability of a new copolymer system*, International Conference on Chemistry and Chemical Engineering RICCE 15, 19-22 September 2007, Sinaia, Romania.
- Zecheru T.**, Zaharia C., Mabileau G., Chappard D., Cincu C., *J. Optoel. Adv. Mater.* 8 (3), 2006, p. 1312 – 1316
- Zecheru, T.**, Zaharia, C., Salageanu, A., Tucureanu, C., Rusen, E., Marculescu, B., Rotariu, T., Cincu, C., *Polymeric biocompatible structures for controlled drug release*, 2nd International Conference on Biomaterials and Medical Devices - BiomMedD'06, 9-11 November 2006, Iasi, Romania.
- ZECHERU, T.**, ZAHARIA, C., MABILLEAU, G., CHAPPARD, D., CINCU, C., *New micron ad nano-sized polymer particles for controlled drug release*, The 4th National Conference „New Research Trends in Material Science ARM-4” – Proceedings, Volum II, September 4-6 2005, Constanta, Romania.
- Zhu G, Schwendeman SP. *Pharm Res.* 2000 Mar;17(3):351-7.
- Zhu G, Mallery SR, Schwendeman SP. *Nat Biotechnol* 2000 Jan;18(1):52-7.
- Ziaie B., Baldi A., Lei M., Gu Y., Siegel R.A., *Advanced Drug Delivery Reviews*, 56, 145-72, 2004.

Internet sites

- www.biomed.brown.edu/.../Pages/emergingq.htm
- http://chsfpc5.chem.ncsu.edu/~franzen/CH795I/lectures/drug_delivery/sld001.htm
- www.eorthopod.com
- <http://www.iam.u-tokyo.ac.jp/chem/theme/thalidomide.jpg>
- www.thalomid.com

LIST OF FIGURES

- Fig. 1-1. Conventional and ideal drug release profiles.
- Fig. 1-2. Powdered drugs encapsulated
- Fig. 1-3. Example of droplets formed by coacervation
- Fig. 1-4. Possible drug release mechanisms for polymeric drug delivery
- Fig. 1-5. Difference between a porous microparticle and a microcapsule
- Fig. 1-6. Some different aggregation morphologies found in low molecular amphiphiles.
- Fig. 1-7. Different types of homopolymer architecture.
- Fig. 1-8. Highly branched dendrimers
- Fig. 1-9. Linear copolymers, statistical or random, alternate and block-copolymers
- Fig. 1-10. Different architectures of block-copolymers.
- Fig. 1-11. Phase diagram and the corresponding self-assembled structures for block-copolymers in bulk.
- Fig. 1-12. Morphologies of block-copolymer aggregates found in aqueous media.
- Fig. 1-13. Use of surface tension measurement to determine the CMC
- Fig. 1-14. a) unimers in solution, di- and triblock respectively b) star and crew cut micelles for a diblock-copolymer, and normal (ABA) and flower-like (BAB) micelles for a symmetric triblock-copolymer, c) vesicle formation for a diblock and triblock-copolymer respectively.
- Fig. 1-15. Constitution of some containers and the multiple modifications possible.
- Fig. 1-16. Growth of a capillary during angiogenesis
- Fig. 1-17. Endothelial cell response to VEGF and ANG1/ANG2 during vasculogenesis and angiogenesis
- Fig. 1-18. Classic foreign body response typically ends with the surrounding of an implant with a dense fibrous layer called the fibrous capsule
- Fig. 1-19. Vascularised tissue response to implants with varying pore sizes
- Fig. 1-20. Mechanism of drug recognition
- Fig. 1-21. (A) Induced Swelling - the result is ionization, swelling, and release of drug, peptide, or protein; (B) Loss of Effective Cross-links - effective cross-links are reversibly lost and release occurs.
- Fig. 1-22. Different administration routes.
- Fig. 1-23. Pharmaceutical carriers
- Fig. 1-24. Mechanisms followed by block-copolymers
- Fig. 1-25. Drug encapsulation in liposomes
- Fig. 1-26. Different strategies for immobilization onto surfaces.
- Fig. 1-27. Schematic representation of macroporous PHEMA hydrogel sponges.
- Fig. 3-1. Chemical synthesis of TIPA monomer
- Fig. 3-2. Chemical structure of p(MMA-co-TIPA) copolymer
- Fig. 3-3. FT-IR spectrum of TIPA monomer

-
- Fig. 3-4. FT-IR spectra of p(MMA-co-TIPA) with different molar ratios
- Fig. 3-5. SEM microphotographs of p(MMA-co-TIPA) copolymers obtained.
- Fig. 3-6. EDX of p(MMA-co-TIPA) copolymers obtained.
- Fig. 3-7. SEM microphotographs of p(MMA-co-TIPA) copolymers obtained.
- Fig. 3-8. Composition diagram of the binary system MMA-TIPA
- Fig. 3-9. Feed composition and copolymer compositions versus conversion
- Fig. 3-10. Conversion versus time for the binary system MMA-TIPA
- Fig. 3-11. Copolymerisation initial rate versus feed composition
- Fig. 3-12. SEM microphotographs of p(MMA-co-TIPA) copolymers incubated in 1x SBF.
- Fig. 3-13. EDX of p(MMA-co-TIPA) copolymers incubated in 1x SBF for 2 weeks.
- Fig. 3-14. Microscopic image of L929 cells in culture after MTT adding.
- Fig. 4-1. Chemical reactions for GuaMA synthesis.
- Fig. 4-2. Chemical structures of the comonomers used: a) HEMA; b) MOEP, and c) GuaMA.
- Fig. 4-3. Chemical structure of ethyl eosin.
- Fig. 4-4. Installation used for suspension polymerisation
- Fig. 4-5. SEM for pHEMA obtained using: a) pBu and 40/60 toluene/2-butanol ratio; b) pBu and 35/65 toluene/2-butanol ratio; c) pBuSt 901 and 40/60 toluene/2-butanol ratio; d) pBuSt 902 and 40/60 toluene/2-butanol ratio; e) pBuSt 905 and 42.5/57.5 toluene/2-butanol ratio; f) pBuSt 905 and 45/55 toluene/2-butanol ratio.
- Fig. 4-6. SEM for p(HEMA-co-MOEP) 5% (left side) and 10% (right side) obtained using: a) pBu and 40/60 toluene/2-butanol ratio; b) pBuSt 905 and 42.5/57.5 toluene/2-butanol ratio; c) pBuSt 905 and 45/55 toluene/2-butanol ratio.
- Fig. 4-7. SEM for p(HEMA-co-GuaMA) 5% (left side) and 10% (right side) obtained using: a) pBu and 40/60 toluene/butanol ratio; b) pBuSt 902 and 40/60 toluene/butanol ratio; c) pBuSt 905 and 45/55 toluene/butanol ratio.
- Fig. 4-8. Microbeads average diameter (μm) versus toluene ratio in the mixture toluene-2-butanol for: a) pHEMA; b) p(HEMA-co-MOEP5%); c) p(HEMA-co-MOEP10%); d) p(HEMA-co-GuaMA5%); e) p(HEMA-co-GuaMA10%).
- Fig. 4-9. Swelling rate of p(HEMA-co-MOEP10%).
- Fig. 4-10. FOM appearance for microbeads containing ethyl eosin: a) pHEMA; b) p(HEMA-co-MOEP); c) p(HEMA-co-GuaMA).
- Fig. 4-11. Microscopic image of L929 cells in culture, in the absence of samples and before the addition of MTT
- Fig. 4-12. Microscopic image of L929 cell line in culture, incubated for 24h with: a) p(HEMA-co-MOEP10%); b) p(HEMA-co-GuaMA10%).
- Fig. 4-13. Microscopic image of L929 cells in culture after incubation for 24h in the presence of: a) p(HEMA-co-MOEP10%); b) p(HEMA-co-GuaMA10%), after the addition of MTT.
- Fig. 4-14. Microbeads injected into rats and distributed within organs after 24h: a) brain; b) lung; c),d) spleen.

-
- Fig. 5-1. Polymers obtained: a) p(HEMA); b) p(HEMA-co-AA); c) p(HEMA-co-MMA); d) p(HEMA-co-MMA-co-AA).
- Fig. 5-2. Average swelling rate (g/g) versus time (min.) for p(HEMA-co-MMA) 90:10 and 80:20 molar ratio in the feed.
- Fig. 5-3. Micro-beads distribution of: a) p(HEMA); and p(HEMA-co-AA) in molar ratios: b) HEMA:AA=95:5; c) HEMA:AA=90:10; d) HEMA:AA=85:15.
- Fig. 5-4. Micro-beads distribution of p(HEMA-co-MMA) in molar ratios: a) HEMA:MMA=95:5; b) HEMA:MMA=90:10; c) HEMA:MMA=85:15; d) HEMA:MMA=80:20; e) HEMA:MMA=70:30; f) HEMA:MMA=60:40.
- Fig. 5-5. Micro-beads distribution of p(HEMA-co-MMA-co-AA) in molar ratios: a) HEMA:MMA:AA=75:20:5; b) HEMA:MMA:AA=70:20:10; c) HEMA:MMA:AA=65:20:15; d) HEMA:MMA:AA=60:20:20.
- Fig. 5-6. Murine fibroblast L929 cell line: a) Blank 1; b) Blank 2.
- Fig. 5-7. Murine fibroblast L929 cell line with: a) p(HEMA-co-MMA5%); b) p(HEMA-co-MMA10%); c) p(HEMA-co-MMA15%); d) p(HEMA-co-MMA20%); e) p(HEMA-co-AA5%); f) p(HEMA-co-AA15%); g) p(HEMA-co-MMA20%-co-AA15%); h) p(HEMA-co-MMA20%-co-AA10%); i) p(HEMA-co-MMA20%-co-AA20%).
- Fig. 6-1. Chemical structure of Nile Red
- Fig. 6-2. Thalidomide's Various Effects in Myeloma
- Fig. 6-3. Pharmacogenic utilities and behaviour of thalidomide
- Fig. 6-4. Chemical structures of Thalidomide and consequences of stereoisomerism
- Fig. 6-5. Chemical structures of the monomers: a) HEMA, b) DADMAC, c) GlyMA, d) MAA, e) MOEAA, f) MOETAC, g) THFMA.
- Fig. 6-6. Polymerisation reactor
- Fig. 6-7. Installation for bulk polymerisation
- Fig. 6-8. Confocal fluorescence microscope
- Fig. 6-9. Fluorescence microphotographs: a) GlyMA (AIBN, 60-65°C), b) GlyMA (PBO, 70-75°C), c) MOEAA (AIBN, 60-65°C), d) MOEAA (PBO, 70-75°C), e) MOETAC (PBO, 70-75°C), f) DMA (PBO, 70-75°C), g) DADMAC (PBO, 70-75°C).
- Fig. 6-10. FOM for: a) p(HEMA-co-MOEAA); b) p(HEMA-co-DADMAC), microbeads stained with Nile Red, in two concentrations.
- Fig. 6-11. Bruker Vertex 70 spectrophotometer
- Fig. 6-12. Senterra microscope
- Fig. 6-13. Comparative FT-IR spectra of the copolymers obtained
- Fig. 6-14. Comparative FT-IR spectra of p(HEMA-co-MOEAA) and p(HEMA-co-MOEAA) loaded with thalidomide
- Fig. 6-15. Comparative Raman spectra of the copolymers obtained
- Fig. 6-16. Comparative Raman spectra of p(HEMA-co-MOEAA) and p(HEMA-co-MOEAA) loaded with Thalidomide

-
- Fig. 6-17. Evolution of the swelling degree versus time (for simplification, it was only mentioned the name of the comonomer)
- Fig. 6-18. Installation for microbeads homogenous turning – calcification tests.
- Fig. 6-19. Installation for pellets stirring – calcification tests.
- Fig. 6-20. SEM coupled with EDX apparatus
- Fig. 6-21. p(HEMA-co-DADMAC) microbeads before (a) and after (b) incubation in 1.5x SBF and pellets before (c) and after (d) incubation in 1.5x SBF.
- Fig. 6-22. p(HEMA-co-GlyMA) microbeads before (a) and after (b) incubation in 1.5x SBF and pellets before (c) and after (d) incubation in 1.5x SBF.
- Fig. 6-23. p(HEMA-co-MAA) microbeads before (a) and after (b) incubation in 1.5x SBF and pellets before (c) and after (d) incubation in 1.5x SBF.
- Fig. 6-24. p(HEMA-co-MOEAA) microbeads before (a) and after (b) incubation in 1.5x SBF, Nile Red-containing microbeads before (c) and after (d) incubation in 1.5x SBF, and pellets before (e) and after (f) incubation in 1.5x SBF.
- Fig. 6-25. p(HEMA-co-MOETAC) microbeads before (a) and after (b) incubation in 1.5x SBF and pellets before (c) and after (d) incubation in 1.5x SBF.
- Fig. 6-26. p(HEMA-co-THFMA) microbeads before (a) and after (b) incubation in 1.5x SBF and pellets before (c) and after (d) incubation in 1.5x SBF.
- Fig. 6-27. Microbeads of p(HEMA-co-MOEAA) loaded with thalidomide.
- Fig. 6-28. EDX graphs of the copolymers after incubation in 1.5x SBF: a) p(HEMA-co-DADMAC), b) p(HEMA-co-GlyMA), c) p(HEMA-co-MAA), d) p(HEMA-co-MOEAA), e) p(HEMA-co-MOETAC), f) p(HEMA-co-THFMA).
- Fig. 6-29. BD FACS Aria Flow Cytometer
- Fig. 6-30. Flow cytometry results for: a) p(HEMA-co-MOEAA) microbeads; b) p(HEMA-co-MOEAA) microbeads stained with Nile Red.
- Fig. 6-31. Flow cytometry results for: a) p(HEMA-co-DADMAC) microbeads; b) p(HEMA-co-DADMAC) microbeads stained with Nile Red.
- Fig. 6-32. Microscopic image of L929 cells in culture, in the absence of samples and before the addition of MTT
- Fig. 6-33. Microscopic image of L929 cell line in culture, incubated for 24h with: a) p(HEMA-co-GlyMA), b) p(HEMA-co-MOETAC).
- Fig. 6-34. Microscopic image of L929 cells in culture after incubation for 24h in the presence of: a) p(HEMA-co-GlyMA), b) p(HEMA-co-MOETAC), after the addition of MTT.
- Fig. 6-35. L929 cell line viability measured by MTT assay performed 4 h after transfection in the presence of polymeric samples (average \pm standard deviation).
- Fig. 6-36. p(HEMA-co-DADMAC) microbeads stained with Nile Red with EA.hy 926 cells: a) after 3 hours; b) after 6 hours.
- Fig. 6-37. p(HEMA-co-MOEAA) microbeads stained with Nile Red with EA.hy 926 cells: a) after 3 hours; b) after 6 hours.

Fig. 6-38. Rat anaesthesia before injecting the suspension of microbeads

Fig. 6-39. Injection of the suspension of microbeads

Fig. 6-40. Rat euthanasia for organs sampling

Fig. 6-41. Rat with metastatic tumours

Fig. 6-42. Organs sampling from a metastatic tumour rat

Fig. 6-43. Microbeads internalised into Sprague-Dawley rats (liver).

Fig. 7-1. Model for polymeric prodrugs proposed by Ringsdorf.

Fig. 7-2. Osteomyelitis

Fig. 7-3. Nafcillin sodium

Fig. 7-4. Swelling rate for the copolymers obtained: a) A1 to A6; b) D1 to D6.

Fig. 7-5. Microphotographs of the copolymers obtained (A1 to A6 and D1 to D6).

Fig. 7-6. Chemical structures of the copolymers obtained: a) p(HEMA-co-dDMA-co-AA); b) p(HEMA-co-dDMA-co-DEAEMA).

Fig. 7-7. Comparative spectra of copolymers obtained: a) A1 to A6; b) D1 to D6.

Fig. 7-8. The composition diagram for the binary system HEMA-AA

Fig. 7-9. Feed composition and copolymer compositions versus conversion

Fig. 7-10. Conversion versus time for HEMA-AA binary system

Fig. 7-11. Composition diagram of AA-dDMA binary system

Fig. 7-12. Feed composition and copolymer compositions versus conversion

Fig. 7-13. Conversion versus time for the AA-dDMA binary system

Fig. 7-14. Initial rate of copolymerisation versus feed composition

Fig. 7-15. Gibbs diagram

Fig. 7-16. Feed composition and copolymer compositions versus conversion

Fig. 7-17. Microscopic image of L929 cells in culture, after MTT addition – negative control

Fig. 7-18. Microscopic image of L929 cells in culture, after MTT addition – positive control, incubated with: a) A1, b) A2, c) A3, d) A4, e) A5, f) A6.

Fig. 7-19. Microscopic image of L929 cells in culture, after MTT addition – positive control, incubated with: a) D1, b) D2, c) D3, d) D4, e) D5, f) D6.

Fig. 7-20. Chemical reactions: a) esterification reaction; b) secondary reaction.

Fig. 7-21. Comparative spectra among A4, A5, A6 and A4N, A5N, A6N and NFPC

Fig. 7-22. SEM microphotographs of: a) A4N; b) A5N; c) A6N.

Fig. 7-23. UV-VIS spectrometer GBC Cintra 303

Fig. 7-24. Calibration of NFPC using UV spectrophotometry

Fig. 7-25. Release kinetics of NFPC from p(HEMA-co-dDMA-co-AA) microbeads.

Fig. 7-26. Fractional drug release versus time curves with different values of exponent n.

Fig. 7-27. Kinetic mechanism of the nafcillin release from: a) A4N; b) A5N; c) A6N.

LIST OF TABLES

- Table 1-1* Global markets for advanced drug delivery systems
- Table 3-1* Comonomer ratios used in the feed compositions for p(MMA-co-TIPA) synthesis
- Table 3-2* EDX results of p(MMA-co-TIPA) copolymers obtained: a) 95:5; b) 93:7; c) 90:10, molar ratios in the feed.
- Table 3-3* Feed compositions of the binary systems
- Table 3-4* Results of the elemental analysis for the binary system MMA-TIPA
- Table 3-5* Calculated molar ratios for the binary system MMA-TIPA
- Table 3-6* Composition of the SBF in ions concentration (mM) versus human body plasma
- Table 3-7* Results of EDX analysis for p(MMA-co-TIPA) copolymers incubated in 1x SBF for 2 weeks
- Table 4-1* Experimental data for the synthesis of pHEMA microbeads
- Table 4-2* Viability of the polymers obtained versus a blank control
- Table 5-1* Compositions of the monomers in the feed mixture
- Table 5-2* Elemental analysis results
- Table 5-3* Viability of the polymers obtained versus a blank control
- Table 6-1* Comonomers used in the study
- Table 6-2* Wavelengths of specific functional groups in the copolymers obtained
- Table 6-3* A and k values
- Table 6-4* Composition of the SBF in ions concentration (mM) versus human body plasma
- Table 6-5* Ca/P ratios obtained from EDX
- Table 6-6* Dosage results for Ca^{2+} and PO_4^{3-} ions
- Table 6-7* Protocol of *in vivo* injection
- Table 7-1* Molar composition of the initial mixture of monomers
- Table 7-2* k and A constants
- Table 7-3* Feed compositions of the binary systems
- Table 7-4* Non-solvents for the binary compositions studied
- Table 7-5* Results of the elemental analysis for the binary system HEMA-AA.
- Table 7-6* Results of the elemental analysis for the binary system AA-dDMA.
- Table 7-7* Results of the copolymerisation of HEMA-AA
- Table 7-8* Results of the copolymerisation of dDMA-AA
- Table 7-9* Compositions of the ternary system
- Table 7-10* Cellular mortality ratio, reported to negative witness (image analysis method)
- Table 7-11* Drug loading efficiency in the polymer samples
- Table 7-12* Calibration of the NFPC standard concentration
- Table 7-15* UV data for nafcillin release
- Table 7-16* Diffusional exponent and mechanism of diffusional release from cylindrical and spherical non-swellable and swellable controlled release systems

Curriculum vitae

Personal information

Surname(s) / First name	ZECHERU Teodora
Address	Str. Săvinești nr. 5, bl. B, ap. 62, Sector 4, 042025 Bucharest
Telephone	+40723.705.972
Fax	+4021.402.27.15
E-mail	teodora.zecheru@yahoo.com
Nationality	Romanian
Date of birth	05.06.1981

Work experience

2002-present	Researcher in over 30 research national projects and programs (RELANSIN, MENER, CEEX, CNCSIS, PN-II), an international project, EUREKA, E!3523 REC-PLASTICS, financial manager in a national CEEX project and director of a TD CNCSIS Grant for young scientists (2007-2008) . Evaluator in the National Program of Research-Development PN-II – Innovation.
2005-present	Teaching at University POLITEHNICA of Bucharest: - coordination of diploma projects - laboratory <i>Polymer Processing Technology</i> – 5th year, Macromolecular Compounds Technology - project <i>Polymer Processing Technology</i> – 5th year, Macromolecular Compounds Technology - laboratory <i>Materiaux Composites</i> – 3rd year, Chemical Engineering – French Department
July – August 2002	Practical stage at ARTECA Jilava, Bucharest
June – September 2001	Research stage in France “Découverte de l’entreprise” – Leonardo da Vinci Grant
April 2000 – April 2001	Inspector in human resources department – SC STRAJA Co. '98 SRL

Education and training

2004-2008	University POLITEHNICA of Bucharest, Faculty of Applied Chemistry and Materials Science, field: polymer chemistry and processing, biopolymers – PhD Student with frequency – Data of thesis defense: 10 October 2008 Publications: 1 book, 11 paperworks in ISI journals, 6 participations in international conferences (publication in volumes), 14 participations in national and international conferences (poster presentations), 3 paperworks published in journals with CNCSIS recognition
2006-present	University of Angers – Faculty of Medicine – cotutelle thesis
January – June 2007	Research program in France – SOCRATES-ERASMUS Grant, University of Angers, Faculty of Medicine
2007	University Centre of Continuous Formation (CUFCO), Angers, DELF diploma in French, international level B2
2006	British Council – English courses, level 5A (graduated with A/A), international level B2
2005	TEM Summer school, Earth Physics Institute, Măgurele, Romania

1999-2004	University POLITEHNICA of Bucharest – Faculty of Engineering in Foreign Languages (5 years) Field: Chemical Engineering – French Division, Diploma of chemical engineer – average 9.58/10
2000	Course of inspector of human resources
1995-1999	High-school: Theoretical high-school “Ion Creangă” of Bucharest, mathematics-physics

Prizes

2008	Student Travel Award for World Biomaterials Congress 2008 - Amsterdam, from the Journal <i>Biomaterials</i>
2007	Price of the jury – Doctoral School of Angers, France – Poster Contest
2000	2 nd price at „Traian Lalescu” University Contest on Physics

Personal skills and competences

Mother tongue	Romanian
Other languages	English <i>European level B2</i> French <i>European level B2</i>

Social skills and competences

2007-present	European Society for Biomaterials
2005-present	Romanian Society of Chemistry, Romanian Society of Biomaterials, Association des <i>Etudiants Francophones</i> – <i>AEF</i>
2003-present	Practical stages in Hospital Prof. Th. Burgehele, different first aid competitions
2004	Course for intervention in case of disaster and first aid
2003-2004	Course of Red Cross volunteer, organised by the Romanian Red Cross National Society

Organisational skills and competences

2005	The 3 rd Edition of Balkans Chemistry Contest, Romania 2005 – organization team
2000-2003	FORUM ENTREPRISES ETUDIANTS, technical support, organisation

Technical skills and competences	- synthesis and characterisation of organic compounds, monomers and polymers with applications in industry, biology, medicine; - data acquisition and processing; - project management.
Computer skills and competences	MS Office, Adobe Photoshop, and Illustrator, Origin, image processing and analysis: ImageJ, Pixel Profile, various software for specific application (FT-IR: JASCO, Bruker; UV-VIS: CINTRA; Housfield Tinius-Olsen 25kN).
Driving licence	B category – since 2000
Interests	- continuous improvement of knowledge in science and software; - project development and management.

LIST OF PAPERWORKS

ISI paperworks

- T. Zecheru**, C. Zaharia, A. Sălăgeanu, C. Țucureanu, E. Rusen, B. Mărculescu, T. Rotariu, C. Cincu, *Polymeric biocompatible structures for controlled drug release*, Journal of Optoelectronics and Advanced Materials, Vol. 9, Iss. 9, 2007, p. 2917-2920.
- Catalin ZAHARIA, **Teodora ZECHERU**, Marie Françoise MOREAU, Florence PASCARETTI-GRIZON, Guillaume MABILLEAU, Bogdan MARCULESCU, Robert FILMON, Corneliu CINCUI, Georges STAIKOS, Daniel CHAPPARD, *Chemical structure of Methylmethacrylate-2-[2',3',5'-triiodobenzoyl]oxoethyl methacrylate copolymer, radio-opacity, in vitro and in vivo biocompatibility*, Acta Biomaterialia, in press, 2008.
- Hervé Nyangoga, **Teodora Zecheru**, Robert Filmon, Michel-Félix Baslé, Corneliu Cincu, Daniel Chappard, *Synthesis and use of pHEMA microbeads with human EA.hy 926 endothelial cells*. Journal of Biomedical Materials Research: Part B - Applied Biomaterials, accepted 2008.
- Romuald BERTHET, Amar ZERROUKHI, Gerald BRUN, **Teodora ZECHERU**, Corneliu CINCUI, *Synthesis and optical properties analysis of a new polymer optical fiber for side lighting*, Revue Roumaine de Chimie, 2007, 52(5), 473-482.
- C. ZAHARIA, E. RUSEN, B. MĂRCULESCU, R. FILMON, M. GĂVAN, N. CONSTANTIN, , D. CHAPPARD, **T. ZECHERU**, C. CINCUI, *New acrylic radio-opaque cement*, Journal of Optoelectronics and Advanced Materials, Vol. 9, No. 8, August 2007, p. 2543-2546.
- Edina Rusen, Cătălin Zaharia, **Teodora Zecheru**, Bogdan Mărculescu, Robert Filmon, Daniel Chappard, Roxana Bădulescu, Corneliu Cincu, *Synthesis and characterisation of core-shell structures for orthopaedic surgery*, Journal of Biomechanics 40 (2007):3349-3353.
- T. Zecheru**, C. Zaharia, G. Mabileau, D. Chappard, C. Cincu, *New HEMA-based polymeric microbeads for drug delivery systems*, Journal of Optoelectronics and Advanced Materials, Vol.3, No.8, 2006, p. 1312-1316.
- Doina Dimonie, Cătălin Zaharia, **Teodora Zecheru**, Ioana Vasile, Denis Panaitescu, *Proprietati de utilizare a unor amestecuri policlorura de vinil – poliuretan termoplastice realizate prin modificare fizica*, Materiale Plastice, 43, nr.3, 2006.
- P. Ghioca, E. Buzdugan, C. Cincu, L. Iancu, C. Zaharia, **T. Zecheru**, *Compozite polietilenice antisoc*, Materiale Plastice Vol. 44, Nr.3, p.175, 2007
- C. ZAHARIA, **T. ZECHERU**, E. RUSEN, A. SĂLĂGEANU, C. CINCUI *Methylmethacrylate-Iodothiophene copolymers for the obtaining of bone and dental cements*, Journal of Optoelectronics and Advanced Materials, Vol. 9, No.11, November 2007, p. 3307-3311.
- Bancu, L., Meghea, A., Simonescu, C., **Zecheru, T.**, *Room temperature synthesis of CdS nanocrystallites*, Molecular Crystals and Liquid Crystals, Volume 483, 15 April 2008, Pages 237-243.

International conferences – publication in volumes

- Eugen Trana, **Teodora Zecheru**, Mihai Bugaru, Tudor Chereches, *Johnson-Cook Constitutive Model for the OL 37 Steel*, The 7th WSEAS International Conference on Electric Power Systems, High Voltages, Electric Machines, 21-23 November 2007, Venice, Italy.
- Goga Doru, Rotariu Traian, Tigianescu Viorel, **Zecheru Teodora**, *Ballistic performances of primers: A new experimental method for evaluation*, 10th Seminar "New Trends in Research of Energetic Materials", 25-27 April 2007, Pardubice, Czech Republic.
- Traian Rotariu, Doru Goga, Sorin Esanu, **Teodora Zecheru**, *Colored smoke pyrotechnic compositions*, The 31st Internationally Attended Scientific Conference Modern Technologies in the XXI Century, 03-04 November 2005, Bucharest, Romania.
- Catalin ZAHARIA, **Teodora ZECHERU**, Corneliu CINCUI, Bogdan MARCULESCU, Daniel CHAPPARD, Robert FILMON, *Iodine-based copolymers with X-Ray Visibility for Biomedical Applications*, Romanian International Conference on Chemistry and Chemical Engineering RICCE XIV, Bucharest ROMANIA 22-24 September 2005, code ISBN 973-718-284-7, code ISBN 973-718-288-X.

International conferences – presentations

- T. Zecheru**, C. Zaharia, E. Rusen, F. Miculescu, C. Cincu, *Synthesis, Physico-Chemical Properties and Biological Evaluation of two new copolymer systems*, World Biomaterials Congress 28 May – 01 June 2008, Amsterdam, The Netherlands.
- Teodora Zecheru**, Cătălin Zaharia, Edina Rusen, Florin Miculescu, Bogdan Mărculescu, Corneliu Cincu, *Synthesis, characterisation and bioavailability of a new terpolymer system*, Romanian International Conference on Chemistry and Chemical Engineering RICCE 15, 19-22 September 2007, Sinaia, Romania.
- Nyangoga H., **Zecheru T.**, Filmon R., Cincu C., Chappard D., *Use of pHEMA microbeads with human endothelial cells*, Romanian International Conference on Chemistry and Chemical Engineering RICCE 15, 19-22 September 2007, Sinaia, Romania.
- Ghioca Paul, Buzdugan Emil, Cincu Corneliu, Iancu Lorena, Spurcaci Bogdan, Zaharia Catalin, **Zecheru Teodora**, *Compozite polietilenice antisoc*, Simpozion International Prioritatile Chimiei pentru o Dezvoltare Durabila (PRIOCHEM), Editia a III-a, Bucuresti, 29-30 October 2007, Bucharest, Romania.
- Zaharia C., Moreau M.F., **Zecheru T.**, Marculescu B., Filmon R., Cincu C., Basle M.F., Chappard D., *A methacrylate polymer containing iodinated monomer usable as bone cement: radio-opacity, in vitro and in vivo biocompatibility*. 34th European Symposium on Calcified Tissues, May 2007, Copenhagen, Denmark, abstract published in CALCIFIED TISSUE INTERNATIONAL 80: S49-S50 Suppl. 1, (2007).
- T. Zecheru**, C. Zaharia, A. Salageanu, C.Tucureanu, E.Rusen,B.Marculescu, T.Rotariu, C.Cincu, *Polymeric biocompatible structures for controlled drug release*, 2nd International Conference on Biomaterials and Medical Devices - BiomMedD'06, 9-11 November 2006, Iasi, Romania.
- Zecheru,T.**, Spulber,C., Borcan,O., Chereches,T., *Spectral screening efficiency of pyrotechnics in atmospheric aerosol release*, Conference on Visibility, Aerosols, and Atmospheric Optics, 3-6 September 2006, Vienna, Austria.

Marilena Constantinescu, Catalin Zaharia, Elena Pau, **Teodora Zecheru**, Corneliu Cincu, *Fibrous materials with potential uses in bone pathology*, XX-e Congress of the International Sericultural Commission – 15-18 december 2005, Bangalore, India.

National conferences – presentations

Corneliu Cincu, Marilena Constantinescu, Catalin Zaharia, **Teodora Zecheru**, Elena Pau, *Chemical Modification Of Some Natural Fibres For Application In Bone Pathology*, Conferința AMCSIT CeEx 2007, "Cercetarea de excelență – premiză favorabilă pentru dezvoltarea spațiului românesc de cercetare", „Excellence research as a way to ERA”, 24-26 October 2007, Brasov, Romania, ISSN 1843-5904.

T. Zecheru, C. Spulber, C.C. Zecheru, T. Chereches, *Advanced technologies and concepts used in diagnosis and treatment*, Fall session 2007 of Romanian Scientists Association (AOSR), 15-16 October 2007, Constanta, Romania.

Teodora ZECHERU, Catalin ZAHARIA, Guillaume MABILLEAU, Daniel CHAPPARD, Corneliu CINCUI, *New micron ad nano-sized polymer particles for controlled drug release*, The 4th National Conference „New Research Trends in Material Science ARM-4” – Proceedings, Volume II, September 4-6 2005, Constanta, Romania, ISBN 973-718-299-5.

Paperworks published in journals with CNCSIS recognition

C. ZAHARIA, **T. ZECHERU**, C. CINCUI, R. FILMON, D. CHAPPARD, *New biomaterials based on glutamic acid for bone pathology*, International Conference on Materials Science and Engineering BRAMAT 2007, published in Bulletin of the Transilvania University of Brasov, Supplement BRAMAT 2007.

Teodora Zecheru, Aurora Salageanu, Corneliu Cincu, Daniel Chappard, Amar Zerroukhi, Poly(HEMA-co-MOEP) microparticles: optimisation of the preparation method and *in vitro* tests, UPB Sci. Bull., Series B, Vol. 70, No. 1 (2008) 45-54.

T. Zecheru, C. Spulber, O Borcan, Obscuration pyrotechnical compositions and their effects in the atmosphere, The 32nd International scientific conference of the Military Technical Academy – Modern Technologies in the 21st Century, 1-2 November 2007, Bucharest, Romania.

Books

Corneliu CINCUI, Catalin ZAHARIA, **Teodora ZECHERU**, *TEHNOLOGII DE PRELUCRARE A POLIMERILOR (Polymer Processing Technologies)*, Ed. PolitehnicaPress, Bucharest 2005, ISBN 973-8449-86-3.